



**HAL**  
open science

# Réticulation non-permanente, chimique ou physique, du caoutchouc naturel époxydé : propriétés dynamiques et recyclage

Lucie Imbernon

► **To cite this version:**

Lucie Imbernon. Réticulation non-permanente, chimique ou physique, du caoutchouc naturel époxydé : propriétés dynamiques et recyclage. Matériaux. Université Pierre et Marie Curie - Paris VI, 2015. Français. NNT : 2015PA066427 . tel-01647206

**HAL Id: tel-01647206**

**<https://theses.hal.science/tel-01647206>**

Submitted on 24 Nov 2017

**HAL** is a multi-disciplinary open access archive for the deposit and dissemination of scientific research documents, whether they are published or not. The documents may come from teaching and research institutions in France or abroad, or from public or private research centers.

L'archive ouverte pluridisciplinaire **HAL**, est destinée au dépôt et à la diffusion de documents scientifiques de niveau recherche, publiés ou non, émanant des établissements d'enseignement et de recherche français ou étrangers, des laboratoires publics ou privés.

Thèse de Doctorat de  
l'Université Pierre-et-Marie-Curie

École doctorale Physique et Chimie des Matériaux - ED 397

*Laboratoire : Matière Molle et Chimie, ESPCI ParisTech-CNRS, UMR7167,  
PSL Research University*

Présentée par

**Lucie IMBERNON**

Pour obtenir le grade de

Docteur de l'Université Pierre-et-Marie-Curie

---

**Réticulation non-permanente, chimique ou physique, du  
caoutchouc naturel époxydé. Propriétés dynamiques et recyclage.**

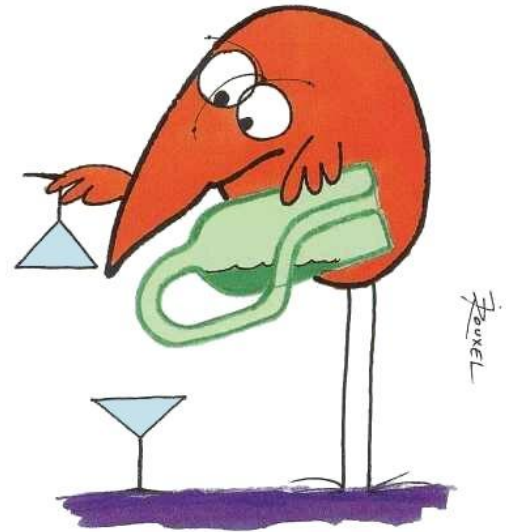
---

Soutenue publiquement le lundi 19 octobre 2015, devant un jury composé de :

M. Dominique HOURDET	Président du jury
M. Ludwik LEIBLER	Directeur de thèse
Mme Sophie NORVEZ	Encadrante
M. Ibon ODRIOZOLA	Examineur
M. Éric PAPON	Rapporteur
M. Jean-François TASSIN	Rapporteur



*Les devises Shadok*



S'IL N'Y A PAS DE SOLUTION  
C'EST QU'IL N'Y A PAS DE PROBLÈME.

*A ma polymère et mon polypère...*



## Remerciements

Comme le dit la chanson : « Voilà, c'est fini ! »

Mais une thèse ça ne se fait jamais seul, et je tiens à remercier ici l'ensemble des gens qui m'ont aidée, soutenue, suivie, et ont fait que je garderai un excellent souvenir de ma journée du 19 octobre 2015, ainsi que de l'ensemble des trois années qui ont précédé cette date. Ce n'est pas sans une petite nostalgie que je m'attaque donc à ce dernier travail d'écriture, pas forcément le plus facile...

Je souhaite tout d'abord remercier très sincèrement **Ludwik Leibler**. Merci de m'avoir accueillie dans le laboratoire toutes ces années, mais également d'avoir accepté d'être mon directeur de thèse. Je suis consciente d'avoir eu une chance exceptionnelle de réaliser ma thèse dans ce cadre privilégié qu'est le MMC. Merci de l'intérêt que vous avez montré pour mon travail, vous m'avez fait confiance et avez toujours été encourageant. J'ai beaucoup apprécié nos réunions, qui m'ont permis d'avancer à chaque fois d'un grand pas. J'ai pu bénéficier de votre vision si claire des choses, de votre recul et de votre connaissance infinie qui m'impressionnent beaucoup.

Un immense merci à **Sophie Norvez**. Tu m'accompagnes dans ma formation depuis maintenant sept ans. D'abord en tant que professeur pendant mes années d'élève-ingénieure, tu m'as ensuite permis de découvrir le MMC lors de mon projet de troisième année qui déjà portait sur le caoutchouc naturel époxydé (j'en profite d'ailleurs pour remercier **Myriam Pire** et **Ilias Iliopoulos** avec qui j'ai eu la chance de travailler également à cette occasion ; Myriam m'a initiée à toutes les techniques d'étude et de mise en forme du caoutchouc disponibles au laboratoire, et Ilias m'a fait partager ses connaissances et m'a donné l'envie de devenir experte en caoutchouc !). Ilias et toi m'avez ensuite proposé de revenir pour mon stage de master pour découvrir un autre type d'élastomère et j'ai finalement postulé pour un financement doctoral que j'ai obtenu. Durant toutes ces années, et particulièrement les trois dernières, tu m'as accompagnée et soutenue aux moments où j'en avais besoin, tu m'as toujours fait entièrement confiance et as montré un enthousiasme à toutes épreuves. On commence à bien se connaître, et j'ai de plus en plus apprécié notre collaboration au long de cette thèse, surtout lorsqu'il s'est agi de rédaction (papiers ou manuscrit de thèse). Je pense qu'avec l'aide précieuse de Ludwik, on forme un binôme efficace et j'espère que d'autres fruits de cette collaboration pourront être publiés rapidement.

Mes sincères remerciements vont aussi à **Jean-François Tassin** et **Éric Papon** qui ont accepté de rapporter ma thèse. Je vous suis extrêmement reconnaissante d'avoir pris le temps de lire et de critiquer mon travail malgré vos emplois du temps certainement plus que chargés. Merci également aux autres membres du jury : **Ibon Odriozola**, qui s'est déplacé depuis l'Espagne (¡ muchas gracias !), et **Dominique Hourdet**, qui a accepté de présider le jury, je sais que vous avez pris part à au moins huit jurys de thèse cet automne et votre participation m'a d'autant plus touchée que vous faisiez également partie du jury qui m'a octroyé une bourse de thèse il y a trois ans !

J'aimerais profiter de ces quelques pages pour remercier l'**ESPCI** et tous ses acteurs pour la formation de haut niveau dont j'ai bénéficié. Je pense que ce choix que j'ai fait en fin de prépa a eu et aura encore beaucoup de conséquences sur mon avenir, et avec le recul que j'ai actuellement je suis vraiment ravie de l'avoir fait !

Durant cette thèse j'ai eu la chance de collaborer avec un certain nombre de personnes que je souhaite remercier chaleureusement ici :

Un grand merci à **Sylvie Tencé-Girault** avec qui j'ai eu la chance de collaborer sur des manip passionnantes ! Merci infiniment d'avoir pris du temps pour moi cette année alors que Sophie était particulièrement prise par ses fonctions à la direction des études de l'ESPCI. Merci aussi pour ta bonne humeur quotidienne, ta disponibilité et toutes les tablettes de chocolat partagées !

Merci à mes autres collaborateurs, tout d'abord **Evi Oikonomou** une personne adorable et talentueuse avec qui j'ai eu grand plaisir à travailler mais aussi à discuter ! Merci à **Pierre-Antoine Albouy** pour qui la cristallisation sous contrainte des caoutchoucs n'a pas de secrets. Merci de nous avoir permis de développer tout un autre aspect d'étude de nos réseaux d'ENR. Je voudrais également remercier **Cédric Lorthioir** qui m'a fait bénéficier de ses connaissances très approfondies en RMN lors de mon stage de master, et **Benoît Le Rossignol** de la société Hutchinson, qui avait suivi mon stage de master et qui a ensuite montré de l'intérêt pour mon travail de thèse, merci pour les échantillons de caoutchouc que vous avez accepté de nous procurer et pour les discussions très enrichissantes par mail ou au téléphone avec Sophie. Enfin, j'ai eu la chance de pouvoir encadrer quatre stages durant ces trois années, et je n'oublie pas les quatre étudiants qui sont venus au labo travailler avec moi sur mon projet. **Louisa Amari** et **Alice Tonnelier** qui ont fait un travail efficace sur le sujet que je leur avais proposé qui ne fait finalement pas partie de ce manuscrit... Désolée pour ça, mais j'ai vraiment beaucoup apprécié votre passage au laboratoire, vous avez été des stagiaires extraordinaires ! Et plus récemment **Guilhem Chenon** et **Raphaël Pauchet** avec qui j'ai également beaucoup aimé travailler !

Je me dois de remercier ici une deuxième fois **Ibon Odriozola** pour m'avoir accueillie durant deux semaines en novembre-décembre 2014 dans son laboratoire à San Sebastián. Ces deux semaines ont été une expérience très enrichissante pour moi, et je voudrais remercier aussi tous les gens avec qui j'ai travaillé là-bas. En particulier **Roberto Martín** qui était lui aussi venu passer une semaine au MMC à Paris, mais également **Alaitz Rekondo**, **Nerea**, **Edurne**, **Alaitz** et les autres...pour leur accueil chaleureux.

Je tiens évidemment à remercier également tous les autres membres du MMC.

Tout d'abord les permanents : **Michel Cloître**, mon tuteur de thèse, que j'ai vu quotidiennement puisque j'ai toujours été entourée de vos étudiants, merci pour votre aide en rhéologie mais aussi pour votre gentillesse de tous les jours ! **Renaud Nicolaÿ**, avec qui j'ai justement aussi partagé le bureau, merci pour nos discussions, tes conseils, scientifiques ou non, j'ai beaucoup apprécié travailler à tes côtés. **François Tournilhac**, que j'ai été très contente de mieux connaître grâce au projet SHINE, **Corinne Soulié-Ziakovic** qui avec

Sophie m'a enseigné la chimie inorganique, **Laurent Corté**, avec qui j'ai fait des manips très intéressantes lors de mon projet de 3A, **Alba Marcellan** avec qui j'ai pu discuter mécanique des polymères durant son passage au laboratoire, **Szilvia Karpati** qui nous a beaucoup aidé pour les observations au TEM, **Anne-Claire Dumanois** et **Isabelle Marlart** pour toute leur aide informatique et pour la GPC, et bien sûr, last but not least : **Marie-France Boucher**, sans qui le laboratoire ne tournerait pas rond, merci pour ta bonne humeur et ton aide plus que précieuse au quotidien !

Une pensée spéciale à tous mes co-bureaux : **Renaud Nicolaÿ**, **Alexandre PrévotEAU**, **Charlotte Pellet**, **Lavanya Mohan**, **Johanna Salvant**, **François Bargain**, **Helen Lentzakis** et la dernière arrivée **Maddalena Mattiello**. Merci pour tous ces bons moments partagés, toutes les discussions, les potins et les sucreries ! Un merci particulier à Charlotte, on se connaît depuis l'entrée à PC il y a déjà sept ans, et après un projet et un stage de master au MMC, on se retrouve finalement face à face au bureau. Ça aura été un grand plaisir de partager tout ça avec toi, et j'ai tout particulièrement apprécié notre synchronisation sur la fin. Donc merci pour tout, le papotage au quotidien, et les petits coups de pouce quand c'était un peu dur pour moi.

Merci aussi à tous les autres membres « non-permanents » du MMC (étudiants et postdocs) pour toute l'aide apportée au labo, mais aussi la bonne humeur, les parties de rigolade et les sorties qui ont fait de ces trois années un super moment.

Merci aux anciens, **Réda Agnaou** et **Jun Mougner** (pour vos blagues et tous vos conseils avisés), **Morgane Leneindre** et **Thomas Vidil** (deux autres anciens de PC qui ont toujours été de bon conseil), **Nga Nguyen** (pour cette bonne humeur constante et communicative), **Nuno Loureiro** (pour ta gentillesse infinie), **Aggeliki Triftaridou** (même si j'ai raté toutes les occasions d'aller manger une glace !), **Cinzia Rotella** (ma coinquilina, merci pour tous les rires qu'on a pu avoir ensemble !), **Francisca Kesten** (quelle joie de vivre !), mais aussi **Miriam Unterlass**, **Monika Gosecka** et **Nebewia Griffete** trois anciennes postdoc de qui je garde également un très bon souvenir.

Merci aux encore plus anciens : **Jessalyn Cortese**, **Mathieu Capelot**, et **Ulysse Naessens** qui étaient là lors de mes débuts de thésarde.

Je pense aussi aux deux autres thésards de la génération 2015 : **David Moreau**, arrivé depuis peu au laboratoire mais déjà bien intégré (merci pour la bonne humeur et le soutien lors des soirées de rédaction un peu -trop- longues) et **Erwan Chabert**.

Mais merci aussi aux nouvelles générations de thésards et de postdocs pour l'ambiance sympathique que vous perpétuez au labo !

La relève des postdocs : **Mikihiro Hayashi**, **Rob van der Weegen**, **Tristan Domenech** et **Raphaël Michel**, I didn't get to know you much, but I am glad to have met you and I wish you all the best!

Merci pour tout et bon courage à **Fanny Angot**, **Rémi Fournier**, **Marie Gracia**, **Adrien Demongeot**, **Aurélié Legrand**, **Lise Devès** et **Max Röttger**, les prochains sur la liste ! Vous

êtes tous des étudiants excellents et je ne me fais aucun souci pour vous. Que ce soit autour de l'extrudeuse pour Adrien, du rhéo pour Rémi, de la traction pour Marie, et même parfois de la pulvérisette pour Max ou tout simplement autour de la table le midi pour Aurélie, Fanny et Lise, j'ai été ravie de vous côtoyer et de travailler avec vous !

Merci enfin aux plus jeunes (au moins en année de thèse) : **Coralie Teulère, François Bargain, Jérémie Lacombe, Thibault Derouineau, Franz Pirolt, Julien Caroux, Maddalena Mattiello, Maïssa Faroux** et **Andre Arnebold**. Vous êtes des collègues géniaux et je vous souhaite de très belles années au labo ! Bon courage à vous, et merci pour tout !

Je remercie aussi les stagiaires qui sont passés par le labo et que j'ai été très contente de connaître, notamment **Benoit, Léo, Blandine, Marc-Antoine, Mailys, Julie**...

Un grand merci aux étudiants et postdocs du **LCMD** avec qui j'ai pu partager les délicieux repas du RU !

J'ai également la chance d'avoir des amis exceptionnels que je tiens à remercier ici. Les Montpelliérains des années Joffre, la prépa aura tissé des liens permanents entre nous, et ceux-là je n'ai aucune envie de les rendre réversibles (héhé, blague de physico-chimiste)! Mais également des amitiés de plus longue date que j'ai réussi à conserver. Merci notamment à **Mélanie, Fanny** (qui était présente le 19 !) et **Sandra**, ainsi qu'à **Allison** qui m'ont permis de faire des pauses bien agréables pendant ma rédaction cet été !

Merci à tous mes amis de PC et pièces rapportées, la promo 127, et surtout la pizza du mercredi. Vous avez rendu ma vie parisienne si agréable, vous allez me manquer ! Merci à **Hugo**, l'initiateur de la fameuse « tradition des cadeaux », et merci à **tous** pour ces animations, j'ai vraiment trop rigolé !

Enfin, merci à la famille. Celle de **Léopold** dans laquelle je suis si bien accueillie : merci pour tout ! Un merci spécial à **Benjamin**, ses talents de photographe mais aussi son modèle m'ont permis d'illustrer ce manuscrit. Et bien évidemment ma famille, merci **Papa, Maman**, vous avez toujours cru sans limite en moi et m'avez permis d'arriver jusqu'ici. Merci pour cet été, ces deux semaines ont été vraiment parfaites pour une thésarde en fin de rédaction. Merci à mes sœurs, **Cécile** pour les bons mots d'une grande sœur, et **Jeanne** qui était là à la toute fin de ma rédaction pour me permettre de m'aérer la tête en courant avec moi la Parisienne. Merci beaucoup à **Matthieu**, ça me touche beaucoup que tu aies fait le déplacement jusqu'à Paris ! Je n'oublie pas non plus **Kévin** qui même s'il n'a pas pu venir a été adorable comme d'habitude. Merci aussi à **Ellen** et **Etienne** qui m'ont tant facilité l'installation à Paris et m'ont aidée à m'y sentir un peu chez moi ! Merci à **Olivier, Noé, Inès** et **Bruno** qui ont fait le déplacement, à **Auntie Marie** pour tous ses encouragements et à mes deux **grand-mères** exceptionnelles !

J'espère n'avoir oublié personne, et si c'est le cas, j'espère que cette personne ne doute pas une seule seconde que je la remercie du fond du cœur ! =)

Il ne me reste donc qu'à remercier **Léopold**, pour avoir accepté de me suivre en Belgique, mais aussi pour tant d'autres choses !...



---

**Introduction générale ..... 1****Chapitre 1 : La chimie dynamique au service du recyclage des élastomères, une revue ..... 10****1. From landfilling to vitrimer chemistry in rubber recycling ..... 10**

Introduction ..... 10

1.1. What is a rubber ?..... 12

1.2. Recycling of conventional elastomer networks ..... 15

1.3. Towards designed recyclability of crosslinked rubbers ..... 22

1.4. Using dynamic chemistry in rubbery materials..... 25

Concluding remarks ..... 55

**2. The choice of Epoxidized Natural Rubber..... 56**

2.1. A product from nature ..... 56

2.2. Epoxidation of NR ..... 58

2.3. ENR properties ..... 59

2.4. A new way to crosslink ENR ..... 61

2.5. A full bio-based system..... 63

**References ..... 64****Chapitre 2 : Échange ou hydrolyse des ponts esters, avantages sur les réseaux permanents ..... 76****1. Dynamic network by transesterification, stress relaxation study..... 78**

1.1. Introduction ..... 79

1.2. Experimental section ..... 80

1.3. Results ..... 83

1.4. Discussion ..... 90

1.5. Conclusions ..... 93

**2. Recyclability of DA-crosslinked ENR through ester hydrolysis..... 96**

2.1. Introduction ..... 96

2.2. Experimental section ..... 96

2.3. Results and discussion.....	97
2.4. Conclusions .....	103
<b>References .....</b>	<b>104</b>

**Chapitre 3 : Retour aux soufres ..... 111**

<b>1. Use of a disulfide-containing diacid.....</b>	<b>114</b>
1.1. Introduction .....	115
1.2. Experimental section .....	117
1.3. Results and discussion.....	120
1.4. Conclusions .....	130
1.5. Supplementary information (SI).....	131
<b>2. Comparison with a sulphur-vulcanized ENR network.....</b>	<b>136</b>
2.1. Introduction .....	136
2.2. Experimental section .....	137
2.3. Results and discussion.....	138
2.4. Conclusions .....	147
Acknowledgments .....	148
Appendix .....	148
<b>References .....</b>	<b>149</b>

**Chapitre 4 : Réticulation physique et cristallisation sous contrainte ..... 154**

<b>1. Strain-induced crystallization in ENR-DA .....</b>	<b>157</b>
1.1. Introduction .....	157
1.2. Experimental section .....	159
1.3. Results and discussion.....	165
1.4. Conclusions .....	176
<b>2. Crystallizable grafts and physical network .....</b>	<b>177</b>
2.1. Introduction .....	177
2.2. Characterization of the BA-grafting onto ENR.....	178
2.3. Properties of BA-grafted ENR25 .....	184
2.4. Summary and conclusions.....	193

<b>3. Dual networks</b> .....	<b>194</b>
<b>Appendix A</b> .....	<b>199</b>
<b>Appendix B</b> .....	<b>200</b>
<b>References</b> .....	<b>203</b>
<b>Conclusion générale</b> .....	<b>205</b>



# **Introduction générale**

---





« *Caoutchouc* »

*Aquarelle, gouache et encre de Chine*

*sur carton*

*Francis Picabia (1879 - 1953)*

*(<https://www.centrepompidou.fr>)*

Ce travail de thèse s'inscrit dans la thématique très actuelle du recyclage des caoutchoucs. Matériaux aux propriétés mécaniques exceptionnelles, les caoutchoucs font partie intégrante de notre vie quotidienne : des pneus aux tétines de biberon en passant par les gants de protection ou encore les semelles de chaussures, le caoutchouc est même utilisé pour confectionner des bijoux. Ces matériaux sont indispensables industriellement dans de nombreux types d'applications tels que l'amortissement ou l'étanchéification. Le caoutchouc naturel, décrit devant l'Académie des sciences pour la première fois au XVIII<sup>e</sup> siècle par Charles-Marie de La Condamine, est longtemps resté le seul élastomère connu, expliquant l'utilisation généralisée du mot *caoutchouc*. Pourtant, le terme *élastomère* est plus générique, et englobe sans ambiguïté tous les polymères naturels ou synthétiques possédant des propriétés élastiques.

Alors que nous sommes actuellement à l'ère du plastique avec une consommation de plus en plus grande de macromolécules synthétiques et naturelles, les élastomères présentent le désavantage de posséder une structure en réseau. En effet, la réticulation des caoutchoucs, qui est nécessaire à leur tenue mécanique, empêche totalement leur recyclage à cause de la création de liens chimiques permanents entre les chaînes de polymère. Les ressources naturelles de la planète, ainsi que sa capacité à gérer les déchets n'étant pas infinies, le recyclage est devenu un problème majeur de notre société.

Le caoutchouc naturel époxydé (epoxydized natural rubber, ENR) est le matériau choisi comme base de ce travail. Il est bien connu au laboratoire Matière Molle et Chimie (MMC) puisqu'il a déjà fait l'objet de la thèse de Myriam Pire en 2011,<sup>1</sup> en collaboration avec l'entreprise Hutchinson, ainsi que de plusieurs articles.<sup>2-7</sup> Ce matériau est directement issu du caoutchouc naturel, ce qui lui confère deux principaux avantages : son origine biosourcée, et

ses bonnes propriétés mécaniques. Peu de solutions existent pour recycler les caoutchoucs réticulés de manière classique. La stratégie utilisée ici est la mise en œuvre de nouvelles méthodes de réticulation utilisant la chimie non-permanente. Cette dernière représente une thématique également largement étudiée au laboratoire MMC, qui a permis le design des matériaux totalement innovants que sont les caoutchoucs auto-cicatrisants<sup>8</sup> et les vitrimères.<sup>9</sup>

Ce manuscrit s'articule en quatre chapitres. Dans une volonté de diffusion de la recherche menée dans le cadre de cette thèse, la majeure partie des résultats de chaque chapitre est rédigée sous la forme d'articles scientifiques. Le manuscrit est donc principalement rédigé en anglais.

Le **Chapitre 1** comprend dans un premier temps une revue bibliographique du recyclage des caoutchoucs. Après une brève présentation de ces matériaux, les techniques de recyclage existantes, concernant les réseaux réticulés de manière classique, sont tout d'abord exposées. Puis, une ouverture est proposée sur l'intérêt de la chimie non-permanente dans ce domaine. L'utilisation d'une telle chimie pour la réticulation d'élastomères est alors détaillée. Cette première partie du chapitre est destinée à être publiée comme article de revue. Dans un deuxième temps, ce chapitre sera aussi l'occasion de présenter plus en détail le système étudié dans cette thèse.

Le **Chapitre 2** marque le début de l'exposition des résultats expérimentaux. L'ENR est réticulé par des diacides carboxyliques qui ouvrent les cycles époxy. Les liens esters obtenus sont potentiellement échangeables par ajout d'un catalyseur (chimie vitrimère). La première partie du chapitre est consacrée à la comparaison de ce réseau catalysé avec un réseau permanent, en termes de relaxation de contrainte et d'adhésion, montrant les avantages de la chimie vitrimère dans le domaine de l'allongement du cycle de vie et du recyclage des élastomères. Cette partie est rédigée sous la forme d'un article qui sera soumis prochainement. Les liens esters présentent un deuxième intérêt en termes de recyclage : leur capacité à être sélectivement rompus par hydrolyse. Cette technique est utilisée dans la deuxième partie du chapitre, pour le recyclage du caoutchouc réticulé chimiquement.

Le soufre est un composé chimique qui a souvent côtoyé les caoutchoucs. En effet, la vulcanisation au soufre est toujours une des techniques de réticulation les plus répandues. Le **Chapitre 3** revient sur l'utilisation de ce composé en termes de chimie dynamique et de recyclage. Comme le précédent, ce chapitre est construit en deux parties. La première partie

est un article intitulé "Chemically crosslinked yet reprocessable epoxidized natural rubber via thermo-activated disulfide rearrangements" paru dans *Polymer Chemistry* en avril 2015.<sup>10</sup> Il s'agit de l'utilisation de diacides fonctionnalisés pour la réticulation de l'ENR. Ces diacides possèdent une liaison disulfure au centre de la chaîne, qui confère des propriétés dynamiques au réseau. Ces propriétés sont caractérisées par des études de relaxation de contrainte, de fluage, d'adhésion et de recyclage. La vulcanisation classique au soufre produit des ponts polysulfures qui sont eux aussi connus pour s'échanger de manière dynamique à haute température. La comparaison de cette technique classique avec la réticulation au diacide fonctionnalisé fera l'objet de la deuxième partie du chapitre.

Enfin, dans le **Chapitre 4**, l'ENR est modifié par greffage. Des monoacides gras sont greffés sur la chaîne d'ENR par estérification, comme dans le cas de la réticulation avec les diacides. Cette modification permet l'obtention d'un réseau physique par cristallisation des greffons. Ce chapitre est l'occasion de présenter une technique de rayons-X sous traction utilisée pour caractériser la cristallisation des greffons, mais aussi la cristallisation sous contrainte de la chaîne d'ENR elle-même. Dans une première partie, l'étude des réseaux chimiques d'ENR réticulé aux diacides permet de mieux comprendre les résultats obtenus par cette technique de rayons-X. Cette partie est rédigée sous la forme d'un article. L'étude du réseau physique constitue la deuxième partie du chapitre. Les deux types de réticulations, chimique ou physique, peuvent être combinés pour obtenir un réseau dit dual, étudié dans la troisième et dernière partie de ce chapitre.

## Références

1. M. Pire, "Caoutouc Naturel Epoxydé et Réticulation par les Acides Dicarboxyliques : Chimie, Cinétique et Propriétés Mécaniques", Thèse de l'Université Pierre-et-Marie-Curie, 2011.
2. M. Pire, S. Norvez, I. Iliopoulos, B. Le Rossignol and L. Leibler, *Polymer*, 2010, **51**, 5903-5909.
3. M. Pire, S. Norvez, I. Iliopoulos, B. Le Rossignol and L. Leibler, *Polymer*, 2011, **52**, 5243-5249.
4. M. Pire, C. Lorthioir, E. K. Oikonomou, S. Norvez, I. Iliopoulos, B. Le Rossignol and L. Leibler, *Polymer Chemistry*, 2012, **3**, 946.
5. L. Imbernon, M. Pire, E. K. Oikonomou and S. Norvez, *Macromolecular Chemistry and Physics*, 2013, **214**, 806-811.
6. M. Pire, E. K. Oikonomou, L. Imbernon, C. Lorthioir, I. Iliopoulos and S. Norvez, *Macromolecular Symposia*, 2013, **331-332**, 89-96.
7. M. Pire, S. Norvez, I. Iliopoulos, B. Le Rossignol and L. Leibler, *Composite Interfaces*, 2014, **21**, 45-50.
8. P. Cordier, F. Tournilhac, C. Soulié-Ziakovic and L. Leibler, *Nature*, 2008, **451**, 977-980.
9. D. Montarnal, M. Capelot, F. Tournilhac and L. Leibler, *Science*, 2011, **334**, 965-968.
10. L. Imbernon, E. Oikonomou, S. Norvez and L. Leibler, *Polymer Chemistry*, 2015, **6**, 4271-4278.

**Chapitre 1**  
**La chimie dynamique au service du recyclage des élastomères,**  
**une revue**

---



<b>Chapitre 1 : La chimie dynamique au service du recyclage des élastomères, une revue .....</b>	<b>10</b>
<b>1. From landfilling to vitrimer chemistry in rubber recycling .....</b>	<b>10</b>
Introduction .....	10
1.1. What is a rubber ?.....	12
1.1.1. Chemistry of rubbers .....	12
1.1.2. Crosslinked networks .....	13
1.1.3. Remarkable properties and industrial applications.....	14
1.2. Recycling of conventional elastomer networks .....	15
1.2.1. Landfill disposal.....	15
1.2.2. Reclaiming of rubber.....	16
1.2.3. Scrap rubber powder as a filler .....	19
1.2.4. Compression moulding.....	20
1.2.5. Power production : heat, fuel.....	21
1.3. Towards designed recyclability of crosslinked rubbers .....	22
1.3.1. Industrial challenges .....	23
1.3.2. Chemical and physical challenges .....	23
1.4. Using dynamic chemistry in rubbery materials.....	25
1.4.1. Physically crosslinked elastomers (thermoplastic elastomers).....	25
1.4.2. Covalent reversible chemistry.....	39
1.4.3. Vitrimer chemistry.....	47
1.4.4. Double networks.....	49
Concluding remarks .....	55
<b>2. The choice of Epoxidized Natural Rubber.....</b>	<b>56</b>
2.1. A product from nature .....	56
2.1.1. Elements of history.....	56
2.1.2. Latex-producing plants .....	57
2.2. Epoxidation of NR .....	58
2.3. ENR properties .....	59
2.4. A new way to crosslink ENR .....	61
2.4.1. Classical crosslinking methods .....	61
2.4.2. Carboxylic diacid as a new crosslinker .....	61
2.5. A full bio-based system.....	63
<b>References .....</b>	<b>64</b>

# **Chapitre 1 : La chimie dynamique au service du recyclage des élastomères, une revue**

## **1. From landfilling to vitrimer chemistry in rubber recycling**

### **Introduction**

Polymers, commonly addressed as “plastics”, are the material of the 21<sup>st</sup> century. They find their use at every step of our day to day life in a very broad range of applications such as automotive, building, aerospace, or pharmacy. From a material scientist’s point of view, they are historically divided in two main classes: thermoplastics and thermosets. On the one hand, thermoplastics are long, entangled polymeric chains. The absence of crosslinks between the chains allows for total malleability of the material. By increasing the temperature, the molecular mobility increases, and the chains are able to diffuse by a phenomenon called reptation.<sup>1, 2</sup> This diffusion process at high temperature enables full processability of the material and shaping/reshaping by simple injection or moulding methods. Thermoplastics are fully recyclable. At the industrial scale, they are thus very convenient, which explains that they represent about 90 % of the total use of polymers nowadays. On the other hand, thermoset materials differ by the existence of chemical crosslinks between the polymer chains. Because of the presence of chemical bonds, the polymer chains can no longer diffuse because of the formation of a polymer network. The presence of the network is however at the origin of a new set of interesting properties. First, no flowing is allowed, even at high temperature: beyond the glass transition temperature, chemical networks present a rubbery plateau that is theoretically infinite. This thermal stability or heat resistance is very useful in high temperature applications. Second, thermosets are insoluble in any kind of solvent allowing the making of hoses and pipes for example. Crosslinking of thermosets also brings very good mechanical properties to the material (hardness or elasticity for example).

Elastomers are a particular class of thermoset materials that present additional exceptional properties of elasticity and resilience. They are widely used in the industry when flexibility is required, to make gaskets and seals, or used as noise reduction and damping materials for example. Elastomers are some of the most versatile engineering materials available. However, thermosets by nature, they present a major recycling problem: crosslinking is necessary to obtain the excellent mechanical properties, but it also implies the existence of irreversible chemical bonds between polymer chains that prevent reprocessing or recycling of the material. Because of the scarcity and increasing prices of natural resources, and of the growing environmental awareness, recycling of materials has become a crucial issue in today's society. It is necessary and industrially relevant to find efficient methods for recycling elastomers, reprocessing them, or even just extending their cycle of life.<sup>3</sup>

Industrial elastomer formulations have been developed and improved for more than a hundred years, making the materials particularly well adapted to their applications and thus hard to replace. The recycling of currently used rubbery objects is thus a very relevant problem, which will be tackled in the second part of this review after a brief introduction on what is a rubber. However, up to now, the recycling of used objects stays limited because of the associated loss of mechanical properties. Another strategy relies on the chemical modification of the crosslinks to design recycling ability. The aim in this case would be to confer thermoplastic's processability to elastomers while maintaining their high elasticity and minimizing the loss of their thermoset characteristics. This represents many chemical and physical challenges that will be exposed in the third part of the review. A new kind of elastomers has been designed and is already used industrially. These so-called thermoplastic elastomers (TPEs) are crosslinked through the use of phase separation and physical interactions but are not fully heat or solvent resistant. Dynamic covalent chemistry is now envisioned as a better solution to produce recyclable elastomers. The design of dynamic rubbery networks through both physical and dynamic covalent interactions will be the focus of the fourth and last part of this review.

## 1.1. What is a rubber ?

The first elastic material referred to as *rubber* was obtained by coagulation of the latex of an exotic tree (*Hevea brasiliensis*). The term “*rubber*” appeared in 1788 because this material exhibited erasing properties. Nowadays, the meaning of *rubber* was extended to any material that shows mechanical properties substantially similar to those of Hevea gum regardless of the chemical composition. The more recent term *elastomer* also refers to any material having rubber-like properties. Both words will be indifferently used in this work to appoint rubber-like materials in general, and Hevea gum will always be called *Natural Rubber* (NR) to avoid any ambiguities.

### 1.1.1. Chemistry of rubbers

*Natural rubber*: Chemically composed of very long molecules of *cis*-1,4-polyisoprene (> 99 %), NR is commercially available under two main forms: liquid (latex, mainly composed of polymer and water), or solid (after coagulation and drying or smoking).

*Synthetic rubbers*: Most of them are produced by the petrochemical industry except from silicon elastomers made from mineral materials (silica). There are three main classes:

- General purpose rubbers: butadiene, styrene-butadiene, polyisoprene...
- Special purpose rubbers: polychloroprene, acrylonitrile butadiene, ethylene-propylene-diene terpolymer, butyl rubber...
- Very special purpose rubbers: silicones, fluoroelastomers, polyacrylates...

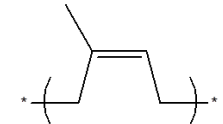
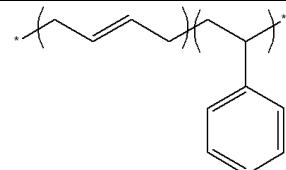
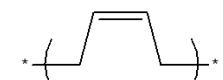
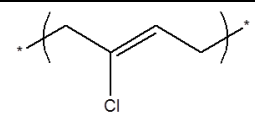
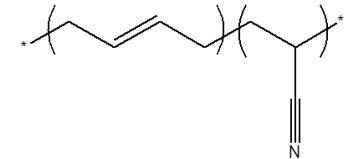
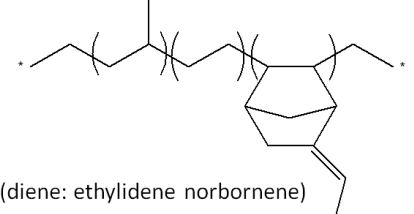
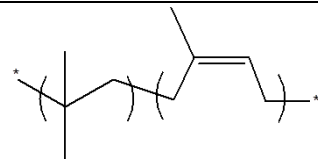
Even if polyisoprene can be synthesized and produced industrially, NR is still used in the industry for its outstanding properties. In particular, a non-negligible percentage of NR is used in the manufacture of truck tires.

*Other types of elastomers*: As we define rubbers by their mechanical properties, any kind of chemistry can be found, for example, an epoxy resin can in some conditions show a rubber-like behaviour.<sup>4</sup>

The chemical composition of some important rubbers is shown in Table 1. In function of this chemical composition, the rubbers have some additional properties like low gas permeability (butyl rubber), high resistance to degradation (chloroprene rubber) or to oils (acrylonitrile rubber), and high resilience (polybutadiene). However, regardless of their precise chemical

composition, they all present good rubbery properties (elasticity with extension ratio in the order of several hundred percent).

Table 1. Chemical structure of some important industrial rubbers

<b>General purpose rubbers</b> (about 82 % of global consumption)	Natural Rubber (NR)	
	Isoprene Rubber (IR)	
	Styrene-Butadiene Rubber (SBR)	
	Butadiene Rubber (BR)	
<b>Special purpose rubbers</b> (about 12 % of global consumption)	Chloroprene Rubber (CR)	
	Nitrile Butadiene Rubber (NBR)	
	Ethylene-Propylene-Diene Monomer (EPDM)	 <p>(diene: ethylidene norbornene)</p>
	Isobutylene Isoprene Rubber (IIR)	
<b>Very special purpose rubbers</b> (about 6 % of global consumption)	Silicone Rubbers (VMQ, PVMQ, FVMQ), Fluoroelastomers (FKM), Acrylic Rubbers (ACM, AEM), Chlorinated or Chlorosulfonated polyethylene (CM, CSM), Hydrogenated Nitrile Rubber (HNBR)...	

### 1.1.2. Crosslinked networks

It is well known that some particular conditions are necessary for a material to exhibit rubber-like elasticity. Treolar cited three main requirements.<sup>5</sup> First, the presence of long chain

molecules with free rotating links is necessary. Second, the secondary forces between molecules should be weak to let the chain take all the variety of statistical conformations rubber-like elasticity depends on. And third, there should be an interlocking of the molecules to form a three-dimensional network. This third condition is the one that allows going from a liquid-like material to a solid-like rubber (with the network structure, the rubber can be considered as an infinite molecule). Thanks to the length of the polymer chains, only a few linkage points are necessary, and the crosslinking does not interfere with the ability of the chains to move and take many configurations.

The first but still widely used way to form a network was sulphur vulcanization, discovered by Charles Goodyear in 1839. Ludersdorf and Hayward had already showed in 1934 the benefits of sulphur on the properties of NR. Since then, sulphur vulcanization has been widely studied and is reasonably understood.<sup>6, 7</sup> This process creates mono-, di- and poly-sulphide links between the rubber chains and enhances greatly the mechanical properties of the material as well as its resistance to heat. Crosslinking of NR may also be achieved using peroxides.<sup>6, 8</sup> In this case, short and stable carbon-carbon bonds are formed between the chains.

Rubber materials are usually extruded and moulded in their liquid state, and acquire rubber elasticity after crosslinking and formation of the network.

### *1.1.3. Remarkable properties and industrial applications*

Among all properties of crosslinked rubbers, elasticity is probably the most impressive. Major theoretical studies have been conducted in order to understand this phenomenon and a theory of rubber elasticity was developed and refined along the years. Kuhn (1942),<sup>9</sup> Guth, James and Matk (1946),<sup>10</sup> Flory (1944-85),<sup>11, 12</sup> Gee (1946)<sup>13</sup> and Treloar (1958)<sup>5</sup> considerably contributed to this work. The rubber elasticity is of entropic origin, conversely to crystalline or glassy materials that present enthalpy driven responses. The decrease of entropy induced by the alignment of the chains upon stretching is the motor of the retractability of the material.

Another important property of rubbers is damping, mostly used in vibration or sound insulation in the building industry for example. Numerous high-tech sealing elements are also made of rubber. The use of rubbers in today's industrial world is extremely wide, going from tires to toys, footwear, hoses, flooring or biomedical applications.<sup>14</sup>

## 1.2. Recycling of conventional elastomer networks

Creating a network, a process called reticulation, is necessary to obtain elastomers. It classically involves the use of sulphur or peroxides that build chemical bonds between the polymer chains. These bonds permanently fix the shape of the objects and impede any full recycling.

In 2012, the global production of elastomers was reaching 26 million tons,<sup>15</sup> 40 % of which being NR and the other 60 % different synthetic rubbers. Among all rubbery objects, tires represent a major recycling challenge because of their abundance and relatively short cycle of life: every year, around 800 million tires are discarded, and this value is increasing by about 2 % per year.<sup>16</sup> In 2010, more than 60 % of the global elastomer production (natural and synthetic) was used in the tire industry,<sup>17</sup> explaining why the recycling problem is often reduced to that of the tire life. A lot of efforts were made towards the amelioration of recycling processes and in 2012 about 8 to 10 % of recycled material was used to make new tires. The main reasons not to increase this percentage are safety matters associated to the loss of mechanical properties.<sup>18</sup> Tires are complex composite material combining elastomeric materials, textiles and metal. Their recycling is thus particularly demanding.

The literature on rubber recycling goes back to the late 19<sup>th</sup> century, following the discovery of sulphur vulcanization. Since that, it has continually evolved with the evolution of society. Some papers are fully devoted to the recycling of tires, for example, Adhikari *et al.*<sup>19</sup> in 2000 or Myhre *et al.*<sup>18</sup> in 2012. An update of the existing methods for recycling all kinds of classically vulcanized rubbery materials is proposed in this second section of the review. A summary is given in Figure 2 at the end of the section.

### 1.2.1. Landfill disposal

Landfill stays the easiest way to discard rubber waste (Figure 1a). However, crosslinked rubbers are not biodegradable, and the landfilling of end of life tires is banned by the European Commission since 1999.<sup>20</sup> The used objects can also be deviated from their main purpose and reused for other applications like holding down the plastic on silage packs, building eco-friendly houses or designing children swings in the case of tires (Figure 1b). However, faced to the ever growing quantity of rubber scraps produced by our society, it becomes crucial to find real recycling processes, at the industrial scale.



**a.**



**b.**

Figure 1. **a.** Used tires discarded in a landfill (from: *Le Monde* 11.12.2012), **b.** Reuse of waste rubber products (courtesy of: Benjamin Mottet)

The more common recycling method is still the grinding of rubber waste. In the case of old tires, the resulting powder is called GTR for “Ground Tire Rubber”.<sup>18, 19</sup> The powder, produced in cryogenic, ambient or humid conditions is then used in various processes for many applications.

### 1.2.2. Reclaiming of rubber

Reclaiming of the polymer from scrap rubber products has much more potential in terms of recycling and protection of the environment. From a tri-dimensional permanent network presenting elastic properties, any process to obtain a low modulus thermoplastic material by breaking the network is called reclaiming. If the reclaiming process selectively breaks crosslinking points, it can also be called devulcanization. Unfortunately none of the existing techniques is fully selective and scission of the main chain is hard to avoid, the reclaimed rubbers usually not recover the original properties of the elastomer. Reclaiming commonly produces a soluble part composed of truncated linear rubber molecules and a lightly crosslinked gel part. The bigger the soluble part and its molecular weight, the better the properties after revulcanization.

No existing reclaiming technique permits to regenerate the polymer exactly as it was before, but the process facilitates the recycling of rubbery products by increasing their compatibility with a virgin matrix. Among all existing techniques of reclaiming, four categories can be distinguished between physical, chemical, physico-chemical, and microbial techniques.

✓ *Physical techniques*

*Mechanical, thermo-mechanical and cryo-mechanical*

Reclaiming of rubber can be achieved mechanically inside a co-rotating twin screw extruder. The resulting material is very dependent on the temperature and the applied shear stress.<sup>21</sup> It can be characterized in terms of sol/gel fraction and crosslink density to determine a reclaiming level.<sup>22</sup> To get a very fine powder, a cryo-mechanical grinding is also feasible.<sup>23</sup> Cooling under the rubber glass transition temperature facilitates the grinding, but the process is more expensive due to the use of liquid nitrogen.

*Microwaves*

Microwave reclaiming is based on the breaking of crosslinks, favoured by the heat produced by microwaves going through the material. This technology was first developed by Goodyear Tire & Rubber in the late 70's. It is probably one of the most selective techniques: by selecting the right amount of energy, mainly sulphur-sulphur and carbon-sulphur bonds are broken, and good tensile properties can be achieved after revulcanization.<sup>19, 24</sup> Yet, main chain scission is unavoidable in the process.<sup>25</sup>

*Ultrasounds*

Isayev *et al.* showed that the application of certain levels of ultrasonic amplitudes, combined to heat and pressure inside an extruder, can efficiently break the network structure of crosslinked rubbers.<sup>26</sup> According to the authors, the ultrasonic devulcanization process is very fast, in the order of one second, and leads to the breaking of mono-, di- and polysulphide links but also carbon-carbon bonds of the main chain. The resulting material is similar to virgin material in terms of processing properties. After devulcanization, the rubber may be mixed again with crosslinking agents and compression moulded to obtain a new crosslinked material. In the case of natural rubber, this technique allows to obtain a recycled material with the same strain at break and 70 % of the tensile strength of the virgin material, making it a good recycling technique. According to the authors, the process would preserve the ability of NR to crystallize under strain.<sup>27</sup>

✓ *Chemical techniques*

Reclaiming of scrap rubber can also be achieved using chemical techniques. Usually powdered rubber is chosen for chemical treatments, the powder minimizing the problem of diffusion of the chemicals inside the network. Chemical methods can be a lot more selective

to the rupture of crosslinking points, which is beneficial for the mechanical properties of the reclaimed material. But the use of organic solvents is a major problem for the industrial scaling-up.

#### *Organic disulphides and mercaptans*

In the case of classical sulphur vulcanization, crosslinking points are mono-, di- and poly-sulphide links that are known to undergo exchange reactions with thiols or disulphides.<sup>28, 29</sup> An excess of those reactants thus partially devulcanizes the network. Diallyl disulphide is commonly used in this process.<sup>19</sup> Only monosulphide links resist to this chemical technique.

#### *Other organic compounds*

More recently, benzoyl peroxide was used to devulcanize NR, up to 46 % devulcanization could be obtained.<sup>30</sup> The process variables were shown to influence greatly the reclaiming.<sup>31</sup>

#### *Inorganic compounds*

For example, nitrous oxide is used for the reclaiming of olefin-containing rubbers. This inorganic compound reacts with double bonds by cycloaddition reactions<sup>32</sup> to yield diene oligomers bearing carbonyl groups (mainly ketones).<sup>33</sup> This technique results in main chain scission and can thus be used with all types of crosslinking processes: classical sulphur vulcanization, but also peroxide and even more original crosslinking methods.

Grubbs catalyst, an organo-metallic complex, can also be used as catalyst for olefin cross-metathesis between main chain double bonds and an olefin-containing transfer agent. Telechelic oligomers can be obtained by this method.<sup>34</sup>

#### *Pyrolysis*

This method that can be counted in chemical methods will be detailed in a subsequent section on energy production.

#### ✓ *Physico-chemical techniques*

Most of the physical reclaiming methods listed above can be coupled with the use of a chemical reclaiming agent to increase the efficiency of the process. It is indeed easy to combine a co-rotating twin screw extruder process at high temperature with the use of a disulphide compound for a better devulcanization of the rubber.<sup>35</sup> Microwaves were also used in combination with inorganic salts and nitric acid for example.<sup>36</sup>

Eventually, supercritical carbon dioxide can also greatly improve the penetration of the most effective devulcanizing reagents into the crosslinked material and thus facilitate the

reaction even in the presence of carbon black or silica.<sup>37</sup> Moreover, CO<sub>2</sub> is a non-toxic material that represents a green alternative to the organic solvents usually used in chemical reclaiming.

✓ *Microbial treatments*

Chemoautotroph organisms, a certain type of bacteria, are capable of oxidizing sulphur. These microorganisms can be used to degrade sulphur-vulcanized rubbers. The major limitation of this technique is that many microorganisms are sensitive to rubber additives, it is thus necessary to find resistant bacteria or to remove additives by immersion in a solvent prior to devulcanization. GTR devulcanization was reported using *Sphingomonas sp.*, a bacteria extracted from coal mines and possessing sulphur oxidizing properties,<sup>38</sup> or *Alicyclobacillus sp.*<sup>39</sup>

The microbial treatment presents the great advantage to be fully selective towards crosslinks and to preserve the integrity of the main chains.

1.2.3. *Scrap rubber powder as a filler*

After grinding, a more or less coarse powder can be obtained from used rubbery objects. For convenience, this powder will be named GTR in the following, even if scrap rubber can result from other objects than tires. This powder can be directly mixed with virgin materials and play the role of a filler.

✓ *In polymer matrices*

Mixing GTR with polymers can potentially improve their mechanical properties. This was tested in thermoplastic matrices,<sup>40</sup> thermoset resins but also in rubbers.<sup>41, 42</sup> However this kind of mixing seems to be beneficial only in the case of thermoplastic elastomers or rubbers.<sup>17</sup> The compatibility between GTR and the matrix is the main problem to overcome as bad compatibility weakens the mechanical properties instead of increasing them. Devulcanization of GTR, as described before, can improve compatibility. For example, in a NR matrix containing 10 % of GTR, devulcanization of the filler makes ultimate stress go from 13.7 to 23.2 MPa (69 % increase). In parallel, strain at break increases by 47 %.<sup>41</sup> A very recent review summarizes the use of GTR as polymer filler.<sup>43</sup>

✓ *In concrete and bitumen*

Elastomers possess exceptional damping properties, that may benefit to the field of building materials, by mixing GTR with asphalt, cement or concrete.<sup>44</sup> Since 1960s, waste rubber has been used for the modification of bitumen to enhance performance of road pavement. This technology is more and more used, but has not been fully adopted worldwide yet, mainly because of poor information and lack of qualified staff.<sup>45</sup>

It is not until 1993 that waste rubber was introduced in concrete to enhance its mechanical properties.<sup>46</sup> Since then, the benefits of this process were demonstrated in particular for structures located in areas exposed to earthquakes or severe dynamic actions such as railway sleepers.<sup>47</sup>

✓ *Other uses*

GTR is also directly used in some more specific applications like artificial grass or green roofs to replace the soil and allow good drainage. This brings energy savings thanks to the thermal insulation provided.<sup>48</sup>

One team reported on the use of GTR as sorbent for the removal of hydrocarbon contaminants in aqueous and gaseous phase. They claimed the removal of 99 % of poly-aromatic hydrocarbons, gasoline components and toluene (at concentrations below their solubility) using only 5 g.L<sup>-1</sup> of crumb rubber. Combined sorption effect of carbon black and rubber was highlighted.<sup>49</sup>

Eventually, waste rubber also has a potential in the field of sound insulation. This kind of application does not rely on the mechanical properties which are usually diminished after recycling, but takes advantage of other properties to valorise the material. Vulcanized rubber is known to be a good acoustic barrier due to its very inhomogeneous crosslinking. This property is transmitted to other materials by mixing with GTR.<sup>50,51</sup> This seems a viable option for use as building material, tackling both problems of noise and environmental pollution.

#### *1.2.4. Compression moulding*

One of the most used crosslinking system, sulphur vulcanization, produces di- and polysulphide links between the polymer chains. Paradoxically, this type of bonds are known to undergo some exchange reactions.<sup>28</sup> While recycling of waste rubber has been studied in literature since the end of the 19<sup>th</sup> century, it is not until 1981 that the GTR was directly reused to obtain a solid object without reclaiming or addition of virgin material. This was initially done by compression moulding of crumb rubber mixed with linking agents (sulphur,

accelerators, etc.).<sup>52</sup> Such process was then also described without the addition of curing compounds and is the object of several patents and articles among which are the major contributions of Farris *et al.*,<sup>53, 54</sup> Bilgili *et al.*,<sup>55, 56</sup> and Gugliemotti *et al.*<sup>16, 57</sup> Many parameters affect the properties of the resulting material including the waste recovery technique (size of GTR particles, devulcanized or not), temperature, presence of additives or pressure. However, the mechanical properties of the recycled rubbers are always significantly under those of the original ones.

#### 1.2.5. Power production : heat, fuel

Combustion of waste rubber is a way to produce heat. This heat can be used for example in cement plants to create energy. This process is efficient because these wastes have heating values higher than coal.<sup>58</sup> However, it brings another source of pollution by the production of fumes, etc., so it cannot be considered as an eco-friendly solution.

Pyrolysis is a thermo-chemical decomposition of products by heat (400 to 800 °C) in the absence of oxygen. This technique decomposes and volatilizes organic solids by heat, without combustion. Once the process is complete, in the case of composite such as tires, the obtained products are hydrocarbons, char (low grade carbon black), and steel. The resulting gas presents an interesting content in methane and ethane assimilated to natural gas. However, due to its high carbon dioxide and monoxide concentration, it cannot be commercialized as a mix with natural gas. The only potential use so far is the production of electricity, either directly (gas turbine) or by production of superheated steam (steam turbine). Meanwhile, some hydrocarbons can be condensed and used as fuel or chemical reagents. The exact composition of these hydrocarbons is temperature dependent.<sup>58</sup> Pyrolysis can also be assisted by microwaves,<sup>59</sup> representing an attractive alternative to conventional pyrolysis since microwaves allow fast heating of any absorbent material. This represents potential time and energy savings.

A last possibility exists in the field of microbial fuel cells whose applications are limited by the high cost of electrode material. Wang *et al.* showed that carbon anodes can be efficiently replaced by waste rubber coated with graphite paint, opening the field to larger scale applications.<sup>60</sup>



Figure 2. Different recycling techniques for industrial rubber objects.

### 1.3. Towards designed recyclability of crosslinked rubbers

Another point of view on recycling consists in looking closer into the chemistry of the crosslinks. As highlighted before, crosslinking is necessary in elastomeric materials to get solvent resistance properties or good elastic behaviour. Crosslinking the polymer by dynamic links to design recyclability upstream appears as a smart pathway (here, *dynamic* includes all kinds of covalent reversible and exchangeable links but also non-permanent chemistries like supramolecular interactions or crystallization). This strategy however is facing many challenges.

Everything in rubber technology is compromises as it is impossible to get at the same time all the desired properties. For example the better ageing resistance of peroxide treatment over sulphur vulcanization is accompanied with poorer fatigue behaviour. An improvement of

the recyclability also in most cases leads to poor solvent resistance and high compression set (e.g. TPE materials). The perfect rubber should combine all classical rubber properties, *i.e.* high elasticity, good ultimate tensile properties, low compression set, damping characteristics and resistance to solvent. In addition, it should also be fully recyclable and reprocessable without any loss in properties over several cycles. In this section, the major challenges arising from this ideal perspective are discussed.

### 1.3.1. Industrial challenges

Many dynamic chemical solutions have been developed for thermosets in general and some of them are successfully used in elastomeric materials as will be seen in a following section. Industrial solutions however impose specific criteria to be fulfilled:

- ✓ *Synthesis*: Only chemically simple and low cost chemical synthesis will be of industrial relevance.
- ✓ *Use of solvents*: Organic solvents are costly and hazardous chemicals that have to be avoided as much as possible. The dynamic properties of the rubber should ideally occur in the bulk state.
- ✓ *Recycling conditions*: Chemical degradation of the polymer obviously has to be avoided.

### 1.3.2. Chemical and physical challenges

We defined a *dynamic rubber* as an elastomeric material crosslinked or polymerized through *dynamic* - that is to say *non-permanent* - chemistry and thus able to undergo network rearrangements providing recyclability. Chemistry will play a crucial role in the obtaining of dynamic rubbers. The main strategies can be classified in two types: modification of an existing rubbery material to enable a dynamic crosslinking, or synthesis of new dynamic networks presenting rubber elasticity. Playing on the chemistry will be an efficient lever to adapt and tune the physical properties.

#### ✓ *Dynamic but strong*

Gels are a class of material presenting many similarities with elastomers. Indeed, they are composed of polymeric chains crosslinked to form a network. The softness and the presence of a solvent provide good mobility to the polymer chains and help the network rearrangements, facilitating the obtaining of dynamic networks.<sup>61, 62</sup> Gels can show elastic properties in some cases,<sup>63</sup> but their mechanical properties are usually far below those of

rubbers. Rubbers have Young's modulus in the order of 1 MPa, and ultimate tensile properties around a few MPa (from 10 to 20) and several hundred percent of deformation,<sup>5</sup> whereas gels present a fragile behaviour with Young's modulus around the kPa. Rubbers are denser than gels as they are solvent-free materials. To introduce a dynamic character in stiff networks having good mechanical properties is a real challenge. Adapting the crosslinking to be dynamic at high temperatures can be a solution. The temperature can increase the mobility of the chains as well as a solvent does, and decrease the viscosity of the material.<sup>4, 64</sup> The obtaining of strong and stable mechanical properties is indeed crucial for most industrial applications.

Among other things, good mechanical properties are related to the presence of long polymer chains presenting a lot of possible conformations. This represents another challenge when the strategy is to synthesize rubbers from dynamically linked small molecules.<sup>65</sup>

✓ *Processable but not liquid*

Self-healing materials are able to retrieve their original properties after being cut and rejoined without any external intervention.<sup>66, 67</sup> This is very valuable for life extension of a material because it enables its continuous healing throughout its life cycle. When the material is in use, self-healing also ensures retention of the mechanical properties through healing of micro-cracks. Self-healing is very dependent on the polymer architecture and real self-healing is theoretically only achieved when the properties of the healed interface are the same than the bulk.<sup>68</sup>

Self-healing becomes possible when the dynamic exchanges occur at room temperature.<sup>69, 70</sup> However, if reorganization can occur without any external stimuli, the material may be subjected to creep and eventually behaves as a liquid at room temperature.<sup>69</sup> A compromise should be found between processability and liquid behaviour. Hydrogen bonds are widely used to create self-healing materials. Leibler and co-workers successfully used hydrogen bonds to get a fully self-healing rubber that showed recoverable extensibility up to several hundred percent and little creep under load.<sup>65</sup>

✓ *Characterization of the dynamic behavior*

Spectroscopic or chromatographic studies can give insights into the chemistry of exchanges in dynamic rubbers.<sup>71, 72</sup> Besides, physical and mechanical characterizations are of greater importance to test the actual recyclability of the materials. Some of the principal implemented tests are mending and welding,<sup>64, 73</sup> reprocessing,<sup>74, 75</sup> healing tests<sup>76</sup> or stress relaxation.<sup>4, 77-79</sup>

For healing tests, tensile geometry is usually chosen for its simplicity. However, it was demonstrated to give limited information and to be very dependent on the experimenter (through the difficult precise repositioning of the cut surfaces).<sup>76</sup> Grande *et al.* implemented a fracture mechanics approach that was shown to give more reliable results.

The interpretation of stress relaxation experiments is somehow more delicate for rubbers than for other dynamic materials. Indeed, Chasset and Thirion pointed out a long time ago a stress relaxation occurring in permanently crosslinked samples of NR.<sup>80</sup> This phenomenon was attributed to the diffusion of dangling chains and other defects inside the rubber network and strongly depends on the crosslink density.<sup>81</sup> The comparison of this inherent stress relaxation and dynamic network relaxation will be the subject of the first part of Chapter 2. Dynamic chemistry may allow complete relaxation of the applied stress, and characteristic relaxation times may be controlled with more efficient triggers than defect diffusion.

## 1.4. Using dynamic chemistry in rubbery materials

Recycling is a common problem to all kinds of thermosetting materials and a lot of efforts was made towards dynamic crosslinking of thermosets.<sup>82-84</sup> In this section, we review the non-permanent crosslinking systems successfully applied in elastomeric materials.

### *1.4.1. Physically crosslinked elastomers (thermoplastic elastomers)*

Physical bonds are weaker than covalent ones. This shortcoming can become an advantage when it comes to recycling, if the bonds are used as crosslinks. Indeed, such links are able of cleaving and reforming in response to a simple stimulus as temperature. Moreover they will be preferably cleaved in the case of damage, keeping the covalent structure of the polymer intact. Crosslinking through the use of supramolecular bonds like hydrogen bonds for example appears as a good dynamic solution with high reactivity as well as repeatability of the repair action. Unfortunately this kind of networks cannot be fully heat- or solvent-resistant as physical bonds indeed are easily cleaved. Nevertheless, physical crosslinking of elastomers has been extensively studied and has given birth to a distinct class of polymers, the thermoplastic elastomers (TPEs). Some of them are of great industrial importance. Numerous combinations of thermoplastic and thermoset materials, taking advantage of phase separation,

crystallization or weak interactions are at the origin of new materials with good mechanical and even solvent resistance properties.

✓ *Industrial TPEs, the use of phase separation and crystallization*

An extensive literature on TPEs exists, including review articles and books.<sup>85, 86</sup> Among the major industrial TPEs are the ABA triblock copolymers (*e.g.* styrene block copolymers as Styrene-Butadiene-Styrene (SBS), Styrene-Ethylene/Butylene-Styrene (SEBS) and Styrene-Isoprene-Styrene (SIS)), thermoplastic olefins, thermoplastic vulcanizates (TPVs), copolyester elastomers and thermoplastic polyurethanes (TPUs). The common feature of those materials is their phase-separated morphology. Pioneering work of Cooper and Tobolsky established the microphase-separated structure of multiblock copolymers composed of soft and hard blocks.<sup>87</sup> In 1980, Leibler published a fundamental article giving the theoretical clues of microphase separation in block copolymers.<sup>88</sup> This physical phenomenon is at the origin of the crosslinking in most TPEs. The “hard segments” (*e.g.* styrene for SBS triblocks) behave at the same time as physical crosslinks and fillers, providing good elasticity, structural strength and also solvent resistance in some cases. The architectures of the main industrial TPEs are schematized in Figure 3.

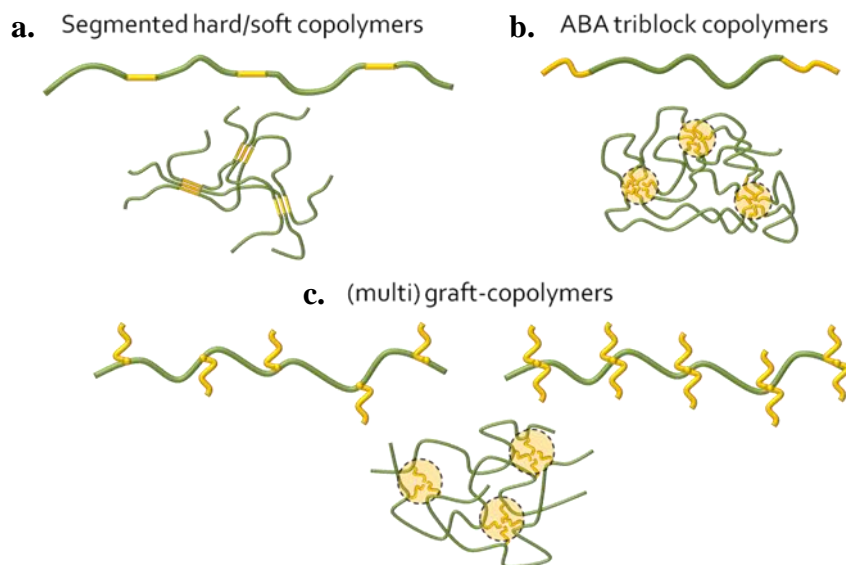


Figure 3. Architecture of the main types of industrial TPEs.

Sustainable ABA triblock copolymers were recently obtained with plant oil as middle block and styrene as end blocks.<sup>89</sup> This strategy is all the more interesting because the obtained recyclable material is partially bio-based.

Dynamic vulcanization, leading to TPVs, is the vulcanization of rubber during its melt-mixing with a plastic material. This mixing produces a very fine dispersion of rubber in the minor plastic phase. Both materials have to be compatible (to allow the dispersion), but not thermodynamically miscible to maintain separate  $T_g$ s and keep both the rubber softness and elasticity as well as the plastic high crystallinity or high  $T_g$  for structural integrity. The finer the dispersion, the better the mechanical properties. Mechanical properties of classically crosslinked rubbers may even be reached if the dispersion is fine enough.<sup>90</sup> A very high number of materials is theoretically achievable thanks to the variety of existing rubbers and plastics, but in practice only relatively few combinations have found industrial relevance. Good examples are crystalline polyolefin plastics mixed with crosslinked polyolefin rubber (*e.g.* polypropylene with ethylene-propylene diene terpolymer (EPDM)).<sup>91</sup> The vulcanization system of the rubber should leave the plastic phase unchanged. Classical sulphur vulcanization is often chosen. In view of the above described morphology of TPVs, an interesting question arises: “why not use GTR to produce TPEs?” This could be a very efficient recycling process for scrap rubber as TPVs are useful and highly-priced industrial materials. As seen in the previous section, the main problem when mixing GTR with virgin matrices is compatibility, the GTR has to be at least partially devulcanized to be more compatible with the plastic matrix. Another possibility is to add virgin rubber to the mix to help compatibilization. Karger-Kocsis and co-workers described TPVs based on low density polyethylene, rubber (NR, SBR, or EPDM) and GTR, dynamically vulcanized by sulphur or peroxide.<sup>92</sup> They showed that some crosslinks between the virgin rubber phase and GTR did help the compatibility and resulted in improved elasticity and mechanical properties.

TPUs are also an important class of TPEs. They are well-known and used in many industrial applications including automobile, footwear, cell phones, packaging, building and medical equipment.<sup>93, 94</sup> They are usually synthesized by addition reactions between a polyol (*e.g.* an aliphatic linear polyether terminated by hydroxyl functions at both ends) and a diisocyanate (most of the time aromatic molecules like methylene diphenyl diisocyanate, which is commonly used for the industrial production of TPUs) to form a prepolymer. This prepolymer is further reacted with a chain extender (usually diols or diamines resulting in urethane or urea bonds) or a chain capper (mono-functional species).<sup>95-97</sup> The chain extenders are called crosslinkers when they are tri-functional, but in this case the resulting material is a thermoset and no longer a TPE. Industrially, the syntheses are carried out under bulk conditions, requiring a full control of viscosity to avoid premature aggregation or crystallization. An example of industrial synthesis is given in Figure 4.

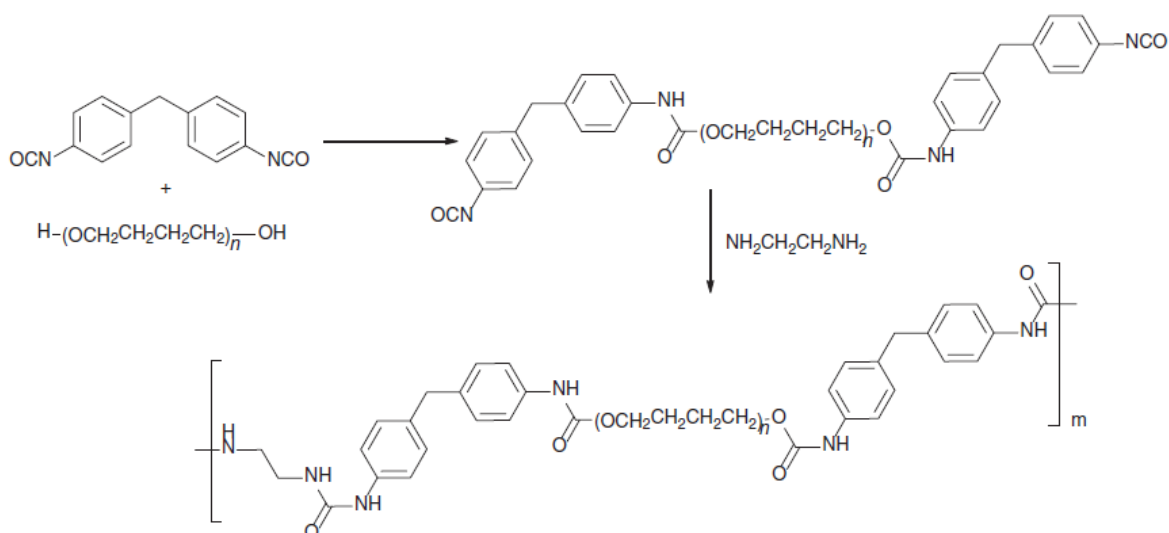


Figure 4. Industrial one-pot synthesis of the industrial polyurethane Spandex™ (adapted from reference<sup>95</sup>).

This step-growth poly-addition results in alternating hard and soft domains. Indeed, the polyols are low  $T_g$  material and bring flexibility to the final polymer, constituting the soft blocks. Conversely, the aromatic diisocyanates, linked with small chain extenders, are more rigid and the resulting portions of chain act as hard segments. The incompatibility between the soft and hard segments is at the origin of a microphase separation. The hard segments self-assemble and crystallize, creating physical crosslinks (Figure 3a). The synthesis conditions have an influence on the phase segregation behaviour, and thus on the properties of the final material, making them an important subject of study.<sup>98-100</sup>

Inspired from TPUs, thermoplastic polyamides can be synthesized easily.<sup>101</sup> Rabani *et al.* showed that the polyamide elastomers had good dynamic and tensile properties, comparable with TPUs. The amide functions are more thermally stable than urethane bonds, and this could be a solution to the tendency of polyurethane to degrade upon heating.<sup>102</sup>

A thermally-healing nitrile rubber (NBR) was obtained by simply mixing NBR with hyperbranched polyethylenimines (PEI) and urea-functionalized PEI amphiphiles.<sup>103</sup> Healing efficiency of 44 % was achieved after annealing for 12 h at 100 °C. The micro-separated morphology of the blends and the migration of PEI were responsible for the observed healing. No backbone modification was required, making this approach industrially attractive.

Crystallization can be a driving force for phase separation and physical crosslinking. In the case of TPU materials, crystallization of hard segments occurs and those segments

segregate into hard domains.<sup>93</sup> In a systematic study of TPVs, Coran and Patel showed that the best properties were obtained with highly crystalline plastics.<sup>104</sup> Classical ABA triblock TPEs use glassy polystyrene as the A hard block and the physical crosslinks result only from incompatibility with the soft blocks and formation of relatively pure domains of the high  $T_g$  polymer that act as physical crosslinks. However, A blocks can also be selected among crystallizing polymers. In this case, the crosslinking is provided by crystallization. Incompatibility between the soft and hard blocks is no longer necessary resulting in lower melt processability and even solvent-resistance in some cases.<sup>105</sup> Crystalline ABA triblocks TPEs were developed using for example isotactic polystyrene as crystalline A blocks,<sup>106</sup> or by combination of soft poly( $\epsilon$ -caprolactone-stat-D,L-lactide) blocks and hard crystalline poly(L-lactide) blocks, which resulted in biodegradable TPEs.<sup>107</sup> More complicated structures with composite crystalline-glassy side blocks were also reported to combine the advantages from both types of A blocks.<sup>108</sup> Crystallization is not limited to the main chain, and side chain crystallization can be used to produce thermoplastic elastomers. Elastomeric materials were obtained by synthesis of polyolefin graft copolymers with crystallizable isotactic polystyrene side chains.<sup>109</sup> Those TPEs showed improved heat distortion temperatures thanks to the rigid PS side chains that melted above 200 °C.

TPEs are reprocessable and healable with temperature. Such trigger can be an advantage but also a drawback in the sense that healing cannot occur without an external stimulus. Self-healing materials exhibiting autonomous ability of repairing have emerged and appear of growing importance in the field of elastomers. However, existing self-healing supramolecular materials are intrinsically limited by the compromise between self-healing efficiency and good mechanical properties. Guan and co-workers tackled this problem by the introduction of hydrogen bonds in the soft segments of conventional hard-soft multiphase TPEs.<sup>110</sup> A brush-like architecture was first chosen with a hard polystyrene backbone grafted with soft polyacrylate amide. A modified styrene block copolymer was also synthesized by introduction of a quadruple hydrogen bonding moiety inside the soft block chain.<sup>111</sup> The resulting supramolecular TPE showed good mechanical and self-healing properties at room or mild temperatures (it could recover more than 90 % of the stress and 75 % of the strain at break after healing for 18 h at 45 °C). Hydrogen bonds were also introduced in the hard phase of TPEs,<sup>112</sup> but this did not lead to self-healing properties.

More complex functional materials can be obtained that respond to stimuli as light for example. Basing them on the same hard and soft block architecture can allow additional good recycling properties.<sup>113</sup>

✓ *Ionomers*

*Ionic interactions* generate dynamic bonds that are able to undergo selective breaking and reformation. Ionomers are a class of polymers that contain small amounts (up to 15 mol %) of ionic groups neutralized with a metal ion, pendant from or incorporated into a hydrocarbon backbone.<sup>114-116</sup> These ionomers are used industrially for shoe making or food packaging for example, due to their interesting combination of properties such as high transparency, toughness, flexibility, adhesion and oil resistance.

The presence of strong intermolecular ionic interactions is the driving force for the organization of the ionic groups in multiplets and clusters and induces microphase separation. The melt processability of ionomers is due to the thermo-labile nature of the ionic crosslinks: the ionic pairs inside the aggregates gain some mobility with temperature; this is the so-called “ion-hopping” mechanism originally proposed by Cooper.<sup>117</sup> Therefore, when based on rubbery low  $T_g$  polymers, ionomers behave like TPEs if the ionic associations are sufficiently weakened at the processing temperature. Among the main types of ionic elastomers are rubber ionomers (mainly from sulphonated and carboxylated rubbers), block copolymer ionomers and ionomeric polyblends (*e.g.* blends of rubber ionomers with different ionomeric plastics based on polyethylene or polypropylene). One example is the metal-neutralized sulphonated EPDM.<sup>118-120</sup> The addition of ionic crosslinks to this material leads to very good mechanical properties comparable to standard vulcanized EPDM in some cases. Lundberg and Makowski have shown that the ionic associations are much stronger in sulphonated ionomers than in their carboxylated analogues.<sup>121</sup> This explains the good properties, but also results in high melt viscosities (2-3 orders of magnitude higher than for carboxylated ionomers). However, sulphonic acid groups are sensitive to high temperature. To avoid degradation, sulphonated ionomers have to be fully neutralized, a disadvantage that explains why carboxylated ionomers are usually preferred.

TPEs can be obtained from graft copolymerization of hard block monomers such as styrene onto natural rubber. Phase separation of this glassy polymer covalently bonded to NR can provide a thermoplastic elastomer.<sup>122</sup> Some authors have reported on thermoplastic ionomers based on styrene-grafted NR, further modified by sulphonation of some of the aromatic rings.<sup>123</sup> The addition of ionic groups improves the tensile strength by a factor of 10, and the resulting material is shown to be completely reprocessable for at least 3 cycles without any loss of mechanical properties.

Metal ions are used to neutralize ionomers. Ibarra *et al.* studied the effect of different metallic oxides on the formation and physical properties of a carboxylated nitrile rubber

(xNBR).<sup>124, 125</sup> They showed that magnesium oxide was able to neutralize xNBR efficiently and gave better mechanical properties than other metallic oxides, *e.g.* calcium oxide, because of the slight reinforcing effect of the former. Goossens, van der Mee and co-workers also showed that the neutralizing cation highly affects the final morphology and properties of the TPE.<sup>126</sup> For example in a maleated EPM rubber, potassium cation ( $K^+$ ) leads to a better phase separation than zinc ( $Zn^{2+}$ ). As a result, the K-ionomers exhibit better mechanical properties. The balance between the molecular weight of the polymer and the grafting density of ionic groups allows for the control of TPEs processing properties.

More recently, Potier *et al.* defined a new family of ionomers by the use of metallic oxo-clusters as crosslinking points.<sup>127</sup> The copolymerization of readily available monomers (n-butyl acrylate) with organic-inorganic nano-building blocks yields elastomeric materials. These networks can be reshaped and fully reprocessed through dynamic bond recombination, lengthening their cycle of life. Interestingly, they also show very good self-healing properties at room temperature.

Ionic liquids (ILs) have been getting more and more attention in the past few years for their potential as green solvents. Their unique properties, such as chemical and thermal stability, low saturated vapour pressure, non-flammability, and good ionic conductivity make them attractive both for the industrial and academic fields for a wide variety of applications. A new kind of thermoplastic elastomer was reported using poly(vinyl alcohol) (PVOH) and a high-melting IL.<sup>128</sup> The IL played a dual role of good solvent and physical junction promoter. The resulting material could be compared to a physical PVOH gel, but the IL solvent was highly non-volatile and had a high melting point, giving rise to stable but reprocessable solid-like elastomers.

#### ✓ *Hydrogen bonds*

Among all supramolecular interactions, *hydrogen bonds* are quite weak (up to  $10 \text{ kcal.mol}^{-1}$ ). Nevertheless, they are extensively used in the field of dynamic elastomers.

The first approach to create reversibly crosslinked elastomers thanks to hydrogen bonds was to graft hydrogen bonding moieties onto existing rubbers. For example, the modification of polymers and copolymers of 1,3-dienes (derivatives of butadiene or isoprene rubbers) through reaction with triazoline diones (Figure 5) yielded hydrogen bonding thermoplastic elastomers.<sup>129</sup>



TPEs. The material could furthermore be reshaped 10 times without any loss of properties making it environmentally friendlier than sulphur-cured NR. Cleavage of the hydrogen bonds occurs around 185 °C, offering a wide temperature range for applications. This chemistry was also adapted to other rubbers with the same success. For example, modified EPM showed very good tensile and recycling properties.<sup>136</sup> A modified polyethylene-octene semi-crystalline elastomer<sup>137</sup> and a plastic/rubber blend<sup>138</sup> were also provided with thermal reparability and recyclability.

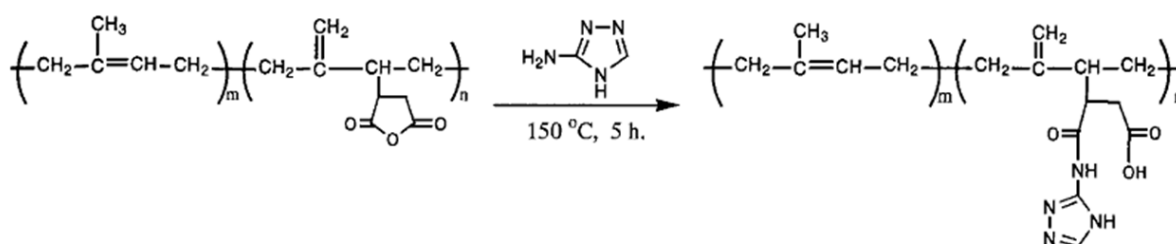


Figure 6. Modification of polyisoprene to graft a six-point hydrogen bonding unit (from reference<sup>135</sup>).

A hydroxy-telechelic poly(ethylene butylene) of low molecular mass was crosslinked by cooperative end-to-end and lateral hydrogen-bonding motifs.<sup>139</sup> The combination of directional strong end-to-end ureido-pyrimidinone associations with lateral bonding of urea or urethane groups (Figure 7a) gave rise to aggregation of end groups in long fibres (Figure 7b). With this design, a low molecular weight polymer was shown to exhibit elastic properties (ultimate strain and strength up to 220 % and 5 MPa) and recyclability.

Silicon elastomers, *e.g.* polydimethyl siloxane (PDMS), are used in various applications ranging from micro-fluidics to food or medical purposes. Their very low  $T_g$  makes them attractive candidates to obtain self-healing ability at room temperature. Roy *et al.* reported an easily synthesized tris-urea-based motif giving rise to six potential hydrogen bonds, that was used to crosslink PDMS.<sup>140</sup> The resulting materials showed good self-healing properties, but were not elastic enough to be tested in tensile tests. Colombani *et al.* reported a hydrogen-bonded TPE obtained by functionalization of PDMS with urea or bis-ureas.<sup>141</sup> The modified PDMS showed good mechanical properties at room temperature, easily tunable thermo-mechanical properties, and could still be processed at higher temperatures. Self-healing properties were not tested.

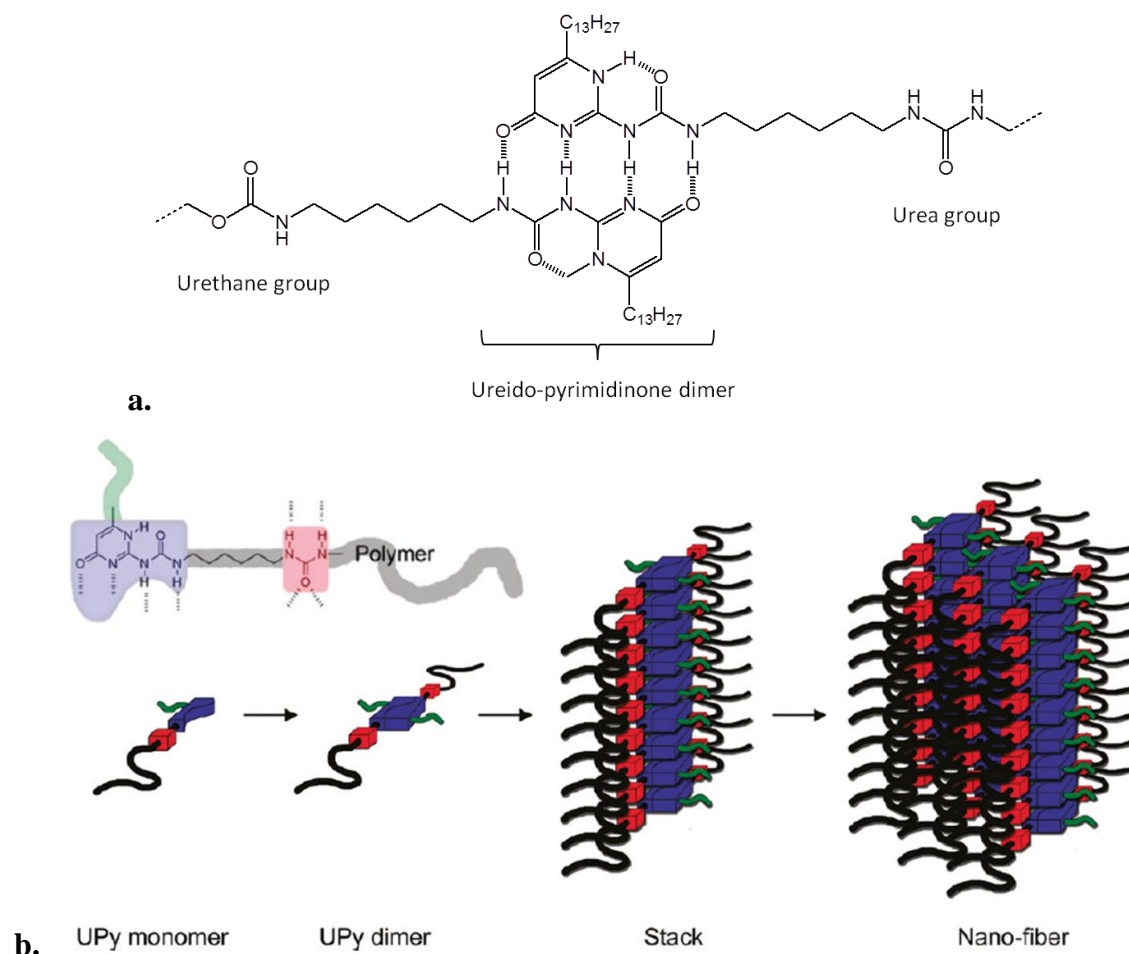


Figure 7. **a.** Strongly dimerized ureido-pyrimidinone units with lateral hydrogen bonding urea and urethane groups. **b.** Organization into fibres (adapted from reference<sup>142</sup>).

A completely different approach to achieve dynamic elastomers was proposed by Leibler and co-workers.<sup>65</sup> The concept was based on the supramolecular assembly of hydrogen bonding small molecules.<sup>143</sup> The main problem for producing rubber-like properties from an assembly of small molecules is the potential crystallization. To overcome this major issue, Leibler *et al.* proposed using mixtures of different hydrogen bonding units based on dimeric and trimeric fatty acids. The different molecular architectures hampered crystallization, and macroscopic phase separation of different species was prevented relying on entropy of mixing and directional specific interactions (Figure 8). With this design, the obtained material is a self-healing supramolecular polymer presenting rubber-like properties. The material was plasticized with dodecane to lower the glass transition temperature and enable elastomeric characteristics. Its properties resembled those of soft rubbers with small residual strains and good elongation ratios. But in addition, it was fully processable by heating

and showed very good self-healing properties at room temperature. The success of this new approach was highly linked to the control of molecular architecture (variety, size, and distribution of the small molecules) and to the use of strong hydrogen bonding interactions.<sup>144-148</sup> The self-healing behaviour of hydrogen bond-based systems is strongly affected by the fracture process. Indeed, damage processes create a high number of available hydrogen bonds. However if the two fractured surfaces are not put into contact rapidly, the hydrogen bonds recombine with each other in each separate piece and the self-healing efficiency decreases. Tack-like experiments were used to explore the self-healing activation and deactivation through the effect of weighting time and temperature.<sup>149</sup> This new concept of reversible association of small molecules to make self-healing rubbery materials was adapted to PDMS-based materials.<sup>150</sup> This allowed lowering the  $T_g$  of the final material without the need for a plasticizer. Rubber-like properties as well as self-healing properties were obtained at room temperature.

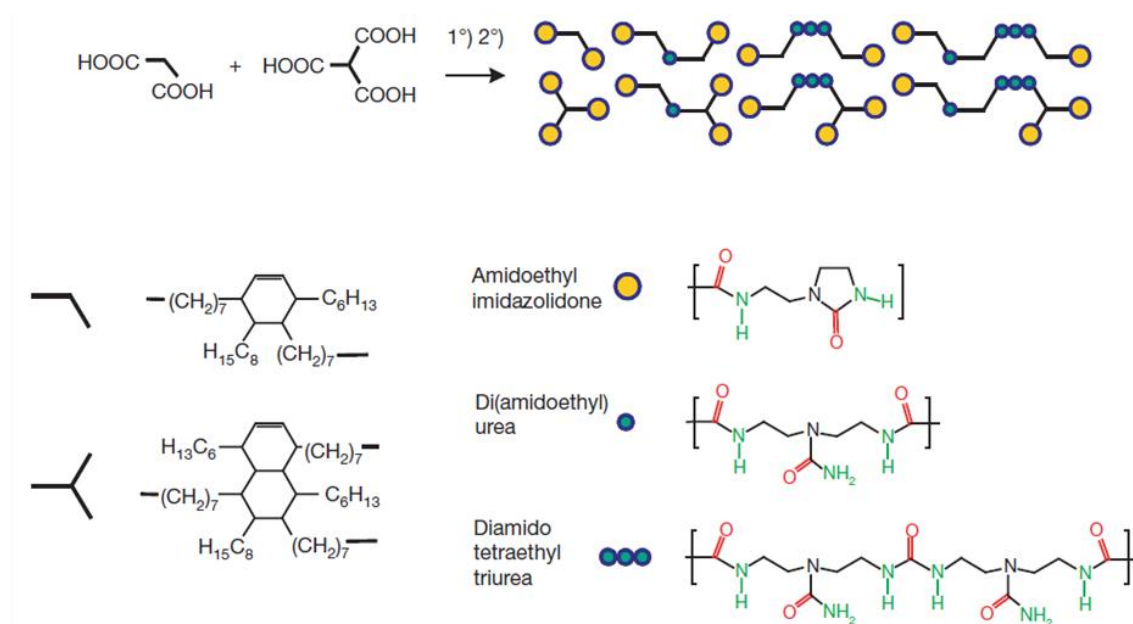


Figure 8. Design and chemistry of a self-healing rubber based on small molecules (from reference<sup>65</sup>).

Combinations of physical bonds can also be used for the dynamic crosslinking of elastomers. Thermoplastic elastomers based on maleated ethylene/propylene copolymers crosslinked by a combination of hydrogen-bonding and ionic interactions were reported.<sup>151</sup> Tensile properties and elasticity were improved by hydrogen bonds and further by the additional ionic bonds.

✓ *Other non-covalent interactions*

Metals can also be used for crosslinking of elastomers through the creation of *coordination bonds*. Those bonds are among the highest energy non-covalent bonds (around 50-80 kcal.mol<sup>-1</sup> compared to 15-50 kcal.mol<sup>-1</sup> for ionic bonds and up to 10 kcal.mol<sup>-1</sup> only for hydrogen bonds). In the case of NBR for instance, the C≡N group becomes a ligand when in contact with the appropriate metal (*e.g.* copper). This was used in a blend of NBR with poly(vinyl chloride) (PVC).<sup>152</sup> The blend was crosslinked with anhydrous copper sulphate (CuSO<sub>4</sub>) particles that also acted as fillers. The *in situ* crosslinking reaction, *i.e.* the coordination between copper and the nitrile groups of NBR occurred during hot pressing of the material, without the need for a solvent. The resulting material showed excellent mechanical properties. PVC behaved as a macromolecular plasticizer improving the fluidity of the system, the mobility of the NBR chains and thus the coordination efficiency. Moreover, PVC was also known to improve ozone and chemical resistance, as well as thermal ageing of NBR. Other authors also used these non-covalent coordination crosslinks to create a reprocessable xNBR with improved thermal stability and compression set.<sup>153</sup> In xNBR, two types of bonds can form upon addition of copper sulphate: ionic bonds, by reaction with carboxylic acid functions, and coordination bonds with the nitrile groups.

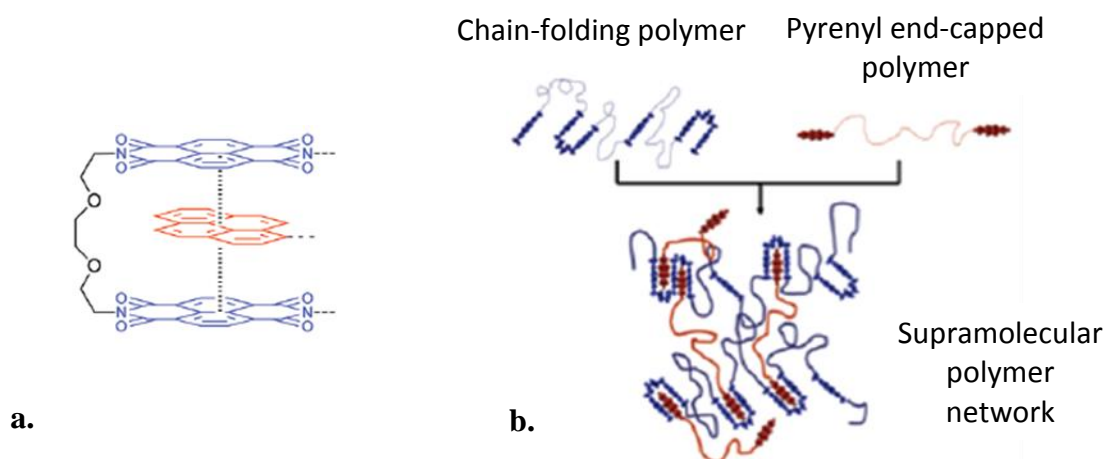


Figure 9. **a.** Proposed structure for the  $\pi$ -stacking interactions; **b.** Principle of the  $\pi$ -stacking network. (Adapted from reference<sup>154</sup>)

The  $\pi$ -stacking occurring between aromatic rings is among the weakest non-covalent interactions. Healable polymers based on  $\pi$ -stacking interactions have been reported.<sup>155</sup> This

concept was also adapted to rubbery materials by Rowan and co-workers, who reported a thermoplastic elastomer made from a blend between a chain-folding aromatic polyimide and a telechelic polyurethane bearing pyrenyl end groups.<sup>154</sup> Compatibilization of the blend was achieved through  $\pi$ -stacking between pyrene and naphthalene (Figure 9). This material presented a nanophase-separated morphology and was healable at high temperature (most of the properties were recovered after 4 h at 100 °C). The strength and healability of this blend was due to the combined effects of  $\pi$ -stacking and hydrogen bonding interactions.

*Host guest interactions* have been shown to be efficient reversible crosslinkers of hydrogels.<sup>156, 157</sup> The originality of these interactions over other supramolecular associations is their selective complementarity. A highly elastic hydrogel, crosslinked by host-guest interactions using cyclodextrin and adamantane as host and guest molecules respectively, was reported (Figure 10). Hydrogels may in some sense be compared with elastomers. We feel that this supramolecular chemistry should have some potential in the field of rubber recycling, especially now that these interactions were reported to operate in bulk to help blending immiscible polymers.<sup>158, 159</sup>

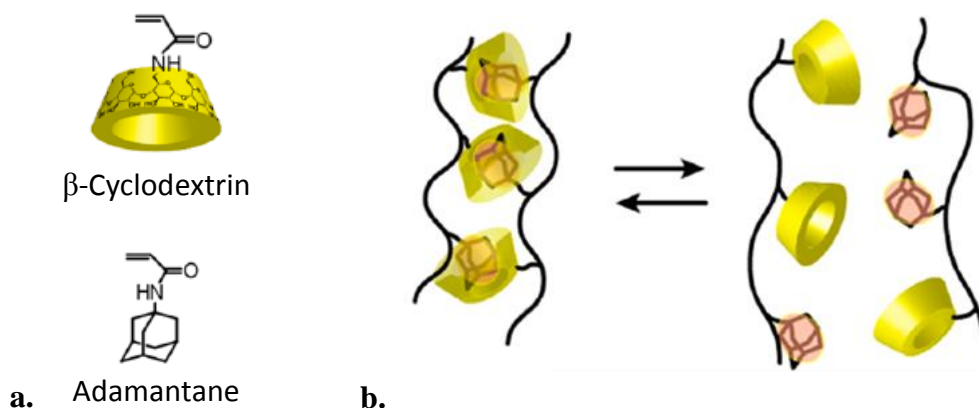


Figure 10. **a.** Monomers bearing host and guest molecules used to create the reversible gel;  
**b.** Reversible host-guest interactions. (Adapted from reference<sup>157</sup>)

*Metallophilic interactions* are metal-metal interactions energetically similar to hydrogen bonds in the case of gold, and slightly weaker for other metals. Odriozola and co-workers took advantage of these interactions to generate dynamically crosslinked elastomers.<sup>160</sup> A thiol-functionalized polyurethane was crosslinked with a silver salt producing Ag(I)-thiolate

argentophilic associations. This material is processable at room temperature and show reasonable elastomeric properties.

✓ *Fillers as dynamic crosslinkers*

To attain the mechanical properties required for industrial applications, elastomers are commonly charged with fillers. Crosslinking elastomer through reversible interactions of the chains with the filler particles (Figure 11) can potentially combine full reprocessability and recycling properties, with good mechanical properties.

Silica, one of the most common fillers, was used by Abetz and co-workers for their previously cited hydrogen-bonding polybutadiene rubber.<sup>161</sup> The surface of the silica nanoparticles was modified to favour hydrogen bonding between the polymer and the silica particles. These filler-matrix interactions helped to get a better dispersion of silica without the use of coupling agents and reduced the Payne effect. The mechanical properties of the composites can be controlled by the degree of rubber modification or the silica loading through the competition and synergy between filler-filler, filler-rubber and rubber-rubber hydrogen bonding interactions. The crosslinking of brominated isobutylene *para*-methylstyrene was also achieved through interactions with silica particles.<sup>162</sup> The tensile strength and degree of bound rubber was found comparable with those of conventionally cured elastomers, but the materials could still be reprocessed by roll milling without much loss in properties (0-8 % loss in ultimate strain and stress). Like in the first example, the concept provides good filler-rubber interactions, inhibition of filler-filler interactions and thus good filler dispersion. According to the author, the interaction could be a nucleophilic substitution reaction between benzylic bromide of the polymer and the silanol groups on the particles. However, such a substitution should lead to non-reversible ether bonds, which is somehow contradictory with the thermoplastic behaviour of the material.

Metal particles are also of interest in this matter. Silver nanoparticles for example, known for their antibacterial activity, can be used to invent materials for biomedical applications. Ag particles were used to crosslink telechelic thiol-functionalized liquid polyisoprene through silver-thiolate coordination bonds, resulting in a thermoplastic elastomer with antibacterial properties.<sup>163</sup> Room temperature self-healing properties could also be obtained through the same interactions.<sup>164</sup> Martin *et al.* showed that in a silicon oil based nanocomposite, the thiolate bonds on the silver nanoparticle surface were in constant exchange at room temperature, allowing for self-healing of the material.

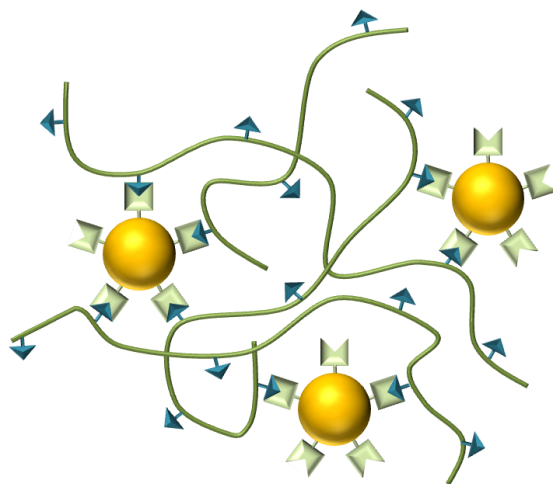


Figure 11. Filler particles as dynamic crosslinkers.

Graphene oxide was also used as a dynamic crosslinker through hydrogen bonding interactions.<sup>165</sup> The advantages of this filler are that it is highly reinforcing and can be used in very low concentrations (< 2 wt%). This permits to preserve the self-healing efficiency of the supramolecular rubber that is usually reduced a lot by the use of fillers. The major drawback of silver or graphene oxide is the cost of the nanoparticles.

#### 1.4.2. Covalent reversible chemistry

*Non-covalent interactions* present the advantage of easy reversibility thanks to their low bond energy. Yet, physically crosslinked materials hardly succeed in equalling covalently bonded elastomers in terms of thermo-mechanical properties. To reach high tensile strength, elasticity or low compression set, covalent crosslinks are undoubtedly more favourable. However, covalent chemistry is inconsistent with recycling, unless the covalent crosslinks are reversible bonds.

##### ✓ *Diels-Alder chemistry*

The Diels-Alder (DA) reaction is an organic chemical reaction between a conjugated diene and an activated alkene referred to as dienophile to give a cyclic product called an adduct (Figure 12a).

This reaction can be reversible with a good choice of reactants under certain conditions of temperature. For example, the reaction between furan (the diene) and maleimide (the dienophile) is known to be an equilibrium in favour of the adduct formation under 60 °C and of its dissociation above 100 °C (Figure 12b). The reverse reaction is known as retro-Diels-

Alder reaction. This reversibility is particularly interesting for the crosslinking of elastomers in that it is an addition and not a condensation process. Therefore, it is a self-contained dynamic system: all atoms of the starting components will be found in the product, nothing is consumed and no by-products are formed during the process. Moreover it does not require the presence of a catalyst.

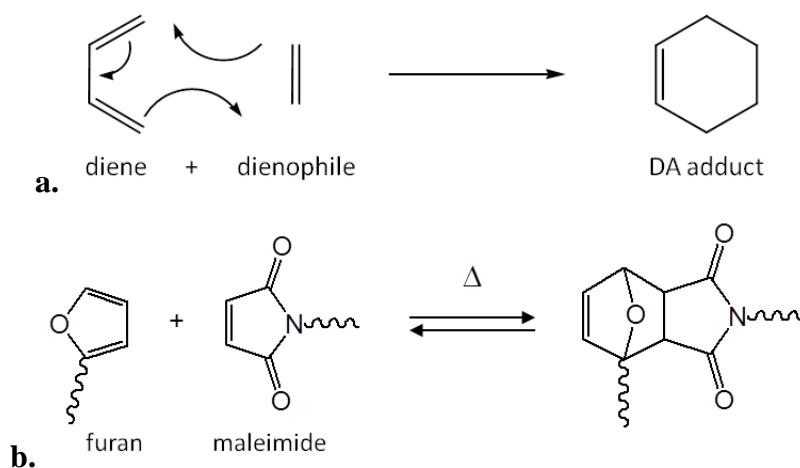


Figure 12. **a.** Diels-Alder reaction between a diene and a dienophile. **b.** Example of the furan/maleimide pair.

DA reaction was extensively studied for the recycling of thermosets, and some examples of elastomeric materials were also developed, most of them based on the classical furan/maleimide pair. A classical approach is the combination of a functional polymer (either a polymeric diene or dienophile) with a small bifunctional molecule (bis(maleimide) or difuran) as crosslinker. Following this approach, acrylic or siloxane backbones were functionalized respectively with pendant furan and maleimide moieties and each resulting polymer was mixed with the complementary bifunctional small molecule (or oligomer, Figure 13).<sup>166</sup> This resulted in fully recyclable low  $T_g$  elastomers. The recycling process occurred by complete thermally induced de-crosslinking of the networks, reverting them into their thermoplastic precursors at high temperature. Another approach was the reaction of linear macro-monomers with di- and tri-functional linkers by DA reaction.<sup>167</sup> The reversible bond is not found only at crosslink points as is the previous example but also in the main chain. The obtained networks showed elastomeric properties and full recyclability upon heating without any loss in elasticity or molecular weight.

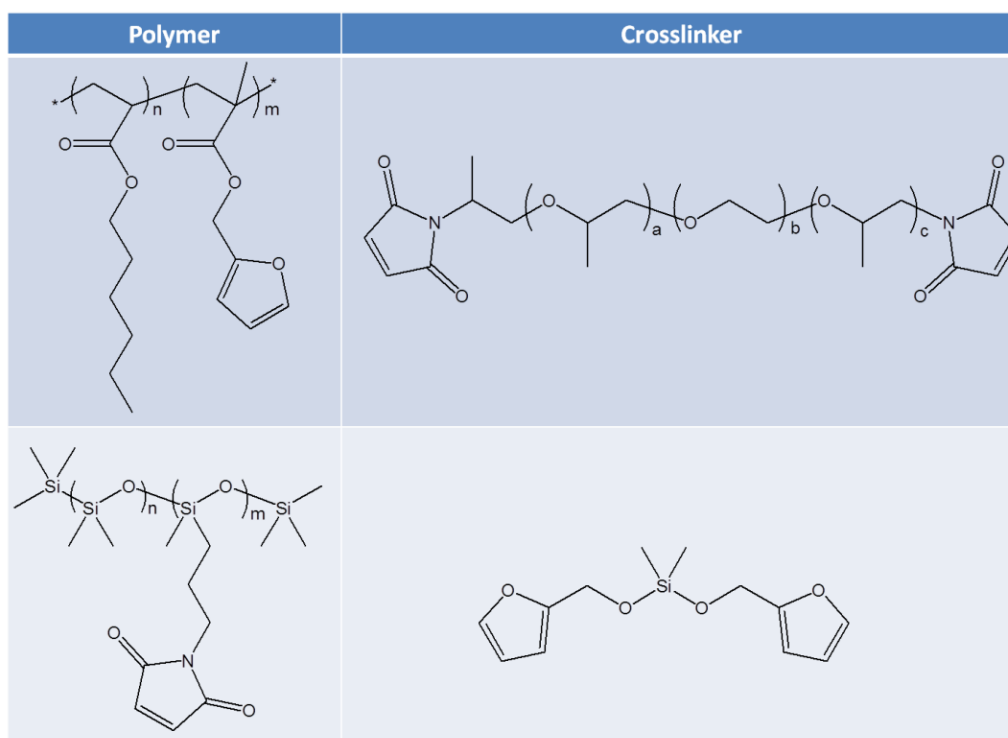


Figure 13. Functional polymers and corresponding crosslinkers of reference<sup>166</sup> for the synthesis of reversibly crosslinked elastomers.

More recently, Gandini and co-workers successfully applied DA chemistry to the crosslinking of poly(butadiene), towards the aim of creating recyclable tires.<sup>168</sup> Their strategy was the functionalization of polybutadiene with furan groups and its crosslinking using bis(maleimide) small molecules. The same material was also reported by another group who showed that the mechanical properties were almost the same before and after reprocessing.<sup>169</sup> However, the crosslinking reaction proceeds in solution, which is industrially not relevant. According to reference<sup>168</sup> Gandini and co-workers are now working on transferring that chemistry to other industrial elastomers like NR. Reversible DA chemistry was also successfully adapted to the crosslinking of maleated EPM rubber.<sup>170</sup> The resulting material could be cut and compression moulded back to the original shape recovering most of its mechanical properties. However, in both of these modified rubbers, the crosslinking reaction proceeds in solution, which is industrially not relevant.

As shown in the previous examples in the case of the furan/maleimide pair, the retro-DA reaction is often activated by high temperatures. Lehn and co-workers reported the occurrence of this reaction at room temperature with a special combination of diene and dienophile (Figure 14).<sup>171</sup> These specific moieties were used to obtain room temperature

dynamic elastomers based on polyethylene glycol.<sup>172</sup> The resulting networks can adapt in ambient conditions, allowing the relaxation of stress and enabling the self-healing of the material.

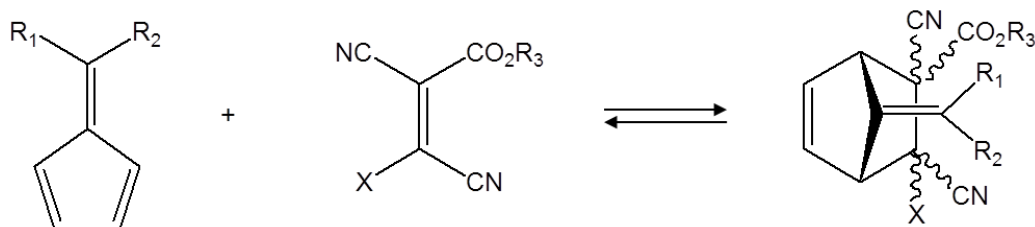


Figure 14. Reversible Diels-Alder reaction described by Lehn and co-workers.<sup>171</sup>

#### ✓ Sulphur chemistry

Sulphur chemistry is a rich tool for material design towards many applications.<sup>29</sup> Reversibly crosslinked elastomers using sulphur chemistry have been widely reported, activated by different triggers.

Scott *et al.* synthesized rubbery networks presenting glass transitions around  $-25\text{ }^{\circ}\text{C}$  through the thiol-ene reaction of small molecules in presence of a photo-initiator (Figure 15a); varying concentrations of a ring-opening monomer (MDTO) were added to include allyl sulphides in the network.<sup>173</sup> The resulting material could undergo reversible photo-mediated backbone cleavage by addition-fragmentation chain transfer at room temperature thanks to the residual photoinitiator (Figure 15b). The chemistry of the networks was unchanged by this radical process, and so was the network connectivity. However, the processability of the materials was limited by termination reactions and the presence of the photo-initiator that is consumed for radical generation. Other examples of photo-stimulated reshuffling reactions were reported by Matyjaszewski and co-workers. A low  $T_g$  ( $-50\text{ }^{\circ}\text{C}$ ) polybutyl acrylate was reversibly crosslinked with trithiocarbonate units. The resulting material was able to self-heal several times by UV irradiation and could be reprocessed through macroscopic fusion of separate pieces.<sup>174</sup> Dynamic polyurethane networks based on the reshuffling of thiuram disulphide units also showed self-healing ability under the stimulation of visible light in air, at room temperature and without solvent.<sup>175</sup>

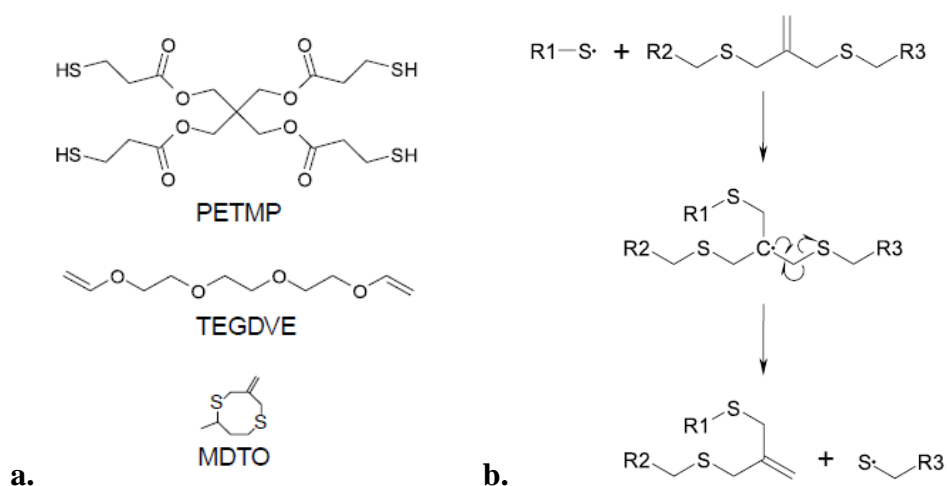


Figure 15. **a.** Monomers used by Scott *et al.* to produce the rubbery networks; **b.** Addition-fragmentation chain transfer enabling the exchange of crosslinks. (Adapted from reference<sup>173</sup>)

Temperature-controlled reversibility was reported by Goossens and co-workers in a disulphide-containing epoxy resin crosslinked with tetra-functional thiols, yielding elastomeric networks having glass transitions around  $-35\text{ }^{\circ}\text{C}$ .<sup>176</sup> These materials showed complete self-healing after one hour at  $60\text{ }^{\circ}\text{C}$ . The healing mechanism was first ascribed to the exchange of disulphide groups, but in a subsequent article, the authors showed that these disulfide exchanges were longer than the measured healing time.<sup>72</sup> They concluded that thiol-disulphide exchanges were responsible for the adaptability of the network. When aromatic disulphides are used, sulphur metathesis can occur at room temperature. Indeed, poly(urea-urethane) elastomers crosslinked by aromatic disulphide bonds showed intrinsic self-healing properties at room temperature.<sup>70</sup> The dynamic process was assigned to aromatic disulphide metathesis combined with reversible hydrogen bonds. Eventually, the use of a catalyst can also be of importance as shown by Lei *et al.*<sup>177</sup> They crosslinked the same type of disulphide-containing epoxy resin used by Goossens<sup>72</sup> by trifunctional disulphide-containing thiols in the presence of a phosphine known to be a catalyst for disulphide metathesis. The resulting elastomeric network was shown to self-heal at room temperature. The process is air-resistant and allows the reprocessing and reshaping of the material. However, phosphines are also known to be efficient reducing agents for disulphides, therefore it is not really clear if the dynamic character goes through disulphide metathesis or thiol-disulphide exchanges.

Copper chloride ( $\text{CuCl}_2$ ) was very recently shown to act as an efficient catalyst for the reshuffling of sulphur-vulcanized polybutadiene networks at  $110\text{ }^{\circ}\text{C}$ , enabling the healing or reprocessing of the material.<sup>178</sup>

Our group recently reported the introduction of disulphide bonds in epoxidized natural rubber (ENR)<sup>74</sup> following a crosslinking method in which ENR was cured by carboxylic diacids through esterification reaction with the epoxy functions.<sup>179, 180</sup> This process creates  $\beta$ -hydroxy esters along the chain<sup>181</sup> and competes with classical sulphur or peroxide vulcanization usually used for the crosslinking of ENR.<sup>182, 183</sup> This crosslinking method also permitted the formation of semi-interpenetrating networks by blending ENRs of different epoxidation ratios and selectively crosslink one of the two phases.<sup>184</sup> The firstly used diacid (dodecanedioic acid) can be obtained from renewable resources,<sup>185</sup> making this system fully bio-based. By selecting a functionalized diacid containing a disulphide function in the middle of the chain, disulphide bonds could be introduced into ENR (Figure 16). The resulting networks showed some reprocessability and adhesion properties. This crosslinking process opens the way to other possibilities of dynamic linkages, as many reversible functions could be introduced *via* the diacid crosslinker.

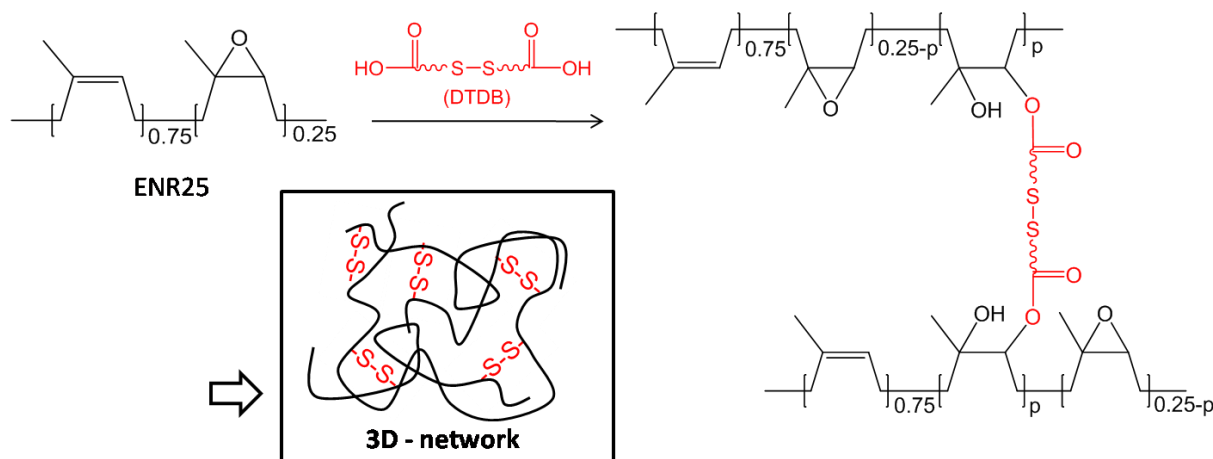


Figure 16. Crosslinking of epoxidized natural rubber by dithiodibutyric acid (from reference<sup>74</sup>).

#### ✓ Other reversible covalent bonds

As early as 1975, the recycling problem of vulcanized rubbers was perceived, and solutions proposed.<sup>186</sup> More patents were filed on the thermally reversible crosslinking of elastomers, showing the industrial importance of this matter.<sup>187, 188</sup> Making use of the reversibility of urethane bonds, reprocessable poly(urethane)s were achieved. The selected urethanes were made using the reaction between benzylic hydroxyl and isocyanate groups for their relatively high reversion onset temperature (from 140 to 180 °C). The networks can thus be used in a

wide temperature range and melt processed just as thermoplastics. High enough above the onset temperature, which depends on the exact chemistry of the components, reverse reaction of urethane bonds occurs and the material can be reprocessed. When cooled down the crosslinks reform and mechanical properties are recovered. Using urea chemistry, another group recently reported elastomers with self-healing properties: the material almost totally recovered its mechanical properties after 12 hours at 37 °C.<sup>189</sup>

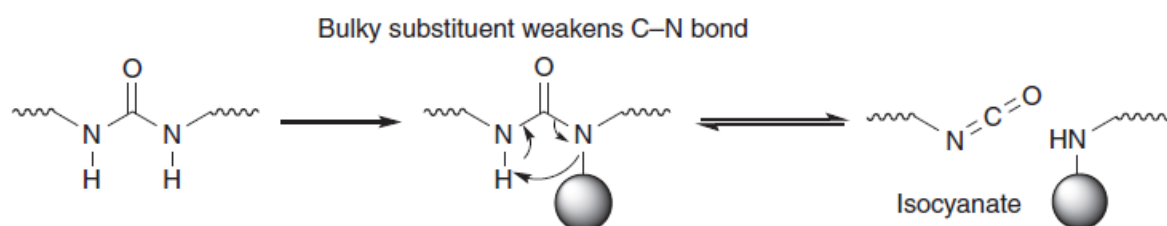


Figure 17. Reversibility of the hindered urea bond (from reference<sup>189</sup>).

The strategy relied on the fact that urea bonds bearing a bulky group on the nitrogen atom can reversibly dissociate into isocyanate and amine at low temperatures (Figure 17). Polyureas and poly(urethane-urea)s are commonly used in applications such as coatings or adhesives in which self-healing properties could be of interest. The hydrogen-bonding potential of urea bonds can also help in improving the mechanical strength. This new type of room temperature reversible urethane bonds is referred to as dynamic hindered urea bonds (HUBs).

Reversible crosslinking of silicon elastomers was achieved thanks to amine-boronate complex formation.<sup>190</sup> The dynamic B–N bond reformation occurs at 60 °C. These complexes are resistant to hydrolysis, opening their use to the crosslinking of elastomers. However, above 130 °C, a permanent change in the elastomeric structure occurs and the exchanges are no longer possible.

Making use of the reversibility of the central C–C bond in diarylbibenzofuranone at room temperature (Figure 18), Otsuka and co-workers reported a self-healing network presenting moderate elastomeric properties (ultimate properties were reported to be 0.8 MPa and 800 % elongation but the network underwent creep at room temperature).<sup>191</sup>

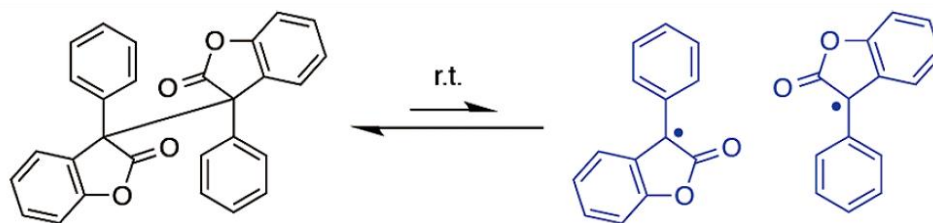


Figure 18. Diarylbibenzofuranone, equilibrium between homolytic bond cleavage and recombination at room temperature (from reference<sup>191</sup>).

Thermally reversible alkoxyamines were also used as elastomer crosslinkers.<sup>192</sup> Fission/recombination of C-ON bonds was used as reversible crosslinking for polyurethanes (Figure 19). The resulting networks could be repeatedly crosslinked and de-crosslinked at 80 °C. The major problem was that this process was sensitive to oxidation and had to be carried out under argon atmosphere. The properties of the healed samples were not the same as the virgin ones, loss in stress and strain at break occurred at each healing cycle. Dynamic exchange of alkoxyamines was also achieved at room temperature by the same authors, allowing the creation of self-healing epoxy elastomers without heating.<sup>193</sup> The homolysis temperature of the bond was lowered by tuning its electronic environment and the reaction was made oxygen-resistant by stabilizing both nitroxide and carbon radicals.

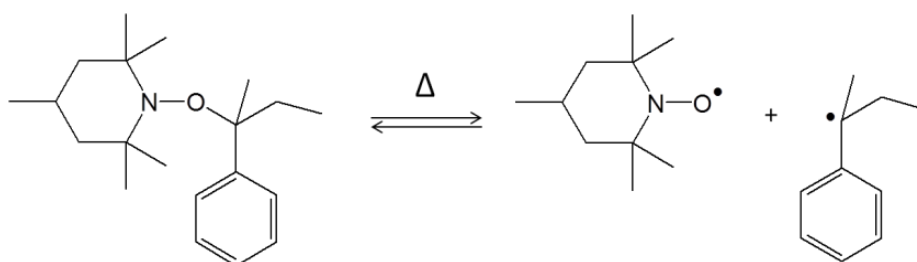


Figure 19. Reversibility of alkoxyamines junction with temperature.

Click chemistry is an easy and efficient tool very useful in macromolecular science.<sup>194</sup> Recently, Du Prez and co-workers reported the reversibility of triazolone dione click chemistry for the creation of dynamic polymer systems.<sup>195</sup> This chemistry has some potential in the field of rubber crosslinking and recycling.

### 1.4.3. Vitrimer chemistry

Vitrimers, introduced in 2011 by Leibler and co-workers,<sup>4</sup> are a new class of polymers at the same level as the two hitherto identified classes, namely thermoplastics and thermosets. The novelty comes from the fact that these chemically crosslinked networks are fully malleable and recyclable but stay insoluble in any solvent even under heating. This behaviour is essentially different from the malleability and solubility of thermoplastics on the one hand, and solvent-resistance but non recyclability of thermosets (like rubbers) on the other hand. The properties of vitrimers are a combination of the most interesting properties of the two other classes of polymers. The key to this behaviour is the use of covalent exchangeable bonds as crosslinking points (Figure 20).

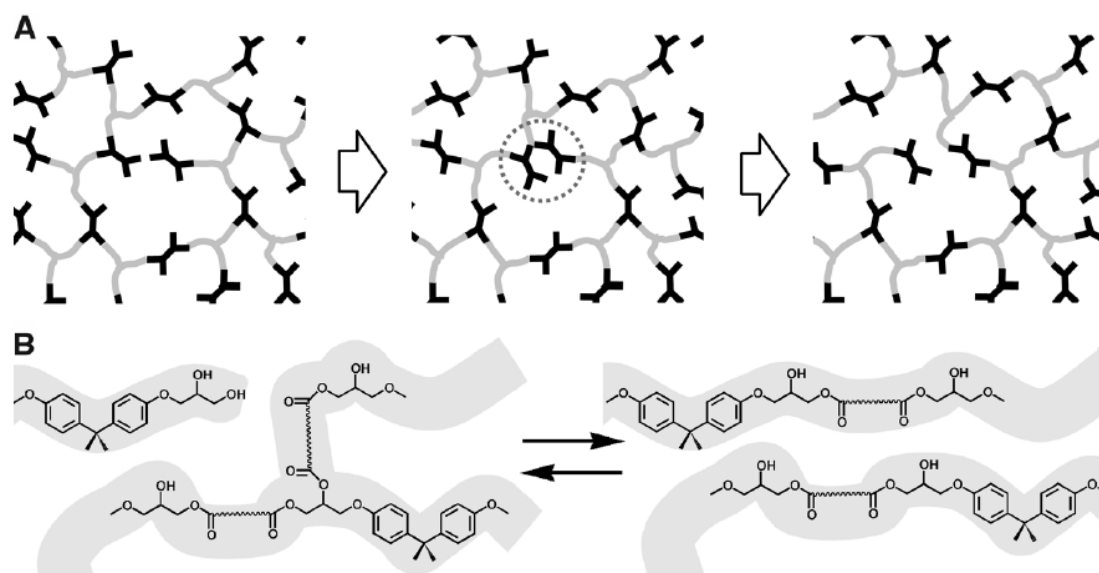


Figure 20. The vitrimer concept explained with the example of epoxy-acid resins. **A.** Topological rearrangements; **B.** Transesterification exchanges. (Reproduced from <sup>4</sup>)

Exchange reactions like transesterification,<sup>4, 64, 196</sup> olefin metathesis,<sup>69</sup> vinylogous transamination,<sup>78</sup> or transalkylation of C–N bonds<sup>79</sup> are used instead of reversible bonds. In exchange chemistry, the number of crosslinking points and the average functionality of the network remain constant, making vitrimers fully malleable and mendable but still insoluble materials.<sup>4, 64, 196</sup> They were called vitrimers because of their similarity with glass (*vitrum* in Latin). Indeed, the topology of the network is quenched by cooling, which fixes the shape of the material by slowing down exchange reactions. The vitrimer transition is thus very similar

to the glass transition but the topology of the network rather than the density of the material is quenched at the transition. A vitrimer material relaxes completely the applied stress under certain conditions (presence of a catalyst and high temperature for epoxy-acid vitrimers<sup>4</sup>), it can be reshaped and reprocessed repeatedly (in theory an infinite number of times as nothing is consumed during the process) and it is fully insoluble in any solvent even in the condition of the exchanges (*e.g.* at high temperature<sup>4</sup>).

In the field of rubbery materials, vitrimer chemistry appears as an excellent way to combine the good mechanical properties of covalently crosslinked elastomers with full recyclability. The first vitrimers were either hard glasses or elastomeric materials depending on the chemistry.<sup>4</sup> The epoxy-acid vitrimer networks show good elastomeric properties at room temperature, and become fully malleable, processable and mendable at higher temperatures.<sup>64</sup> As in the case of glass, the processability is achieved in a wide time-temperature window. The processing of these materials is thus much more flexible than in the case of thermoplastics. Moreover, the vitrimer glass transition can be tuned by the use of the proper catalyst.<sup>196</sup>

The concept of vitrimers was rapidly extended to other chemistries than transesterification<sup>197</sup> and used in the field of rubbers. Lu *et al.* reported vitrimer properties in a peroxide-crosslinked polybutadiene network by addition of an olefin metathesis catalyst (Grubbs catalyst). The resulting material was fully processable but still insoluble.<sup>69, 73</sup> This system is however different from previously described epoxy-acid elastomers because vitrimer properties occur at room temperature and are not triggerable anymore. The approach is potentially applicable to all olefin containing rubbers, which represents a lot of industrial materials (NR, SBR, etc.). However, Grubbs catalysts are very expensive, which can be a serious limitation for industrial applications. Moreover, it is likely that rubbers like NR will not maintain, after olefin metathesis, the well-defined *cis*-configuration that makes them outstanding materials. Siloxane anionic equilibration was rediscovered and pointed out as an efficient method to create healable and reprocessable elastomeric networks.<sup>198</sup> This process can be seen as a metathesis of siloxane bonds but has some limitations such as the volatility of cyclic oligomers potentially formed upon rearranging of the network.

The vitrimer chemistry was also adapted to renewable crosslinked elastomers.<sup>77</sup> Polylactide-based vitrimers containing Sn(Oct)<sub>2</sub> as transesterification catalyst were shown to exhibit remarkably short relaxation times of less than 50 s at 140 °C. However their properties after healing were not exactly the same as before (smaller strain at break), which could be due to secondary reactions.

Other vitrimer chemistries were developed without the necessity of a catalyst. New materials exhibiting vitrimer properties through vinylogous transamination were synthesized.<sup>78</sup> Even though not elastomers ( $T_g$  above 80 °C), they present very short relaxation times (85 s at 170 °C) and are made from easily accessible chemicals, opening the way to elastomeric vinylogous vitrimers. Boronic ester transesterification also was used to create dynamic elastomeric networks.<sup>199</sup> The authors interestingly showed that the small molecule exchange kinetics were transferrable to the malleability and processability of the networks, allowing their control.

Many fields of applications can benefit from the vitrimer technology. For example, Obadia *et al.* described the synthesis of ion-conducting vitrimers inspired from poly(ionic liquid)s.<sup>79</sup> The involved exchange mechanism is transalkylation of C–N bonds, a process controlled by temperature. The materials have potential as solid electrolytes such as supercapacitors, batteries, fuel cells, or separation membranes. They have elastomeric properties with a  $T_g$  around –10 °C. The liquid-crystalline elastomers described by Terentjev and co-workers are another example of the great benefits of vitrimer chemistry.<sup>200</sup> The exchangeable bonds allow for macroscopic orientation of the liquid-crystal required for reversible actuations, which otherwise is hard to achieve in practice. The resulting elastomers are reshapable like classical vitrimers. This technology could open the way to artificial muscles.

#### 1.4.4. Double networks

To always design further innovative materials, the combination of two networks composed of different types of crosslinks is an option. The interest of double networks for reinforcing gels has been widely illustrated by Gong and co-workers.<sup>63</sup> This technology was then transferred to elastomers by Ducrot *et al.*<sup>201, 202</sup> The principle of the reinforcement is the presence of at least two interpenetrated networks. One of the networks is pre-constrained by the polymerization of the other and breaks when the material is stressed. The sacrificial bonds are responsible for energy dissipation, giving rise to a substantial gain in mechanical properties. The major problem of this approach is the lack of reversibility. Once the materials have been stressed, the sacrificial bonds remain irreversibly broken. Under the maximum tested strain no other bonds are broken and the good mechanical properties are lost.

Using dynamic chemistry in double networks could enable at the same time improvement of mechanical properties and extension of the materials cycle of life. By coupling with a covalent network, the material cannot be expected to be fully recyclable. However, major improvements in mechanical and damping properties can potentially be

achieved. For example, carboxylated nitrile butadiene rubber (xNBR) was dually crosslinked.<sup>203</sup> Photochemical thiol-ene reaction was used to form chemical crosslinks and additional ionic crosslinks using ZnO permitted to improve the tensile strength of the materials. Such a double network design could also enable the healing of micro-cracks and a better compatibilization of fillers with the matrix. Montarnal *et al.* designed epoxy elastomers combining covalent bonds and hydrogen bonds that could be useful for filled materials: hydrogen bonding may improve the matrix-filler interaction, what would favorably affect the mechanical properties.<sup>204</sup>

One way to consider recycling in such a dual covalent-dynamic system is to stay under the percolation threshold of the chemical network (that is to say under the gel point). Ibarra and co-workers added covalent crosslinks to ionic thermoplastic rubbers in order to enhance the compression set and the properties at high temperature while keeping the processing properties of ionomers.<sup>205</sup> xNBR was crosslinked with both magnesium oxide (ionic crosslinks) and dicumyl peroxide (permanent crosslinks). The covalent crosslinks were shown to influence ionic aggregation: the aggregation number decreased and the number of aggregates increased with increasing crosslinker concentration. Processability was retained below a certain peroxide concentration. Small improvements were observed on some of the properties of the dually crosslinked samples (the hardness and modulus at 100 % and 300 % deformation increased), however tensile and tear strengths were negatively affected by the few permanent crosslinks.

In terms of recyclability, the combination of two different dynamic systems has much more potential. In a previous section, we reviewed some works combining two types of non-covalent bonds. For example the introduction of hydrogen bonds in microphase-separated hard/soft TPEs can provide the material with self-healing properties. The combination of ionic crosslinks with hydrogen bonds was also shown to improve mechanical properties. Those materials are fully recyclable. However, even if supramolecular bonds potentially offer self-healing properties, covalent bonds are incontestably the best type of crosslinks in terms of mechanical properties and resistance to solvents. Hence, the most favorable combination appears to be the coupling of dynamic covalent bonds with non-covalent ones. Lehn and co-workers synthesized doubly crosslinked self-healing elastomers based on PDMS.<sup>206</sup> They combined chemically reversible imine linkages with multiple hydrogen-bonded urea groups. The material exhibited properties similar to those of synthetic rubbers (*e.g.* Young's modulus) and self-healing was very efficient. The combination of hydrogen bonds and covalent bonds that become reversible only with temperature reduces the creep observed in purely

supramolecular networks. This allowed the obtaining of healable materials showing partial repair at room temperature without being subject to creep. These networks could be almost completely healed by increasing the temperature.<sup>207</sup> Guan and co-workers combined a vitrimer network by exchangeable covalent bonds with a network based on hydrogen bonds.<sup>208</sup> Their concept was the use of double dynamic crosslinking to reversibly improve the poor mechanical properties shown by existing self-healing polymers. This was made possible through the introduction of sacrificial hydrogen bonds. The reinforcement mechanism is based on energy dissipation as in Gong's double network gels. In addition, the labile nature of hydrogen bonds brings the lacking reversibility. The obtained elastomeric material was reprocessable and recyclable. To reach at the same time good self-healing, strong mechanical behaviour and solvent resistance, it is necessary to increase the number of both chemical and supramolecular bonds. However, this is limited by the functionality of monomers. Tournilhac and co-workers tackled this problem and devised a chemical platform permitting to tune the number of chemical bonds without decreasing the number of hydrogen bonds.<sup>209</sup> With this platform, many self-healing hybrid networks with tuneable properties can potentially be achieved.

Odriozola and co-workers showed that combination of two dynamic covalent networks could simply be achieved by mixing the two dynamic polymers. The thermo-mechanical blending process created a new material with improved mechanical properties and a co-continuous microstructure.<sup>210</sup>

To summarize, the relevant properties of the main new recyclable rubbers presented in this fourth section have been gathered in Table 2.

Table 2. Compared properties of the main dynamic rubbers.

<sup>a</sup>stress at break; <sup>b</sup>strain at break, HB: Hydrogen Bonds, NT: Non Tested, RT: Room Temperature

	Type of dynamic crosslinks	Base polymer	T <sub>g</sub> [°C]	σ <sub>max</sub> <sup>a</sup> [MPa]	ε <sub>max</sub> <sup>b</sup> [%]	Compression set	Healing efficiency and conditions	Ref
Vitrimers	trans-esterification	epoxy-acid thermoset resin	≈ 15	9	175	NT	100 % injection moulding at 200°C	4
	olefin metathesis	peroxide crosslinked polybutadiene	very low	0.6	80	potentially high at RT	100 % 1 h at 30°C, Grubbs catalyst	69, 73
Covalent reversible	Diels-Alder	linear macro-monomers with di- and tri-functional linkers	-34	40	700	NT	100 % rDA: 20 min at 145 °C and immediately dissolved in RT-CHCl <sub>3</sub> DA: 60 °C, 15 h	167
	dynamic hindered urea bonds (HUBs)	cross-linked poly(urethane-urea)	-52	0.93	300	NT, a priori high	87 % (strain recovery) 12 h at 37°C	189
	disulphides	Disulphide-containing epoxy resin cured with tetra-functional thiols	-35	0.5	70	NT	100 % 1 h at 60 °C	72, 176
	aromatic disulphides	polyurethane	-50	0.8	3000	potentially high at RT	97 % 24 h at RT or 150 °C, 30 bar for 20 min	70
Non-covalent	Metallophilic interactions	polyurethane	-64	0.35	120	potentially high at RT	100% hot press for 20 min, 100 °C and 30 bar or 24 h, RT and a pressure of 3 kg.cm <sup>-2</sup>	160

Non-covalent	HB and $\pi$ -stacking	polyurethane	-20	4	170	NT	95% (tensile modulus) 91% (strain) 77% (toughness) 4 h at 100 °C (same over 5 break-heal cycles)	154
	HB charges as dynamic crosslinker	Silica filled Brominated Isobutylene para-MethylStyrene	< 0	8	295	NT	$\geq 90$ % (stress and strain) remilled 5 min at 120°C and compression molded for 20 min at 180°C	162
	HB charges as dynamic crosslinker	Thiol-functionalized silicon oils	$\leq$ RT	0.3	70	potentially high at RT	100 % 24 h at RT	164
	HB charges as dynamic crosslinker	tri-fatty acids reacted with amine to form hydrogen bonding amide	[-5;9] depends on the filler content	0.26	550	potentially high at RT	98 % 1 h healing at RT	165
				0.8	200		53 % 1 h healing at RT	
	HB	Small molecules + dodecane as plasticizer	8	3.5	600	potentially high at RT	$\geq 85$ % 180 min at RT	65
	HB	polyisoprene	-60	15	600	NT no creep	Re-forming ability more than 10 times without significantly degrading mechanical properties	135
	HB	ethylene - propylene rubber (EPM)	-42.6	9.3	660	38% (70 °C, 22 h, 25 % compression )	Re-forming ability more than 10 times degrading mechanical properties	136
hybrid organic-inorganic ionic interactions	poly(n-butyl acrylate)	-49	0.2	1600	NT high at RT	75 % (strain) $\geq 60$ % (stress) 60 h at 90 °C	127	

Non-covalent	Ionomers	Maleated Ethylene/Propylene Copolymers	-50	9.9	820	15 % (23 °C) 39 % (70 °C)	100 % repeatedly compression molded into smooth and homogeneous films at 200 °C	126
	phase separation (hard/soft)	polyamide elastomers	-73	30	1200	NT 29 % tensile set (after 300 % strain)	melting above 190 °C	101
	Ionomers	zinc sulfonated styrene grafted NR	Low	7.5	200	NT	100% Mastication and moulding for 5+5 min at 150°C (upon 3 cycles of reprocessing)	123
Combinations of two types of crosslinks	phase separation (hard/soft) + HB	brush: polystyrene backbone and polyacrylate amide soft arms with HB	2-5°C (soft blocks)	0.9	1600	potentially high at RT	≥ 75 % (strain) 24 h at RT	110
	coordination + ionic bonds	xNBR	4.5	19	350	9 % (22 h at 70 °C)	NT	153
	HB + ionic bonds	Maleated ethylene/propylene copolymers (MAN-g-EPM)	-50	5.2	800	20 % (22 h at RT with 25% deformation)	remoulded several times at 80 °C	151
	olefin metathesis + HB	amide-containing cyclooctene networks by ROMP	NT	1.7	950	NT (high a priori)	100 % (stress) 90 % (strain) 90 % (toughness) 3 h at 50 °C	208
	Trans-esterification + HB	epoxy resin	12	3.1	230	NT should be better than HB alone	70 % 24 h at RT (up to 100 % for other compositions)	209

## Concluding remarks

Rubber recycling has become one of the major environmental problems because of the extensive use of these materials in day to day life. This recycling is complicated by the intrinsically permanent thermoset nature of elastomers. However, dynamic chemistry offers many different solutions to design the recyclability upstream. This chemistry has the potential to meet the different chemical and physical challenges of rubber recycling. Each dynamic solution has advantages and shortcomings: in dynamic rubbers as in classical rubbers, everything is about compromises.

Thermoplastic elastomers are already widely used industrial materials; they represent a good compromise between the tensile properties of rubbers and the full processability of thermoplastics. Yet, they also present shortcomings that prevent them from certain more demanding applications.

One of the best solutions to obtain a material with both very good rubber properties (elasticity, high tensile properties, resistance to solvent, high damping characteristics, etc.) and full recyclability would probably be to provide an industrial rubber with vitrimer crosslinks. Indeed, the base rubber is crucial to take advantage of its good elastomeric mechanical properties, and the vitrimer chemistry is the only dynamic chemistry that combines recyclability with full solvent resistance. Provide natural rubber with vitrimer properties is still a very interesting challenge to tackle.

## 2. The choice of Epoxidized Natural Rubber

### 2.1. A product from nature

Epoxidized Natural Rubber (ENR) is obtained by direct epoxidation of Natural Rubber (NR). The later material and its use being part of history, a few historical facts are developed here to satisfy the curiosity of the reader. Then, ENR is presented in more detail, and eventually the previous work done in our laboratory is reviewed as it constitutes the basis of the present work.

#### 2.1.1. Elements of history

Rubber was already used a long time ago by pre-Columbian civilizations in Central and South America for the manufacturing of game balls for example. However, it is not before the middle of the 18<sup>th</sup> century that Charles-Marie de la Condamine, a French explorer, brought latex samples back to France allowing identification of the rubber tree (*Hevea brasiliensis*, Figure 21) by François Fresneau de la Gataudière in 1747. The French term “caoutchouc” (rubber in English) was adapted by Charles-Marie de la Condamine from the term “caotchu” that means “crying wood” in the Quechuan language.



Figure 21. *Hevea brasiliensis* or rubber tree (illustration from reference<sup>211</sup>).

From this period, people started to grow Heveas in Asia (Sri Lanka, Malaysia, Thailand...) and Africa (*Hevea brasiliensis* originally comes from Brazil). The new material was at this time widely used for waterproofing fabrics or sealing. However, its properties were too

dependent on temperature: it became sticky with the heat of the sun and fragile during winter. In 1839, Charles Goodyear (1800-1860) accidentally found a solution to this problem by dropping raw rubber mixed with sulphur into a hot stove. He noticed that the material had acquired better thermal properties and got a patent on sulphur vulcanization of NR. His discovery was closely linked to the work of Friedrich Ludersdorf and Nathaniel Hayward who independently showed in 1834 that mixing sulphur to raw natural rubber helped to prevent the material from becoming sticky.

Since then, sulphur vulcanization has been widely studied and used in the industry. This process which creates mono-, di- and polysulphide bridges between the rubber chains highly enhances mechanical properties and thermal resistance of the material.

### *2.1.2. Latex-producing plants*

Natural rubber is produced by certain type of plants to protect themselves against external aggressions. A stable dispersion of polymer micro-particles in an aqueous medium is found in the latex of the plant, constituting the cytoplasm of laticifer cells. These cells are arranged in a network of laticiferous vessels located in the inner bark of the trees. When the tree is armed, the latex flows and then coagulates on exposure to air. This is a natural protection mechanism.



*Figure 22. Harvesting of latex from Hevea brasiliensis in India (courtesy of: Sophie Norvez).*

Latex is collected by periodic incision of the bark (called “tapping”, Figure 22). Numerous steps of stabilization, coagulation, and drying are then necessary to finally obtain rubber bales.

Although around 2000 different plant species produce latex,<sup>212</sup> *Hevea brasiliensis* is the only species that produces commercially viable quantities of high-quality rubber (30–50 % by volume of fresh latex). However, numerous studies are conducted to find alternatives to face the increasing demand in NR. According to the work of a French team in Montpellier, guayule (Figure 23), could potentially be a good candidate for the production of NR in the Mediterranean region.<sup>213</sup>



Figure 23. Guayule field, latex-producing plant well adapted to the Mediterranean climate.  
(from: Cirad Montpellier, S. Palu)

## 2.2. Epoxidation of NR

From a chemical point of view, NR is mainly composed of *cis*-1,4-polyisoprene (Figure 24a). Chemical modification of existing polymers is an efficient way to obtain new materials with specific properties. People have tried to modify NR from the mid twenties to improve for example its resistance to oils. To do that, some of the double bonds can be epoxidized to obtain more polar chains and improve the oil-resistance of the material. Epoxidized natural rubber (ENR, Figure 24b) is obtained by reaction with peracids such as peracetic or performic acid.<sup>214, 215</sup>

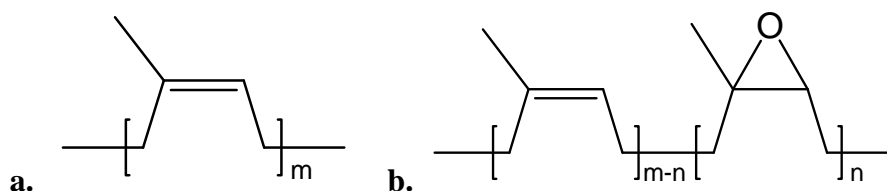


Figure 24. Chemical molecules of: **a.** NR (polyisoprene) and **b.** ENR.

The epoxidation step must be conducted carefully to avoid any side reaction such as furanization or ring opening reactions producing carboxyl or hydroxyl pendant groups. The temperature of the medium and concentration of peracid must be precisely controlled.<sup>216, 217</sup> The epoxidation can be performed under the latex form, before coagulation, by adding a preformed peracid. However, for economic reasons, the peracid is usually formed *in situ* by adding carboxylic acid (formic acid) and hydrogen peroxide.<sup>218</sup> All degrees of epoxidation can be reached by this method.

The epoxidation ratio is easily determined by spectroscopic methods. For example, using <sup>1</sup>H NMR, this ratio is calculated from the respective integration of the peak at 2.7 ppm (proton on the oxirane group) and the one at 5.1 ppm (allylic proton). Using infrared spectroscopy, it is possible to compare the intensities of the peaks at 870 cm<sup>-1</sup> and 835 cm<sup>-1</sup> that respectively correspond to the asymmetric deformation of the epoxy rings and the out-of-plane deformation of =C-H bonds.<sup>219</sup> Coupling titration methods with infrared spectroscopy and DSC (Differential Scanning Calorimetry) measurements, Davey and Loadman showed that epoxy rings were randomly placed on the chain.<sup>219</sup> Bradbury and Perera confirmed one year later this random distribution thanks to <sup>13</sup>C NMR measurements.<sup>220</sup> They concluded that NR epoxidation was a random process in homogeneous solution but also in the latex phase.

### 2.3. ENR properties

NR has unique mechanical properties. However, very few materials derived from NR are actually used in industry, ENR being one of the only examples. The Strain Induced Crystallization (SIC) of NR chains is at the origin of the exceptional performances (ultimate properties and resistance to tearing and crack propagation).<sup>221</sup> ENR retains this ability to crystallize when stretched and exhibits the same kind of mechanical properties than NR.<sup>222</sup> This is possible because the epoxidation reaction retains the *cis* conformation of the chain and minor rearrangements of the crystal lattice allow the inclusion of the epoxy co-units in the polymer crystals. SIC is observed until 95 % of epoxidation and the average crystallinity at 400 % strain is constant until 50 % modification. After that, this percentage decreases dramatically.

ENR properties vary with the epoxidation ratio. Only two grades are commercially available nowadays (ENR25 and ENR50 with respectively 25 and 50 mol% epoxidation). In

this study, we used ENR25 only. The glass transition temperature varies linearly with the epoxidation ratio (Figure 25), causing an increase in damping (lower resilience).

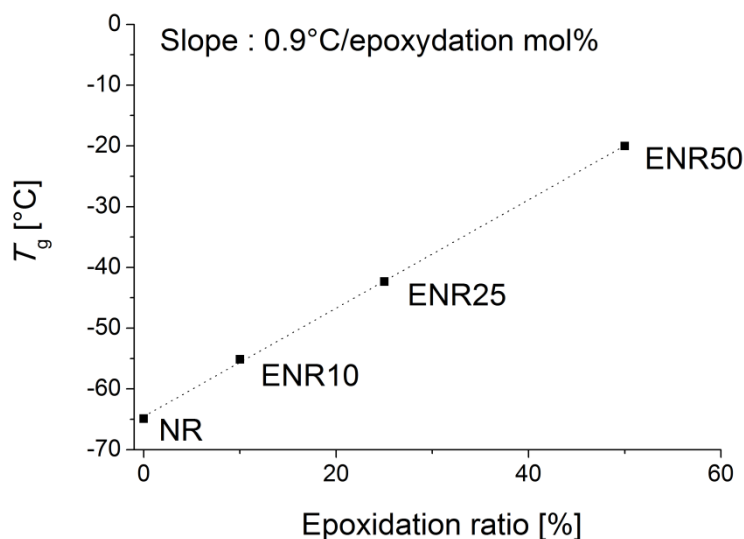


Figure 25.  $T_g$  evolution of NR with the epoxidation ratio.<sup>223</sup>

ENR chains are more polar than NR owing to the presence of the oxirane groups. This permits a better resistance to oils,<sup>224, 225</sup> a lower gas permeability,<sup>226</sup> and a better compatibility with polymers bearing polar groups as polyamide<sup>227</sup> or polyvinyl chloride (PVC).<sup>228</sup> It is also beneficial for the compatibilization of fillers with the matrix. Indeed, in ENR, the same degree of reinforcement can be obtained with silica than with carbon black without coupling agents, which is not possible in NR.<sup>217</sup> Specific interactions of epoxy sites with silanols help compatibilization. Conversely to carbon black, silica reinforcement gives the opportunity to create colored vulcanizates.

Thermal stability of ENR was also studied in the literature. Thermo-gravimetric analyses showed that the thermal degradation of ENR in inert atmosphere is a one-step process.<sup>229</sup> Heping *et al.* showed that the temperature of thermal degradation and the activation energy increase with the epoxidation ratio, indicating a better stability of highly epoxidized samples.<sup>230</sup> Thermo-oxidative degradation is a much more complex multi-step process. Degradation reactions can affect both double bonds and epoxy functions; nevertheless, the formed species are the same than for NR (mostly hydro-peroxides, carbonyls or hydroxyls).<sup>231</sup> The oxidation rate increases with the epoxidation ratio in a supposed auto-catalytic process.

## 2.4. A new way to crosslink ENR

### 2.4.1. Classical crosslinking methods

In spite of the new functionality present on the ENR chain, this rubber is usually crosslinked as NR through classical sulphur or peroxide vulcanizations. Like in NR, sulphur reacts preferentially near the double bonds; however, sulphur vulcanization of ENR is more efficient. This is due to several factors. Firstly, ENR possess isolated double bonds, which reduces the formation of intramolecular links and increases the crosslink density. Secondly, the epoxy functions are thought to play an activation role on the adjacent double bonds. That would explain why the reaction starts earlier in highly epoxidized materials.<sup>232</sup> Peroxide crosslinking was less studied in the literature.<sup>233, 234</sup> This process is known to produce thermally more stable materials showing better ageing properties.

Each crosslinking process possesses advantages and drawbacks in terms of material properties. Sulphur vulcanization produces polysulphide links known to undergo exchange reactions,<sup>28</sup> which leads to good mechanical properties and fatigue resistance.<sup>235</sup> The energy of the S-S bond is relatively low (25-40 kcal.mol<sup>-1</sup>)<sup>236</sup> so it will break before C-C bonds ( $\approx 90$  kcal.mol<sup>-1</sup>)<sup>236</sup> and will be able to reform. However, sulphur-vulcanized rubber show poor ageing properties due to the easy oxidation of the sulphur bridges. Moreover, studies have shown that thermal decomposition of sulphur compounds produces acids that will catalyze ring opening reactions of the epoxy functions.<sup>237</sup> Conversely, peroxide vulcanization produces very stable carbon-carbon bonds that are more resistant over time. However, C-C bonds do not possess any reversible character, which significantly weakens the material during repeated solicitations. In the case of NR, it has been shown that polysulphide-containing materials resist two or three times longer to fatigue solicitation than monosulphide- or peroxide-crosslinked ones.<sup>6</sup>

### 2.4.2. Carboxylic diacid as a new crosslinker

The PhD thesis of Myriam Pire, a former student of the MMC laboratory, was dedicated to this problem, in collaboration with Hutchison SA. The aim was to find a compromise between fatigue and ageing properties.<sup>223</sup> Industrially, classical methods described in the previous paragraph are predominant for the curing of ENR. However, ENR can also be crosslinked through opening of the epoxy functions.<sup>238-244</sup> Myriam showed that a good compromise was reached using carboxylic diacids to open epoxy rings.<sup>183</sup> On the one hand, this new

crosslinking process creates covalent ester bonds that show a good stability over time. On the other hand, the use of long diacids (Dodecanedioic Acid, DA, containing 12 carbon atoms in the chain) brings flexibility. The resulting DA-crosslinked ENR is thus resistant to ageing and present acceptable fatigue properties.

Curing behaviour and mechanical properties of reactive blends of ENR with DA were investigated during Myriam's PhD.<sup>179</sup> The efficiency of crosslinking increased with increasing epoxy contents and the reaction kinetic was shown to be of first order regarding to DA. The ratio of epoxy functions per diacid molecules was defined as  $p$ . Optimum mechanical properties for ENR25 were obtained for  $p = 25$ , corresponding to one diacid molecule for 25 epoxy functions. The crosslinking reaction was shown to be highly promoted by the presence of 1,2-dimethylimidazole (DMI).<sup>180</sup> This base does not act as a catalyst but as an accelerator for the epoxy reaction through activation of DA by formation of the corresponding imidazolium salt. This salt is more soluble in ENR and ensures the good dispersion of the curing agent in the rubber matrix. The acceleration of the crosslinking reaction shortens drastically the curing time which is beneficial for the mechanical properties of the final material.

The mechanism of the reaction was studied by solid-state NMR spectroscopy.<sup>181</sup> The formation of  $\beta$ -hydroxy esters along the chains was confirmed (Figure 26). The imidazolium dicarboxylate preferentially opens the epoxy at the less substituted side in accordance with a mechanism associated to basic conditions. Moreover, it could be shown that DMI-induced acceleration of the crosslinking process reduces secondary reactions that are otherwise favoured by long curing times.

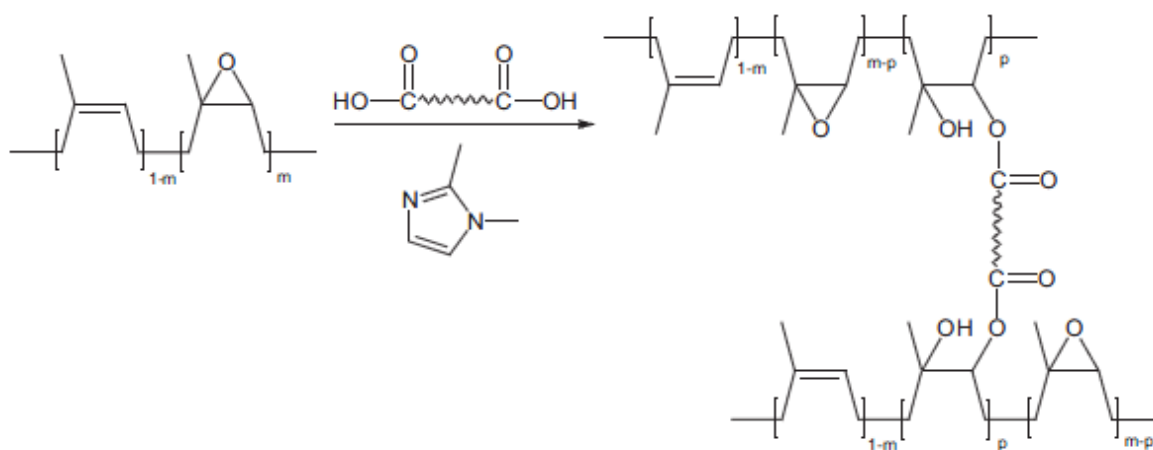


Figure 26. Crosslinking of ENR in the presence of DMI (reproduced from reference<sup>180</sup>).

The new crosslinking process was shown to compete with standard sulphur and peroxide vulcanizations in terms of curing conditions and mechanical properties.<sup>182, 183</sup> It was also possible to create semi-interpenetrated ENR networks by mixing ENRs of different epoxidation ratios and selectively crosslinking one of the two immiscible phases.<sup>184</sup> The difference of solubility of the diacid in both matrices and the faster curing rate of more epoxidized ENR play important roles into this selective crosslinking process.

In the following, the DA-cured ENR25 will be referred to as ENR-DA.

## 2.5. A full bio-based system

The basic diacid used for ENR crosslinking was Dodecanedioic Acid (DA). This diacid is widely used for various applications in the production of corrosion inhibitors, antiseptics, surfactants, paints, molding resins, as well as adhesives or powder coatings. It is also very important for the production of Nylon 6,12. Traditionally produced from butadiene *via* a multi-step chemical process, it is found under the form of white flakes. The growing demand for high performances Nylon 6,12 encourages DA production and does not seem to be declining. Evonik, Ube or Invista are among the main producers of petroleum-based DA. However, faced to the growing environmental awareness and the very unstable petrol prices, some companies have started to re-think the production and find bio-based alternatives. The American company Verdezyne is now able to produce a bio-based DA from raw materials derived from plants. Their process has the additional benefit to be cheap.

ENR being itself directly issued from a natural product, our ENR-DA system is completely bio-based.<sup>185</sup> This represents a major advantage of this new type of crosslinking. The accelerator, DMI (Figure 26, under the arrow), is often used as catalyst in polyurethanes,<sup>245</sup> or hardener in epoxy resins.<sup>246</sup> DMI is a biodegradable product that can be completely assimilated by a bacterial consortium after only 31 days.<sup>247</sup> Compared to sulphur vulcanization that uses toxic products like zinc oxide (ZnO, particularly poisonous for the aquatic environment) or N-cyclohexyl-2-benzothiazolylsulfenamide (CBS, widely used accelerator), this new crosslinking process thus appears as an efficient and environmentally friendly alternative.

## References

1. P.-G. De Gennes, *Scaling concepts in polymer physics*, Cornell university press, 1979.
2. M. Doi and S. F. Edwards, *The theory of polymer dynamics*, Oxford University Press, USA, 1988.
3. *US 6512051 B2 Pat.*, 2003.
4. D. Montarnal, M. Capelot, F. Tournilhac and L. Leibler, *Science*, 2011, **334**, 965-968.
5. L. R. G. Treloar, *The physics of rubber elasticity*, Oxford university press, 1975.
6. B. L. Chan, D. J. Elliott, M. Holley and J. F. Smith, *Journal of Polymer Science: Polymer Symposia*, 1974, **48**, 61-86.
7. A. Coran, *Journal of Applied Polymer Science*, 2003, **87**, 24-30.
8. X. Liu, T. Zhou, Y. Liu, A. Zhang, C. Yuan and W. Zhang, *RSC Advances*, 2015, **5**, 10231-10242.
9. W. Kuhn and F. Grun, *Kolloid-Z*, 1942, **101**, 248-271.
10. E. Guth, H. James and H. Mark, *Advances in Colloid Science*, 1946, **2**, 253.
11. P. J. Flory, *Chemical Reviews*, 1944, **35**, 51-75.
12. P. J. Flory, *Polym J*, 1985, **17**, 1-12.
13. G. Gee, *Transactions of the Faraday Society*, 1946, **42**, 585-598.
14. R. M. Nascimento, F. L. Faita, D. L. S. Agostini, A. E. Job, F. E. G. Guimarães and I. H. Bechtold, *Materials Science and Engineering: C*, 2014, **39**, 29-34.
15. <http://www.lecaoutchouc.fr/>, *Diaporama 150 ans SNCP Etat de la filière en 2013*, Syndicat National du Caoutchouc et des Polymères.
16. C. Lucignano, A. Gugliemotti and F. Quadrini, *Polymer-Plastics Technology and Engineering*, 2012, **51**, 340-344.
17. J. Karger-Kocsis, L. Mészáros and T. Bárány, *J Mater Sci*, 2013, **48**, 1-38.
18. M. Myhre, S. Saiwari, W. Dierkes and J. Noordermeer, *Rubber Chemistry and Technology*, 2012, **85**, 408-449.
19. B. Adhikari, D. De and S. Maiti, *Progress in Polymer Science*, 2000, **25**, 909-948.
20. *Landfill of waste directive. Brussels, Belgium: European Commission. Council Directive 1999/31/EC, (1999).*
21. H. Yazdani, M. Karrabi, I. Ghasmi, H. Azizi and G. R. Bakhshandeh, *Journal of Vinyl and Additive Technology*, 2011, **17**, 64-69.
22. G. Tao, Q. He, Y. Xia, G. Jia, H. Yang and W. Ma, *Journal of Applied Polymer Science*, 2013, **129**, 2598-2605.
23. S. B. Liang, D. P. Hu, C. Zhu and A. B. Yu, *Chemical Engineering & Technology*, 2002, **25**, 401-405.
24. P. S. Garcia, F. D. B. de Sousa, J. A. de Lima, S. A. Cruz and C. H. Scuracchio, *express Polymer Letters*, 2015, **9**, 1015-1026.
25. A. Zanchet, L. N. Carli, M. Giovanela, J. S. Crespo, C. H. Scuracchio and R. C. R. Nunes, *Journal of Elastomers and Plastics*, 2009, **41**, 497-507.
26. A. I. Isayev, J. Chen and A. Tukachinsky, *Rubber Chemistry and Technology*, 1995, **68**, 267-280.
27. M. Tapale and A. I. Isayev, *Journal of Applied Polymer Science*, 1998, **70**, 2007-2019.
28. A. V. Tobolsky, W. J. MacKnight and M. Takahashi, *The Journal of Physical Chemistry*, 1964, **68**, 787-790.
29. M. Le Neindre and R. Nicolay, *Polymer Chemistry*, 2014, **5**, 4601-4611.
30. S. Rooj, G. C. Basak, P. K. Maji and A. K. Bhowmick, *J Polym Environ*, 2011, **19**, 382-390.

31. M. Sabzekar, M. P. Chenar, S. M. Mortazavi, M. Kariminejad, S. Asadi and G. Zohuri, *Polymer Degradation and Stability*, 2015, **118**, 88-95.
32. K. Dubkov, S. Semikolenov, D. Ivanov, D. Babushkin and V. Voronchikhin, *Iran Polym J*, 2014, **23**, 881-890.
33. K. A. Dubkov, S. V. Semikolenov, D. P. Ivanov, D. E. Babushkin, G. I. Panov and V. N. Parmon, *Polymer Degradation and Stability*, 2012, **97**, 1123-1130.
34. F. Sadaka, I. Campistron, A. Laguerre and J.-F. Pilard, *Polymer Degradation and Stability*, 2013, **98**, 736-742.
35. H. Yazdani, I. Ghasemi, M. Karrabi, H. Azizi and G. R. Bakhshandeh, *Journal of Vinyl and Additive Technology*, 2013, **19**, 65-72.
36. G. D. Paulo, D. Hirayama and C. Saron, *Advanced Materials Research*, 2012, **418-420**, 1072-1075.
37. Y. Ikeda, in *Chemistry, Manufacture and Applications of Natural Rubber*, eds. S. Kohjiya and Y. Ikeda, Woodhead Publishing, 2014, pp. 436-451.
38. Y. Li, S. Zhao and Y. Wang, *J Polym Environ*, 2012, **20**, 372-380.
39. C. Yao, S. Zhao, Y. Wang, B. Wang, M. Wei and M. Hu, *Polymer Degradation and Stability*, 2013, **98**, 1724-1730.
40. L. Mészáros, T. Bárány and T. Czvikovszky, *Radiation Physics and Chemistry*, 2012, **81**, 1357-1360.
41. X. Zhang, C. Lu and M. Liang, *J Polym Res*, 2009, **16**, 411-419.
42. N. Roche, M. N. Ichchou, M. Salvia and A. Chettah, *Journal of Elastomers and Plastics*, 2011, **43**, 317-340.
43. S. Ramarad, M. Khalid, C. Ratnam, A. L. Chuah and W. Rashmi, *Progress in materials science*, 2015, **72**, 100-140.
44. X. Shu and B. Huang, *Construction and Building Materials*, 2014, **67, Part B**, 217-224.
45. D. Lo Presti, *Construction and Building Materials*, 2013, **49**, 863-881.
46. N. N. Eldin and A. B. Senouci, *Cement, Concrete and Aggregates*, 1993, **15**, 74-84.
47. F. Pacheco-Torgal, Y. Ding and S. Jalali, *Construction and Building Materials*, 2012, **30**, 714-724.
48. G. Pérez, A. Vila, L. Rincón, C. Solé and L. F. Cabeza, *Applied Energy*, 2012, **97**, 347-354.
49. L. Alamo-Nole, O. Perales-Perez and F. R. Roman, *Desalination and Water Treatment*, 2012, **49**, 296-306.
50. R. Maderuelo-Sanz, M. Martín-Castizo and R. Vílchez-Gómez, *Applied Acoustics*, 2011, **72**, 823-828.
51. R. Maderuelo-Sanz, A. V. Nadal-Gisbert, J. E. Crespo-Amorós and F. Parres-García, *Applied Acoustics*, 2012, **73**, 402-408.
52. *U.S. Patent 4244841 Pat.*, 1981.
53. *U.S. Patent 0101004 A1 Pat.*, 2002.
54. A. R. Tripathy, J. E. Morin, D. E. Williams, S. J. Eyles and R. J. Farris, *Macromolecules*, 2002, **35**, 4616-4627.
55. *U.S. Patent 5904885 Pat.*, 1999.
56. E. Bilgili, A. Dybek, H. Arastoopour and B. Bernstein, *Journal of Elastomers and Plastics*, 2003, **35**, 235-256.
57. A. Gugliemotti, C. Lucignano and F. Quadrini, *Plastics, Rubber and Composites*, 2012, **41**, 40-46.
58. M. Miranda, F. Pinto, I. Gulyurtlu and I. Cabrita, *Fuel*, 2013, **103**, 542-552.
59. A. Undri, L. Rosi, M. Frediani and P. Frediani, *Fuel*, 2014, **115**, 600-608.

60. H. Wang, M. Davidson, Y. Zuo and Z. Ren, *Journal of Power Sources*, 2011, **196**, 5863-5866.
61. Y. Zhang, B. Yang, X. Zhang, L. Xu, L. Tao, S. Li and Y. Wei, *Chemical Communications*, 2012, **48**, 9305-9307.
62. J. N. Hunt, K. E. Feldman, N. A. Lynd, J. Deek, L. M. Campos, J. M. Spruell, B. M. Hernandez, E. J. Kramer and C. J. Hawker, *Advanced Materials*, 2011, **23**, 2327-2331.
63. J. P. Gong, *Soft Matter*, 2010, **6**, 2583-2590.
64. M. Capelot, D. Montarnal, F. Tournilhac and L. Leibler, *Journal of the American Chemical Society*, 2012, **134**, 7664-7667.
65. P. Cordier, F. Tournilhac, C. Soulié-Ziakovic and L. Leibler, *Nature*, 2008, **451**, 977-980.
66. R. P. Wool, *Soft Matter*, 2008, **4**, 400-418.
67. M. D. Hager, P. Greil, C. Leyens, S. van der Zwaag and U. S. Schubert, *Advanced Materials*, 2010, **22**, 5424-5430.
68. S. J. Garcia, *European Polymer Journal*, 2014, **53**, 118-125.
69. Y.-X. Lu, F. Tournilhac, L. Leibler and Z. Guan, *Journal of the American Chemical Society*, 2012, **134**, 8424-8427.
70. A. Rekondo, R. Martin, A. R. de Luzuriaga, G. Cabañero, H. J. Grande and I. Odriozola, *Materials Horizons*, 2014, **1**, 237-240.
71. M. Abdollahzadeh, C. Esteves, A. Catarina, S. Zwaag and S. J. Garcia, *Journal of Polymer Science Part A: Polymer Chemistry*, 2014, **52**, 1953-1961.
72. M. Pepels, I. Filot, B. Klumperman and H. Goossens, *Polymer Chemistry*, 2013, **4**, 4955-4965.
73. Y.-X. Lu and Z. Guan, *Journal of the American Chemical Society*, 2012, **134**, 14226-14231.
74. L. Imbernon, E. Oikonomou, S. Norvez and L. Leibler, *Polymer Chemistry*, 2015, **6**, 4271-4278.
75. R. Martin, A. Rekondo, A. R. de Luzuriaga, G. Cabañero, H. J. Grande and I. Odriozola, *Journal of Materials Chemistry A*, 2014, **2**, 5710-5715.
76. A. Grande, S. Garcia and S. van der Zwaag, *Polymer*, 2015, **56**, 435-442.
77. J. P. Brutman, P. A. Delgado and M. A. Hillmyer, *ACS Macro Letters*, 2014, **3**, 607-610.
78. W. Denissen, G. Rivero, R. Nicolaÿ, L. Leibler, J. M. Winne and F. E. Du Prez, *Advanced Functional Materials*, 2015, **25**, 2451-2457.
79. M. M. Obadia, B. P. Mudraboyina, A. Serghei, D. Montarnal and E. Drockenmuller, *Journal of the American Chemical Society*, 2015, **137**, 6078-6083.
80. R. Chasset and P. Thirion, *Proceedings of the International Conference on Non-Crystalline Solids*, 1965.
81. J. G. Curro and P. Pincus, *Macromolecules*, 1983, **16**, 559-562.
82. S. Billiet, X. K. D. Hillewaere, R. F. A. Teixeira and F. E. Du Prez, *Macromolecular Rapid Communications*, 2013, **34**, 290-309.
83. S. Burattini, B. W. Greenland, D. Chappell, H. M. Colquhoun and W. Hayes, *Chemical Society Reviews*, 2010, **39**, 1973-1985.
84. P. Tyagi, A. Deratani and D. Quemener, *Israel Journal of Chemistry*, 2013, **53**, 53-60.
85. J. G. Drobny, *Handbook of thermoplastic elastomers*, Elsevier, 2nd edn., 2014.
86. R. J. Spontak and N. P. Patel, *Current Opinion in Colloid & Interface Science*, 2000, **5**, 333-340.
87. S. L. Cooper and A. V. Tobolsky, *Journal of Applied Polymer Science*, 1966, **10**, 1837-1844.
88. L. Leibler, *Macromolecules*, 1980, **13**, 1602-1617.

89. Z. Wang, L. Yuan, N. M. Trenor, L. Vlaminck, S. Billiet, A. Sarkar, F. E. Du Prez, M. Stefik and C. Tang, *Green Chemistry*, 2015, **17**, 3806-3818.
90. J. Karger-Kocsis, in *Polypropylene*, ed. J. Karger-Kocsis, Springer Netherlands, 1999, vol. 2, ch. 116, pp. 853-858.
91. A. Y. Coran and R. P. Patel, in *Polypropylene Structure, blends and composites*, ed. J. Karger-Kocsis, Springer Netherlands, 1995, ch. 6, pp. 162-201.
92. C. R. Kumar, I. Fuhrmann and J. Karger-Kocsis, *Polymer Degradation and Stability*, 2002, **76**, 137-144.
93. J. G. Drobny, in *Handbook of Thermoplastic Elastomers*, William Andrew Publishing, Norwich, NY, 2007, ch. 9, pp. 215-234.
94. S. K. Smart, G. A. Edwards and D. J. Martin, in *Rubber Nanocomposites*, John Wiley & Sons, Ltd, 2010, pp. 239-254.
95. K. A. Houton and A. J. Wilson, *Polymer International*, 2015, **64**, 165-173.
96. P. Krol, *Progress in materials science*, 2007, **52**, 915-1015.
97. Y. He, D. Xie and X. Zhang, *J Mater Sci*, 2014, **49**, 7339-7352.
98. M. Sánchez-Adsuar, E. Papon and J. J. Villenave, *Journal of Applied Polymer Science*, 2000, **76**, 1602-1607.
99. M. Sánchez-Adsuar, E. Papon and J. J. Villenave, *Journal of Applied Polymer Science*, 2000, **76**, 1596-1601.
100. M. Sánchez-Adsuar, E. Papon and J. J. Villenave, *Journal of Applied Polymer Science*, 2000, **76**, 1590-1595.
101. G. Rabani, G. M. Rosair and A. Kraft, *Journal of Polymer Science Part A: Polymer Chemistry*, 2004, **42**, 1449-1460.
102. D. Joel and A. Hauser, *Die Angewandte Makromolekulare Chemie*, 1994, **217**, 191-199.
103. A. C. Schüssele, F. Nübling, Y. Thomann, O. Carstensen, G. Bauer, T. Speck and R. Mülhaupt, *Macromolecular Materials and Engineering*, 2012, **297**, 411-419.
104. A. Coran and R. Patel, *Rubber Chemistry and Technology*, 1981, **54**, 892-903.
105. M. Morton, *Rubber Chemistry and Technology*, 1983, **56**, 1096-1110.
106. B. T. Gall, R. Thomann and R. Mülhaupt, *Journal of Polymer Science Part A: Polymer Chemistry*, 2011, **49**, 2339-2345.
107. Y. Nakayama, K. Aihara, H. Yamanishi, H. Fukuoka, R. Tanaka, Z. Cai and T. Shiono, *Journal of Polymer Science Part A: Polymer Chemistry*, 2015, **53**, 489-495.
108. J. P. Bishop and R. A. Register, *Macromolecules*, 2010, **43**, 4954-4960.
109. B. T. Gall, J. McCahill, D. W. Stephan and R. Mülhaupt, *Macromolecular Rapid Communications*, 2008, **29**, 1549-1553.
110. Y. Chen, A. M. Kushner, G. A. Williams and Z. Guan, *Nature Chemistry*, 2012, **4**, 467-472.
111. J. Hentschel, A. M. Kushner, J. Ziller and Z. Guan, *Angewandte Chemie International Edition*, 2012, **51**, 10561-10565.
112. A. Gooch, C. Nedolisa, K. A. Houton, C. I. Lindsay, A. Saiani and A. J. Wilson, *Macromolecules*, 2012, **45**, 4723-4729.
113. X. Wang, J. Vapaavuori, Y. Zhao and C. G. Bazuin, *Macromolecules*, 2014, **47**, 7099-7108.
114. A. Eisenberg, *Ions in polymers*, American Chemical Society Washington, DC, 1980.
115. M. R. Tant, K. A. Mauritz and G. L. Wilkes, *Ionomers: synthesis, structure, properties and applications*, Springer Science & Business Media, 1997.
116. P. Antony and S. K. De, *Journal of Macromolecular Science, Part C*, 2001, **41**, 41-77.
117. W. Cooper, *Journal of Polymer Science*, 1958, **28**, 195-206.
118. P. K. Agarwal and R. D. Lundberg, *Macromolecules*, 1984, **17**, 1918-1928.

119. W. J. MacKnight and R. D. Lundberg, *Rubber Chemistry and Technology*, 1984, **57**, 652-663.
120. A. U. Paeglis and F. X. O'Shea, *Rubber Chemistry and Technology*, 1988, **61**, 223-237.
121. R. D. Lundberg and H. S. Makowski, in *Ions in Polymers*, AMERICAN CHEMICAL SOCIETY, 1980, vol. 187, ch. 2, pp. 21-36.
122. P. Phinyocheep, in *Chemistry, Manufacture and Applications of Natural Rubber*, eds. S. Kohjiya and Y. Ikeda, Woodhead Publishing, 2014, pp. 68-118.
123. T. Xavier, J. Samuel and T. Kurian, *International Journal of Polymeric Materials and Polymeric Biomaterials*, 2003, **52**, 251-264.
124. L. Ibarra and M. Alzorriz, *Journal of Applied Polymer Science*, 2003, **87**, 805-813.
125. L. Ibarra and M. Alzorriz, *Journal of Applied Polymer Science*, 2007, **103**, 1894-1899.
126. M. A. J. van der Mee, R. M. A. l'Abee, G. Portale, J. G. P. Goossens and M. van Duin, *Macromolecules*, 2008, **41**, 5493-5501.
127. F. Potier, A. Guinault, S. Delalande, C. Sanchez, F. Ribot and L. Rozes, *Polymer Chemistry*, 2014, **5**, 4474-4479.
128. J. Yoon, H.-J. Lee and C. M. Stafford, *Macromolecules*, 2011, **44**, 2170-2178.
129. K.-W. Leong and G. B. Butler, *Journal of Macromolecular Science: Part A - Chemistry*, 1980, **14**, 287-319.
130. R. Stadler and L. de Lucca Freitas, *Colloid & Polymer Sci*, 1986, **264**, 773-778.
131. C. Hilger and R. Stadler, *Die Makromolekulare Chemie*, 1990, **191**, 1347-1361.
132. C. Hilger and R. Stadler, *Macromolecules*, 1992, **25**, 6670-6680.
133. J. Hellmann, C. Hilger and R. Stadler, *Polymers for Advanced Technologies*, 1994, **5**, 763-774.
134. C.-C. Peng and V. Abetz, *Macromolecules*, 2005, **38**, 5575-5580.
135. K. Chino and M. Ashiura, *Macromolecules*, 2001, **34**, 9201-9204.
136. K. Chino, *Kgk-Kautschuk Gummi Kunststoff*, 2006, **59**, 158-162.
137. M. Kashif and Y.-W. Chang, *Polymer International*, 2014, **63**, 1936-1943.
138. Y.-W. Chang, J. K. Mishra, S.-K. Kim and D.-K. Kim, *Materials Letters*, 2006, **60**, 3118-3121.
139. H. Kautz, D. Van Beek, R. P. Sijbesma and E. Meijer, *Macromolecules*, 2006, **39**, 4265-4267.
140. N. Roy, E. Buhler and J.-M. Lehn, *Chemistry – A European Journal*, 2013, **19**, 8814-8820.
141. O. Colombani, C. Barioz, L. Bouteiller, C. Chanéac, L. Fompérie, F. Lortie and H. Montès, *Macromolecules*, 2005, **38**, 1752-1759.
142. W. P. J. Appel, G. Portale, E. Wisse, P. Y. W. Dankers and E. W. Meijer, *Macromolecules*, 2011, **44**, 6776-6784.
143. J.-M. Lehn and J. Sanders, *Angewandte Chemie-English Edition*, 1995, **34**, 2563.
144. D. Montarnal, P. Cordier, C. Soulié-Ziakovic, F. Tournilhac and L. Leibler, *Journal of Polymer Science Part A: Polymer Chemistry*, 2008, **46**, 7925-7936.
145. D. Montarnal, F. Tournilhac, M. Hidalgo, J.-L. Couturier and L. Leibler, *Journal of the American Chemical Society*, 2009, **131**, 7966-7967.
146. F. Tournilhac, P. Cordier, D. Montarnal, C. Soulié-Ziakovic and L. Leibler, *Macromolecular Symposia*, 2010, **291-292**, 84-88.
147. J. Cortese, C. Soulié-Ziakovic, M. Cloitre, S. Tencé-Girault and L. Leibler, *Journal of the American Chemical Society*, 2011, **133**, 19672-19675.
148. J. Cortese, C. Soulié-Ziakovic, S. Tencé-Girault and L. Leibler, *Journal of the American Chemical Society*, 2012, **134**, 3671-3674.

149. F. Maes, D. Montarnal, S. Cantournet, F. Tournilhac, L. Corte and L. Leibler, *Soft Matter*, 2012, **8**, 1681-1687.
150. A. Zhang, L. Yang, Y. Lin, L. Yan, H. Lu and L. Wang, *Journal of Applied Polymer Science*, 2013, **129**, 2435-2442.
151. C. Sun, M. Van der Mee, J. Goossens and M. Van Duin, *Macromolecules*, 2006, **39**, 3441-3449.
152. F. Shen, H. Li and C. Wu, *Journal of Polymer Science Part B: Polymer Physics*, 2006, **44**, 378-386.
153. L. Ibarra, A. Rodríguez and I. Mora-Barrantes, *Polymer International*, 2009, **58**, 218-226.
154. S. Burattini, B. W. Greenland, D. H. Merino, W. Weng, J. Seppala, H. M. Colquhoun, W. Hayes, M. E. Mackay, I. W. Hamley and S. J. Rowan, *Journal of the American Chemical Society*, 2010, **132**, 12051-12058.
155. S. Burattini, H. M. Colquhoun, B. W. Greenland and W. Hayes, *Faraday discussions*, 2009, **143**, 251-264.
156. M. Nakahata, Y. Takashima, H. Yamaguchi and A. Harada, *Nature Communications*, 2011, **2**, 511.
157. T. Kakuta, Y. Takashima and A. Harada, *Macromolecules*, 2013, **46**, 4575-4579.
158. X. Ji, J. Chen and M. Xue, *Macromolecular Chemistry and Physics*, 2014, **215**, 536-543.
159. M. Dionisio, L. Ricci, G. Pecchini, D. Masseroni, G. Ruggeri, L. Cristofolini, E. Rampazzo and E. Dalcanale, *Macromolecules*, 2014, **47**, 632-638.
160. A. Ruiz de Luzuriaga, A. Rekondo, R. Martin, G. Cabañero, H. J. Grande and I. Odriozola, *Journal of Polymer Science Part A: Polymer Chemistry*, 2015, **53**, 1061-1066.
161. C.-C. Peng, A. Göpfert, M. Drechsler and V. Abetz, *Polymers for Advanced Technologies*, 2005, **16**, 770-782.
162. W. K. Wong, *Macromolecular Symposia*, 2005, **221**, 137-144.
163. S. Bokern, Z. Fan, C. Mattheis, A. Greiner and S. Agarwal, *Macromolecules*, 2011, **44**, 5036-5042.
164. R. Martin, A. Rekondo, J. Echeberria, G. Cabanero, H. J. Grande and I. Odriozola, *Chemical Communications*, 2012, **48**, 8255-8257.
165. C. Wang, N. Liu, R. Allen, J. B. H. Tok, Y. Wu, F. Zhang, Y. Chen and Z. Bao, *Advanced Materials*, 2013, **25**, 5785-5790.
166. R. Gheneim, C. Perez-Berumen and A. Gandini, *Macromolecules*, 2002, **35**, 7246-7253.
167. M. Watanabe and N. Yoshie, *Polymer*, 2006, **47**, 4946-4952.
168. E. Trovatti, T. M. Lacerda, A. J. F. Carvalho and A. Gandini, *Advanced Materials*, 2015, **27**, 2242-2245.
169. J. Bai, H. Li, Z. Shi and J. Yin, *Macromolecules*, 2015, **48**, 3539-3546.
170. L. M. Polgar, M. van Duin, A. A. Broekhuis and F. Picchioni, *Macromolecules*, 2015, DOI: 10.1021/acs.macromol.5b01422
171. P. J. Boul, P. Reutenauer and J.-M. Lehn, *Organic Letters*, 2005, **7**, 15-18.
172. P. Reutenauer, E. Buhler, P. J. Boul, S. J. Candau and J. M. Lehn, *Chemistry – A European Journal*, 2009, **15**, 1893-1900.
173. T. F. Scott, A. D. Schneider, W. D. Cook and C. N. Bowman, *Science*, 2005, **308**, 1615-1617.
174. Y. Amamoto, J. Kamada, H. Otsuka, A. Takahara and K. Matyjaszewski, *Angewandte Chemie*, 2011, **123**, 1698-1701.

175. Y. Amamoto, H. Otsuka, A. Takahara and K. Matyjaszewski, *Advanced Materials*, 2012, **24**, 3975-3980.
176. J. Canadell, H. Goossens and B. Klumperman, *Macromolecules*, 2011, **44**, 2536-2541.
177. Z. Q. Lei, H. P. Xiang, Y. J. Yuan, M. Z. Rong and M. Q. Zhang, *Chemistry of Materials*, 2014, **26**, 2038-2046.
178. H. Xiang, H. Qian, Z. Lu, M. Rong and M. Zhang, *Green Chemistry*, 2015, **17**, 4315-4325.
179. M. Pire, S. Norvez, I. Iliopoulos, B. Le Rossignol and L. Leibler, *Polymer*, 2010, **51**, 5903-5909.
180. M. Pire, S. Norvez, I. Iliopoulos, B. Le Rossignol and L. Leibler, *Polymer*, 2011, **52**, 5243-5249.
181. M. Pire, C. Lorthioir, E. K. Oikonomou, S. Norvez, I. Iliopoulos, B. Le Rossignol and L. Leibler, *Polymer Chemistry*, 2012, **3**, 946-953.
182. M. Pire, E. K. Oikonomou, L. Imbernon, C. Lorthioir, I. Iliopoulos and S. Norvez, *Macromolecular Symposia*, 2013, **331-332**, 89-96.
183. M. Pire, S. Norvez, I. Iliopoulos, B. Le Rossignol and L. Leibler, *Composite Interfaces*, 2014, **21**, 45-50.
184. L. Imbernon, M. Pire, E. K. Oikonomou and S. Norvez, *Macromolecular Chemistry and Physics*, 2013, **214**, 806-811.
185. C. Ding and A. S. Matharu, *ACS Sustainable Chemistry & Engineering*, 2014, **2**, 2217-2236.
186. US3898253 A Pat., 1975.
187. US6559263 B1 Pat., 2003.
188. US20070149711 A1 Pat., 2007.
189. H. Ying, Y. Zhang and J. Cheng, *Nature Communications*, 2014, **5**, 3218.
190. L. Dodge, Y. Chen and M. A. Brook, *Chemistry – A European Journal*, 2014, **20**, 9349-9356.
191. K. Imato, A. Takahara and H. Otsuka, *Macromolecules*, 2015, **48**, 5632-5639.
192. C. Yuan, M. Z. Rong and M. Q. Zhang, *Polymer*, 2014, **55**, 1782-1791.
193. Z. P. Zhang, M. Z. Rong and M. Q. Zhang, *Polymer*, 2014, **55**, 3936-3943.
194. P. Espeel and F. E. Du Prez, *Macromolecules*, 2015, **48**, 2-14.
195. S. Billiet, K. De Bruycker, F. Driessen, H. Goossens, V. Van Speybroeck, J. M. Winne and F. E. Du Prez, *Nature Chemistry*, 2014, **6**, 815-821.
196. M. Capelot, M. M. Unterlass, F. Tournilhac and L. Leibler, *ACS Macro Letters*, 2012, **1**, 789-792.
197. W. Denissen, J. M. Winne and F. E. Du Prez, *Chemical Science*, 2015, DOI:10.1039/C5SC02223A.
198. P. Zheng and T. J. McCarthy, *Journal of the American Chemical Society*, 2012, **134**, 2024-2027.
199. O. R. Cromwell, J. Chung and Z. Guan, *Journal of the American Chemical Society*, 2015.
200. Z. Pei, Y. Yang, Q. Chen, E. M. Terentjev, Y. Wei and Y. Ji, *Nature Materials*, 2014, **13**, 36-41.
201. E. Ducrot, Y. Chen, M. Bulters, R. P. Sijbesma and C. Creton, *Science*, 2014, **344**, 186-189.
202. E. Ducrot, H. Montes and C. Creton, *Macromolecules*, 2015, **48**, 7945-7952.
203. D. Lenko, S. Schlögl, A. Temel, R. Schaller, A. Holzner and W. Kern, *Journal of Applied Polymer Science*, 2013, **129**, 2735-2743.
204. D. Montarnal, F. Tournilhac, M. Hidalgo and L. Leibler, *Journal of Polymer Science Part A: Polymer Chemistry*, 2010, **48**, 1133-1141.

205. I. Mora-Barrantes, M. Malmierca, J. Valentin, A. Rodriguez and L. Ibarra, *Soft Matter*, 2012, **8**, 5201-5213.
206. N. Roy, E. Buhler and J. M. Lehn, *Polymer International*, 2014, **63**, 1400-1405.
207. B. Zhang, Z. A. Digby, J. A. Flum, E. M. Foster, J. L. Sparks and D. Konkolewicz, *Polymer Chemistry*, 2015, DOI: 10.1039/c5py01214g.
208. J. A. Neal, D. Mozhdehi and Z. Guan, *Journal of the American Chemical Society*, 2015, **137**, 4846-4850.
209. F. Sordo, S.-J. Mougner, N. Loureiro, F. Tournilhac and V. Michaud, *Macromolecules*, 2015, **48**, 4394-4402.
210. R. Martin, A. Rekondo, A. Ruiz de Luzuriaga, A. Santamaria and I. Odriozola, *RSC Advances*, 2015, **5**, 17514-17518.
211. W. Brandt, M. Gürke, F. E. Köhler, G. Pabst, G. Schellenberg and M. Vogtherr, *Köhler's Medizinal-Pflanzen in naturgetreuen Abbildungen mit kurz erläuterndem Texte : Atlas zur Pharmacopoea germanica, austriaca, belgica, danica, helvetica, hungarica, rossica, suecica, Neerlandica, British pharmacopoeia, zum Codex medicamentarius, sowie zur Pharmacopoeia of the United States of America*, Fr. Eugen Köhler, 1887.
212. R. A. Backhaus, *Israel journal of botany*, 1985, **34**, 283-293.
213. N. Sfeir, T. Chapuset, S. Palu, F. Lançon, A. Amor, J. García García and D. Snoeck, *Industrial Crops and Products*, 2014, **59**, 55-62.
214. I. Gelling, *Rubber chemistry and technology*, 1985, **58**, 86-96.
215. S.-N. Gan and Z. A. Hamid, *Polymer*, 1997, **38**, 1953-1956.
216. D. R. Burfield, K. L. Lim and K. S. Law, *Journal of applied polymer science*, 1984, **29**, 1661-1673.
217. C. Baker, I. Gelling and R. Newell, *Rubber chemistry and technology*, 1985, **58**, 67-85.
218. I. R. Gelling, *British Pat 2113692*, 1982.
219. J. E. Davey and M. J. R. Loadman, *British polymer journal*, 1984, **16**, 134-138.
220. J. Bradbury and M. Perera, *Journal of applied polymer science*, 1985, **30**, 3347-3364.
221. A. Gent, *Transactions of the Faraday Society*, 1954, **50**, 521-533.
222. C. Davies, S. Wolfe, I. Gelling and A. Thomas, *Polymer*, 1983, **24**, 107-113.
223. M. Pire, *PhD. Thesis "Caoutchouc Naturel Epoxydé et Réticulation par les Acides Dicarboxyliques : Chimie, Cinétique et Propriétés Mécaniques"*, 2011, UPMC.
224. A. S. Hashim and S. Kohjiya, *Kautschuk Gummi Kunststoffe*, 1993, **46**, 208-213.
225. V. Tanrattanakul, B. Wattanathai, A. Tiangjunya and P. Muhamud, *Journal of applied polymer science*, 2003, **90**, 261-269.
226. T. Johnson and S. Thomas, *Polymer*, 1999, **40**, 3223-3228.
227. A. N. Bibi, D. A. Boscott, T. Butt and R. S. Lehrle, *European Polymer Journal*, 1988, **24**, 1127-1131.
228. S. N. Koklas, D. D. Sotiropoulou, J. K. Kallitsis and N. K. Kalfoglou, *Polymer*, 1991, **32**, 66-72.
229. S. D. Li, Y. Chen, J. Zhou, P. S. Li, C. S. Zhu and M. L. Lin, *Journal of applied polymer science*, 1998, **67**, 2207-2211.
230. Y. Heping, L. Sidong and P. Zheng, *Journal of thermal analysis and calorimetry*, 1999, **58**, 293-299.
231. B. Poh and K. Lee, *European Polymer Journal*, 1994, **30**, 17-23.
232. A. Sadequl, U. Ishiaku and B. Poh, *European Polymer Journal*, 1999, **35**, 711-719.
233. S. Varughese and D. K. Tripathy, *Polymer Degradation and Stability*, 1992, **38**, 7-14.
234. T. Johnson and S. Thomas, *Journal of Macromolecular Science-Physics*, 1997, **B36**, 401-416.

235. H. Chun and A. Gent, *Rubber chemistry and technology*, 1996, **69**, 577-590.
236. S. Tamura and K. Murakami, *Polymer*, 1980, **21**, 1398-1402.
237. I. Gelling and N. Morrison, *Rubber chemistry and technology*, 1985, **58**, 243-257.
238. M. Akiba and A. Hashim, *Progress in polymer science*, 1997, **22**, 475-521.
239. A. Hashim and S. Kohjiya, *Journal of Polymer Science Part A: Polymer Chemistry*, 1994, **32**, 1149-1157.
240. Y. W. Chang, J. K. Mishra, J. H. Cheong and D. K. Kim, *Polymer International*, 2007, **56**, 694-698.
241. A. S. Hashim, S. Kohjiya and Y. Ikeda, *Polymer International*, 1995, **38**, 111-117.
242. R. Alex, P. De and S. De, *Journal of Polymer Science Part C: Polymer Letters*, 1989, **27**, 361-367.
243. T. Lin, X. Zhang, Z. Tang and B. Guo, *Green Chemistry*, 2015.
244. L. Mascia, J. Clarke, K. S. Ng, K. S. Chua and P. Russo, *Journal of applied polymer science*, 2015, **132**.
245. F. M. Casati, H. R. Penaloza and F. W. Arbir, *US Patent 4431753 A*, 1984.
246. R. Dowbenko, C. Anderson and W.-H. Chang, *Industrial & Engineering Chemistry Product Research and Development*, 1971, **10**, 344-351.
247. S. Stolte, S. Abdulkarim, J. Arning, A.-K. Blomeyer-Nienstedt, U. Bottin-Weber, M. Matzke, J. Ranke, B. Jastorff and J. Thöming, *Green Chemistry*, 2008, **10**, 214-224.

**Chapitre 2**  
**Échange ou hydrolyse des ponts esters, avantages sur les**  
**réseaux permanents**

---



<b>Chapitre 2 : Échange ou hydrolyse des ponts esters, avantages sur les réseaux permanents .....</b>	<b>76</b>
<b>1. Dynamic network by transesterification, stress relaxation study .....</b>	<b>78</b>
1.1. Introduction .....	79
1.2. Experimental section .....	80
1.2.1. <i>Materials</i> .....	80
1.2.2. <i>Blend preparation</i> .....	81
1.2.3. <i>Characterization techniques</i> .....	81
1.3. Results .....	83
1.3.1. <i>DA-crosslinked ENR</i> .....	83
1.3.2. <i>Peroxide-crosslinked ENR</i> .....	85
1.3.3. <i>Adhesion enhancement</i> .....	89
1.4. Discussion .....	90
1.5. Conclusions .....	93
<b>2. Recyclability of DA-crosslinked ENR through ester hydrolysis .....</b>	<b>96</b>
2.1. Introduction .....	96
2.2. Experimental section .....	96
2.2.1. <i>Materials</i> .....	96
2.2.2. <i>Recycling procedure</i> .....	96
2.2.3. <i>Characterizations</i> .....	97
2.3. Results and discussion .....	97
2.3.1. <i>Re-crosslinking of the hydrolyzed material</i> .....	98
2.3.2. <i>NMR study</i> .....	99
2.3.3. <i>GPC results</i> .....	102
2.4. Conclusions .....	103
<b>References .....</b>	<b>104</b>

## Chapitre 2 : Échange ou hydrolyse des ponts esters, avantages sur les réseaux permanents

La nouvelle méthode de réticulation de l'ENR développée au laboratoire Matière Molle et Chimie par Myriam Pire (décrite au Chapitre 1) résulte en la création de fonctions  $\beta$ -hydroxy esters le long des chaînes d'ENR (Figure 1). Dans ce chapitre, nous nous proposons d'étudier cette réticulation sous un angle différent.

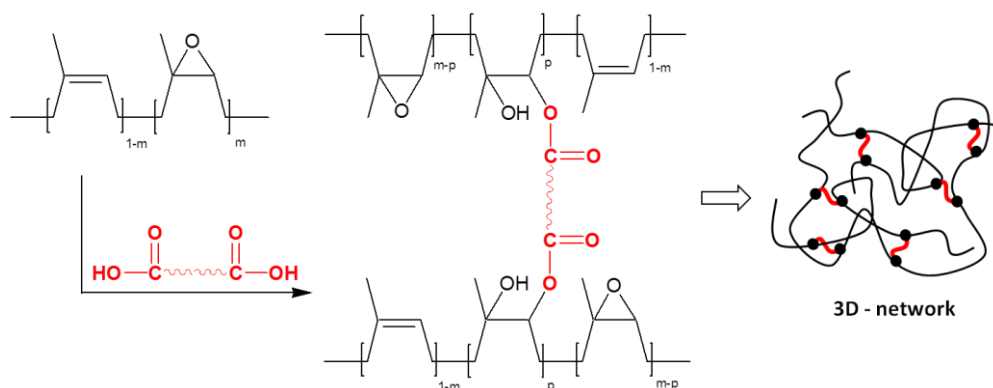


Figure 1. Réticulation de l'ENR par réaction de l'acide dodécanedioïque (DA).

En effet, une autre équipe du laboratoire a introduit récemment le concept de vitrimères, révolutionnant la vision classique de la séparation entre thermoplastiques et thermosets.<sup>1-3</sup> La réaction chimique ayant permis de développer les premiers vitrimères est la transestérification. Activée par la température et la présence d'un catalyseur adapté, cette réaction permet des échanges de liaisons au sein du réseau ; le matériau vitrimère devient totalement malléable et recyclable mais pourtant toujours insoluble en bon solvant (Figure 2). La topologie du réseau est modifiée au cours de la réaction, mais le nombre de points de réticulation et la fonctionnalité moyenne du réseau restent constants, ce qui est la clef des propriétés innovantes du vitrimère. La forme du matériau est fixée à basse température car les réactions d'échange sont très lentes et la topologie du réseau est bloquée. La réticulation de l'ENR par des diacides produisant des liens esters et des fonctions hydroxyles, on pourrait penser obtenir un matériau vitrimère par transestérification.

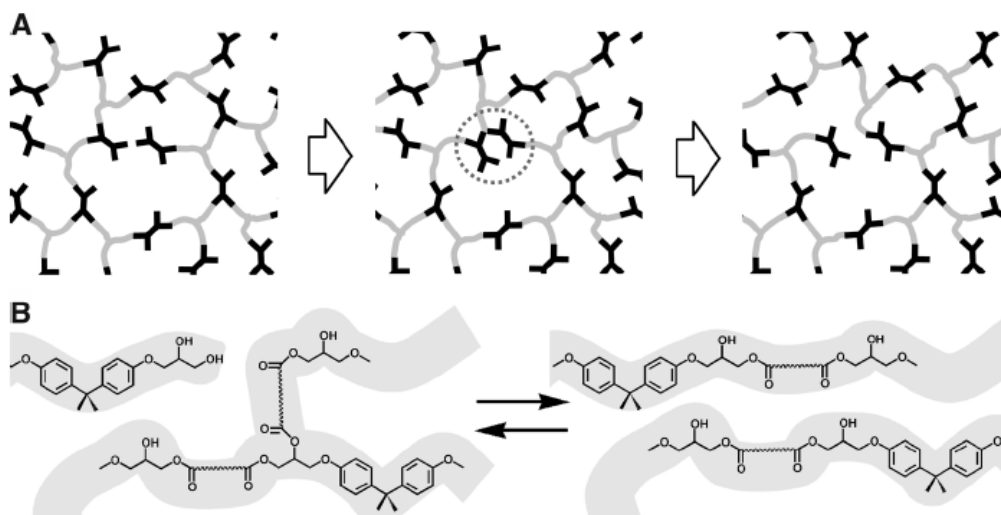


Figure 2. Transestérification dans les matériaux vitrimères époxy-acide (adapté de Montarnal et al.<sup>1</sup>).

Des propriétés de réparation ont été reportées pour des caoutchoucs réticulés de manière permanente, mais présentant une faible densité de réticulation.<sup>4</sup> La chimie vitrimère, grâce à des réactions d'échange bien contrôlées, permet également d'obtenir ce type de comportement.<sup>2</sup> La première partie de ce chapitre sera consacrée à l'étude des avantages de la chimie vitrimère sur ces réseaux permanents faiblement réticulés, en termes de relaxation de contrainte et d'adhésion. Cette étude est rédigée sous la forme d'un article « On the Advantages of the Vitrimer-Like Transition in Crosslinked Rubbers ».

Outre leur potentiel de transestérification, les esters sont également connus pour réagir relativement facilement avec l'eau dans certaines conditions acido-basiques pour donner l'acide carboxylique (ou l'ion carboxylate) et l'alcool correspondants. Cette fragilité du lien ester offre une possibilité unique de recyclage du réseau chimique par dissolution dans un bon solvant. Le recyclage du matériau par hydrolyse des esters sera étudié dans la deuxième partie du chapitre.

# 1. Dynamic network by transesterification, stress relaxation study

## On the Advantages of the Vitrimer-Like Transition in Crosslinked Rubbers

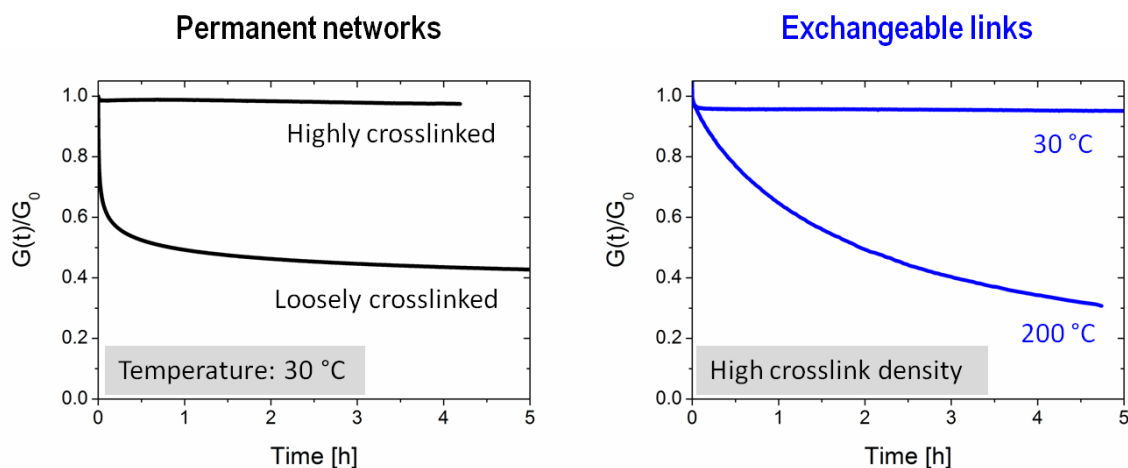
by Lucie Imbernon, Sophie Norvez and Ludwik Leibler

*Matière Molle et Chimie, ESPCI ParisTech - CNRS, UMR-7167, PSL Research University.*

*To be submitted*

### Abstract

To get intrinsic adhesion or healing properties in a crosslinked rubber, two levers are possible: the inherent relaxation in permanently but lightly crosslinked elastomers or the relaxation due to exchange reactions as recently reported in the case of vitrimers. The former is associated with dangling chain diffusion and cannot be controlled. Lightly crosslinked rubbers may show interesting adhesion and healing properties, but at the expense of mechanical properties: ultimate properties are limited and materials are subjected to creep even at low temperature. Conversely, exchange reactions may be triggered by temperature, providing the healable materials with strong elastomeric properties in a wide temperature range. Here a model system based on epoxidized natural rubber is presented which enables to differentiate and quantify the part of each process. A comparative study including stress relaxation, swelling experiments and adhesion measurements highlights the advantages of the vitrimer chemistry on inherent relaxation as a proof of concept.



## 1.1. Introduction

Permanently crosslinked elastomeric materials present a well-known long term stress relaxation which depends on the density of crosslinks.<sup>5</sup> This relaxation has been extensively studied in relation with the topology of the network and theories have emerged.<sup>6-9</sup> It is thought to be due to the diffusion of dangling chains and defects by reptation. The lower the crosslink density, the higher this effect. A low crosslink density thus appears as an efficient lever to produce healable materials, as molecular mobility of the free chain ends facilitates interdiffusion. Taking advantage of this process, a self-healing peroxide-vulcanized rubber system can be obtained, the healing ability being allowed only by the diffusion of dangling chains and defects.<sup>4</sup> Yet, too low crosslink densities are also responsible for poor mechanical properties and creep at room temperature. If crosslink density is increased, the self-healing capacity rapidly decreases and then disappears.<sup>4</sup> Lightly crosslinked rubbers are thus of little practical use.

Vitrimers, discovered by Leibler and co-workers a few years ago, are chemically crosslinked networks that can rearrange by exchange reactions while keeping the number of crosslinks constant.<sup>1</sup> The first exchangeable links were ester bonds, but other chemistries were then reported.<sup>1, 3, 10-13</sup> With this design, materials are fully processable and mendable but stay insoluble even under heating in a good solvent. The malleable vitrimer objects can be worked out above the vitrimer transition and the shape is quenched by slowing down the exchange reactions at low temperature. This new class of polymeric material combines advantageous properties of both thermoplastics and thermosets: chemically crosslinked vitrimer materials can be completely recycled, healed or mended.

In this manuscript, we propose to make a quantitative comparison of both processes: vitrimer-like exchanges and crosslink density effect. The study is performed in the case of natural rubber derivatives. Natural rubber (NR) is a material of great interest because of outstanding properties obtained after crosslinking. Like all thermosets, NR is usually crosslinked by permanent bonds and can no longer be reshaped or welded after curing. Nowadays, there is no satisfactory way to recycle NR: most of waste rubber is discarded in landfills, or out of use objects are reduced into powders used as fillers for virgin NR.<sup>14</sup> A rubber capable of mending or recycling would be of major industrial interest.

Different ways may be envisioned to obtain a vitrimer-like rubber. Since NR presents reactive double bonds, olefin metathesis could be considered to introduce adaptive properties

in rubber networks.<sup>11, 15</sup> However, the exceptional mechanical properties of NR are linked to the well-defined stereochemistry of the macromolecules: all units are in the *cis* configuration, allowing for strain induced crystallization.<sup>16</sup> Olefin metathesis, as a probable source of *cis-trans* isomerization,<sup>17, 18</sup> would impair the mechanical properties of the material. A vitrimer-like behaviour could alternatively be obtained through transesterification reactions in ester-containing natural rubber networks. Our group recently showed that epoxidized natural rubber (ENR, a unique elastomer retaining most of the properties of NR from which it derives<sup>19, 20</sup>) could be efficiently crosslinked using dicarboxylic acids.<sup>21, 22</sup> This new type of crosslinking, which produces  $\beta$ -hydroxy esters along the chain,<sup>23</sup> competes with standard sulphur or peroxide vulcanizations<sup>24, 25</sup> and also offers the opportunity to create reprocessable rubbers by introduction of functional diacid crosslinkers,<sup>26</sup> or semi-interpenetrated networks by blending and selective crosslinking.<sup>27</sup> When combined with a transesterification catalyst, these ester containing networks could provide the crosslinked rubber with vitrimer-like properties. To compare with a reference network and probe the effect of crosslink density, ENR was alternatively crosslinked with peroxides, what creates stable carbon-carbon bonds and leads to a permanent network.

Quantitative stress relaxation and adhesion measurements are used to compare both processes. The relaxation study highlights the difference in characteristic times between a slow exchangeable chemistry and the physical effects of the crosslinking density. Lightly crosslinked networks show some adhesion at room temperature at the expenses of the mechanical properties, but increasing the crosslink density impedes the adhesion properties which are due to defects and dangling chain ends. Vitrimer chemistry brings the opportunity to develop strong networks showing high crosslink densities and still adaptable.<sup>10</sup>

## 1.2. Experimental section

### 1.2.1. Materials

ENR25, containing 25 mol% epoxy groups, kaolin and dicumyl peroxide (DCP) were kindly provided by Hutchinson SA Research Center, France. The kaolin used in the formulations was Polestar 200R. DCP is supported on calcium carbonate (40 wt% of active product). Dodecanedioic acid (DA, 99 %, Acros), 1,2-dimethylimidazole (DMI, 98 %, Sigma-Aldrich) and zinc acetate dihydrate ( $\text{Zn}(\text{OAc})_2 \cdot 2\text{H}_2\text{O}$ , 98-101 %, Alfa Aesar) were all used as received.

### 1.2.2. Blend preparation

Mixtures of ENR25, DA (3.2 phr: parts per hundred parts of rubber by weight), DMI (2.7 phr) and  $\text{Zn}(\text{OAc})_2$  were masticated in a Haake Polydrive mixer at 40 °C for about 17 minutes, following a protocol already described.<sup>22</sup> During mixing the temperature increases to about 70 °C. DMI, liquid in the mixing conditions (mp  $\approx$  38 °C), was premixed with kaolin (1:2 w/w), an inert filler, to facilitate its incorporation into the rubber. After blending, samples were cured in a CARVER press under 8 tons pressure at 180 °C for the appropriate time (determined by rheology experiments, 40 or 45 min).

A mixture of ENR25 and DCP was prepared in the same conditions. The resultant reactive blend contains 6 phr of supported DCP.

### 1.2.3. Characterization techniques

*Curing:* The cross-linking process was followed using an Anton Paar MCR 501 rheometer in plate-plate geometry (25-mm diameter, 1 Hz frequency, 0.1 % strain). Samples of 26-mm diameter were cut in 1.5 mm thick uncured sheets of rubber pressed for 5 min at 80 °C. To ensure a good contact between the rubber disc and the plates, an axial force of 20-30 N was first applied to the sample for about 15 minutes before the experiment. The axial force was then maintained to 2 or 5 N by adjusting the gap during the experiment. In these conditions, results of the measurements were comparable with the ones obtained in a Moving Die Rheometer.<sup>21</sup> The temperature was raised from 30 °C to 150 or 180 °C at 1 °C.s<sup>-1</sup>, and then the sample was left under oscillatory shear at this high temperature for curing. Every step of the curing process is conducted under a nitrogen atmosphere to prevent oxidation.

*Frequency sweep:* The samples (uncured or fully cured inside the rheometer) were submitted to a frequency ramp from 0.01 to 15 Hz (5 points per decade) under constant temperature, strain ( $\gamma = 0.1$  %) and normal force (2 N to ensure a good contact between the rubber disc and the plates).

*Stress relaxation:* Stress relaxation experiments were conducted in the rheometer right after crosslinking the sample, under nitrogen atmosphere. After 15 min of temperature equilibration from the curing temperature to the chosen temperature, a 1 % strain step was applied and the resulting stress was monitored over time. The good contact between the plates and the geometry is insured by the *in situ* curing process.

*Mechanical properties:* Stress-strain behaviour was studied using an Instron machine with a crosshead speed of  $500 \text{ mm}\cdot\text{min}^{-1}$ , until break. Dumbbells of 25 mm effective length and 4 mm width were cut in a 1.5 mm thick cured rubber sheet. At least five samples were run for each blend. Strain was followed using a video extensometer.

*Adhesion procedure:* For ENR-DA samples, cured sheets were cut into pieces of 100x45 mm. Two pieces of the same material were put in contact and tightened in a home-made system (Figure S1a) that compresses the two sheets together over a length of 50 mm. The intensity of the compression was kept constant between different samples through controlling the displacement of the upper part of the system. The strain thus depends on the initial thickness of the rubber sheets (between 30 and 40 % in our case). This set-up was then placed under vacuum at 200 °C for 3.5 hours. The adhered sheets are cooled down and at least five samples (5x100 mm) are cut for T-peel experiments. These samples present an adhered zone and a free zone of 50 mm length each as shown in Figure S1b. Several T-peel samples were tested for each material.

For ENR-DCP samples, the cured rubber was cut into rectangular strips (5x100 mm). Two strips were superimposed and tightened in the same home-made system (strain was also around 30 to 40 %). The set up was left at room temperature during 3.5 hours without controlling the atmosphere. Three T-peel samples were tested for each material (same geometry than ENR-DA T-peel samples).

*T-peel experiments:* The samples are peeled apart symmetrically by pulling the free zone ends in opposite directions in an Instron machine. The peel rate was  $100 \text{ mm}\cdot\text{min}^{-1}$  and the peel strength (load/width) was taken as the average plateau of the peel strength-strain curve (N/m).

*Swelling measurements:* Disc samples of 5 or 7 mm-diameter cut in 1.5 mm thick sheets of cured rubber were immersed in chloroform. Their weight was followed over time till equilibrium swelling. Samples were then dried and weighted again to determine the sol fraction.

### 1.3. Results

#### 1.3.1. DA-crosslinked ENR

Three different materials were prepared containing varying percentages of  $\text{Zn}(\text{OAc})_2$  (0, 10 and 20 mol% compared with the number of acid functions). The amount of diacid in all cases corresponds to one DA molecule per 100 monomers, *i.e.* one per 25 epoxy groups for ENR25, and the quantity of DMI was in stoichiometry with acid functions. Considering that the diacid fully reacts, this insured a same level of crosslinking in the three materials.

The crosslinking kinetics of the blends were followed by the evolution of the elastic modulus  $G'$  when heating at 180 °C in the rheometer (Figure 3). During the rapid heating ramp,  $G'$  first decreases because the rubber softens. Then the sudden  $G'$  increase shows the beginning of the crosslinking reaction. For sample ENR-DA0, containing 0 %  $\text{Zn}(\text{OAc})_2$ , a plateau is reached in about 40 minutes showing that the reaction with the diacid is complete. This was also checked in a previous work by solid NMR.<sup>23</sup> By addition of 10 %  $\text{Zn}(\text{OAc})_2$  (sample ENR-DA1), the same shape of crosslinking curve is observed, with a plateau about 10 % lower. With the highest percentage of catalyst (ENR-DA2), the  $G'$  modulus is even lower.

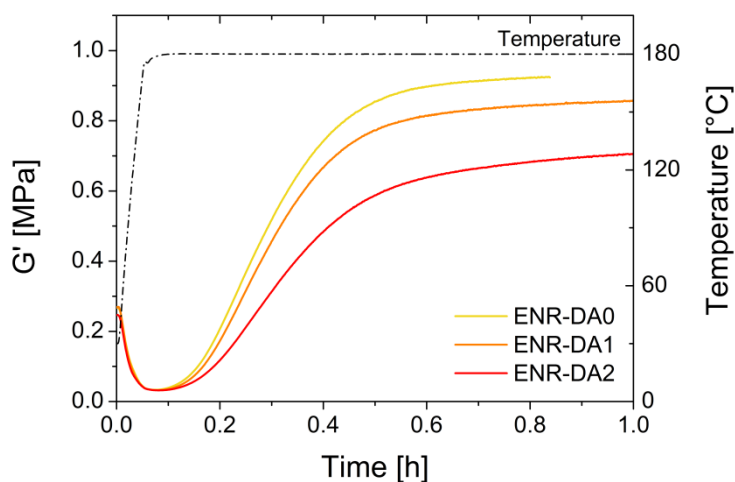


Figure 3. Crosslinking kinetics of ENR25/DA/ $\text{Zn}(\text{OAc})_2$  blends are followed in the rheometer

We previously showed that the plateau value varied linearly with the crosslinking density of the material (Figure S2).<sup>21</sup> Here the plateau value evolution indicates that the crosslink density decreases with increasing quantities of  $\text{Zn}(\text{OAc})_2$ . This is likely due to  $\text{Zn}^{2+}$  ability to complex

the carboxylic acid functions, preventing DA from reacting with epoxy sites. The crosslink densities of the three samples, cured 40 minutes for 0 and 10 mol% of  $\text{Zn}(\text{OAc})_2$  and 45 minutes for 20 mol% according to rheological measurements (time to attain 98 % of the modulus at 1 hour) were compared by swelling measurements in chloroform, a good solvent for ENR. The mass swelling ratios defined as  $Q_m = \frac{m_s - m_d}{m_d}$  are  $8.4 \pm 0.1$ ,  $9.2 \pm 0.1$  and  $9.9 \pm 0.1$  for sample ENR-DA0, -1 and -2, respectively.  $m_s$  is the mass of the swollen sample and  $m_d$  its de-swollen mass. This measurement confirms that the crosslink densities of the three samples are slightly different. In each case the sol fraction is low: between 4 and 5 %.

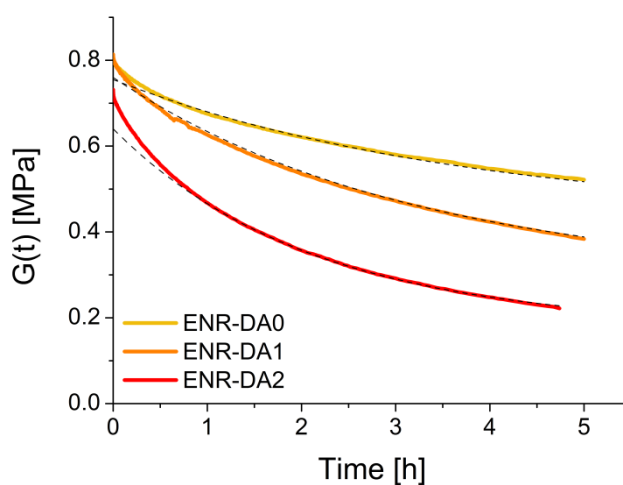


Figure 4. Stress relaxation experiments at 200 °C in DA-crosslinked ENR

The stress relaxation behaviour of the materials was tested at 200 °C in the rheometer after *in situ* curing. The temperature was first equilibrated for 20 minutes at 200 °C. The relaxation moduli  $G(t)$  are plotted in Figure 4. The curves can be fitted at long times with Equation (1).

$$G(t) = y_0 + Ae^{-\frac{t}{t_0}} \quad (1)$$

Fit parameters are gathered in Table 1. The  $t_0$  time, which decreases with the quantity of catalyst, is proportional to the characteristic time of transesterification. Without catalyst, transesterification reaction is very slow, the relaxation time is as long as  $t_0 \approx 4$  hours. By addition of 20 mol% catalyst, this time is divided by two, but is still very long compared with the Maxwell relaxation time in epoxy-acid vitrimers catalyzed by zinc at comparable temperatures (25 minutes at 190 °C).<sup>1</sup>

Table 1. Parameters of the stress relaxation fit according to Equation (1)

Sample	$y_0$ [MPa]	A [MPa]	$t_0$ [h]
<b>ENR-DA0</b> (0 mol% Zn(OAc) <sub>2</sub> )	0.43	0.325	3.8
<b>ENR-DA1</b> (10 mol% Zn(OAc) <sub>2</sub> )	0.29	0.47	3.2
<b>ENR-DA2</b> (20 mol% Zn(OAc) <sub>2</sub> )	0.18	0.46	2.1

Stress relaxation was tested at different temperatures for the sample containing the highest quantity of catalyst (ENR-DA2, Figure 5). No relaxation occurred at 30 or 120 °C, the temperature is not high enough, and the topology of the network is frozen. The initial relaxation modulus increases with temperature, in accordance with the typical increase of shear modulus with temperature in rubbery materials.<sup>28</sup>

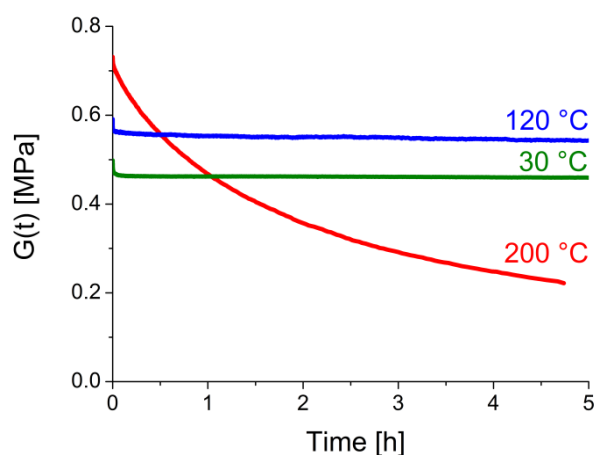


Figure 5. Stress relaxation in ENR-DA2 at different temperatures

### 1.3.2. Peroxide-crosslinked ENR

The crosslinking reaction of ENR25 by DCP was followed by rheological measurements (Figure 6). The crosslinking time of the reactive blend was varied from 500 to 4200 seconds, to get vulcanizates with different crosslink densities. After the desired time at 150 °C, temperature was quickly decreased to 30 °C to stop the crosslinking process. The plateau moduli of each sample at 30 °C are collected in Table 2. The samples are named ENR-DCPi where the i index increases with the crosslinking time at 150 °C in the rheometer: 500, 700, 900, 1300, 1700 and 4200 seconds (the latter is fully crosslinked:  $G'$  reached a plateau). The

crosslinked samples were swollen in chloroform till equilibrium and then dried. This allowed to calculate the sol fraction and the equilibrium mass swelling ratio  $Q_m$ . The crosslink density varies conversely to  $Q_m$ . The data collected in Table 2 show an evolution of the crosslink density. The longer the crosslinking time, the higher the crosslink density and the lower the sol fraction of the sample.

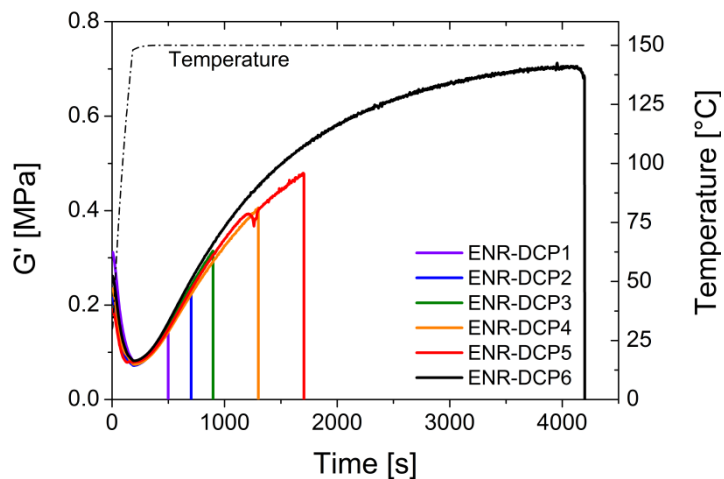


Figure 6. Vulcanizates at different degrees of crosslinking are obtained by varying the peroxide-curing time at 150 °C.

Table 2. Crosslink data for ENR-DCP samples cured for different times.

Sample	ENR-DCP1	ENR-DCP2	ENR-DCP3	ENR-DCP4	ENR-DCP5	ENR-DCP6
Crosslinking time [s]	500	700	900	1300	1700	4200
Plateau modulus after equilibration at 30 °C [MPa]	0.31	0.315	0.34	0.37	0.43	0.55
Equilibrium mass swelling ratio $Q_m$	44	21	16	13	11	9
sol fraction wt%	18.5	7.1	5.5	4.4	4.0	2.8

Right after crosslinking in the rheometer, the samples were submitted to stress relaxation measurements. The temperature of stress relaxation was fixed to 30 °C to avoid degradation by high temperature. The relaxation modulus of each sample is plotted against time in Figure 7. The Chasset and Thirion's law (Equation (2))<sup>5</sup> was used to fit the data, permitting a

quantitative comparison of the different samples. The corresponding parameters are listed in Table 3. The empirical law was found to be in very good agreement with our data (*Figure 7a*).

$$G(t) = G_{\infty} \left[ 1 + \left( \frac{t}{\tau_0} \right)^{-m} \right] \quad (2)$$

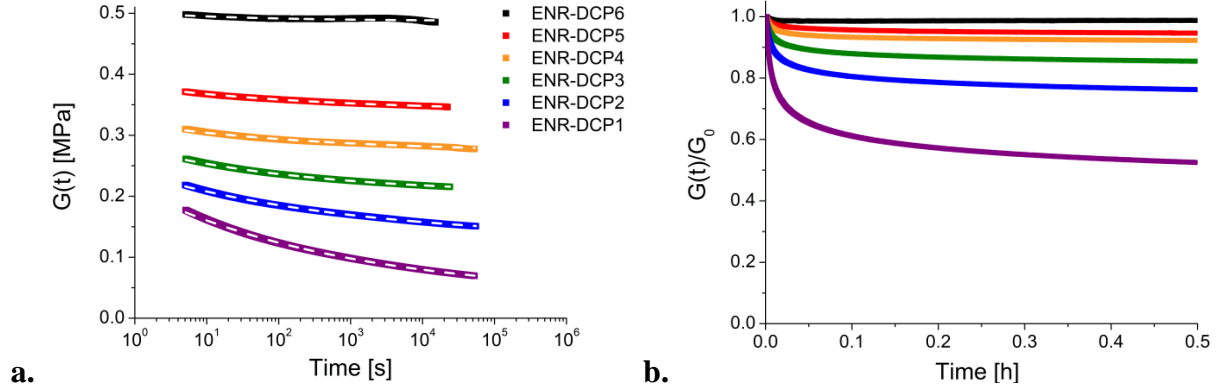


Figure 7. Stress relaxation experiment at 30 °C; **a.** semi-logarithmic representation (white slashes: fit of the curves with the Chasset-Thirion experimental law) **b.** linear reduced representation.

Table 3. Fit parameters for the Chasset and Thirion's law

Sample	$G_{\infty}$ (MPa)	$\tau_0$ (s)	$m$
ENR-DCP1	0.05	$6 \cdot 10^4$	0.149
ENR-DCP2	0.15	$4 \cdot 10^{-1}$	0.14
ENR-DCP3	0.20	$4 \cdot 10^{-3}$	0.175
ENR-DCP4	0.25	$2 \cdot 10^{-5}$	0.16
ENR-DCP5	0.35	$3 \cdot 10^{-6}$	0.163
ENR-DCP6	0.50	$9 \cdot 10^{-7}$	0.256

The stress relaxation data can be superimposed onto a single master curve (Figure 8) by applying a time-crosslink density reduction with a reduction constant  $a_v$  (Equation (3)):<sup>6</sup>

$$a_v = \left( \frac{v}{v_0} \right)^{-2/m} \quad (3)$$

$v_0$  is the reference density (chosen as the crosslink density of sample ENR-DCP3) and  $m$  is the Chasset-Thirion parameter for the same reference sample ( $m = 0.175$ , Table 3).

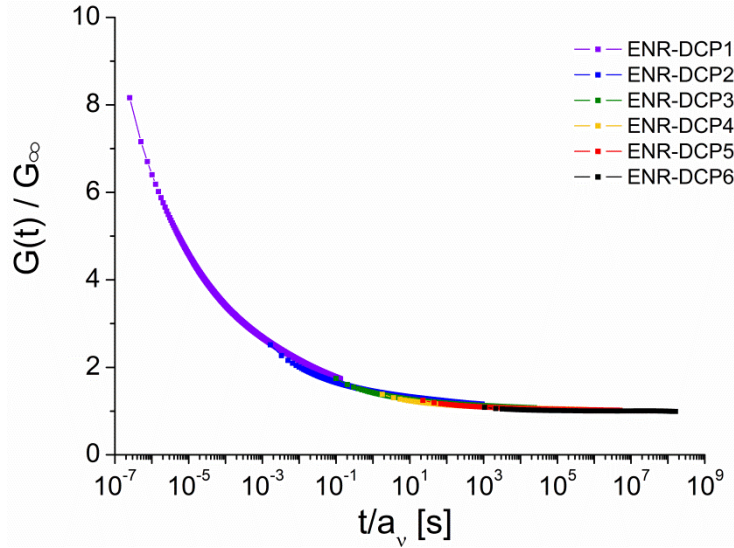


Figure 8. Time-crosslink density superposition of the relaxation data for ENR-DCPi

The stress relaxation fits permit to obtain the relaxation modulus in a fully relaxed state  $G_{\infty}$ . This modulus is directly linked to the number of crosslinks and should not include the entanglements and network defects that have already relaxed. In a first approximation, the crosslink density  $\nu$  of the different samples is thus calculated using the relation (4), where  $\rho$  is the density of the rubber and  $M_c$  the molecular mass between crosslinks.

$$\nu = \frac{\rho}{M_c} = \frac{G_{\infty}}{RT} \quad (4)$$

Frequency sweeps at different temperatures were performed on the uncured material, and a master curve could be obtained by time-temperature superposition with a reference temperature of 30 °C (Figure 9). The data at 160 °C do not superimpose because at this temperature, the peroxide was activated and the crosslinking reaction started. From Figure 9, we can extrapolate a plateau value of  $G_N^0 = 0.17$  MPa for the uncrosslinked material. This enables the calculation of a molar mass between entanglements,  $M_e = \frac{\rho RT}{G_N^0} \approx 14\,000$  g.mol<sup>-1</sup>.  $T$  is the temperature,  $R$  the gas constant, and  $\rho$  the density of the rubber ( $\rho \approx 0.97$  for ENR25). Since rubber chains are very long (about 10<sup>6</sup> g.mol<sup>-1</sup> for this bio-based polymer), the polymer is considerably entangled despite the high value of  $M_e$ . This is also supported by the fact that  $G'$  and  $G''$  do not cross at low frequency: the uncrosslinked polymer chains are too long and entangled to flow.

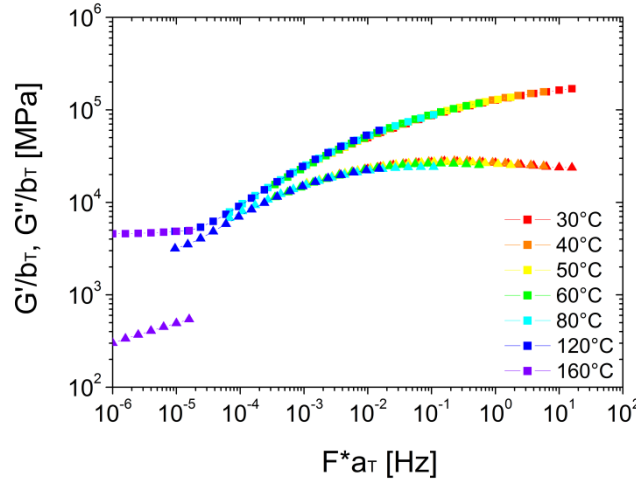


Figure 9. Time-temperature superposition for the uncured reactive blend.  $G'$ : ■,  $G''$ : ▲.  $a_T$  was found to follow a Williams-Landel-Ferry law and  $b_T$  stays relatively close to the unity ( $T_{ref} = 30\text{ °C}$ ).

### 1.3.3. Adhesion enhancement

For samples ENR-DA0, -1, -2, T-peel tests were conducted as described in the experimental part. The force needed to peel the samples was measured. An average of this force divided by the width of the sample was then calculated to evaluate the detachment energy  $G_a$  according to formula (5):<sup>29</sup>

$$G_a = 2 \frac{F}{w} \quad (5)$$

The obtained values of detachment energy are plotted against catalyst content in Figure 10a. The presence of 10 mol% catalyst largely doubles the adhesion energy. With 20 mol% catalyst, this energy is multiplied by a factor five. The catalyst significantly improves the interfacial adhesion of crosslinked ENR. It is worth noticing that 20 mol% of catalyst represents only 1 wt% of  $\text{Zn}(\text{OAc})_2 \cdot 2 \text{H}_2\text{O}$ .

The same T-peel tests were conducted on samples ENR-DCP1, 3 and 6. Here the adhesion step was done at room temperature to prevent any further peroxide crosslinking and thus to test the adhesion resulting only from chain and defects interdiffusion. The corresponding detachment energy is plotted against decreasing crosslink densities in Figure 10b. The detachment energy varies by a factor 10 by decreasing the crosslinking time from 4200 to 500 s, which decreases the crosslink density. For a highly crosslinked sample (ENR-DCP6), there is almost no adhesion between the two pieces of rubber. When the crosslink density decreases, the detachment energy increases up to 140 J/m<sup>2</sup>, still lower than the values obtained for the samples showing vitrimer exchanges at high temperatures.

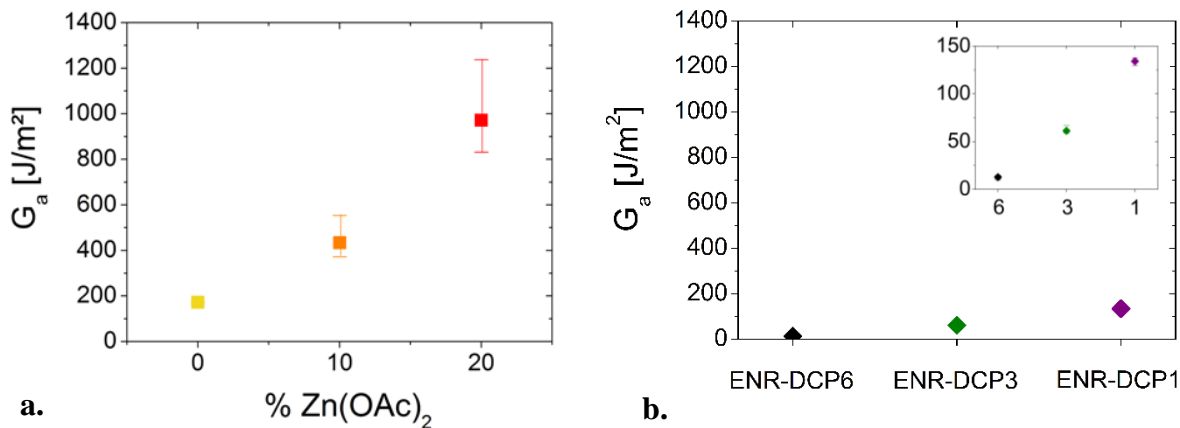


Figure 10. **a.** Adhesion at 200 °C for ENR-DA samples with varying catalyst concentration (in mol%). **b.** Adhesion at room temperature for ENR-DCP samples with decreasing crosslink densities (zoom in inset).

## 1.4. Discussion

Complete stress relaxation is a major feature of adaptable materials. However, in the stress relaxation behaviour of a material, a non negligible part of the degree of crosslinking may be involved. To assess the effect of the crosslink density on stress relaxation of ENR, model networks composed of ENR crosslinked by dicumyl peroxide (DCP) were prepared. Using DCP, the crosslinks are permanent carbon-carbon bonds. The effect of the crosslink density on stress relaxation at 30 °C was investigated by varying the curing time. Viscoelastic behaviour of elastomers has long ago been studied in relation with the topology of the network. In the early 60's, Chasset and Thirion pointed out a long term relaxation of rubbery materials and proposed a law (Equation (2)) that fitted their experimental data on natural rubber crosslinked by peroxides.<sup>5</sup> More theoretical studies were conducted by Ferry who suggested that branched structures in the presence of entanglements were responsible for the very long term relaxation.<sup>8</sup> The branched structures are supposed to relax slowly because of topological constraints (entanglements). Then, de Gennes introduced the concept of reptation.<sup>7, 30</sup> According to his theory, reptation is the way a dangling chain can reach equilibrium when put in a perturbed state. The first molecular interpretation of the long term relaxation of elastomers was given by Curro and Pincus.<sup>6</sup> Their theory was based on the reptation of dangling chain ends in a crosslinked entangled network. Assuming that the stress

due to a dangling chain of length  $n$  is proportional, not to the part that has relaxed as de Gennes postulated, but to the part which has not relaxed, Curro and Pincus were able to extract an equation identical to Equation (2). Our relaxation data on ENR-DCP samples nicely fit this equation, indicating that, as for other properties, ENR retains the relaxation behaviour of NR from which it derives. The Table 3, collecting the fitting parameters, permits a comparison between samples. First, the longer the curing time, the higher the crosslink density (this was also checked by swelling measurements, Table 2).  $G_{\infty}$  increases of about one order of magnitude with the crosslink density. This is related to the amount of dangling chains but also with the amount of uncrosslinked chains (the soluble fraction of the samples that is decreasing with the crosslinking time, Table 2). Secondly, the values of the relaxation times  $\tau_0$  are in agreement with the data found in the literature on natural rubber.<sup>9,31</sup> The evolution of  $\tau_0$  is consistent with the supposed role of dangling ends. The longer the time of crosslinking at 150 °C, the shorter the dangling chains. The time of reptation through the network is supposed to increase with the length of the chain and this phenomenon is at the origin of the observed stress relaxation. Finally, as long as the rubber is not fully crosslinked, the parameter  $m$  is approximately constant ( $m \approx 0.17$ ). It does not depend linearly on crosslink density as predicted by Curro and Pincus's theory. Besides, a time-crosslink density reduction can be applied to obtain a superposition of the data at different crosslink densities.<sup>32</sup> It was reported that such a superposition is incompatible with a linear dependence of  $m$  on the crosslink density.<sup>9</sup> In our case, the data superimpose satisfactorily in the time-crosslink density reduction (Figure 8), in accordance with the constancy of the  $m$  factor.

In this study, ENR crosslinked with dicarboxylic acids was expected to behave as an adaptable network thanks to transesterification reactions. DMI was added as an esterification accelerator for crosslinking and  $\text{Zn}(\text{OAc})_2$  as the transesterification catalyst, known to be efficient in already described epoxy-acid vitrimer systems.<sup>3</sup> A well crosslinked material was obtained in each case (samples ENR-DA0, -1 and -2) as confirmed by rheology (a  $G'$  plateau around 1 MPa is reached, ranking the material among standard unfilled industrial rubbers) and by swelling experiments (samples swell but do not dissolve in a good solvent). Stress relaxation was performed to evaluate the adaptability of the network at high temperature (Figure 4). Some relaxation is observed, but the relaxation modulus does not go down to zero even after several hours. If the only crosslinks were ester bonds able to exchange quickly like in vitrimer systems,<sup>1,10</sup> the modulus should decrease to zero. The transesterification exchange is thus limited in our material. The lack, and low reactivity of free hydroxyl groups, could explain the slowness of the reaction. Indeed, the only available hydroxyl functions are

obtained by opening of the epoxy groups. We previously showed that such ring opening was stereoselective in our system,<sup>23</sup> so most of the hydroxyl groups are hindered by a methyl group (Figure 11) and therefore few available for exchanges. As the hydroxyl functions have a crucial importance in transesterification-based vitrimers,<sup>10</sup> here the scarcity of free hydroxyl groups impedes the exchange process.

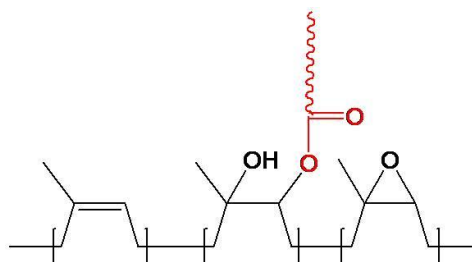


Figure 11. Stereoselective opening of ENR epoxy groups by carboxylic acids gives rise to hindered hydroxyl groups.

ENR is also known to undergo some oxidation reactions at elevated temperatures that could be source of permanent crosslinks (other than esters).<sup>33</sup> The stress relaxation curves are correctly fitted at long times by addition of a constant part to a Maxwell model (Equation (1), Table and Figure 4). This constant, which can be associated to secondary reactions, decreases as the concentration of catalyst increases. Transesterification goes faster in the presence of catalyst, so permanent links start forming in a more relaxed state, giving rise to a lower constant.

The mass swelling ratio measured for the three ENR-DA samples in the same solvent than for the ENR-DCP samples (chloroform) are in between 8 and 10, which is comparable to samples ENR-DCP5 and -6 (the more crosslinked ones). The low sol fraction (4-5 %) also attests high crosslink density of ENR-DA samples. The effect of the density of crosslinks on the stress relaxation of the ENR-DA samples is thus negligible. Therefore the significant relaxation in ENR-DA is not due to the diffusion of dangling ends and can be attributed to transesterification exchanges. In *Figure 7b*, it is clear that the most important effect of the crosslink density on stress relaxation appears at short times (< 0.1 hour). Conversely, the relaxation observed in ENR-DA samples is distributed all over the time scale studied, and the characteristic times associated to transesterification are long (a few hours, Figure 4). In ENR-

DA system, the characteristic times related either to the crosslink density (physical effect) or to the transesterification reaction (dynamic covalent chemistry) may be well separated.

The DA-crosslinked samples were shown to be highly crosslinked networks, whose stress relaxation is not complete even at high temperature in presence of a transesterification catalyst. Therefore, the material is unlikely to show full processability like vitrimers. Nevertheless the material relaxes considerably at 200 °C, and even better in the presence of the catalyst owing to transesterification reactions. Such rearrangements promote thermally triggered adhesion between pieces of rubber. Adhesion tests show that only 1 wt% catalyst indeed increases significantly the adhesion energy.

## 1.5. Conclusions

The effect of crosslink density on elastomeric stress relaxation was studied within a permanent model network of epoxidized natural rubber (peroxide-cured). Low degrees of crosslinking give rise to significant relaxation at room temperature, due to the diffusion of dangling chains. The characteristic times of this physical relaxation are estimated to be < 0.1 hour for most samples.

In parallel, ENR was fully crosslinked with dodecanedioic acid (DA) to obtain an ester-containing network. In presence of a transesterification catalyst, DA-cured samples exhibit a large stress relaxation at high temperature. Contrarily to peroxide-cured ENR, no sharp decrease of the modulus is observed at short times, but the relaxation is distributed over a large period of time. Compared swelling experiments between peroxide- and diacid-cured ENR samples show that physical relaxation is negligible in highly crosslinked ENR-DA systems. The large stress relaxation is due to transesterification reaction at high temperatures, whose characteristic time ( $\approx$  2-3 hours) is much longer than the observed effect of crosslink density. Since the transesterification reaction is slower in ENR than in classical vitrimers, our system enables distinction between both characteristic times.

Zinc acetate catalyst promotes the relaxation dynamics of the crosslinked rubber, improving self-adhesion of the rubber at high temperature. Addition of only 1 wt% of catalyst increases the detachment energy by a factor of five. An interesting compromise is reached: at

room and moderate temperatures the rubber exhibits great mechanical properties without undesired creeping whereas at high temperatures it shows adhesion and potential healability.

This ENR system cannot be considered as a true vitrimer system since secondary reactions make it inadequate for full reprocessing; another chemistry should be conceived. Nevertheless, the presented results should be understood as a proof of principle of the interest of vitrimer chemistry in the design of new rubbers combining temperature and catalyst controlled healability with strong elastomeric properties at working temperatures.

**Acknowledgements:** This work was founded by the French government, Department of Higher Education and Research (L. Imbernon). The authors gratefully thank Benoît le Rossignol from Hutchinson SA, Montargis Research Center, France for the gift of ENR25. Erwan Chabert is warmly thanked for his help in sample preparation for T-peel tests.

Supplementary information

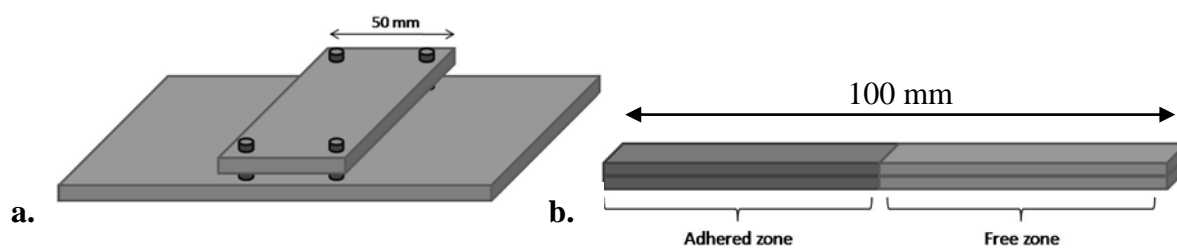


Figure S1. **a.** Set-up for preparation of adhered samples. **b.** T-peel samples.

The composition of the materials is summarized in Table S1.

Table S1. Composition of the samples (phr: parts per hundred rubber).

Sample name	ENR-DA0	ENR-DA1	ENR-DA2
ENR	100	100	100
DA	3.2	3.2	3.2
DMI	2.7	2.7	2.7
Kaolin	5.4	5.4	5.4
Zn(ac) <sub>2</sub> mol% <sup>a</sup>	0	10	20

<sup>a</sup> molar percent compared with the number of diacid functions

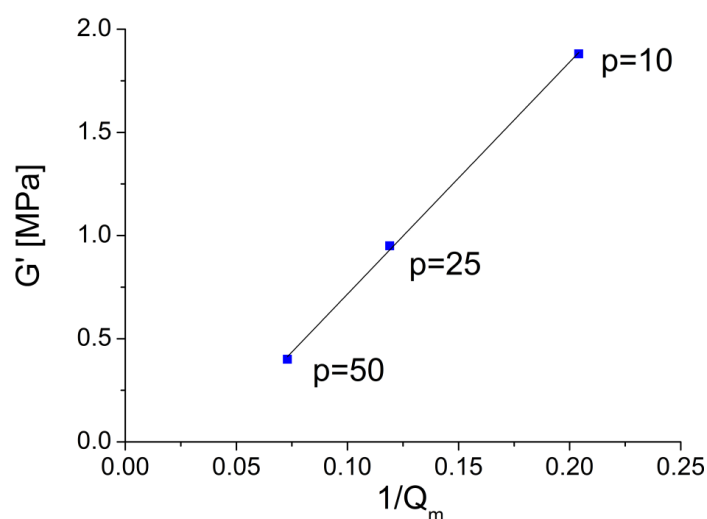


Figure S2.  $G'$  plateau value in function of the inverse of mass swelling ratio  $1/Q_m$  chosen to represent the crosslink density ( $p$  is the number of epoxy functions for one diacid molecule).

## 2. Recyclability of DA-crosslinked ENR through ester hydrolysis

### 2.1. Introduction

Chemical networks swell in a good solvent but not dissolve, the swelling ratio depending on the density of crosslinks. The dissolution of crosslinked networks can only occur through the cleavage of chemical bonds. For rubbers, in the case of peroxide crosslinking, chains are linked by very stable carbon-carbon bonds and there is no easy chemical way to cleave them. Conversely, sulphur vulcanization produces polysulphide bridges sensitive to oxidation. Using dithiothreitol or tributylphosphine for example,<sup>26, 34</sup> di- and polysulphide bonds can easily be cleaved in two thiols. However, sulphur-vulcanized rubber cannot be fully recycled through dissolution because of the mono-sulphide bonds that have a higher energy and are not easily broken.

As shown by Pire *et al.*,<sup>23</sup> carboxylic acids can open the epoxy functions of ENR, creating  $\beta$ -hydroxy esters along the chains (Figure 1). The DA-crosslinked ENR is thus a chemical network containing sensitive ester links. The ester functional group is known to undergo hydrolysis under acid or basic conditions. In this section, we will use hydrolysis to “decrosslink” ENR-DA and recycle the polymer.

### 2.2. Experimental section

#### 2.2.1. Materials

The ENR chemical network used for this study is ENR25 crosslinked with DA referred to as ENR-DA0 in the previous section. Sodium hydroxide (NaOH,  $\geq 97\%$ ) and solvents were obtained from the Sigma-Aldrich Co. and used as received.

#### 2.2.2. Recycling procedure

*Rubber recovery:* In a round bottom flask equipped with a condenser, a piece of ENR network (1 g, 0.26 mmol of ester function) was heated to 50 °C and left under magnetic stirring in a mixture of NaOH (80-90 mg, 2-2.3 mmol) in THF:MeOH:H<sub>2</sub>O (30 mL:10 mL:1mL) under nitrogen bubbling. After about 2 hours, the piece of network was completely dissolved. The

content of the flask was dried using a rotary evaporator and dissolved again in pure toluene. This organic phase was washed at least three times with water in a separatory funnel to eliminate the excess of NaOH. Eventually, the polymer was retrieved by precipitation in MeOH and dried under vacuum at room temperature until constant weight.

*Crosslinking of the hydrolyzed rubber:* The hydrolyzed rubber was once again crosslinked using DA. The reclaimed quantity being too small to proceed by mixing in the internal mixer, the blending was done in solution. The recycled polymer (0.5 g) was dissolved in 5 mL of dichloromethane ( $\text{CH}_2\text{Cl}_2$ ). The appropriate amounts of DA and DMI were added to the mixture to reach approximately the same degree of crosslinking as in the initial ENR-DA. As DA is not soluble in  $\text{CH}_2\text{Cl}_2$ , a few drops of dimethyl sulfoxide were added. The mixture was left stirring at room temperature for about three hours and poured in a stainless steel plate. The solvent was slowly evaporated overnight under the hood. The resulting film was then cured at 180 °C for 40 min in a vacuum oven.

### 2.2.3. Characterizations

*Nuclear Magnetic Resonance spectroscopy (NMR):*  $^1\text{H}$  NMR spectra were recorded in  $\text{CDCl}_3$  using a Bruker Avance 400 spectrometer (400 MHz).

*Gel Permeation Chromatography (GPC):* Molecular weights and dispersities were determined using GPC, with a Malvern GPC1000 pump and a Viscotek TDA 305 triple detection array with three thermostatically controlled columns (LT5000L). Tetrahydrofuran was used as eluent at 35 °C at a flow rate of 1 mL.min<sup>-1</sup>. The apparatus was used in a single detection mode and the apparent molecular weights ( $M_n$  and  $M_w$ ) and dispersities ( $M_w/M_n$ ) were obtained using a poly(methyl methacrylate) (PMMA) conventional calibration.

## 2.3. Results and discussion

Esters may be hydrolyzed in acid or basic media. For example, the ester-containing molecule can be heated under reflux in dilute hydrochloric or sulphuric acid. This acid-catalyzed reaction is an equilibrium, excess of water should be used to produce a complete hydrolysis. Unfortunately, the oxirane ring present in ENR is also sensitive to acidic conditions and can be quite easily opened.<sup>35</sup> An acidic treatment is thus undesirable here, given that the aim is to recover the initial polymer with as few modifications as possible. The

second option is the use of dilute alkali. In this case the reaction is not an equilibrium which is an advantage. This second option was thus chosen for the recycling of ENR-DA. The principle of the recycling process is drawn in Figure 12.

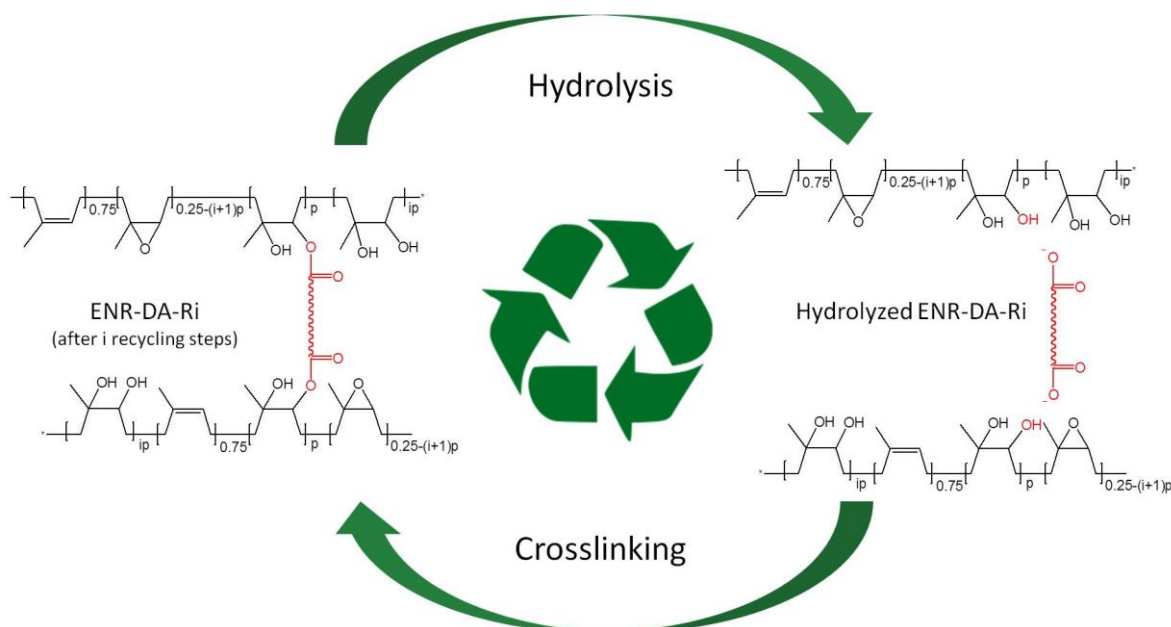


Figure 12. Principle of the recycling of ENR-DA. The ENR-DA network is hydrolyzed and the resulting linear polymer is re-crosslinked with DA. (Both epoxy functions and hydroxyl moieties formed after hydrolysis can theoretically take part in the re-crosslinking reaction).

By combining the use of NaOH, water and heat, the cured rubber was fully solubilized in a good solvent. The hydrolyzed product was characterized to detect a possible degradation in alkaline conditions. The linear polymer was then crosslinked again with DA through our standard esterification reaction. The obtained network is called ENR-DA-R1. More generally ENR-DA-R<sub>i</sub> will refer to the network obtained after *i* recycling cycles (hydrolysis followed by re-crosslinking).

### 2.3.1. Re-crosslinking of the hydrolyzed material

The recovered hydrolyzed polymer was crosslinked again with DA (same proportions than the initial ENR-DA network). After curing in a vacuum oven for 40 min at 180 °C, the recycled

rubber was left in tetrahydrofuran during 48 hours. The material swelled without dissolving, confirming the crosslinked structure as shown in Figure 13.

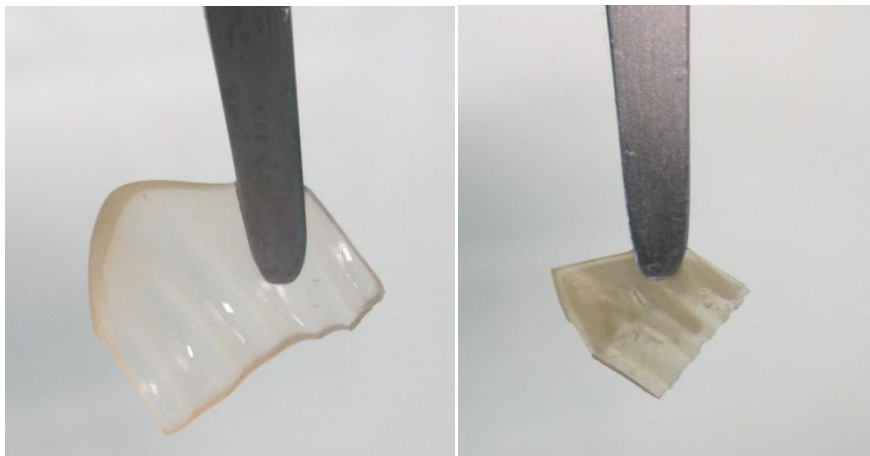


Figure 13. Picture of the recycled sample after swelling for 48 hours (left) and drying (right)

The sample dissolved again in the presence of NaOH in THF:MeOH:H<sub>2</sub>O, confirming the ester nature of the crosslinks of the recycled rubber.

### 2.3.2. NMR study

All linear polymers were characterized by liquid <sup>1</sup>H NMR in CDCl<sub>3</sub>. In the spectrum of ENR, two characteristic peaks allow for calculation of the epoxidation ratio. The peak at 5.1 ppm corresponds to the ethylenic proton and the one at 2.7 ppm corresponds to the proton of the epoxy monomer. The epoxidation ratio  $X_{epoxy}$  is thus calculated using Equation (6):

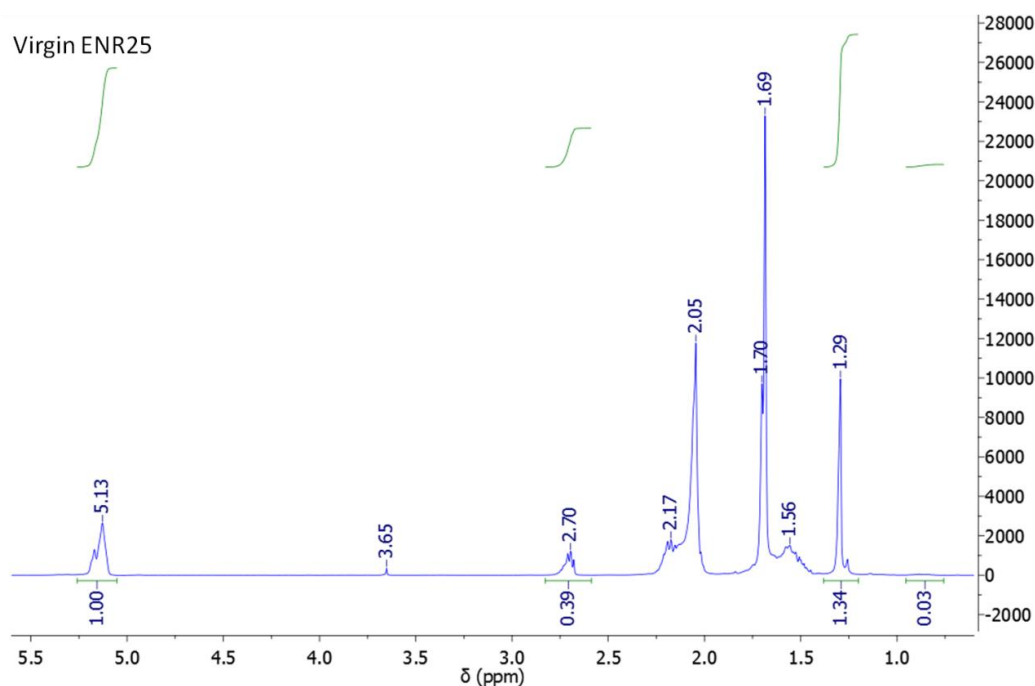
$$X_{epoxy} = \frac{I_{2.7}}{I_{2.7} + I_{5.1}} \times 100 \quad (6)$$

On the presented NMRs (Figure 14), the integration of the peak at 5.1 ppm was fixed to 1 to facilitate comparisons. The epoxidation ratios of the three linear polymers are collected in Table 4.

Table 4. Epoxidation ratio of the polymers before crosslinking and after each hydrolysis

Sample	Virgin ENR25	Hydrolyzed ENR-DA	Hydrolyzed ENR-DA-R1
X <sub>epoxy</sub> (%)	28	24.5	23

The initial ENR, sold as ENR25 by the supplier, actually presented an epoxidation ratio of 28 %, as measured by NMR. To crosslink ENR25, a epoxy/diacid ratio of one diacid molecule for 25 epoxy rings ( $p = 25$  with our notation) was chosen because this ratio was shown to give good mechanical properties in a previous work.<sup>21</sup> If all diacid molecules would react, the theoretical number of opened epoxy functions after crosslinking would be 8 %. The <sup>1</sup>H NMR spectra of the material after two hydrolysis steps look very similar to the one of virgin ENR25 (Figure 14). One can notice that the peak at 2.7 ppm corresponding to the epoxy monomer proton decreased after hydrolysis. The theoretical epoxidation ratio left after a consumption of 8 % of epoxy function is around 26 %. The 24.5 % measured by NMR are thus in the expected range. A few epoxy functions may have reacted with NaOH but most of them resisted to the hydrolysis step. The same conclusions are drawn for the second hydrolysis after the first recycling step.



a.

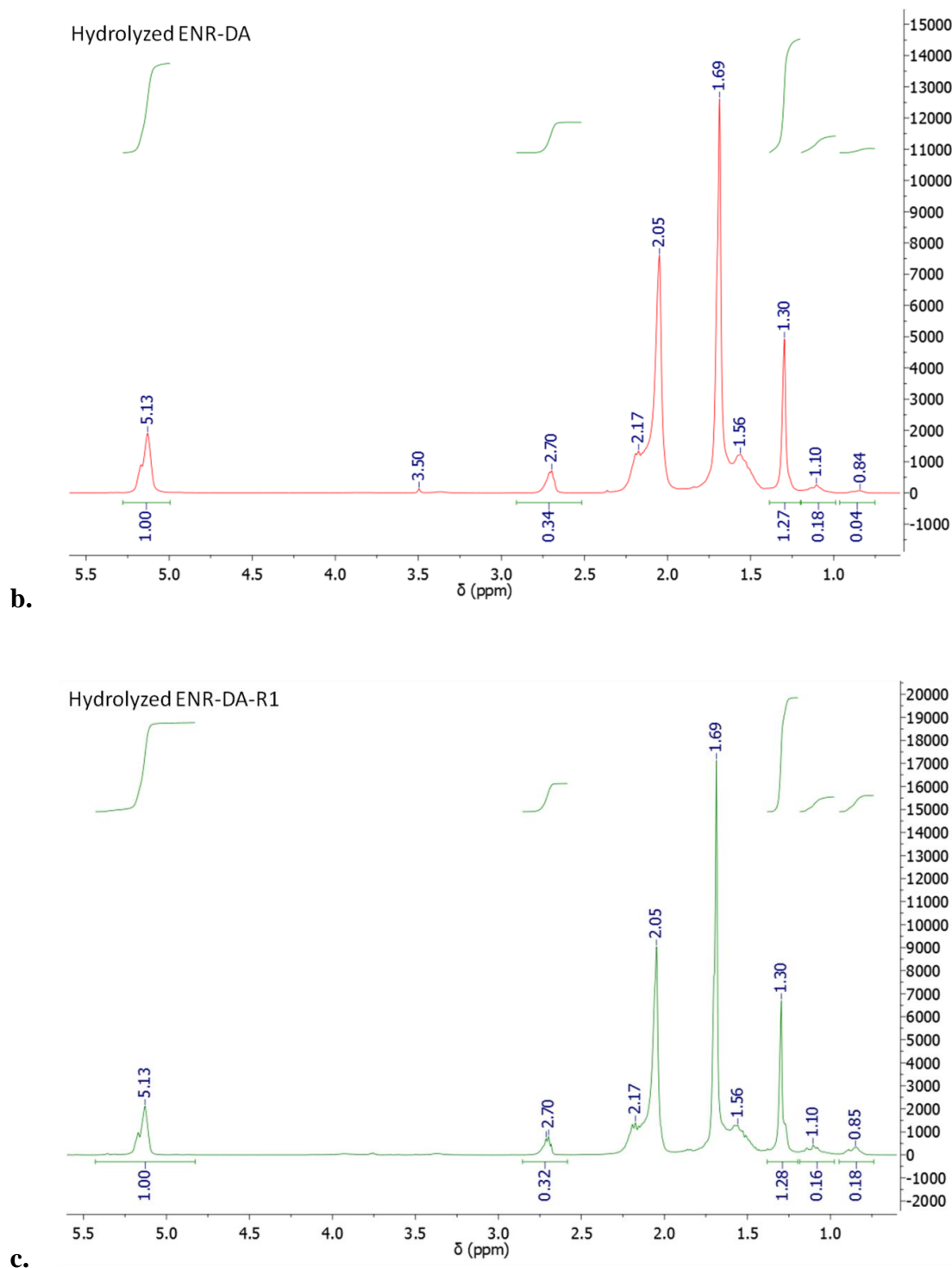


Figure 14.  $^1\text{H}$  NMR characterization of the different linear polymers.

**a.** Initial ENR25, **b.** Polymer recovered after hydrolysis of ENR-DA, **c.** Polymer recovered after hydrolysis of ENR-DA-R1 (second hydrolysis).

After hydrolysis of ENR-DA, the low percentage of hydrolyzed monomers can be visualized in the  $^1\text{H}$  NMR spectrum by zooming (for example after the first hydrolysis, Figure 15). Most of the hydrolyzed monomers corresponds to the ones opened by DA during crosslinking, but some can also be epoxy rings opened during the hydrolysis step. A new peak appeared at 3.36 ppm, corresponding to the C-H protons of the hydrolyzed monomers. The NMR of high molecular mass polymers is not precise enough to conclude quantitatively, but the integration of this peak is in the expected range (about 8 % of the initial number of epoxy).

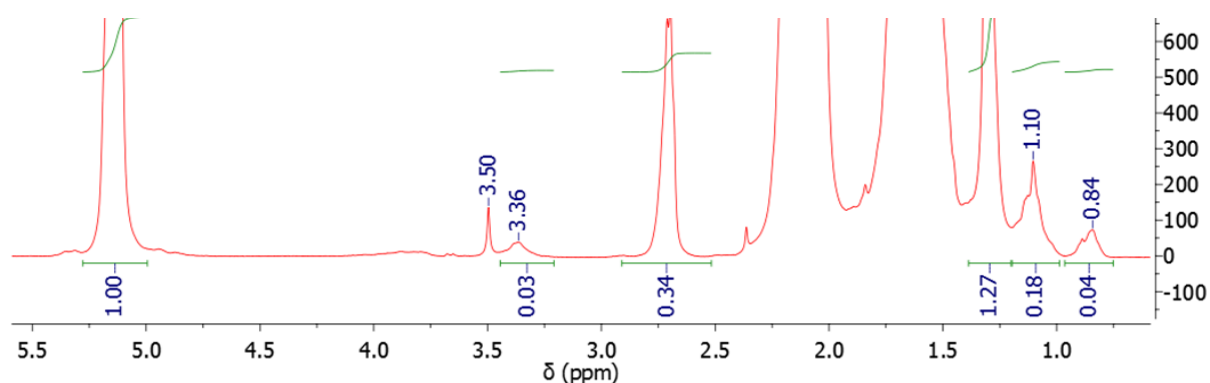


Figure 15.  $^1\text{H}$  NMR spectrum of hydrolyzed ENR-DA, zoom.

This NMR study clearly shows that the chemical structure of ENR is well preserved during recycling.

### 2.3.3. GPC results

At each step of the recycling process, the linear polymers were characterized by GPC to check chain lengths. The measurement of the molecular weights was complicated by the non negligible initial gel part of ENR25 that prevented from using triple detection, because the precise sample concentration was not accessible after filtering. Hence, a standard had to be chosen between PS and PMMA. Both polymers are quite different from ENR but PMMA was selected as it contains oxygen atoms and has a higher polarity mimicking the increasing polarity of ENR after hydrolysis. All cited molecular weight values must be taken with caution and conclusions will only be drawn by comparison between samples.

The process of mixing a polymer in an internal mixer can potentially break the chains. In the case of ENR, this is particularly important because of the initial high molecular weight ( $\geq 10^6 \text{ g}\cdot\text{mol}^{-1}$ ). Hence, the molecular weight of the polymer after blending in the internal

mixer but before curing was measured and taken as the basis of our comparisons ( $M_w$  (ENR25) = 410 000 g.mol<sup>-1</sup>). After the first hydrolysis step, the recovered ENR is about 5 or 6 times shorter than the initial one ( $M_w$  (hydrolyzed ENR-DA) = 71 000 g.mol<sup>-1</sup>). Chain scission occurred during the hydrolysis of the ester bonds. As simple or double carbon-carbon bonds are not particularly sensitive to basic conditions, the scission process could be an oxidation of the 1,2-diol in two carbonyl functions.

The second recycling step leads to a lower loss in molecular weight: it is divided by less than a factor 2 ( $M_w$  (Hydrolyzed ENR-DA-R1) = 41 300 g.mol<sup>-1</sup>). Both recovered linear polymers remain elastic solids at room temperature.

## 2.4. Conclusions

ENR-DA, a chemical network with good mechanical properties,<sup>25</sup> could be recycled through ester hydrolysis in mild conditions. The process is reproducible several times: the recycled material can be dissolved and crosslinked again. Such a recycling process is not attainable with standard sulphur or peroxide vulcanizations. In the case of ENR-DA, as long as non-hydrolyzed epoxy rings are present, the rubber can be crosslinked using diacids and is recyclable. When all oxirane rings are opened, the linear polymer can still be crosslinked by the use of peroxide or sulphur vulcanizations, the final network becoming non-recyclable.

The linear ENR obtained after ester hydrolysis has a lower molecular weight probably due to chain scissions during the hydrolysis process. However, after two hydrolysis steps the molecular weight of ENR is still high enough for the linear polymer to be an elastic solid at room temperature. This work should be considered as a proof of concept and the process could most probably be optimized.

## References

1. D. Montarnal, M. Capelot, F. Tournilhac and L. Leibler, *Science*, 2011, **334**, 965-968.
2. M. Capelot, D. Montarnal, F. Tournilhac and L. Leibler, *JACS*, 2012, **134**, 7664-7667.
3. M. Capelot, M. M. Unterlass, F. Tournilhac and L. Leibler, *ACS Macro Letters*, 2012, **1**, 789-792.
4. M. A. Rahman, L. Sartore, F. Bignotti and L. Di Landro, *ACS Applied Materials & Interfaces*, 2013, **5**, 1494-1502.
5. R. Chasset and P. Thirion, "Proceedings of the Conference on Physics of Non-Crystalline Solids", Amsterdam, 1965.
6. J. G. Curro and P. Pincus, *Macromolecules*, 1983, **16**, 559-562.
7. P. G. de Gennes, *Scaling Concepts in Polymer Physics*, Cornell University Press, 1979.
8. J. D. Ferry, *Viscoelastic Properties of Polymers*, Wiley, New York, 3rd edn., 1980.
9. G. B. McKenna and R. J. Gaylord, *Polymer*, 1988, **29**, 2027-2032.
10. M. Capelot, D. Montarnal, F. Tournilhac and L. Leibler, *Journal of the American Chemical Society*, 2012, **134**, 7664-7667.
11. Y.-X. Lu, F. Tournilhac, L. Leibler and Z. Guan, *Journal of the American Chemical Society*, 2012, **134**, 8424-8427.
12. W. Denissen, G. Rivero, R. Nicolaÿ, L. Leibler, J. M. Winne and F. E. Du Prez, *Advanced Functional Materials*, 2015, **25**, 2451-2457.
13. M. M. Obadia, B. P. Mudraboyina, A. Serghei, D. Montarnal and E. Drockenmuller, *Journal of the American Chemical Society*, 2015, **137**, 6078-6083.
14. B. Adhikari, D. De and S. Maiti, *Progress in Polymer Science*, 2000, **25**, 909-948.
15. Y.-X. Lu and Z. Guan, *Journal of the American Chemical Society*, 2012, **134**, 14226-14231.
16. S. Trabelsi, P. A. Albouy and J. Rault, *Macromolecules*, 2003, **36**, 7624-7639.
17. S. Gutierras, S. M. Vargas and M. A. Tlenkopatchev, *Polymer Degradation and Stability*, 2004, **83**, 149-156.
18. M. S. Sanford, J. A. Love and R. H. Grubbs, *Journal of the American Chemical Society*, 2001, **123**, 6543-6554.
19. S.-N. Gan and Z. A. Hamid, *Polymer*, 1997, **38**, 1953-1956.
20. I. R. Gelling, *Rubber Chemistry and Technology*, 1985, **58**, 86-96.
21. M. Pire, S. Norvez, I. Iliopoulos, B. Le Rossignol and L. Leibler, *Polymer*, 2010, **51**, 5903-5909.
22. M. Pire, S. Norvez, I. Iliopoulos, B. Le Rossignol and L. Leibler, *Polymer*, 2011, **52**, 5243-5249.
23. M. Pire, C. Lorthioir, E. K. Oikonomou, S. Norvez, I. Iliopoulos, B. Le Rossignol and L. Leibler, *Polymer Chemistry*, 2012, **3**, 946-953.
24. M. Pire, E. K. Oikonomou, L. Imbernon, C. Lorthioir, I. Iliopoulos and S. Norvez, *Macromolecular Symposia*, 2013, **331-332**, 89-96.
25. M. Pire, S. Norvez, I. Iliopoulos, B. Le Rossignol and L. Leibler, *Composite Interfaces*, 2014, **21**, 45-50.
26. L. Imbernon, E. K. Oikonomou, S. Norvez and L. Leibler, *Polymer Chemistry*, 2015, **6**, 4271-4278.
27. L. Imbernon, M. Pire, E. K. Oikonomou and S. Norvez, *Macromolecular Chemistry and Physics*, 2013, **214**, 806-811.
28. D. W. Van Krevelen and P. J. Hoftyzer, *Properties of polymers: their estimation and correlation with chemical structure*, Elsevier, 1976.

29. R. J. Chang and A. N. Gent, *Journal of Polymer Science: Polymer Physics Edition*, 1981, **19**, 1619-1633.
30. P. G. De Gennes, *J. Phys. France*, 1975, **36**, 1199-1203.
31. S. Mitra, S. Chattopadhyay and A. Bhowmick, *J Polym Res*, 2011, **18**, 489-497.
32. D. J. Plazek, *Journal of Polymer Science Part A-2: Polymer Physics*, 1966, **4**, 745-763.
33. B. T. Poh and K. S. Lee, *European Polymer Journal*, 1994, **30**, 17-24.
34. M. Le Neindre and R. Nicolay, *Polymer Chemistry*, 2014, **5**, 4601-4611.
35. C.-C. Peng and V. Abetz, *Macromolecules*, 2005, **38**, 5575-5580.



**Chapitre 3**  
**Retour aux sulfures**

---



<b>Chapitre 3 : Retour aux soufres .....</b>	<b>111</b>
<b>1. Use of a disulfide-containing diacid.....</b>	<b>114</b>
1.1. Introduction .....	115
1.2. Experimental section .....	117
1.2.1. <i>Materials</i> .....	117
1.2.2. <i>Blend preparation</i> .....	118
1.2.3. <i>Crosslinking process</i> .....	118
1.2.4. <i>Stress relaxation</i> .....	118
1.2.5. <i>Reprocessing procedure</i> .....	118
1.2.6. <i>Strain recovery profile</i> .....	118
1.2.7. <i>Adhesion measurements</i> .....	119
1.2.8. <i>Tensile tests</i> .....	119
1.2.9. <i>Swelling experiments</i> .....	119
1.2.10. <i>Gel permeation chromatography</i> .....	120
1.2.11. <i>Nuclear Magnetic Resonance spectroscopy</i> .....	120
1.3. Results and discussion.....	120
1.3.1. <i>DTDB is an efficient crosslinker of ENR, comparable with DA</i> .....	120
1.3.2. <i>The presence of disulphide bonds enables network rearrangements</i> .....	123
1.3.3. <i>The rearrangements of the network can promote good adhesion behaviour</i> . 126	
1.3.4. <i>Thermo-activated adhesion enables recycling of the rubber</i> .....	128
1.4. Conclusions .....	130
1.5. Supplementary information (SI).....	131
1.5.1. <i>Reprocessing experiment</i> .....	131
1.5.2. <i>Reproducibility of the simple tensile tests</i> .....	132
1.5.3. <i>Swelling experiment</i> .....	132
1.5.4. <i>Study of the dissolved DTDB-cured network in reductive conditions</i> .....	133
1.5.5. <i>Determination of Young's Modulus</i> .....	134
<b>2. Comparison with a sulphur-vulcanized ENR network.....</b>	<b>136</b>
2.1. Introduction .....	136
2.2. Experimental section .....	137
2.2.1. <i>Materials</i> .....	137
2.2.2. <i>Blend preparation</i> .....	137
2.2.3. <i>Characterization methods</i> .....	137
2.3. Results and discussion.....	138
2.3.1. <i>Curing and crosslink density</i> .....	138
2.3.2. <i>Stress relaxation behaviour</i> .....	140
2.3.3. <i>Reprocessing of the material</i> .....	142
2.3.4. <i>Thermo-oxydative properties</i> .....	143
2.3.5. <i>Creep measurement</i> .....	145

2.4. Conclusions .....	147
Acknowledgments .....	148
Appendix .....	148
<b>References</b> .....	<b>149</b>

## Chapitre 3 : Retour aux sulfures

Dans le chapitre précédent, nous avons vu que la transesterification est limitée dans notre système ENR-DA, d'autant plus en l'absence de catalyseur. Les liaisons esters de ce système non catalysé pourront donc être considérées comme permanentes sur des échelles de temps de quelques heures à 180 °C. Le diacide réticulant peut cependant servir de vecteur pour l'introduction d'une fonction dynamique au sein du réseau, voir Figure 1.

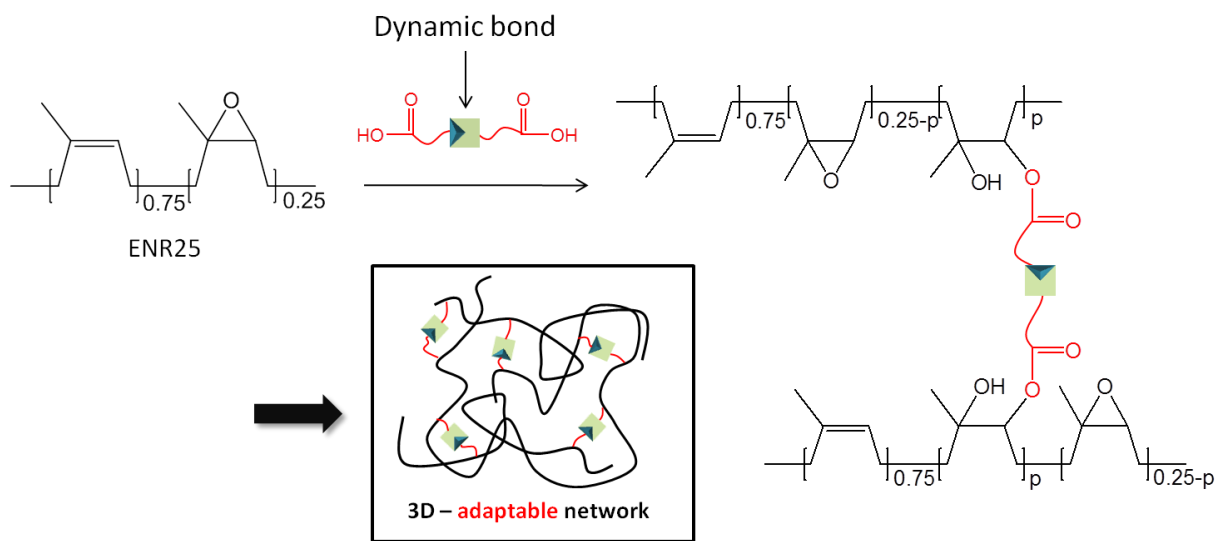


Figure 1. Introduction d'une fonction dynamique dans le réseau d'ENR par l'agent réticulant.

La vulcanisation classique au soufre est une technologie utilisée industriellement depuis plus de 150 ans. Au long de toutes ces années, elle a été affinée, optimisée, et elle est aujourd'hui particulièrement bien maîtrisée. Le procédé introduit des ponts di-, tri-, tétra- et polysulfures entre les chaînes du caoutchouc. Cette méthode de réticulation est classiquement considérée comme produisant des liens permanents. Paradoxalement, les liens polysulfures sont connus pour s'échanger à haute température.<sup>1</sup> La réversibilité de ces liens est d'ailleurs à l'origine des bonnes propriétés en fatigue du caoutchouc vulcanisé au soufre par rapport à une vulcanisation au peroxyde. Ce dernier procédé crée des liens C-C courts et non réversibles, qui sont définitivement rompus lors de sollicitations répétées. La relaxation de contrainte à haute température des caoutchoucs vulcanisés (au soufre et au peroxyde) a été étudiée par Tobolsky d'une part, et Berry et Watson de l'autre, au milieu du XX<sup>e</sup> siècle.<sup>2, 3</sup> Ces auteurs

ont débattu des mécanismes de dégradation mis en jeu lors de cette relaxation, ainsi que de l'effet de l'atmosphère (présence ou non d'oxygène) sans vraiment arriver à se mettre d'accord.<sup>4-8</sup> Pour tous, la relaxation de contrainte observée est forcément liée à la dégradation du réseau puisque la contrainte enregistrée est directement proportionnelle au nombre de chaînes élastiquement actives. Quelques années plus tard, Tamura et Murakami ont étudié plus en détail l'effet de l'oxygène sur cette relaxation.<sup>9</sup> Dans leur étude, trois réseaux sont comparés : l'un contenant des liens polysulfures, le deuxième des liens mono- et disulfures, et le troisième des liens mono-sulfures seulement. Ils invoquent également la rupture de chaînes qui d'après eux est la rupture homolytique des liaisons C-C situées à côté des points de réticulation mono- et disulfures par formation de radicaux. Cependant, ils soulignent aussi l'effet des liens polysulfures qui peuvent s'échanger et provoquent donc une relaxation de la contrainte sans augmenter la partie soluble du caoutchouc. Avec les vitrimères,<sup>10</sup> Leibler *et al.* ont montré qu'un réseau chimique peut même dans certains cas totalement relaxer les contraintes tout en gardant un nombre de lien constant, par échange de liaisons.

Quelques articles existent sur la « revulcanisation » de caoutchouc vulcanisé au soufre puis pulvérisé.<sup>11-13</sup> La poudre est moulée par compression à une température suffisante pour que des échanges de liens polysulfures aient lieu. Ce procédé permet d'obtenir un nouvel objet en caoutchouc à partir de déchets vulcanisés. Cependant, la vulcanisation au soufre implique l'utilisation de composés toxiques, notamment pour l'environnement (par exemple l'oxyde de zinc ZnO, ou le N-cyclohexyl-2-benzothiazolylsulfenamide, accélérateur classiquement utilisé). Le présent chapitre décrit l'introduction de liaisons disulfures comme points de réticulation de l'ENR en évitant la vulcanisation au soufre, et tous les produits toxiques associés. Nous tirons parti de la nouvelle réticulation de l'ENR mise en place au laboratoire et étudiée au chapitre précédent en choisissant comme réticulant un diacide contenant une liaison disulfure centrale (l'acide dithiodibutyrique, DTDB, Figure 2).

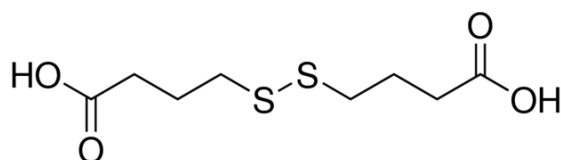


Figure 2. Formule chimique de l'acide dithiodibutyrique, DTDB.

Les liaisons disulfures sont étudiées dans la littérature pour leur capacité d'échange, permettant la création de matériaux auto-réparants.<sup>14-17</sup> Le matériau réticulé par DTDB sera ici étudié pour ses propriétés de relaxation de contrainte, de remise en forme après réticulation et d'adhésion notamment. Cette première partie du chapitre est un article récemment publié dans *Polymer Chemistry*.<sup>18</sup>

Dans une deuxième partie, les propriétés de l'ENR réticulé par DTDB seront comparées à celles d'un ENR vulcanisé au soufre en termes de relaxation de contrainte, de capacité de « revulcanisation » mais aussi de résistance à la thermo-oxydation, connue pour être plutôt mauvaise dans les matériaux vulcanisés au soufre. L'utilisation du soufre produit un mélange de liens mono-, di- et polysulfures. La chimie présentée ici est mieux définie puisque les points de réticulation ne sont en théorie que des liaisons disulfures, ce qui pourrait permettre d'espérer une meilleure tenue en vieillissement.

## 1. Use of a disulfide-containing diacid

### Chemically crosslinked yet reprocessable epoxidized natural rubber *via* thermo-activated disulphide rearrangements

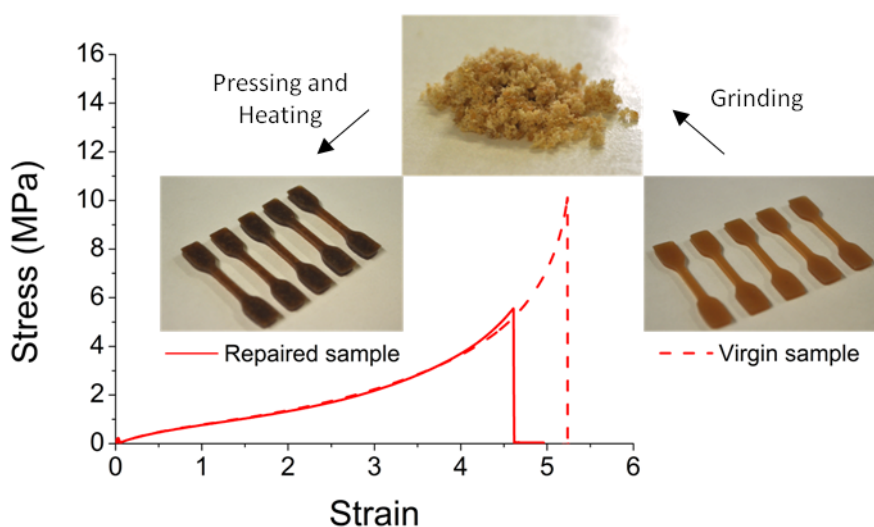
by Lucie Imbernon, Evdokia K. Oikonomou, Sophie Norvez and Ludwik Leibler

*Matière Molle et Chimie, ESPCI ParisTech - CNRS, UMR-7167, PSL Research University.*

*Polym. Chem.*, 2015, **6**, 4271-4278

#### Abstract

The thermo-activated reprocessing ability of a chemically crosslinked epoxidized natural rubber (ENR) is investigated. Disulphide groups are introduced into the rubber using dithiodibutyric acid (DTDB) as a crosslinker. DTDB-cured ENR presents strong elastomeric properties due to the high molecular weight of the rubber and efficient crosslinking. The material behaves like a standard natural rubber until 100 °C and becomes reprocessable above 150 °C, owing to disulphide rearrangements. After grinding to a fine powder, the crosslinked rubber can be reprocessed and recovers most of its initial mechanical properties. The heat-triggered disulphide rearrangements are characterized in terms of stress relaxation, creep/recovery, adhesion tests, and swelling experiments. Comparison is made with ENR samples crosslinked by permanent links.



*Disulphide crosslinks introduced in an ENR matrix enable the thermo-activated reprocessing of the chemically crosslinked rubber, studied in terms of stress relaxation and adhesion experiments.*

## 1.1. Introduction

The rubber industry faces a major recycling problem due to the irreversibility of the crosslinked networks. Indeed, to exhibit good mechanical properties such as elasticity and high toughness as well as solvent resistance, rubbers must be chemically crosslinked. Afterwards however, the chemical network prevents the reshaping or recycling of rubbery objects. This irreversibility problem common to all thermoset polymers draws a lot of work in the chemistry community. Covalently adaptable networks exhibiting reversible covalent chemistry appeared as a possible way to overcome this issue.<sup>19-23</sup> However, these networks can potentially be depolymerized under certain conditions (heat for example). Vitrimers, recently introduced by Leibler and co-workers, are a new class of polymers.<sup>10</sup> The novelty comes from the fact that vitrimers are fully processable but still insoluble materials. This behaviour is essentially different from those of two hitherto identified classes of polymers: thermoplastics, that are malleable and soluble, and thermosets (like rubbers), which are insoluble and cannot be reshaped once synthesized. Vitrimers consist of a network containing exchangeable bonds. Exchange reactions like transesterification,<sup>10, 24, 25</sup> olefin metathesis,<sup>26</sup> or vinylogous transamination<sup>27</sup> are used instead of reversible bonds. The number of crosslinking points and the average functionality of the network remain constant, making vitrimers fully malleable and mendable but still insoluble materials.<sup>10, 24, 25</sup> Shape is fixed by cooling, which slows down exchange reactions and quenches the topology of the network. The vitrimer transition is analogous to a glass transition but the topology of the network rather than the density of the material is quenched at the transition.

Around 1840, Goodyear and Hancock independently reinvented rubber by introducing the vulcanization process, involving combination with sulphur and heating. Vulcanization is thus an old industrial process, but much of its chemistry yet remains unclear. Nevertheless, there is a general agreement that the outstanding mechanical properties, in particular fatigue resistance, of sulphur-vulcanized rubbers is associated to polysulphide rearrangements. A very few papers, mostly directed towards industrial applications, have reported the recycling of sulphur-vulcanized NR by compression moulding of pulverized rubber waste<sup>11-13</sup> but no mechanistic studies were described. Model systems containing disulphide bonds have attracted considerable interest recently to produce self-healing materials under various stimuli like heat, light or redox conditions.<sup>14-17, 28-34</sup> Only a limited number of studies however have focused on chemically crosslinked solvent-free polymer networks. Amamoto *et al.* showed

the complete self-healing of a crosslinked polyurethane by exposure to visible light at room temperature.<sup>32</sup> The network contained thiuram disulphide moieties in the main chain which permitted the reshuffling of the bonds. Recently, the Odriozola group reported a synthetic polyurethane that self-healed without external stimuli *via* rearrangements of aromatic disulphide bonds.<sup>16, 34</sup> Self-healing occurred at room temperature, partly due (50 %) to the presence of hydrogen bonds. In the meantime, Lei *et al.* showed that tributylphosphine catalyzed the self-healing of a polysulphide network at room temperature.<sup>17</sup> Heat was also used as a stimulus as shown by Klumperman, Goossens and co-workers.<sup>14</sup> Their disulphide-based epoxy resin produced a healable thermoset system that regained 100 % of the original mechanical properties after healing for 1 hour at 60 °C. The self-healing was mostly attributed to thiol-disulphide reversible reshuffling.<sup>29</sup> Yet, all these systems present relatively weak elastomeric properties. At the rupture point, the strain is usually limited to 200 % and the stress inferior to 1 MPa, where a standard industrial rubber may be expected to reach at least 500 % elongation and 10 MPa stress before reinforcement by fillers.<sup>35</sup> Using the disulphide reversible chemistry in a natural rubber presenting intrinsic strong elastomeric properties could combine reprocessing ability and good mechanical behaviour.

Widely used in the rubber industry, Epoxidized Natural Rubber (ENR) is a unique elastomer obtained by epoxidation of natural rubber harvested from Hevea trees. ENR mechanical properties are very similar to those of NR up to 50 mol% epoxidation.<sup>35</sup> Owing to the polar nature of the oxirane groups, ENR demonstrates interesting additional properties, like low gas permeability<sup>36</sup> or oil resistance,<sup>37</sup> as well as enhanced compatibility with polymers bearing polar groups.<sup>38, 39</sup> Self-healing properties after ballistic damage were reported in a low molecular weight ENR slightly crosslinked by dicumylperoxide.<sup>40</sup> The self-healing was attributed to small chain inter-diffusion process. Self-healing properties decreased and rapidly disappeared as the crosslinking density increased, since the crosslinking hindered the diffusion process. Here we investigate reprocessing properties in a highly crosslinked high molecular weight ENR exhibiting strong elastomeric properties.

Our group recently showed that ENR can be efficiently crosslinked by dicarboxylic acids in the presence of 1,2-dimethylimidazole acting as an accelerator.<sup>41-43</sup> The crosslinking reaction of this bio-based polymer relies on the opening of the epoxy rings by the acid functions, resulting in the formation of  $\beta$ -hydroxy esters along the main chains.<sup>44</sup> This new type of crosslinking competes efficiently with conventional vulcanizations using sulphur or peroxides.<sup>45</sup> It also offers the opportunity to introduce different chemical functions in the rubber by the way of the carboxylic diacid crosslinker. In this work, a disulphide function was

incorporated in ENR using dithiodibutyric acid (DTDB) as the crosslinker (Figure 3). Thermo-activated rearrangements in the crosslinked rubber are studied by stress-relaxation and creep/recovery experiments. Comparison with ENR crosslinked by aliphatic diacid enlightens the importance of disulphide bonds in the relaxation process, which allow partial recycling of the rubber.

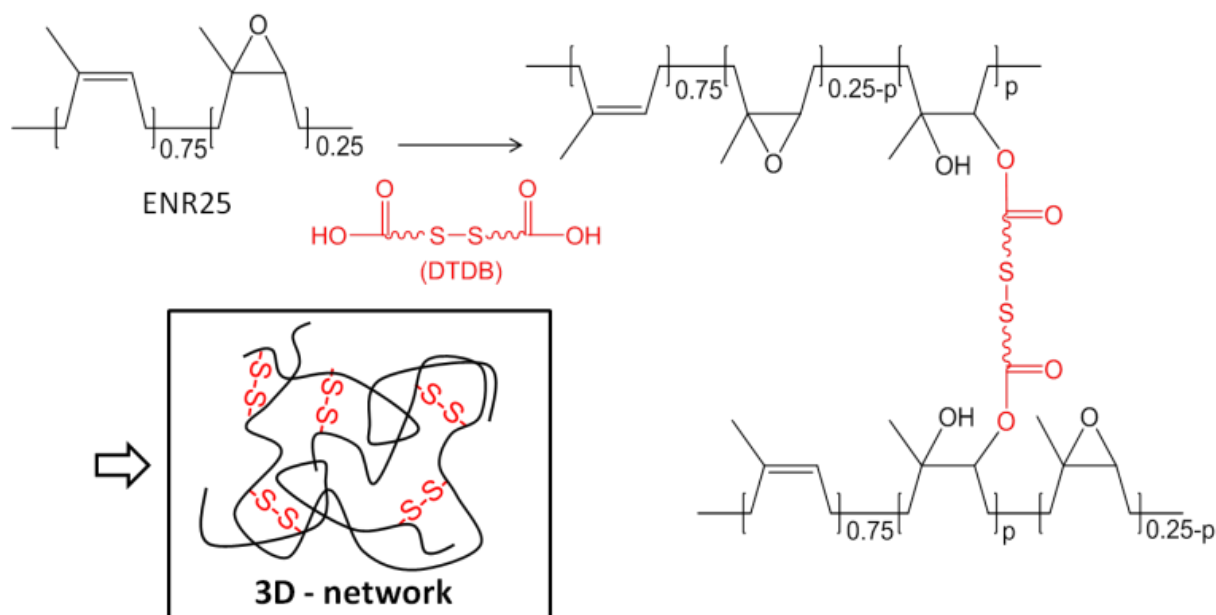


Figure 3. Crosslinking of ENR25 (25 mol% epoxidized): Schematic representation of the disulphide containing network. The ratio of epoxy function per diacid molecule is fixed to 25 to provide the network with optimal mechanical properties.<sup>41</sup>

## 1.2. Experimental section

### 1.2.1. Materials

ENR25, containing 25 mol% epoxy groups, and kaolin were kindly provided by Hutchinson SA Research Center, France. Dithiodibutyric acid (DTDB, 95%) and 1,2-dimethylimidazole (DMI, 98%) were obtained from Sigma–Aldrich and dodecanedioic acid (DA, 99%) was purchased from Acros.

### 1.2.2. Blend preparation

Mixtures of ENR25, diacids, and DMI were prepared in a Haake Polydrive mixer at 40 °C for about 12 min, following a protocol already described.<sup>41</sup> The amount of diacid was fixed to one molecule of diacid per 100 monomers, that is to say, one per 25 epoxy groups for ENR25. DMI, liquid in the mixing conditions (mp  $\approx$  38 °C), was premixed with kaolin (1:2, w/w), an inert filler, to facilitate its incorporation in the rubber. After blending, samples were cured in a Carver press under 8 tons pressure at 180 °C for the appropriate time (time determined by rheology experiment, about 40 min in both cases).

### 1.2.3. Crosslinking process

The cross-linking process was followed using a Anton Paar MCR 501 rheometer, in plate - plate geometry (25 mm-diameter, 1 Hz frequency, 0.1 % strain). Samples of 26 mm-diameter were cut in 1.5 mm thick uncured sheets pressed at 80 °C. To ensure a good contact between the rubber disc and the plates, an axial force of 10 N was first applied to the sample for 5 min before the experiment. The axial force was then maintained to 2 N by adjusting the gap during the experiment. In these conditions, results of the measurements were comparable with the ones obtained in a Moving Die Rheometer.<sup>41</sup> The temperature was quickly raised from 30 to 180 °C, and then the sample was left under oscillatory shear at 180 °C for curing.

### 1.2.4. Stress relaxation

After *in situ* curing, the samples were analyzed by stress relaxation experiments in a Anton Paar rheometer. The temperature was fixed at 180 °C and a 1 % strain step applied. The resulting relaxation modulus was monitored over time.

### 1.2.5. Reprocessing procedure

A piece of crosslinked rubber was reduced to a fine powder using a Fritsch Pulverisette 14. Liquid nitrogen was used to process below the  $T_g$  of the sample and facilitate the grinding. The obtained powder was then heated at 180 °C for 40 minutes in a Carver press under 8 tons pressure. Dumbbells for tensile tests were punched out from the cured material. The same experiment was conducted on DTDB- and DA-cured ENR (Figure Sa in SI).

### 1.2.6. Strain recovery profile

Strain-recovery profiles were recorded using a DMA Q800 series TA Instrument in tension-film mode. Rectangular samples (5 x 20 x 1.6 mm) were cut in a film of cured ENR. At a

fixed temperature, the force applied to the sample was alternatively fixed to 0.5 and 0 N. In a typical simple test a 0.5 N force was applied for 300 min before a 300 min-recovery period (0 N). For cyclic creep/recovery, periods of 15 minutes were chosen. In each case, the corresponding strain profile was recorded over time.

#### 1.2.7. Adhesion measurements

Lap-shear geometry was adopted for adhesion measurements. Rectangular samples (5 x 100 x 1.5 mm) were cut in a cured film and superimposed on a 20 mm length. This lap joint was then put under pressure with a controlled 30 % deformation in a home-made set up and left in a vacuum oven at 180 °C for different adhesion times. The resulting lap shear specimen was tested on a Instron machine with a crosshead speed of 100 mm.min<sup>-1</sup>, at room temperature, with no humidity control, until complete peeling or break. Rectangular samples of the same geometry but without overlapping region were tested in the same conditions to determine the Young modulus  $E$  of the material.  $E$  was taken as the slope of the stress/strain curve at low strains and was used in the calculation of adhesion energies.

#### 1.2.8. Tensile tests

The stress–strain behaviour was studied using an Instron machine with a crosshead speed of 500 mm.min<sup>-1</sup>, at room temperature, with no humidity control, until break. Dumbbells of 10 mm effective length and 2 mm width were cut in a 1.5 mm-thick cured rubber sheet (about 2 mm for reprocessed samples) (Figure Sb and c). Strain was followed using a video extensometer. At least five samples (see Figure S2) were tested for each material. To calculate the ultimate tensile properties, an average number of stress and strain at break on all tested specimens was taken.

#### 1.2.9. Swelling experiments

Toluene was used as a good solvent of ENR for the simple swelling experiments. The swelling ratio  $Q$  is defined as  $Q = \frac{(m_s - m_u)}{m_u}$ ,  $m_s$  and  $m_u$  being the swollen and unswollen mass of the sample, respectively. The swelling behaviour of DTDB-cured material was studied before and after reprocessing. A piece of each material (virgin 1.6 x 5.23 x 5.34 mm and reprocessed 2.16 x 5.04 x 5.15 mm) was left in toluene for a few days and the weight was followed over time (Figure S3).

For the reductive swelling experiments, tetrahydrofuran (THF) was preferred to toluene because of its miscibility with water. The samples (1.5 mm thickness discs of 5 mm diameter) were immersed in THF and their weight evolution was followed over time. When the equilibrium swelling was reached, a small excess of tri-*n*-butylphosphine (TBP) and a few drops of water were added under magnetic stirring.

#### 1.2.10. Gel permeation chromatography

Molecular weights and dispersities were determined using SEC, with a Malvern GPC1000 pump and a Viscotek TDA 305 triple detection array with three thermostatically controlled columns (LT5000L). Tetrahydrofuran (THF) was used as eluent at 35 °C and at a flow rate of 1 mL.min<sup>-1</sup>. The apparatus was used in a single detection mode and the apparent molecular weights ( $M_n$  and  $M_w$ ) and dispersities ( $M_w/M_n$ ) were obtained with a polystyrene conventional calibration.

#### 1.2.11. Nuclear Magnetic Resonance spectroscopy

<sup>1</sup>H NMR spectra were recorded in CDCl<sub>3</sub> using a Bruker Avance 400 spectrometer (400 MHz).

### 1.3. Results and discussion

#### 1.3.1. DTDB is an efficient crosslinker of ENR, comparable with DA

Crosslinking of ENR by DTDB is followed in a rheometer (Figure 4). Comparison is made with dodecanedioic acid (DA), an aliphatic crosslinker which contains no disulphide bond.<sup>41</sup>  
<sup>42</sup> After a fast heating ramp from 25 to 180 °C, the temperature is maintained at 180 °C for crosslinking. During the temperature ramp, the elastic modulus  $G'$  first decreases due to softening of the rubber. At 180 °C, the sharp increase of  $G'$  shows that the crosslinking reaction takes place. Kinetics of crosslinking are very similar for both materials, as indicated by the identical  $G'$  initial slopes. A swelling experiment in toluene indicated that after curing for 40 minutes at 180 °C, both networks have similar crosslinking densities (the swelling ratio  $Q$  is  $3.0 \pm 0.1$  for DA-cured and  $3.3 \pm 0.2$  for DTDB-cured samples). The crosslinking process in the case of DTDB is thus believed to be similar to the one observed with aliphatic diacid containing no disulphide bonds: diacids opens the epoxy groups to create  $\beta$ -hydroxyesters

along the main chains.<sup>44</sup> If this was strictly the case, the network should be the one drawn in Figure 3 and it should be possible to fully solubilize the rubber by selectively breaking disulphide bonds.

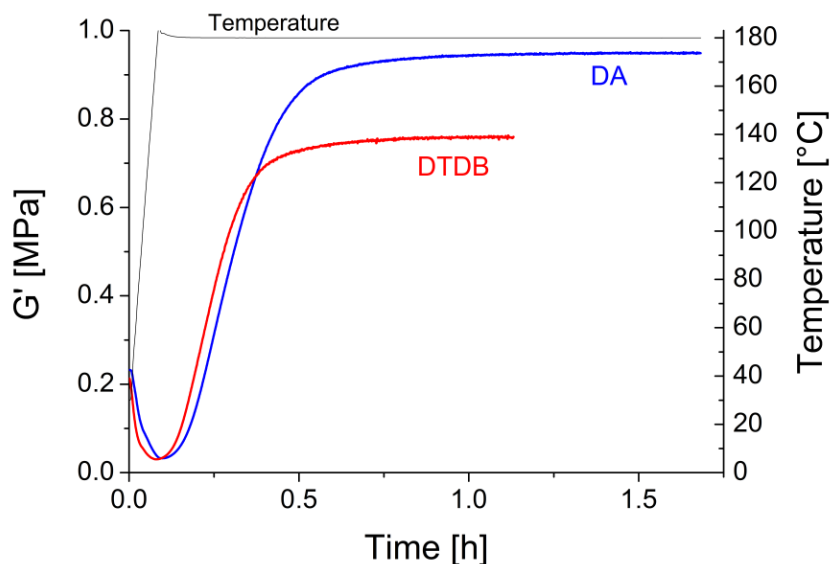
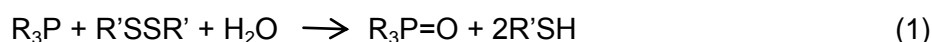


Figure 4. Kinetic study of the curing at 180 °C in the rheometer. ENR25 + DTDB is compared with the reference material (ENR25 + DA).

Two important features arise from this rheological experiment (Figure 4): the crosslinking reaction is complete in about half an hour at 180 °C, and the resulting material exhibits a shear modulus in the range of 1 MPa, which ranks our system among standard unfilled rubbers used in industry. To test the presence of disulphide bonds after the curing process at 180 °C, reductive swelling experiments were conducted in THF. A piece of rubber was swollen in the good solvent until equilibrium and then a reductive agent was added. Trialkylphosphines,  $R_3P$ , are known to quantitatively reduce organic disulphides into thiols in the presence of water (equation (1)).



After equilibrium swelling in pure THF, an excess of tri-*n*-butylphosphine (TBP) and water (to the theoretical number of disulphide bonds) was added and the additional swelling (if any) measured (Figure 5).

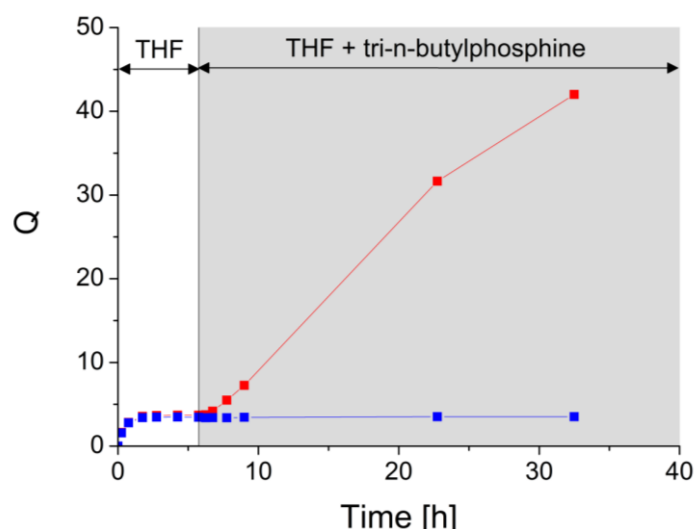


Figure 5. Reductive swelling experiment (Red: DTDB-cured sample, Blue: DA-cured sample). The reductive agent was introduced after 6 hour-equilibration in pure THF.

After addition of the reductive agent, the rubber behaves very differently as it contains disulphides or not. The swelling ratio of DA-cured network remains stable whereas DTDB-cured network swells a lot, due to the reduction of disulphide crosslinks into separate thiols. We checked that when no TBP was added, the DTDB-cured network behaved exactly like the reference material. This confirms that disulphide bonds are still present after crosslinking at 180 °C. The very large swelling of the disulphide-containing network weakens the material a lot. Under magnetic stirring, the piece of rubber finally dissolves. Gel permeation chromatography and  $^1\text{H-NMR}$  indicated that the material obtained after swelling was degraded (chains much shorter than in initial ENR, see Figure S4), preventing quantitative weight measurements and estimation of the permanent/reversible bonds ratio in the system. However, it is very likely that a few permanent bonds are created during the curing process. When increasing the temperature, disulphide bonds can break either into radical or into thiols that can react with another disulphide bond (reversible covalent chemistry). But thiyl radicals can also react with the double bonds of ENR (as for classical sulphur vulcanization of NR). This kind of these side reactions creates permanent crosslinks (monosulphide bonds). The high temperature (180 °C) necessary for crosslinking ENR by dicarboxylic acids favours these side reactions. Thus, after curing, we likely obtain a dual network mainly composed of disulphide crosslinks, but which most probably also contains a few permanent crosslinks.

### 1.3.2. The presence of disulphide bonds enables network rearrangements

Stress relaxation experiments were conducted at high temperature after *in situ* curing inside the rheometer. Relaxation modulus *versus* time is plotted in Figure 6.

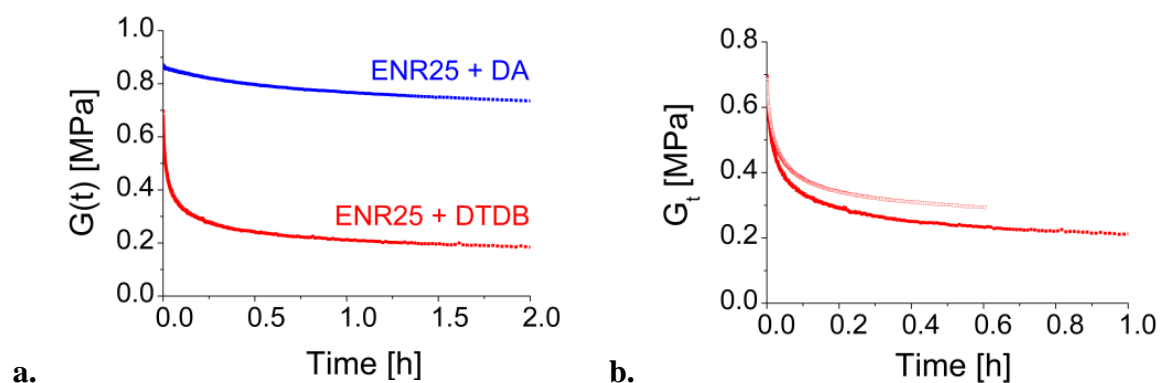


Figure 6. Stress relaxation experiment at 180 °C after curing in the rheometer. **a.** Comparison between DA- and DTDB-cured materials, **b.** First stress relaxation (filled symbols), second stress relaxation (void symbols) of DTDB-cured ENR.

The relaxation of ENR crosslinked with dodecanedioic acid (DA) is presented for comparison. In the latter system, the network has no possibility of rearrangement as it does not contain disulphide bonds. In Figure 6a, the sample containing disulphide bonds exhibits a substantial relaxation of stress whereas the control material shows a mostly flat curve. The *in situ* curing of the sample prevents any slipping effect during stress relaxation experiments. The slight relaxation observed in the control material is likely due to the diffusion of dangling chains.<sup>46</sup> Another possibility could be ester linkages undergoing transesterification. However, transesterification is not favoured in our system because of scarcity and little availability of free hydroxyl groups,<sup>24</sup> as well as the absence of transesterification catalyst.<sup>25</sup> The difference in behaviour between the DTDB- and DA-cured networks indicates a major contribution of disulphide bonds to the relaxation process. Nevertheless, the relaxation of DTDB-cured sample is not complete within the two-hour experiment, likely because side reactions at high temperature generate non reversible bonds. In Figure 6b, we compare two successive stress relaxations on the same DTDB-cured sample. The second relaxation is very similar to the first one. The initial modulus is the same and then a substantial relaxation is observed, indicating that the material still contained a lot of disulphide bonds after the first relaxation experiment.

However, the second relaxation seems slower, the corresponding relaxation modulus remaining higher than during the first relaxation experiment. The slowdown of the relaxation dynamics may be associated to the consumption of some reversible bonds by side reactions happening at high temperatures. The shear modulus  $G'$  is still very similar before and after the relaxation experiment, indicating that the number of crosslinks did not increase much. This tends to prove that the effect of side reactions stays limited at this time scale.

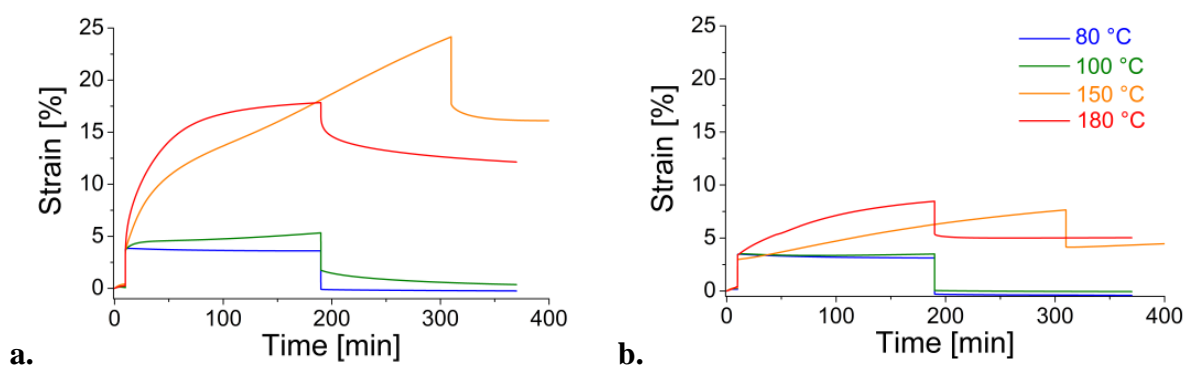


Figure 7. Creep/Recovery tests at different temperatures. **a.** DTDB-cured ENR, **b.** DA-cured ENR. A force of 0.5 N is applied for 180 min and then released.

To complete stress relaxation data, creep experiments were performed in the DMA. Chemically crosslinked rubbers usually recover their original shape after stretching. Force-controlled creep/recovery tests at different temperatures were performed on the DTDB-cured rubber (Figure 7a). The results of the same tests for DA-cured samples are plotted for comparison (Figure 7b). Both rubbers can withstand temperatures as high as 100 °C without residual deformation, but their behaviour at higher temperature greatly differs. The slight increase of the strain observed for the control material at 150 °C and 180 °C can probably be related to some degradation of the material. On the other hand the disulphide-containing material deforms much more and faster. This pronounced elongation may be associated with rearrangements of disulphide bonds activated at high temperature. Yet, the slope of deformation decreases with time when the experiment is conducted at 180 °C. This phenomenon is the mark of the side reactions that impedes disulphide rearrangements. It is much more present and rapid at 180 °C indicating the effect of temperature on the probability and rate of side reactions.

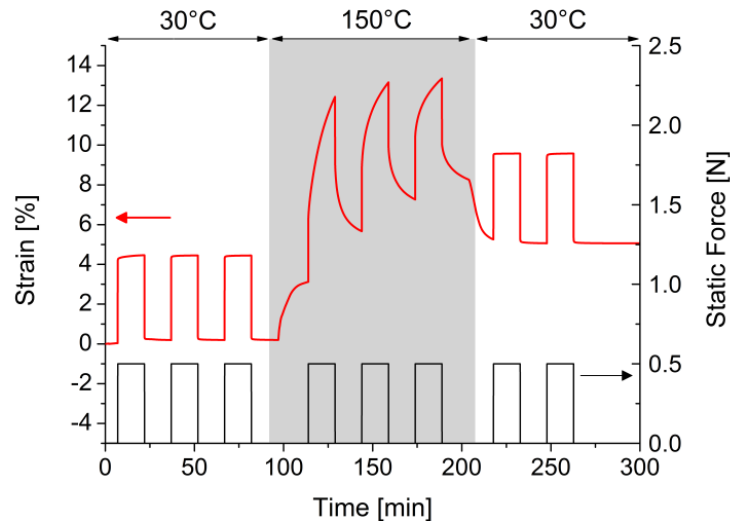


Figure 8. Cyclic strain/recovery profiles on ENR25 crosslinked with DTDB at different temperatures (black: applied force, red: strain response of the material).

Cyclic strain/recovery experiments were performed, before, during, and after heating to test the reversibility of the dynamic behaviour with temperature (Figure 8). As expected from the previous experiment, at 30 °C our material behaves like a standard rubber and recovers its original shape after removing the force. The material response is reproducible whatever the number of solicitations (three cycles presented here). After equilibrating the temperature at 150 °C for 5 minutes, the response of the material to the same experiment is completely different. First, an increase in strain during heating and equilibration should be noticed, likely due to thermal expansion of the material. Upon application of a 0.5 N force, the rubber deforms about 10 % and does not recover its initial length after removing the applied force. After three cycles, the strain of the unstretched material has increased from 3 to 8 % thanks to the rearrangements of the network. However, the deformation seems to decrease at each cycle. This is probably caused by side reactions that impede the material from reshaping. Repeating the experiment after decreasing the temperature back to 30 °C, the response of the material is the same as during the first three cycles (with a remaining strain of 5 % due to the rearrangements that occurred at 150 °C). The network has stopped rearranging, the material behaves like a classical chemically crosslinked rubber again. Therefore, it is possible to activate the rearrangement of the network by heating and stop it completely by cooling.

1.3.3. *The rearrangements of the network can promote good adhesion behaviour*

We showed that the temperature activates chemical rearrangements in a disulphide-containing ENR network. The rearrangements are a combination of disulphide rearrangements and side reactions that both result in the creation of new crosslinks. Adhesion experiments were conducted to quantify a possible mendability of the crosslinked rubber. Lap shear geometry was selected as it is well documented<sup>47</sup> and easy to implement. Lap shear measurements are independent of the length of the joint as long as it is above about four times the joint thickness,<sup>47</sup> so a length of 20 mm was selected for our 3-mm thickness samples. After an adhesion time of 30 min at 180 °C (Figure 9a), DA-cured samples rapidly peel and the maximum force is less than 5 N, whereas for DTDB-cured samples, the force goes up to 20 N, where the sample breaks instead of peeling. The adhesion between DTDB-cured samples is thus much higher compared to the reference material. The adhered joints were swollen into a good solvent to characterize the physical or chemical nature of the adhesion. The DA-cured joint rapidly lifts off upon swelling whereas the DTDB-cured joint swells a lot without breaking, showing the presence of chemical bonds between the two pieces of rubber. Chemical rearrangements create new bonds between the samples and are responsible for the good adhesion properties.

The effect of contact time and temperature was investigated on DTDB-cured rubber. Joints adhered for different times at 180 °C were tested; the corresponding force/strain profiles are plotted in Figure 9b. The temperature was also varied keeping the contact time constant at 30 min (Figure 9c). At short adhesion times or low temperatures, as for DA-cured rubber, the samples completely peel enabling to calculate an adhesion energy using the Kendall's formula (equation (2)):<sup>47</sup>

$$G = \frac{F^2}{4 w^2 E h} \quad (2)$$

where  $F$  is the measured force,  $E$  the Young's modulus,  $w$  the width and  $h$  the thickness of the sample (joint is thus  $2 \times h$  thick).

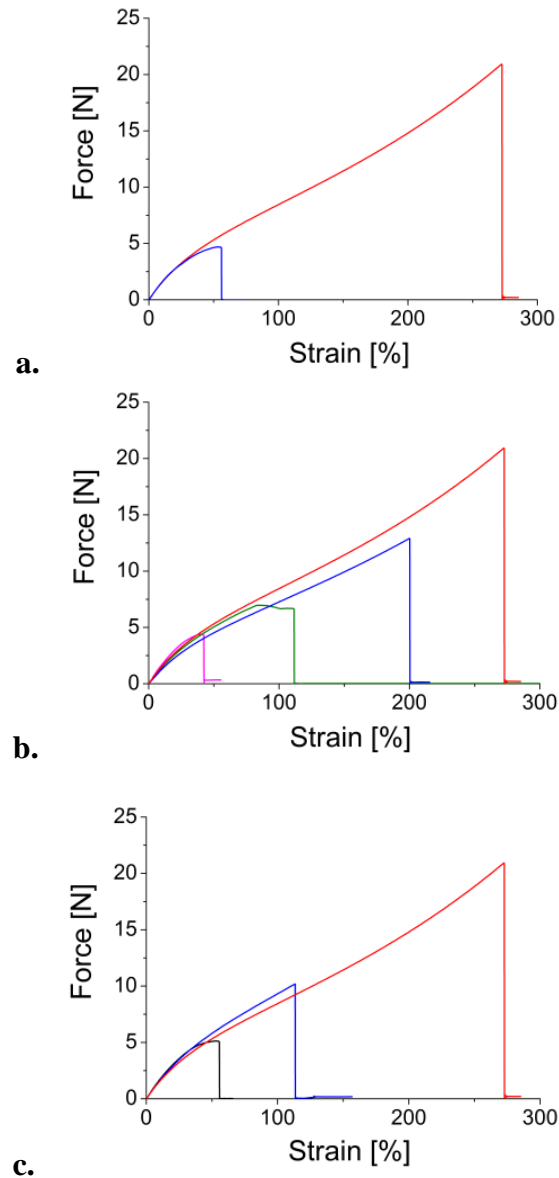


Figure 9. Lap shear tests on cured rubbers: **a.** Comparison between DA- (blue) and DTDB-(red) cured rubbers, adhesion for 30 min at 180 °C, **b.** DTDB-cured rubber adhered at 180 °C for varying times (pink: 5 min, green: 10 min, blue: 20 min and red: 30 min), **c.** DTDB-cured rubber adhered for 30 min at different temperatures (black: 100 °C, blue: 150 °C and red: 180 °C).

Calculated adhesion energies are summarized in Table 1. For the highest adhesion times, the joint becomes stronger than the material itself and the sample breaks as already observed in Figure 9a. In this case, it is impossible to calculate an adhesion energy but the adhesion is obviously higher than for shorter adhesion times. For a 30 min adhesion of the reference material at 180 °C, the calculated energy is only 90 J/m<sup>2</sup> which is comparable to the 80 J/m<sup>2</sup> measured for the disulphide-containing sample at 100 °C, temperature at which no

rearrangement reactions are observed. It confirms that this low adhesion of the test material is probably only due to chain inter-diffusion between the two pieces of material.

Table 1. Results of adhesion measurements

Sample	DTDB-cured					DA-cured	
	180 °C				150 °C	100 °C	180 °C
Adhesion time (min)	5	10	20	30	30	30	30
Adhesion energy (J/m <sup>2</sup> )	70	230	Sample breaks	Sample breaks	Sample breaks	80	90

#### 1.3.4. Thermo-activated adhesion enables recycling of the rubber

For recycling experiments, DTDB-cured sample was reduced to a fine powder using a variable speed rotor mill and then heated at 180 °C for 40 minutes in a heating press (Figure 10). The same reprocessing experiment was conducted on a DA-cured sample for comparison. After the heat treatment, the integrity of the DA-crosslinked sample is not recovered (Figure S1). Specimens could still be cut and tested showing that the “reformed” material has completely lost its properties after grinding and heating. The behaviour of the disulphide-containing network is completely different. The integrity of the sample is fully restored after heating as shown in Figure 10a. Most of the mechanical properties are recovered: the reprocessed sample shows about 50 % of the initial stress and 80 % of the initial, strain at break (Figure 10b). After fine grinding of the rubber, when grains of powder are pressed together at high temperature, rearrangements occur. In these conditions, chains start to interpenetrate and chemical reactions will then “mend” the grains together. Side reactions generating permanent bonds limit the rearrangements inside each grain of powder, but they take part into the mending process creating bonds between and inside particles, even if the created bonds are not dynamic anymore. All this process can be seen as relaxation allowing intimate adhesion of the powder grains.

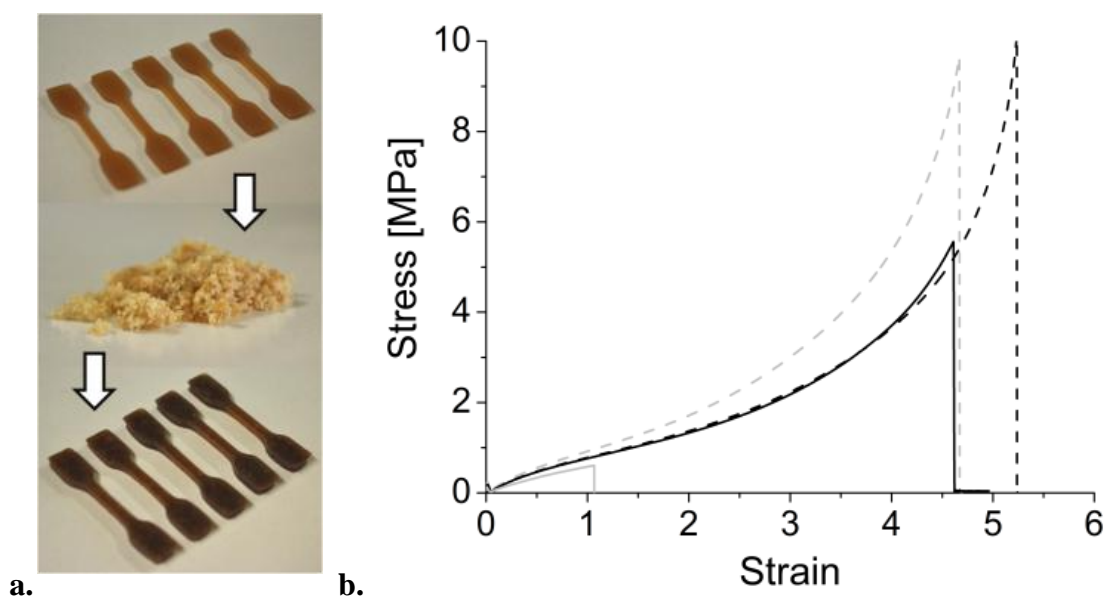


Figure 10. Recycling experiment. **a.** The cured rubber is finely grinded then reshaped by compression moulding. **b.** Tensile test before and after the recycling experiment (black: DTDB-cured; grey: DA-cured; dashed: before; line: after).

The properties of both samples are listed in Table 2. It is worth noticing that for DTDB-cured material, the Young's modulus remains identical after reforming the sample (Figure S5). Swelling experiments in toluene (Table 2 and Figure S3) confirmed that the crosslinking density is comparable before and after reforming.

Table 2. Mechanical properties of ENR crosslinked by DTDB or DA, before grinding and after reprocessing.

	Stress at break [MPa]	Strain at break	Young's modulus [MPa]	Equilibrium swelling ratio Q
DTDB_virgin	$12 \pm 2$	$5.3 \pm 0.2$	$1.67 \pm 0.02$	3.5
DTDB_reprocessed	$5 \pm 1$	$4.2 \pm 0.2$	$1.66 \pm 0.02$	3.3
DA_virgin	$10 \pm 1$	$4.6 \pm 0.2$		
DA_reprocessed	$1.0 \pm 0.1$	$0.6 \pm 0.1$		

## 1.4. Conclusions

A dynamic covalent network was obtained by crosslinking ENR with a disulphide-containing carboxylic diacid. The resulting rubber was shown to be a dual network containing mostly disulphide crosslinks (considered as dynamic) and a few permanent crosslinks resulting from unavoidable side reactions. The dynamic nature of the disulphide bonds was highlighted through stress relaxation, creep and adhesion experiments. The network presents strong elastomeric properties at temperatures as high as 100 °C and is able to rearrange at higher temperatures (above 150 °C). The processing of the rubber at high temperature is limited because of the dual nature of the network, but even after several cycles at high temperature rearrangements still occur. The material can be recycled and recovers most of its mechanical properties after grinding to a fine powder and remoulding. A compromise is obtained: despite the formation of some permanent bonds, the object, even used at high temperatures, may be reshaped at the end of its life cycle. This could be optimized, by the use of a catalyst for example. Furthermore, the good adhesion properties of this rubber should permit the repairing of cracks by heating and thus lead to fatigue improvement. Our comparison of DA- and DTDB-cured systems shows the importance of the disulphide rearrangements in the stress relaxation process, the adhesion properties and recycling capability of DTDB-cured ENR rubber.

Other kinds of chemical functions could be introduced in ENR *via* the internal chain of a carboxylic diacid. We thus can envision developing rubbers sensitive to other stimuli than temperature or even materials having a fully reversible behaviour if side reactions can be avoided.

### **Acknowledgements**

This research has been supported by the European Seventh Framework NMP program, SHINE project - grant agreement 309450-2. Benoît le Rossignol from Hutchinson SA, Montargis Research Centre, France, is warmly acknowledged for the gift of ENR25, as are Michel Cloître and Renaud Nicolaÿ for helpful discussions on rheological measurements and disulphide chemistry, respectively, as well as Erwan Chabert for his help in adhesion sample preparation.

### 1.5. Supplementary information (SI)

This section is adapted from the electronic supplementary information section published in *Polymer Chemistry* in order to avoid too many repetitions.

#### 1.5.1. Reprocessing experiment

During a recycling experiment, a piece of crosslinked rubber was reduced to a fine powder and subsequently compression moulded at 180 °C to allow for disulphide rearrangements.

The same experiment was conducted on DTDB- and DA-cured ENR and the comparison of the two resulting materials is shown in Figure Sa. In this photo, it is clear that the samples behave very differently. The integrity of the sample is fully recovered in the case of the disulphide containing network (on the left) whereas for the test material (DA-cured ENR on the right), the powder is only partially agglomerated. In the case of DA-cured material, the agglomeration can be due to the effect of compression and to a limited inter-diffusion of the crosslinked polymer chains but no chemical reversible reaction is possible. In the case of DTDB-cured ENR, the disulphide rearrangements happening at high temperatures transform the powder back to a one-piece material.

Three specimens could still be cut from the DA-cured reprocessed material to test the tensile properties. Photos of the samples before and after reprocessing are given in Figure S1b and c.

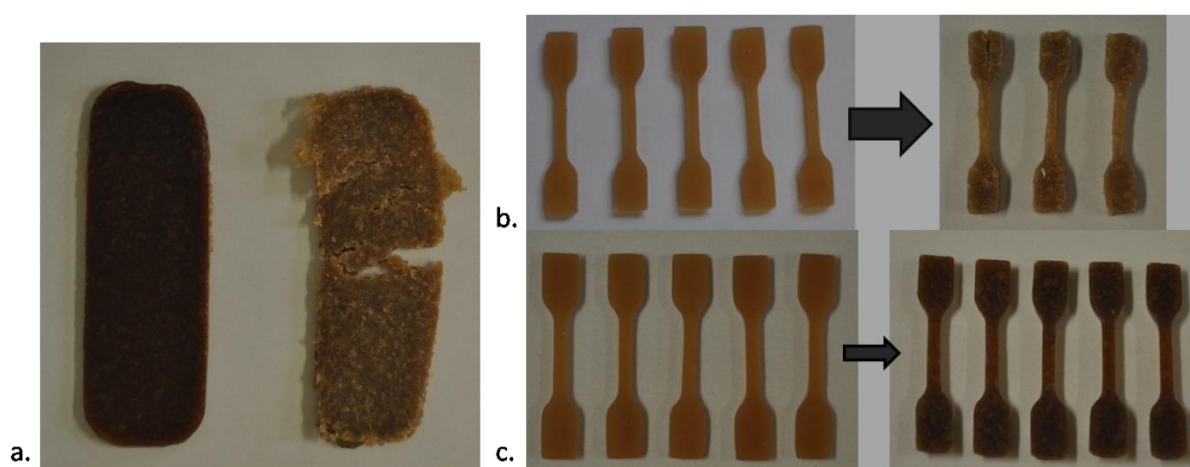


Figure S1. Reprocessing of a grinded sample: **a.** Materials obtained after the reprocessing procedure (left: DTDB-cured ENR, right: DA-cured ENR) **b.** DA-cured samples before and after reprocessing, **c.** DTDB-cured samples before and after reprocessing.

1.5.2. Reproducibility of the simple tensile tests

Stress-strain behaviour is determined by tensile tests until break. At least five different specimens of the same material were systematically studied to test reproducibility and take an average of the properties (except for the DA-cured reprocessed ENR from which only three samples could be punched, but they show a very good reproducibility). The dumbbell shaped samples are shown in Figure S**b** and **c**. In Figure S2, one can see the good reproducibility of the tensile experiment.

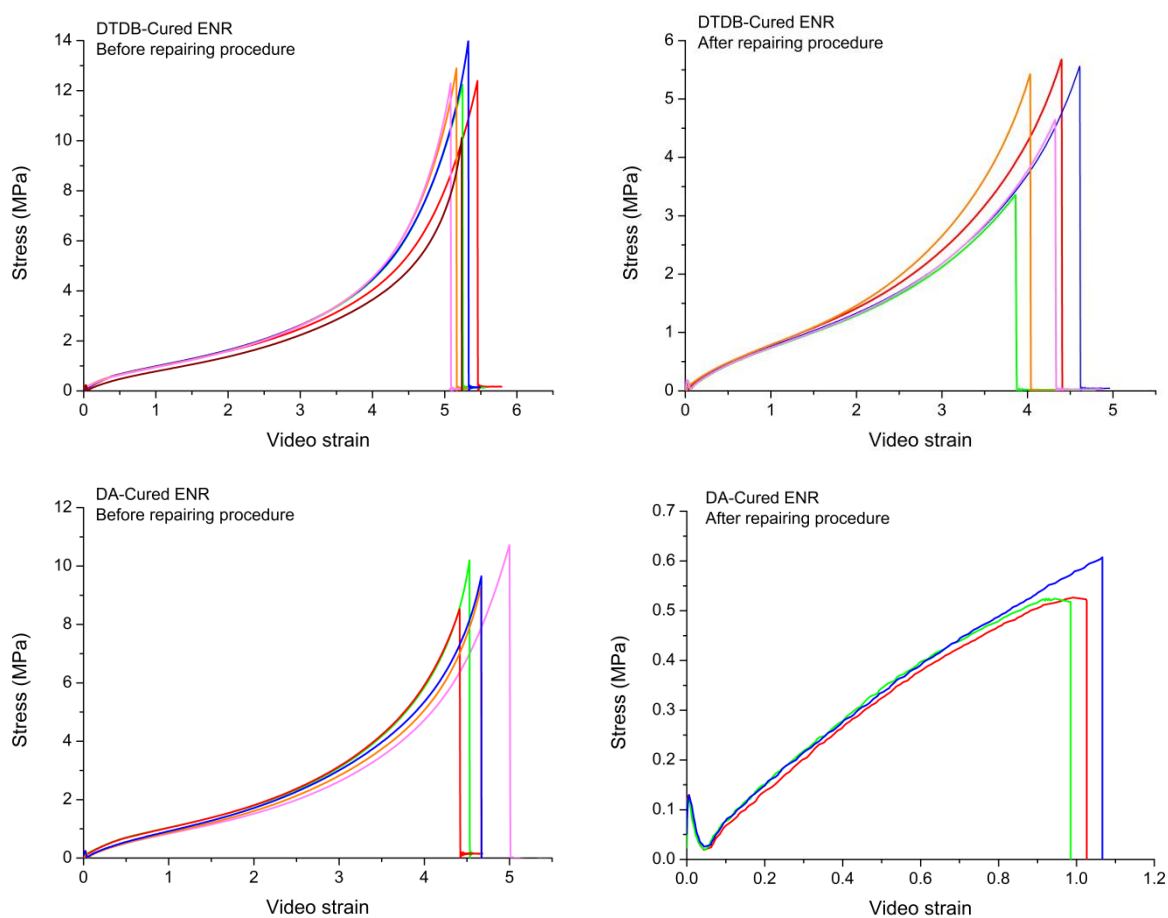


Figure S2. Stress-strain profiles of the specimen before and after reprocessing (up: DTDB-cured material, down: DA-cured)

1.5.3. Swelling experiment

The swelling ratio  $Q$  of DTDB-cured ENR before and after reprocessing is plotted against time in Figure S3. After a few hours, the weight remained constant indicating that the samples

reached their equilibrium swelling. The corresponding equilibrium ratio is very similar before and after reprocessing meaning that the density of crosslinks in the two networks is almost the same.

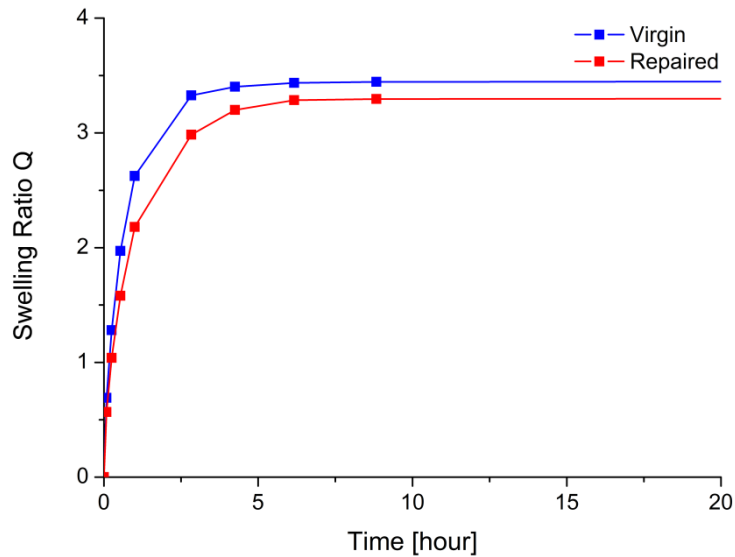


Figure S3. Swelling behaviour of the DTDB-cured rubber before and after reprocessing.

#### 1.5.4. Study of the dissolved DTDB-cured network in reductive conditions

By using reductive conditions, disulphide links can be broken into thiols. It causes very large swelling of the disulphide-containing network that weakens the material a lot. Eventually, the material dissolves, but it is degraded. Indeed, on the one hand  $^1\text{H-NMR}$  indicated that the chemistry of the material is the same (epoxidized polyisoprene with 25 % epoxy groups, see Figure S4), but on the other hand gel permeation chromatography showed much shorter chains than in initial ENR ( $M_w \approx 10\,000\text{--}20\,000\text{ g.mol}^{-1}$  instead of almost  $10^6\text{ g.mol}^{-1}$  for virgin ENR).

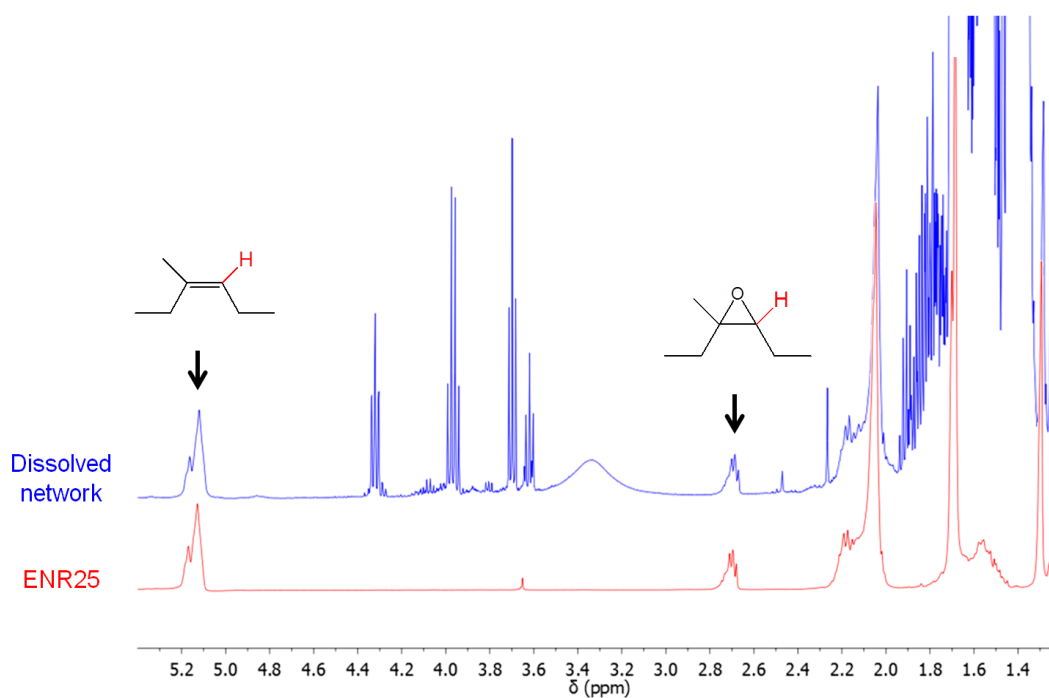


Figure S4.  $^1\text{H}$ -NMR superposition of ENR25 in red and the dissolved material in blue

This NMR was done on a piece of DTDB-cured network that was dissolved in THF with the presence of water and a very large excess of TBP (to accelerate the dissolving process). When dissolved, the material was filtered and the solvent was completely evaporated. Comparison is made with virgin ENR25. On the blue curve of Figure S4, the peaks of TBP appeared (a mix of its native form and oxidized form) because of the large excess. By comparing to the spectrum of pure ENR25 (in red), one can see that the characteristic peaks of ENR25 are present in the good ratio, confirming that the ENR structure is not altered (olefinic proton at 5.1 ppm and proton of the epoxy ring around 2.7 ppm).

#### 1.5.5. Determination of Young's Modulus

Young's modulus of DTDB-cured ENR was also determined using tensile measurements. Rectangular specimens were used for a better reproducibility. The specimen (5 x 30 mm) were cut in a film of the tested material (width was around 1.6 mm for the virgin cured sample and 2 mm for the reprocessed one). For this test, the strain speed was fixed at  $10 \text{ min}^{-1}$  which corresponds to a crosshead speed of about  $200 \text{ mm} \cdot \text{min}^{-1}$  (effective length of the specimens was around 20 mm in each case). The corresponding curves are given in Figure S5.

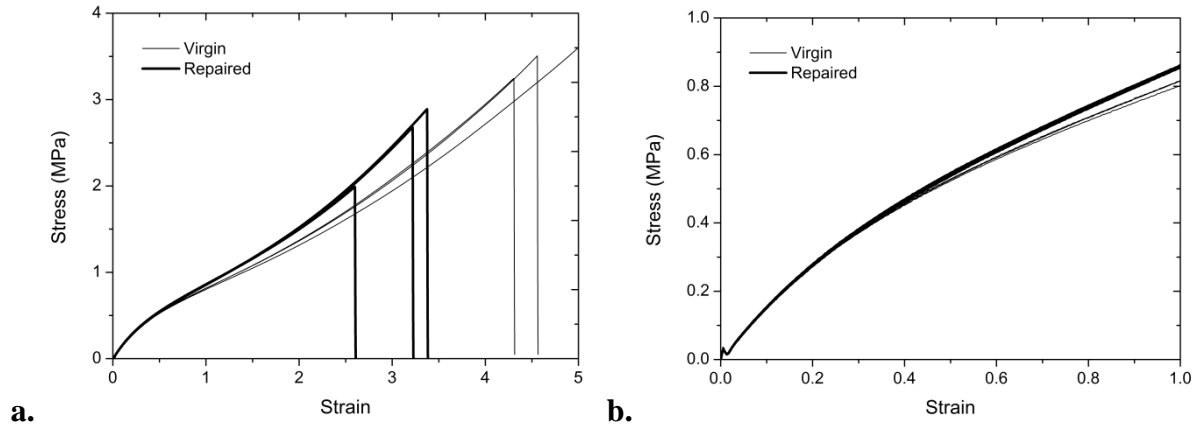


Figure S5. Tensile test for the determination of Young's Modulus on DTDB-cured ENR  
(a. Stress-strain profile, b. Zoom.)

The beginning of the curves is very reproducible so we did only three measurements for each material. Considering that the Young's modulus is the slope of the stress-strain curve at low strain, it is possible to deduce from these measurements that  $E$  is around 1.5-1.6 MPa for both the virgin and the reprocessed samples. However  $E$  can also be found by another method that should be somehow more precise. For a uniaxial tensile test, the affine model gives the stress  $\sigma$  in function of the elongation ratio  $\lambda$ :

$$\sigma = G \left( \lambda - \frac{1}{\lambda^2} \right)$$

The Young's modulus can thus be obtained by plotting

$$\frac{\sigma}{\lambda + \frac{1}{\lambda^2}} = f(\lambda)$$

which is a constant  $K$  at low strains. In this case the Young's modulus can be taken as  $E = 3K$  (indeed for rubbers, the Poisson's coefficient is 0.5 which gives  $E = 3G$ ). With this second method, Young's moduli were found to be respectively 1.67 and 1.66 MPa with an error of only about  $\pm 0.02$  MPa.

## 2. Comparison with a sulphur-vulcanized ENR network

### 2.1. Introduction

The DTDB-cured rubber presented in the previous section is crosslinked through disulphide bridges (and most probably a small amount of permanent C-C or C-S crosslinks from side reactions). Conversely, sulphur vulcanization produces a complex mix of mono-, di- and polysulphides. It is thus potentially interesting to compare the two types of crosslinking. However, one should keep in mind that sulphur vulcanization results in different types of bridges depending on the chosen cure recipe. Indeed, by varying the sulphur/accelerator ratio for example, the crosslinks can go from a majority of long polysulphide links (standard sulphur vulcanization) to mostly mono- and disulphides (efficient vulcanization).

As seen in the introduction of this chapter, sulphur vulcanized rubbers were studied for their relaxation properties a long time ago.<sup>2, 3, 5</sup> This relaxation phenomenon at high temperatures is due in part to degradation, but also to polysulphide rearrangements. Tetrasulphides have been shown to rearrange much faster (about 10 times) than disulphides.<sup>48</sup> This supposed stability of disulfide links is somehow in contradiction with our previous results on reprocessability of DTDB-cured ENR compared with DA-cured. However, Owen *et al.* based their interpretation on stress relaxation experiments carried out at 120 °C whereas the temperature used to reprocess DTDB samples was higher: 180 °C.

In this section, we compare the DTDB-cured material to a standard sulphur-vulcanized ENR (containing polysulphide links). Reprocessing properties and ageing resistance were compared. Polysulphide links are known to poorly resist to thermal oxidation. The poor ageing behaviour of sulphur-vulcanized ENR networks is partly explained by acid-catalyzed opening reactions of epoxy rings. Indeed, acids are formed by thermal decomposition of oxidized sulphides.<sup>49, 50</sup> The use of DTDB instead of sulphur could thus have a positive effect on the ageing resistance of the material.

## 2.2. Experimental section

### 2.2.1. Materials

All materials and methods used for the DTDB-cured ENR were already described in the first part of this chapter. Sulphur (S<sub>8</sub>) was obtained from Sigma-Aldrich Co. Zinc oxide (ZnO, > 99 %), stearic acid (97 %) and N-cyclohexyl-2-benzothiazolylsulfenamide (CBS, > 95 %) were respectively purchased from Fluka, Acros and TCI Co.

### 2.2.2. Blend preparation

Mixtures of ENR25, S<sub>8</sub>, ZnO, stearic acid and CBS were prepared in a Haake Polydrive mixer at 40 °C for about 20 min. The exact composition of this mix can be found in Table 3. After blending, samples were cured in a CARVER press under 8 tons pressure at 150 °C for the appropriate time (30 min, determined by rheology experiment).

Table 3. Recipe of vulcanized rubber samples (phr: parts per hundred rubber)

Component	Amount (phr)
ENR 25	100
Sulphur	3.5
Zinc Oxide	6
Stearic acid	0.5
CBS	0.5

### 2.2.3. Characterization methods

All the characterization methods (rheology, tensile testing, dynamic mechanical analysis and reprocessing experiment) were already described in the previous section (1.2). For swelling experiments, chloroform was used as a good solvent for ENR and the samples were discs of 5 mm diameter and 1.5 mm thickness. The swelling ratio Q was also defined in section (1.2). Thermo-oxidation was performed by placing the dog bone shaped tensile samples in an air-circulating oven for a determined period of time at a controlled temperature. The tensile properties of the materials were tested before and after ageing.

## 2.3. Results and discussion

### 2.3.1. Curing and crosslink density

There are three types of sulphur vulcanization systems depending on the sulphur/accelerator ratio:

- ✓ *Conventional vulcanization systems*: with a high content of sulphur, this kind of systems results in polysulfide containing materials.
- ✓ *Efficient vulcanization systems*: when the sulphur content is lower than the accelerator content, the resulting crosslinks are mainly mono- and disulfide links.
- ✓ *Semi-efficient vulcanization systems*: this is the case where both reactants are used in the same proportion and is a compromise between the two above mentioned systems.

In our case, the sulphur/accelerator ratio was fixed at 7 to obtain a polysulphidic network. The corresponding recipe is indicated in Table 3. In this mix, sulphur is used as the crosslinker, zinc oxide is an activator, and CBS an accelerator. A saturated fatty acid, stearic acid, is added to the formulation to help the compatibilization of ZnO with the matrix. Sometimes, retarding agents or anti-degradants are used in industrial formulations to respectively block the reaction before a certain time and temperature, and preserve the material from oxidative degradation. No retarding agent or anti-degradant were added here. The vulcanized sample will be referred to as ENR-S<sub>8</sub> in the following, and compared with ENR-DTDB (the DTDB-cured material of the previous section).

The kinetic of the crosslinking reaction was followed in the rheometer. Four identical samples were tested. As shown in Figure 11, the results are quite dispersed in terms of  $G'$  values. This can be explained by some air trapped between the sample and the rheometer, or by the fact that some samples contained bubbles. However, the shape of the curve is very reproducible,  $G'$  reaches a plateau within 45 minutes. As most of the reaction seems to occur before 15 minutes, the crosslink time was fixed to 30 minutes at 150 °C (to reach 90-95 % of the plateau value).

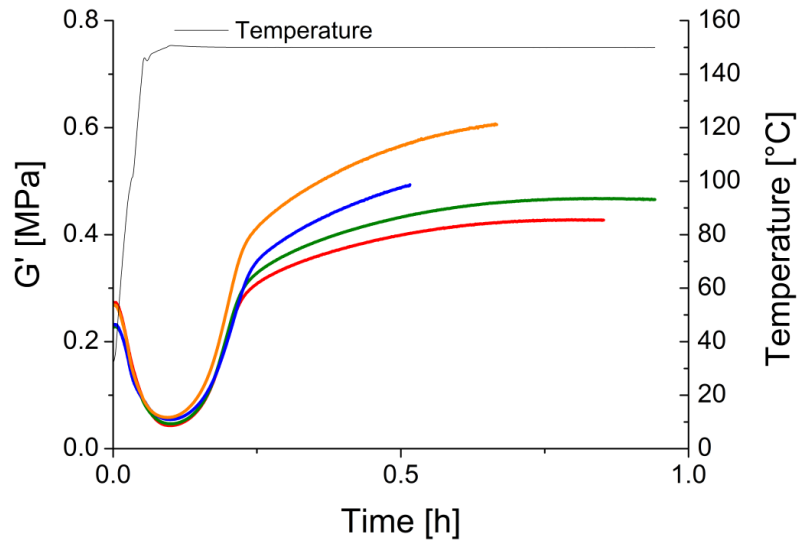


Figure 11. Kinetic study of the sulphur vulcanization of ENR25 at 150 °C in the rheometer (4 samples of the same formulation).

The aim here is to compare two types of ENR networks. For the comparison to be meaningful, the crosslink density of the materials should be similar. ENR-DTDB and ENR-S<sub>8</sub> were swollen in chloroform in order to have an idea of the extent of crosslinking. Three samples were tested for each material. Both networks rapidly swell to a comparable equilibrium swelling ratio around 8 or 9 (Figure 12). This indicates that both networks have similar crosslink density, allowing their comparison.

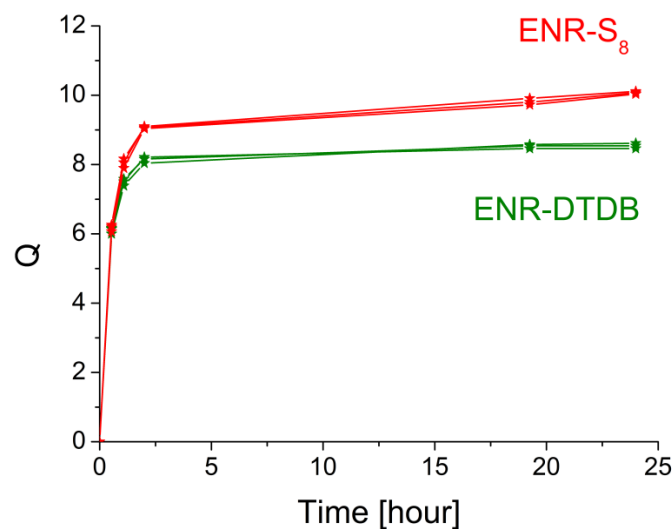


Figure 12. Compared swelling ratios of ENR-S<sub>8</sub> and ENR-DTDB in chloroform.

### 2.3.2. Stress relaxation behaviour

All stress relaxation experiments were performed under nitrogen flux in the rheometer. The samples were cured *in situ* and subsequently tested after the chosen curing time at the appropriate temperature (ENR-DTDB is cured for 40 minutes at 180 °C and ENR-S<sub>8</sub> for 30 minutes at 150 °C). The stress relaxations were carried out right after curing at the same temperature which is thus different for ENR-DTDB and ENR-S<sub>8</sub>. The reduced relaxation moduli are plotted in Figure 13 for comparison.

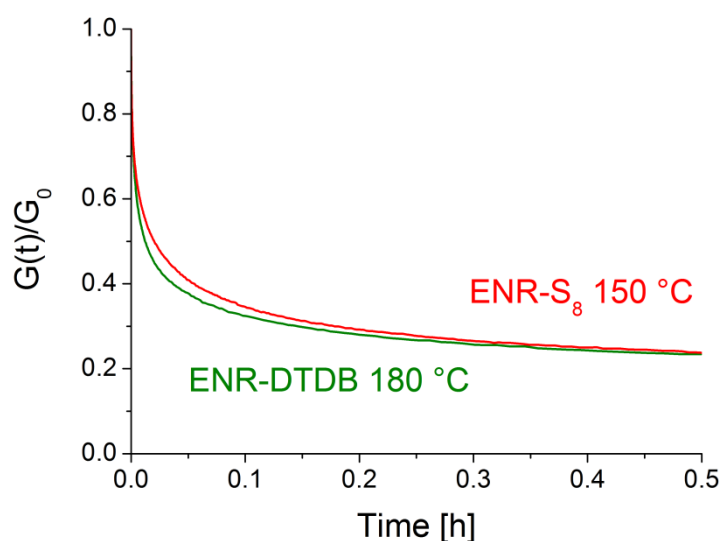


Figure 13. Stress relaxation experiment of ENR-S<sub>8</sub> and ENR-DTDB after curing in the rheometer.

The stress relaxation of ENR-DTDB at 180 °C is very similar to that of ENR-S<sub>8</sub> at 150 °C. This indicates that disulfide bonds can be cleaved at 180 °C just as polysulphidic links at 150 °C. For both materials, the shear modulus  $G'$  (measured in oscillation) is very similar before and after the relaxation experiment, indicating that the number of crosslinks did not change much which confirms that the crosslinks are reformed.

From the results of the previous section on ENR-DTDB, we suspected that side reactions occurred at high temperatures. More relaxation experiments were carried out after different curing times in the rheometer (Figure 14) to check the effect of this parameter on the stress relaxation of the samples.

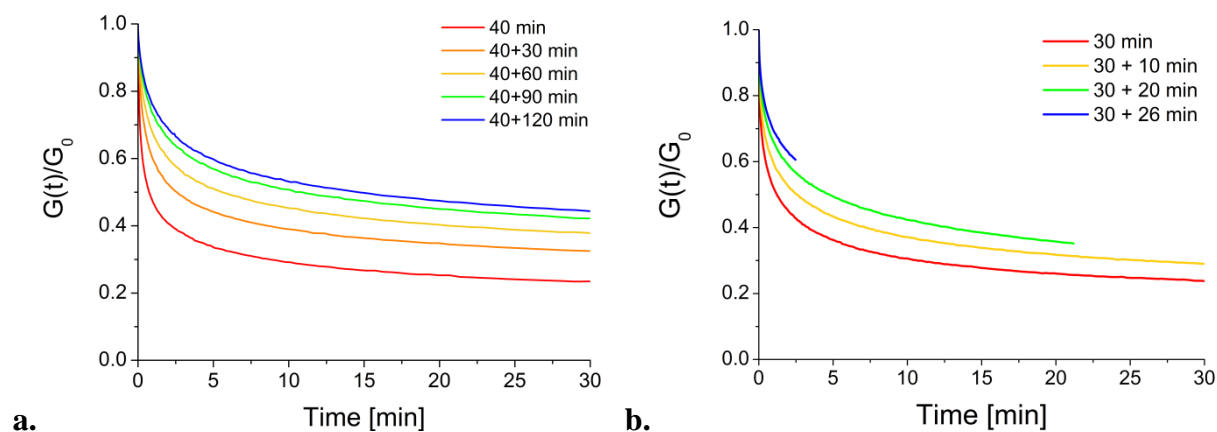


Figure 14. Effect of the curing time on the stress relaxation properties

**a.** ENR-DTDB at 180 °C, **b.** ENR-S<sub>8</sub> 150°C.

The legends are the curing time before relaxation (at 180 °C for ENR-DTDB and 150°C for ENR-S<sub>8</sub>)

Both materials show the same behaviour. With increasing curing times, the shape of the relaxation curve is modified.  $G(t)/G_0$  seems to reach an plateau in each case, and the longer the curing time the higher this plateau. The stress relaxation is believed to occur through rearrangements of sulphidic bonds. The decreasing extent of relaxation observed for longer curing times is thus probably linked with modifications of the network chemistry. In the case of ENR-DTDB, we concluded in the previous section that some reversible disulphide bonds are consumed by side reactions happening at high temperature. The same explanation can be given here for ENR-S<sub>8</sub>. However, instead of transforming a reversible bond into a permanent one, the side reactions of a polysulphide network may be more gradual. From a polysulfide link of more than 4 sulphur atoms, two shorter polysulphides can be obtained that will then potentially be affected by side reactions. As our vulcanization system should result in a majority of long polysulphidic links, the side reaction process limiting stress relaxation could be slowed down in ENR-S<sub>8</sub> compared to ENR-DTDB. However, this is not what is observed. Quantitatively, the value of the reduced modulus at 10 minutes of relaxation,  $G(t = 10 \text{ min})/G_0$ , increases of 0.12 for ENR-S<sub>8</sub> for an increase of vulcanization time of 20 minutes but it only increases of 0.1 in the case of ENR-DTDB for an increase of vulcanization time of 30 minutes. Side reactions are faster in ENR-S<sub>8</sub>. This result is probably linked with the already observed fact that polysulphides are more reactive than disulphides. They must be also more prone to side reactions even at lower temperature (150 °C instead of 180 °C).

### 2.3.3. Reprocessing of the material

ENR-DTDB showed good reprocessing properties (Figure 10 in section (1.3.4)). Similar properties have already been reported for sulphur-vulcanized natural rubber.<sup>11-13</sup> In these examples, GTR powder is compression moulded at high temperature without the use of virgin gum or curing agents. The properties of the obtained materials are not as good as the initially cured rubber, but the reprocessed materials exhibit rubbery characteristics with acceptable rupture properties. The case of GTR is somewhat special due to the presence of fillers that could have an effect on the reprocessing properties. The reprocessing properties of our filler-free ENR-S<sub>8</sub> samples were tested in order to compare both vulcanization systems (polysulphides for sulphur vulcanization and disulfides for DTDB). The mechanical properties of ENR-S<sub>8</sub> before and after reprocessing are shown in Figure 15.

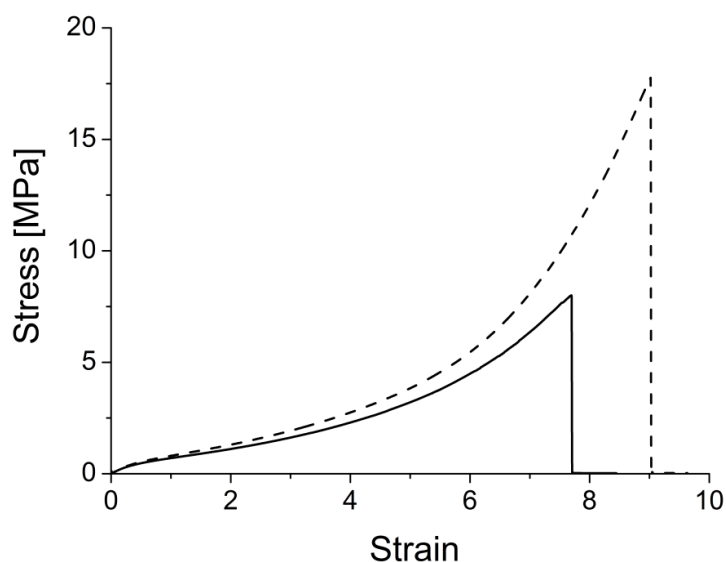


Figure 15. Tensile test before (dashed) and after (line) the recycling experiment of ENR-S<sub>8</sub>.

The results of this experiment are qualitatively similar for ENR-S<sub>8</sub> (Figure 15) and ENR-DTDB (Figure 10b): some of the initial properties are recovered. One can however notice that both curves superimpose for ENR-DTDB whereas the strain of the reprocessed ENR-S<sub>8</sub> is lower than the one of the virgin sample. This loss in modulus could result from a loss in crosslink density or some chain scission.

Table 4. Ultimate mechanical properties of ENR-S<sub>8</sub> and ENR-DTDB before and after reprocessing

	ENR-DTDB			ENR-S <sub>8</sub>		
	Virgin	Revulcanized	% recovery	Virgin	Revulcanized	% recovery
$\sigma_{\max}$ [MPa]	12 ± 2	5 ± 1	42	17.1 ± 2	7.7 ± 1	45
$\epsilon_{\max}$	5.3 ± 0.2	4.2 ± 0.2	80	8.9 ± 0.4	7.5 ± 0.4	84

The results can be interpreted more quantitatively with the values of stress and strain at break that are collected in Table 4. Both materials have very similar reprocessing properties. The disulphide bond is dynamic enough at 180 °C to provide rearrangements and compete with polysulfide bonds.

#### 2.3.4. Thermo-oxydative properties

It is well known that sulphur vulcanization provides the material with quite poor ageing properties. In this section, we compare ENR-DTDB to ENR-S<sub>8</sub> to see if the selective use of disulfide is beneficial for this matter.

Ageing experiments should be conducted over some years to get representative results about the life of materials. At the laboratory scale, the experiment is accelerated by the use of temperature. Samples are put in air circulating ovens for determined periods of time at a controlled temperature. As our materials do not contain antioxidants, a moderate temperature of 70 °C was first chosen. The mechanical properties after ageing are shown in Figure 16. Each curve is chosen as the representative curve among the five tested samples (at least five, and sometimes up to seven). The same curves but with all the samples for each time of ageing are shown in Appendix 1, Figure 20, to appreciate the increased dispersities.

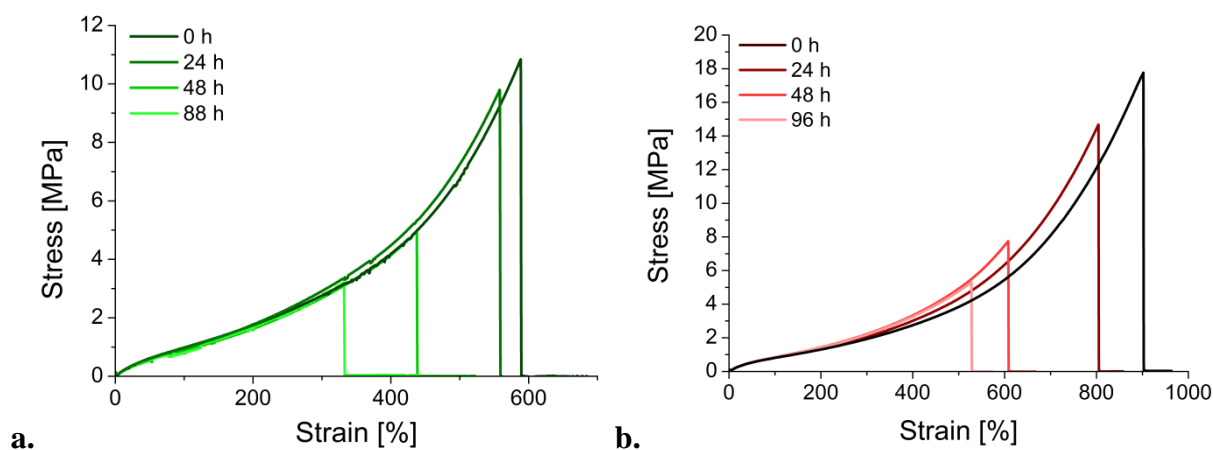


Figure 16. Mechanical properties after ageing at 70 °C for different times. **a.** ENR-DTDB, **b.** ENR-S<sub>8</sub>

Over the 3 or 4 days at 70 °C, the ultimate properties of our materials decrease constantly as expected for sulphur crosslinking. The only qualitative difference seen on these plots is the fact that all the stress-strain curves superimpose for ENR-DTDB whereas they do not in the case of ENR-S<sub>8</sub>. Classically, in ageing experiments, the rising of the modulus at the same strain is a sign of over-crosslinking. Conversely, if it decreases, chain scission is the dominating ageing process. Eventually, if the curves superimpose, it can be that over-crosslinking and chain scission compensate each other. In our case, ENR-S<sub>8</sub> seems to over-crosslink whereas in ENR-DTDB this over-crosslinking is compensated by some chain scissions.

As disulphide rearrangements were shown to happen only above 150 °C, the ageing properties of both materials were also tested at 150 and 180 °C. For the longer ageing times, the reproducibility decreases and the results are more dispersed. For a better comparison of the ultimate properties, average values were calculated. The loss percentages relative to the non-aged samples were plotted against the ageing time at each temperature in Figure 17. At 70 °C, the loss in mechanical properties is very similar for ENR-DTDB and ENR-S<sub>8</sub>. Over the three days of test, the loss in tensile strength is significant (only 20-30 % of the initial properties are retained). Even if ENR-DTDB shows slightly higher values of relative strain at break, it can be concluded that both crosslinking types lead to thermo-oxidation sensitive materials. By testing at 150 °C, a beneficial effect of the disulphide links over polysulphides is highlighted. The time scale is much shorter, but ENR-DTDB is clearly more resistant, probably thanks to the lower reactivity of disulphides. The highest temperature is too high and

both samples are completely degraded; in less than 1 hour for ENR-S<sub>8</sub> and about 1.5 hours for ENR-DTDB.

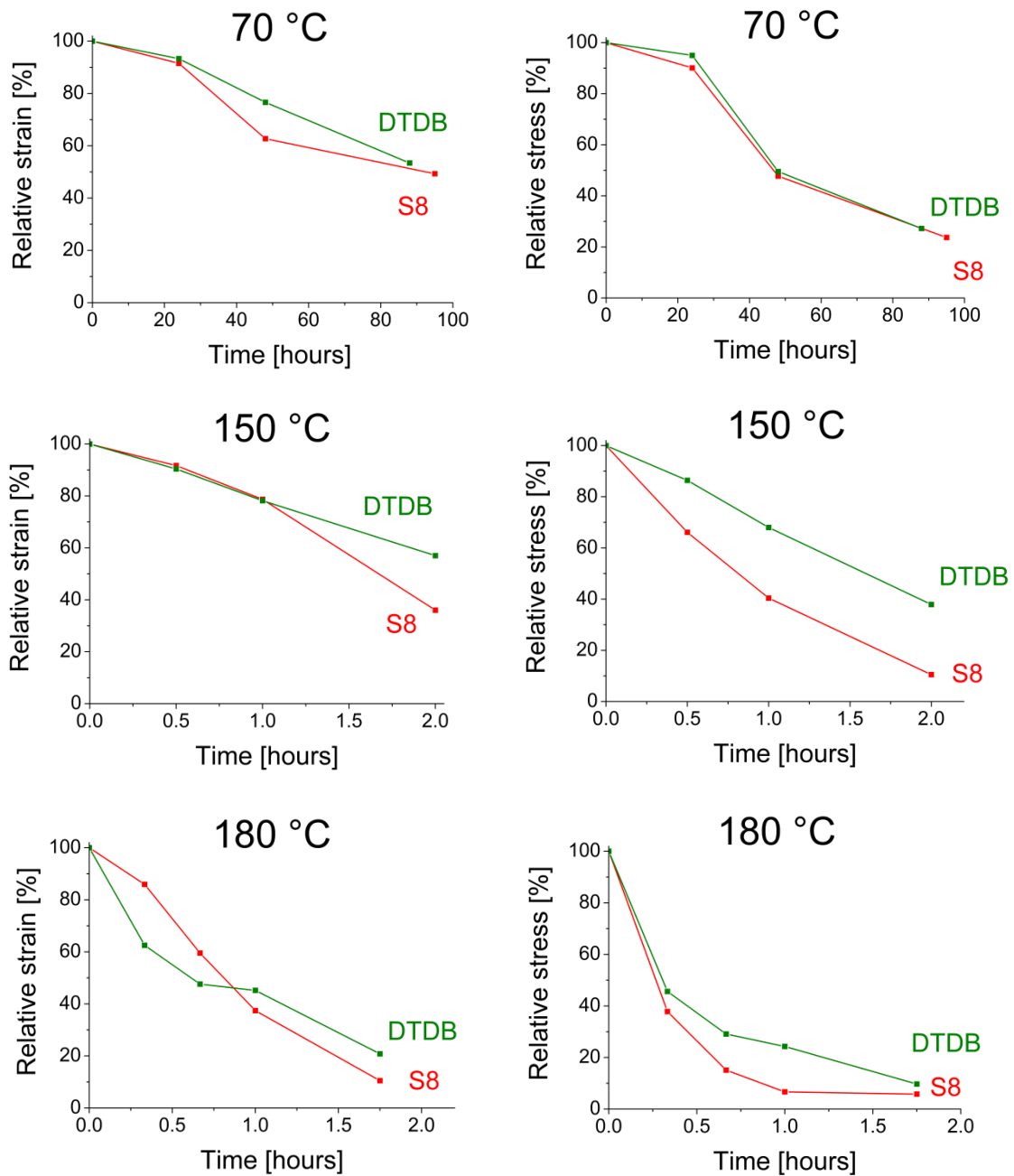


Figure 17. Ultimate properties after ageing, relative to the non-aged samples.

### 2.3.5. Creep measurement

Through creep measurements, DTDB-cured samples were shown to resist to relatively high temperatures (up to 100 °C) without any deformation, but started to rearrange above 150 °C.

The same experiments were conducted on ENR-S<sub>8</sub> (Figure 18). For ENR-DTDB, this experiment was shown in Figure 7a.

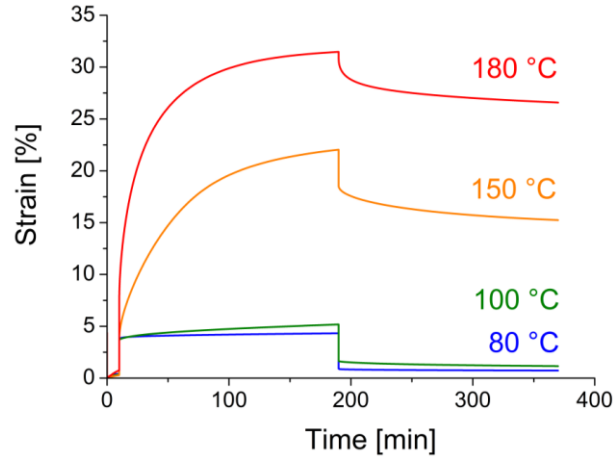


Figure 18. Creep properties of ENR-S<sub>8</sub> at different temperatures (a force of 0.5 N is applied during 180 min and released).

Again, at first sight, both materials have similar qualitative behaviours: they withstand the applied force without much residual strain at 100 °C and start to significantly deform above 150 °C. However, looking closer and more quantitatively, one can see that at 100 °C the final residual strain is 1.2 % whereas it was only 0.36 % for ENR-DTDB. This difference could be of importance in applications where the precise shape of the samples needs to be retained.

For more convenience, the comparison between ENR-DTDB and ENR-S<sub>8</sub> at 150 °C is plotted in Figure 19.

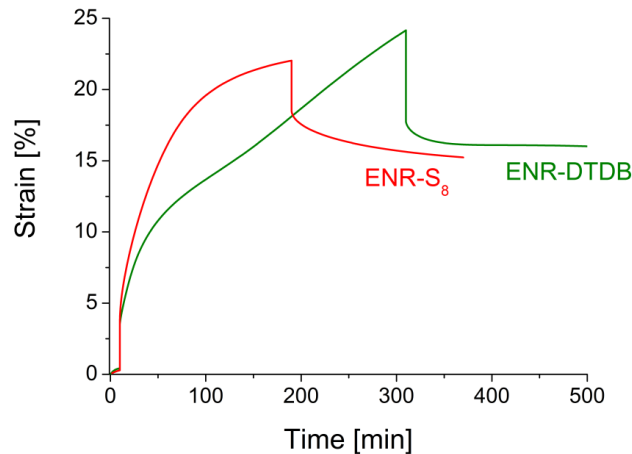


Figure 19. Creep test. Comparison of ENR-DTDB with ENR-S<sub>8</sub> at 150 °C.

The initial slope of the curve is more elevated for ENR-S<sub>8</sub>, confirming the higher reactivity of polysulphides. However, after about 100 min, this slope tends to decrease, which is not the case of ENR-DTDB. This decrease was already observed for ENR-DTDB at 180 °C (Figure 7a in section (1.3.2)) and was attributed to the effect of secondary reactions that consume dynamic bonds and create permanent ones. This creep experiment shows that side reactions are faster and more limiting at 150 °C in the polysulphide-containing network, an argument in favour of the DTDB-cured system.

## 2.4. Conclusions

Classical sulphur vulcanization produces dynamic networks through polysulphide exchanges. The cured materials show stress relaxation and reprocessing properties. However, the sulphur curing recipe contains toxic additives like ZnO or CBS which are highly detrimental to the environment. This is a major drawback because sulphur vulcanization is nowadays widely used in the industry. In the first part of this chapter, we showed that well defined disulfide bonds may be introduced as the crosslink points of an ENR network. This material possesses reprocessing and adhesion properties. The aim of the second part of this chapter was to compare a polysulfide network obtained by classical sulphur vulcanization with this new, more environmentally friendly, disulphide crosslinking.

All tested properties are quite similar for the two types of crosslinks. The introduction of dynamic bonds enables reprocessing of the material. The extent of property recovery is in the same range in both cases (about 45 % of the tensile strength and 80 % of the strain at break). However, some differences are found in favour of the disulphide crosslinking. Indeed, ENR-DTDB can for example withstand temperatures as high as 100 °C with very low residual deformations. Generally, polysulphides were shown to be more reactive than disulphides. This lower reactivity of disulphides is not detrimental to the dynamic character of the network and sulphidic rearrangements can still occur at high temperature. Moreover, the lower reactivity of disulphides makes them less prone to the secondary reactions which degrade the quality of the dynamic network. DTDB thus appears as a good competitor for sulphur in the crosslinking of ENR.

## Acknowledgments

Guilhem Chenon is warmly thanked for his experimental participation to Section (2) during his internship in the laboratory.

## Appendix

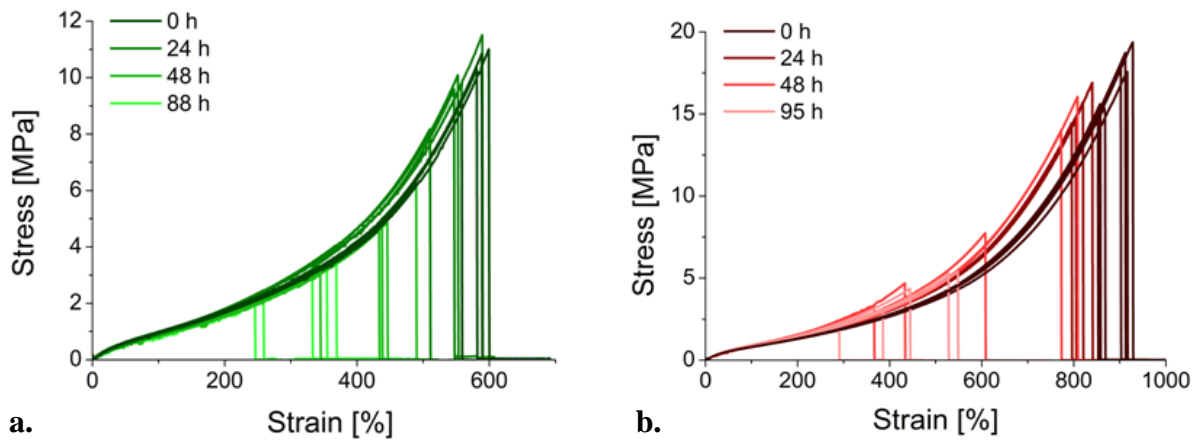


Figure 20. Mechanical properties after ageing at 70 °C for different times.  
(For each time all the curves are shown) **a.** ENR-DTDB, **b.** ENR-S<sub>8</sub>

## References

1. A. Tobolsky, W. MacKnight and M. Takahashi, *The Journal of Physical Chemistry*, 1964, **68**, 787-790.
2. A. V. Tobolsky, I. B. Prettyman and J. H. Dillon, *Journal of Applied Physics*, 1944, **15**, 380-395.
3. J. Berry and W. Watson, *Journal of Polymer Science*, 1955, **18**, 201-213.
4. J. P. Berry, *Journal of Polymer Science*, 1956, **21**, 505-517.
5. A. V. Tobolsky, *Journal of Applied Physics*, 1956, **27**, 673-685.
6. J. P. Berry and W. F. Watson, *Journal of Polymer Science*, 1957, **25**, 493-494.
7. A. Tobolsky, *Journal of Polymer Science*, 1957, **25**, 494-497.
8. J. Berry and W. Watson, *Journal of Polymer Science*, 1957, **25**, 497-498.
9. S. Tamura and K. Murakami, *Polymer*, 1980, **21**, 1398-1402.
10. D. Montarnal, M. Capelot, F. Tournilhac and L. Leibler, *Science*, 2011, **334**, 965-968.
11. B. Adhikari, D. De and S. Maiti, *Progress in Polymer Science*, 2000, **25**, 909-948.
12. E. Bilgili, A. Dybek, H. Arastoopour and B. Bernstein, *Journal of Elastomers and Plastics*, 2003, **35**, 235-256.
13. A. Gugliemotti, C. Lucignano and F. Quadrini, *Plastics, Rubber and Composites*, 2012, **41**, 40-46.
14. J. Canadell, H. Goossens and B. Klumperman, *Macromolecules*, 2011, **44**, 2536-2541.
15. H. Otsuka, S. Nagano, Y. Kobashi, T. Maeda and A. Takahara, *Chemical Communications*, 2010, **46**, 1150-1152.
16. A. Rekondo, R. Martin, A. Ruiz de Luzuriaga, G. Cabanero, H. J. Grande and I. Odriozola, *Materials Horizons*, 2014, **1**, 237-240.
17. Z. Q. Lei, H. P. Xiang, Y. J. Yuan, M. Z. Rong and M. Q. Zhang, *Chemistry of Materials*, 2014, **26**, 2038-2046.
18. L. Imbernon, E. Oikonomou, S. Norvez and L. Leibler, *Polymer Chemistry*, 2015, **6**, 4271-4278.
19. C. N. Bowman and C. J. Kloxin, *Angewandte Chemie International Edition*, 2012, **51**, 4272-4274.
20. X. Chen, M. A. Dam, K. Ono, A. Mal, H. Shen, S. R. Nutt, K. Sheran and F. Wudl, *Science*, 2002, **295**, 1698-1702.
21. G. Deng, C. Tang, F. Li, H. Jiang and Y. Chen, *Macromolecules*, 2010, **43**, 1191-1194.
22. C. J. Kloxin and C. N. Bowman, *Chemical Society Reviews*, 2013, **42**, 7161-7173.
23. R. J. Wojtecki, M. A. Meador and S. J. Rowan, *Nature Materials*, 2011, **10**, 14-27.
24. M. Capelot, D. Montarnal, F. Tournilhac and L. Leibler, *JACS*, 2012, **134**, 7664-7667.
25. M. Capelot, M. M. Unterlass, F. Tournilhac and L. Leibler, *ACS Macro Letters*, 2012, **1**, 789-792.
26. Y.-X. Lu, F. Tournilhac, L. Leibler and Z. Guan, *Journal of the American Chemical Society*, 2012, **134**, 8424-8427.
27. W. Denissen, G. Rivero, R. Nicolaÿ, L. Leibler, J. M. Winne and F. E. Du Prez, *Advanced Functional Materials*, 2015, **25**, 2451-2457.
28. M. Le Neindre and R. Nicolaÿ, *Polymer Chemistry*, 2014, **5**, 4601-4611.
29. M. Pepels, I. Pilot, B. Klumperman and H. Goossens, *Polymer Chemistry*, 2013, **4**, 4955-4965.
30. U. Lafont, H. van Zeijl and S. van der Zwaag, *ACS Applied Materials & Interfaces*, 2012, **4**, 6280-6288.

31. J. A. Yoon, J. Kamada, K. Koynov, J. Mohin, R. Nicolaÿ, Y. Zhang, A. C. Balazs, T. Kowalewski and K. Matyjaszewski, *Macromolecules*, 2012, **45**, 142-149.
32. Y. Amamoto, H. Otsuka, A. Takahara and K. Matyjaszewski, *Advanced Materials*, 2012, **24**, 3975-3980.
33. R. Nicolaÿ and Y. Kwak, *Israel Journal of Chemistry*, 2012, **52**, 288-305.
34. R. Martin, A. Rekondo, A. Ruiz de Luzuriaga, G. Cabanero, H. J. Grande and I. Odriozola, *Journal of Materials Chemistry A*, 2014, **2**, 5710-5715.
35. C. K. L. Davies and S. V. Wolfe, *Polymer*, 1983, **24**, 107-113.
36. T. Johnson and S. Thomas, *Polymer*, 1999, **40**, 3223-3228.
37. A. S. Hashim and S. Kohjiya, *Kautschuk Gummi Kunststoffe*, 1993, **46**, 208-213.
38. A. N. Bibi, D. A. Boscott, T. Butt and R. S. Lehrle, *European Polymer Journal*, 1988, **24**, 1127-1131.
39. S. N. Koklas, D. D. Sotiropoulou, J. K. Kallitsis and N. K. Kalfoglou, *Polymer*, 1991, **32**, 66-72.
40. M. A. Rahman, L. Sartore, F. Bignotti and L. Di Landro, *ACS Applied Materials & Interfaces*, 2013, **5**, 1494-1502.
41. M. Pire, S. Norvez, I. Iliopoulos, B. Le Rossignol and L. Leibler, *Polymer*, 2010, **51**, 5903-5909.
42. M. Pire, S. Norvez, I. Iliopoulos, B. Le Rossignol and L. Leibler, *Polymer*, 2011, **52**, 5243-5249.
43. L. Imbernon, M. Pire, E. K. Oikonomou and S. Norvez, *Macromolecular Chemistry and Physics*, 2013, **214**, 806-811.
44. M. Pire, C. Lorthioir, E. K. Oikonomou, S. Norvez, I. Iliopoulos, B. Le Rossignol and L. Leibler, *Polymer Chemistry*, 2012, **3**, 946.
45. M. Pire, S. Norvez, I. Iliopoulos, B. Le Rossignol and L. Leibler, *Composite Interfaces*, 2014, **21**, 45-50.
46. R. Chasset and P. Thirion, "Proceedings of the Conference on Physics of Non-Crystalline Solids", North Holland Publishing Co., Amsterdam, 1965.
47. K. Kendall, *Journal of Physics D-Applied Physics*, 1975, **8**, 512-522.
48. G. D. T. Owen, W. J. MacKnight and A. V. Tobolsky, *The Journal of Physical Chemistry*, 1964, **68**, 784-786.
49. I. Gelling and N. Morrison, *Rubber chemistry and technology*, 1985, **58**, 243-257.
50. S. Kohjiya and Y. Ikeda, *Chemistry, manufacture and applications of natural rubber*, Elsevier, 2014.

**Chapitre 4**  
**Réticulation physique et cristallisation sous contrainte**

---



<b>Chapitre 4 : Réticulation physique et cristallisation sous contrainte.....</b>	<b>154</b>
<b>1. Strain-induced crystallization in ENR-DA .....</b>	<b>157</b>
1.1. Introduction .....	157
1.2. Experimental section .....	159
1.2.1. <i>Materials</i> .....	159
1.2.2. <i>Sample preparation</i> .....	159
1.2.3. <i>Characterization</i> .....	160
1.2.4. <i>X-ray data processing</i> .....	161
1.3. Results and discussion.....	165
1.3.1. <i>Crosslinking and thermo-mechanical characterisation of ENR-DA networks</i>	165
1.3.2. <i>Tensile tests and in situ X-ray experiments</i> .....	168
1.3.3. <i>Comparison with literature</i> .....	175
1.4. Conclusions .....	176
<b>2. Crystallizable grafts and physical network .....</b>	<b>177</b>
2.1. Introduction .....	177
2.2. Characterization of the BA-grafting onto ENR.....	178
2.2.1. <i>Grafting reaction</i> .....	178
2.2.2. <i>Thermo-physical characterization of the grafting</i> .....	178
2.2.3. <i>Spectroscopic characterization</i> .....	181
2.3. Properties of BA-grafted ENR25 .....	184
2.3.1. <i>Thermo-mechanical properties</i> .....	184
2.3.2. <i>Morphology and structure of the physical network</i> .....	185
2.3.3. <i>Mechanical properties and X-ray scattering</i> .....	186
2.4. Summary and conclusions.....	193
<b>3. Dual networks.....</b>	<b>194</b>
<b>Appendix A .....</b>	<b>199</b>
<b>Appendix B.....</b>	<b>200</b>
<b>References .....</b>	<b>203</b>

## Chapitre 4 : Réticulation physique et cristallisation sous contrainte

Dans les deux chapitres précédents, nous avons étudié la réticulation de l'ENR par des liens covalents. Des propriétés d'adhésion, de relaxation de contrainte et même de recyclage ont pu être obtenues grâce à la chimie covalente dynamique (liens esters échangeables par transestérification en présence d'un catalyseur, ou réarrangements de liaisons disulfures avec la température). Ici, on se propose de réticuler l'ENR de manière physique pour obtenir un élastomère thermoplastique.

Les élastomères thermoplastiques (TPE) ont été beaucoup étudiés dans la littérature, et ont fait l'objet d'un développement industriel important.<sup>1, 2</sup> Les propriétés de ces matériaux sont limitées par une faible résistance aux solvants et à la température, mais on les trouve cependant dans des applications variées telles que l'isolation de câbles, les adhésifs ou même les chaussures, applications pour lesquelles la température limite d'utilisation ne pose pas de problème. Les TPEs les plus importants commercialement sont des copolymères à blocs à base de polyuréthane, polyester, polyamide ou encore polystyrène/élastomère. Ces copolymères se structurent par séparation de phase. Des parties « dures » constituent des points de réticulation entre les parties « molles », lesquelles permettent de conserver le caractère souple et élastique d'un élastomère. A partir du caoutchouc naturel, il est possible d'obtenir des TPEs par greffage. La copolymérisation d'un monomère vinylique par greffage sur le caoutchouc naturel a été largement utilisée pour en modifier les propriétés. On distingue deux procédés : le « grafting from » lors duquel le greffage se fait par polymérisation d'un monomère sur un site actif du caoutchouc et le « grafting onto » qui consiste à greffer une chaîne préformée sur un site actif du polymère. Généralement, le greffage a lieu en solution ou en phase latex (plus intéressant d'un point de vue écologique).

Ici, nous étudions le greffage de chaînes cristallisables (acide béhénique, Figure 1) sur l'ENR par extrusion réactive. L'intérêt de ce type de greffage est l'absence de solvant, ce qui facilite le procédé d'un point de vue industriel. Les propriétés mécaniques du matériau greffé

seront testées pour vérifier la capacité des greffons à se comporter comme des points de réticulation physique, permettant un comportement d'élastomère.

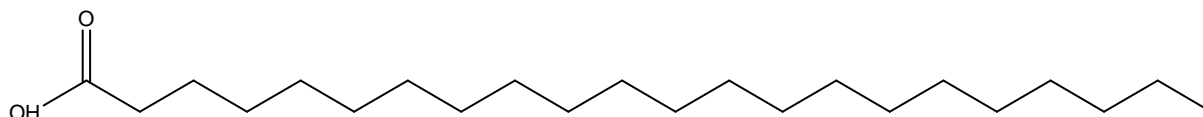


Figure 1. Formule développée de l'acide béhénique (22 atomes de carbone).

Le caoutchouc naturel, ainsi que sa version époxydée, présentent la capacité de cristalliser sous l'application d'une grande déformation (Chapitre 1). Cette propriété, connue sous le nom de cristallisation sous contrainte, est à l'origine des très bonnes propriétés mécaniques du caoutchouc. Elle est généralement étudiée par des mesures de diffraction des rayons X,<sup>3-9</sup> technique également utilisée pour l'étude des matériaux semi-cristallins.<sup>10, 11</sup> L'acide béhénique (C22) étant cristallisable, l'ENR greffé présente potentiellement des similitudes avec les matériaux semi-cristallins ; son étude par diffraction des rayons X peut donc s'avérer doublement intéressante. En effet, des informations sur la cristallisation des greffons C22 mais aussi sur la cristallisation des chaînes d'ENR au cours de la traction peuvent être obtenues.

Une collaboration avec Pierre-Antoine Albouy du Laboratoire de Physique des Solides d'Orsay (LPS) a permis de profiter de son expertise sur la cristallisation sous contrainte dans les caoutchoucs naturels. Le LPS possède une machine de traction combinée à une source de rayons X, permettant des mesures dynamiques de diffraction des rayons X au cours de la traction, avec laquelle nous avons étudié l'ENR greffé. A titre de comparaison, nous avons également étudié la capacité de cristallisation sous contrainte de notre matériau de base, l'ENR-DA.

La première partie de ce chapitre sera consacrée à la caractérisation de la cristallisation sous contrainte du réseau chimique (ENR-DA) et sera l'occasion de mieux comprendre les informations obtenues lors de cette expérience de WAXS sous traction. Cette étude d'ENR-DA est présentée sous la forme d'un article en cours de rédaction, « Strain-induced crystallization of sustainably crosslinked epoxidized natural rubber », dans lequel nous étudions également l'effet de la densité de réticulation sur la cristallisation sous contrainte.

L'étude de l'ENR greffé C22 constitue la deuxième partie du chapitre, avec tout d'abord la caractérisation chimique du greffage, puis l'étude du réseau physique obtenu aux rayons X sous traction. Enfin, dans une troisième et dernière partie, nous étudierons des réseaux doubles obtenus par combinaison de la réticulation physique et de la réticulation chimique. L'appareil permettant de réaliser des mesures de diffraction de rayons X aux grands angles (Wide Angle X-ray Scattering, WAXS) au cours de la traction est décrit brièvement en annexe de ce chapitre.

# 1. Strain-induced crystallization in ENR-DA

## Strain-induced crystallization in sustainably crosslinked epoxidized natural rubber

by Lucie Imbernon,<sup>a</sup> Raphaël Pauchet,<sup>a</sup> Myriam Pire,<sup>a</sup> Pierre-Antoine Albouy,<sup>b</sup> Sylvie Tencé-Girault<sup>a</sup> and Sophie Norvez<sup>a</sup>

<sup>a</sup> *Matière Molle et Chimie, ESPCI ParisTech - CNRS, UMR-7167, PSL Research University.*

<sup>b</sup> *Laboratoire de physique des solides, CNRS, UMR-8502, Université Paris-Sud.*

*To be submitted*

### Abstract

Strain-induced crystallization (SIC) is studied in networks of epoxidized natural rubber crosslinked with eco-friendly dodecanedioic acid, by X-ray scattering measurements during cyclic stretching. An orientation parameter is calculated to quantitatively describe the behaviour of the amorphous phase during loading and unloading. Our samples are compared to sulphur-vulcanized NR and ENR. SIC lattice parameters are found independent of the nature of the crosslinks, but the crosslink density affects the onset of crystallization. The demonstrated SIC behaviour is at the origin of the good mechanical properties observed in our sustainable material.

### 1.1. Introduction

Natural Rubber (NR) is an outstanding material considered environmentally friendly owing to its bio-based origin. Besides its impressive elasticity, it possesses very good mechanical and rupture properties as well as low heat build-up that make it priceless in many demanding applications. Indeed, NR is still used for the manufacturing of truck tires in particular, in spite of the fact that synthetic polyisoprene is available.

Modification of polymers is an efficient way to tune materials properties. Chemical modification of NR was developed at the beginning of the 19<sup>th</sup> century. However, epoxidized natural rubber (ENR) is nowadays one of the only commercial derivatives of NR. Industrial production of ENR started in Malaysia in 1988,<sup>12</sup> and two grades are available today on the market (ENR25 and ENR50 having 25 and 50 mol% epoxidation, respectively).

NR is able to crystallize upon elongation. Such strain-induced crystallization (SIC) is at the origin of the high resistance to crack propagation and excellent fatigue performances of the material.<sup>13, 14</sup> Discovered in 1925 by Katz and Bing,<sup>15</sup> this property was then studied in detail in a large number of publications.<sup>4-9</sup> The crystallization of NR chains is possible thanks to their well-defined *cis* configuration. The epoxidation reaction preserves the *cis* configuration, transferring the ability to crystallize to the new material. ENR thus retains NR's remarkable mechanical properties, may be explaining why it is the only commercial derivative. Contrarily to NR, very few studies on the SIC of ENR were reported. In 1983, Davies *et al.* studied static X-ray diffraction of stretched sulphur-vulcanized ENR, showing the ability of the material to crystallize upon stretching.<sup>3</sup> The authors showed that the epoxy groups were incorporated into the crystals, resulting in a variation of the unit cell parameters. Since then, no X-ray scattering study was conducted on ENR networks to our knowledge.

Our group recently reported on a new way to crosslink ENR, different from classical sulphur and peroxide vulcanization.<sup>16,17</sup> Carboxylic diacids were used as crosslinking agents through esterification of the epoxy functions. This crosslinking process results in  $\beta$ -hydroxy esters along the chains<sup>18</sup> and competes with classical vulcanizations.<sup>19, 20</sup> It can also be used to produce semi-interpenetrated networks by blending ENRs with different degrees of epoxidation,<sup>21</sup> or reprocessable crosslinked materials by using a functionalized diacid.<sup>22</sup> Dodecanedioic acid (DA) used as crosslinker of ENR is obtained from renewable resources which makes our material completely bio-based.<sup>23</sup> Following the increasing interest in environmentally friendly materials, further attempts were made lately in that direction. Crosslinking of ENR with renewable conjugated acids *via* oxa-Michael reaction<sup>24</sup> or by reaction with renewable and biodegradable lignin was recently reported.<sup>25</sup>

SIC is a very important feature of ENR as it is at the origin of its good mechanical properties. Only one paper relates some X-ray diffraction measurements on innovative ENR networks (crosslinked by lignin).<sup>25</sup> However, the authors showed that their material did not crystallize upon stretching; the rubber still presented acceptable mechanical properties thanks to the reinforcing effect of lignin. ENR was also crosslinked with zinc diacrylate (ZDA) through oxa-Michael reaction,<sup>26</sup> or with dodecyl succinic anhydride through ring-opening of epoxy functions,<sup>27, 28</sup> and some authors discussed the strain-induced crystallization ability of ENR networks through tensile tests and Mooney-Rivlin plots.<sup>29, 30</sup> However, none of these ENR networks was proven to undergo strain-induced crystallization by X-ray measurements. Here, the SIC behaviour of ENR crosslinked with a carboxylic diacid is studied by X-ray diffraction during mechanical cycling. The material is shown to well crystallize upon

stretching and the lattice parameters of ENR crystals are measured. The SIC is compared with what was reported for sulphur-vulcanized NR and ENR, and the effect of the crosslink density is discussed.

## 1.2. Experimental section

### 1.2.1. Materials

ENR25, containing 25 mol% epoxy groups, and kaolin were kindly provided by Hutchinson SA Research Center, France. Dodecanedioic acid (DA, 99%) was purchased from Acros and 1,2-dimethylimidazole (DMI, 98%) from the Sigma-Aldrich Co. All chemicals were used as received. The kaolin used in the formulations was Polestar 200R.

### 1.2.2. Sample preparation

Mixtures of ENR, DA and DMI were made using a DSM micro-extruder with a capacity of 15 cm<sup>3</sup>. Blending was performed with a 60 rpm screw rotation speed under N<sub>2</sub> flow to prevent oxidation of the extruded material. ENR25 was first introduced at 120 °C and masticated alone for 30 minutes at 180 °C. The other components were consecutively added after cooling at 60 °C to avoid crosslinking reactions and the blending was carried on for 7 minutes. Three different compositions were studied by varying the DA-content. We define a  $p$  ratio as the number of epoxy rings available per diacid molecule. The exact formulations of the materials are given in Table 1. The resulting rubber will be referred to as ENR-DA.

Table 1. Composition of the mixes. Amounts are given in phr (part per hundred rubber)

Component	$p = 25$	$p = 50$	$p = 100$
ENR25	100	100	100
DA	3.3	1.6	0.9
DMI	2.8	1.4	0.7
kaolin	5.5	5.5	5.5

DMI is liquid in the mixing conditions ( $T_m \approx 38$  °C), so kaolin was used as an inert filler to facilitate its incorporation. After blending, samples were cured in a Carver hydraulic press

under 8 tons in the appropriate conditions of time at 180 °C (to reach 90 % of the shear modulus plateau obtained by rheological measurements).

### 1.2.3. Characterization

#### *Rheological measurements*

An Anton Paar MCR 501 rheometer was chosen to follow the crosslinking process using plate-plate geometry (25 mm-diameter, 1 Hz frequency, 0.1 % strain). Samples were 26 mm-diameter discs cut in 1.5 mm thick uncured sheets pressed at 80 °C. An axial force of 10 N was applied to the sample during 5 min before the experiment to ensure a good contact between the rubber and the plates. This force was then maintained around 2 N during the experiment by adjusting the gap. In these conditions, results of the measurements were shown to be comparable with the ones obtained in a Moving Die Rheometer.<sup>16</sup> The temperature was quickly raised from 30 to 180 °C, and the sample was left under oscillatory shear at 180 °C for curing.

#### *Swelling test*

Chloroform was used as a good solvent of ENR25. Discs of 5 mm-diameter were immersed until equilibrium swelling (around 24 hours). Their weight was followed and used to calculate the equilibrium swelling ratio  $Q$  defined in Equation (1):

$$Q = \frac{m_s - m_u}{m_u} \quad (1)$$

where  $m_s$  and  $m_u$  are respectively the swollen and unswollen mass of the sample. These swelling measurements can usually serve to determine the crosslink density through the Flory-Rehner theory.<sup>9</sup> However, the obtained results are very dependent on the value of the Flory-Huggins parameter  $\chi$  that is not precisely known in the case of ENR. In this work, we will thus only compare the swelling measurements by calculating  $1/Q$  that can be seen as an apparent crosslink density.

#### *In situ X-ray tensile tests*

The stretching apparatus was already described in detail elsewhere.<sup>7, 9</sup> It is placed on a rotating copper anode X-ray generator operating at 40 kV and 40 mA ( $K_\alpha$  wavelength  $\lambda_{Cu} = 0.1542 \text{ nm}$ ). The extension of the sample is symmetric relative to the fixed point where the X-ray beam is focalized. All the tests were performed at a strain rate of  $1.25 \text{ min}^{-1}$ . Scattering patterns were recorded using a CCD camera with an acquisition time of 10 s. As

data transfer takes about 6 s, the chosen tensile speed allowed an appropriate number of experimental points during traction. The extension ratio was calculated from the displacement and the initial length of the samples (20 mm). The force applied to the samples was measured with a 300 N load sensor and the true stress was calculated from the load  $F$  and extension ratio  $\lambda$  as:

$$\sigma_{true} = \frac{F}{S_0} \lambda = \sigma \lambda \quad (2)$$

where  $S_0$  is the initial section of the unstretched sample, and  $\sigma$  the engineering stress.

A home-made mould was used to obtain samples well fitted to the clamps of the stretching apparatus (Figure 2). The samples are long strips with a cylinder on each side. Thickness of the strips was about 1.25 mm and their width 6 mm (Figure 2b). In a typical measurement, the sample was put inside the clamps, allowed to stabilize at 20 °C for about 5 min and then submitted to stretching. Two cycles were carried out until about 90-95 % of the rupture strain, and finally, after 5 minutes waiting, the sample was stretched until break.



Figure 2. Clamps (a) and samples (b) for in situ X-ray scattering tensile experiments.

#### 1.2.4. X-ray data processing

From X-ray experiments, we can deduce the inter-reticular distances of the crystalline rubber, an evaluation of the degree of crystallinity and a measure of the orientation of the amorphous (molten) chains. The X-ray diffraction geometry is presented in Figure 3a, along with typical diffraction patterns obtained during stretching (Figure 3b-c-d).

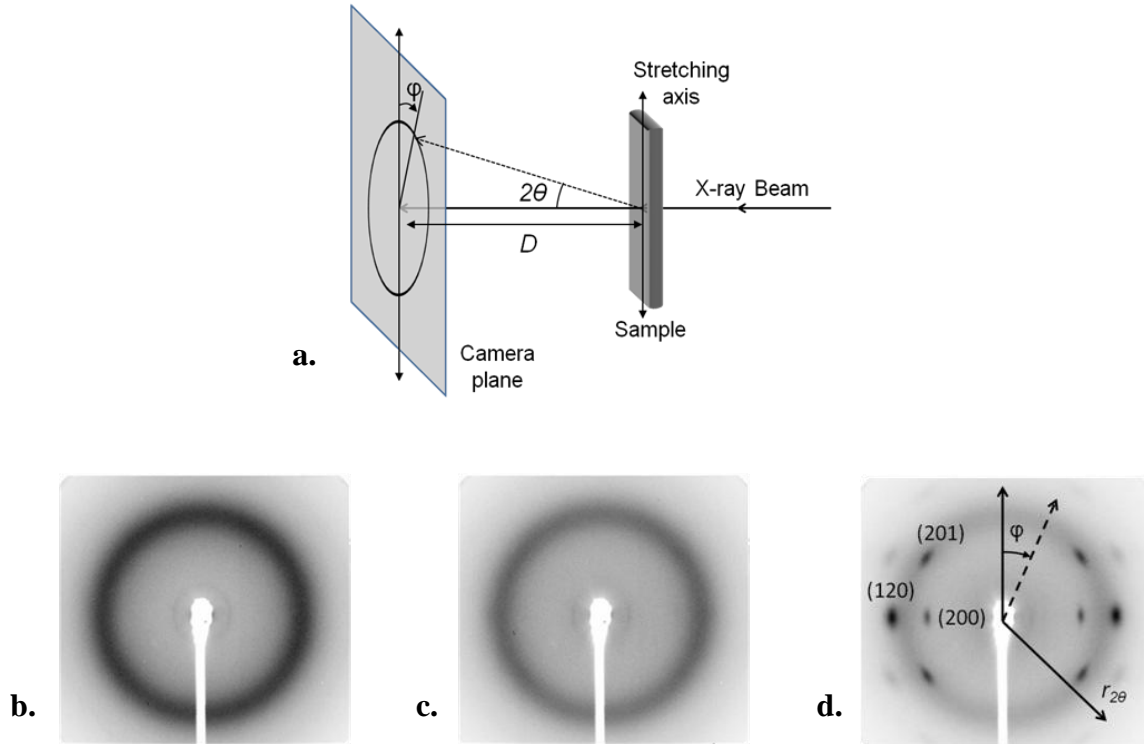


Figure 3. **a.** Scheme of the X-ray diffraction geometry. Typical diffraction patterns: **b.** amorphous and isotropic, **c.** amorphous and oriented **d.** semi-crystalline and oriented, with crystallographic indexation of the main peaks (orthorhombic lattice).

The diffraction pattern corresponds to the intersection of the cone of half top angle  $2\theta$  with the plane of the detector. Knowing the distance  $D$  between the sample and the camera plane, the measure of  $r_{2\theta}$  on the diffraction pattern allow the calculation of the corresponding angle  $2\theta$  using relation (3):

$$r_{2\theta} = D \tan 2\theta \quad (3)$$

Inter-reticular distances can then be deduced from the Bragg's formula:

$$2d_{hkl} \sin\theta = \lambda_{Cu} \quad (4)$$

During the tensile experiment, the X-ray patterns evolve from an isotropic amorphous signal to a semi-crystalline oriented one. From these patterns, two types of information were extracted: the orientation of the amorphous phase (through calculation of an amorphous phase orientation parameter  $\langle P_2^{RX}(\cos\varphi) \rangle$ ) and the degree of crystallinity as well as the lattice parameters of the crystal cell.

### Orientation of the amorphous phase

The orientation of the amorphous phase can be quantified with the orientation order parameter  $\langle P_2^{RX}(\cos\varphi) \rangle$  defined as:

$$\langle P_2^{RX}(\cos\varphi) \rangle = \frac{3 \langle \cos^2 \varphi \rangle - 1}{2} \quad (5)$$

where  $\varphi$  is the azimuthal angle, counted from the stretching direction (vertical direction on the pattern, Figure 3). The mean value of  $\cos^2 \varphi$  is calculated as follow:

$$\langle \cos^2 \varphi \rangle = \frac{\int_0^\pi I_{am}(\varphi) \cdot \cos^2 \varphi \cdot \sin \varphi \cdot d\varphi}{\int_0^\pi I_{am}(\varphi) \cdot \sin \varphi \cdot d\varphi} \quad (6)$$

with  $I_{am}(\varphi)$  the azimuthal scan of the amorphous intensity.

The procedure to extract the intensity  $I_{am}(\varphi)$  is explained in Figure 4. The recorded intensity was integrated radially over the range between the two scattering angles determined by the black circles in Figure 4a (between  $2\theta_{min} \approx 12^\circ$  and  $2\theta_{max} \approx 23^\circ$ ). This allowed taking into account the amorphous ring and the most intense crystallization peaks indexed as (200), (120) and (201) in Figure 3d.

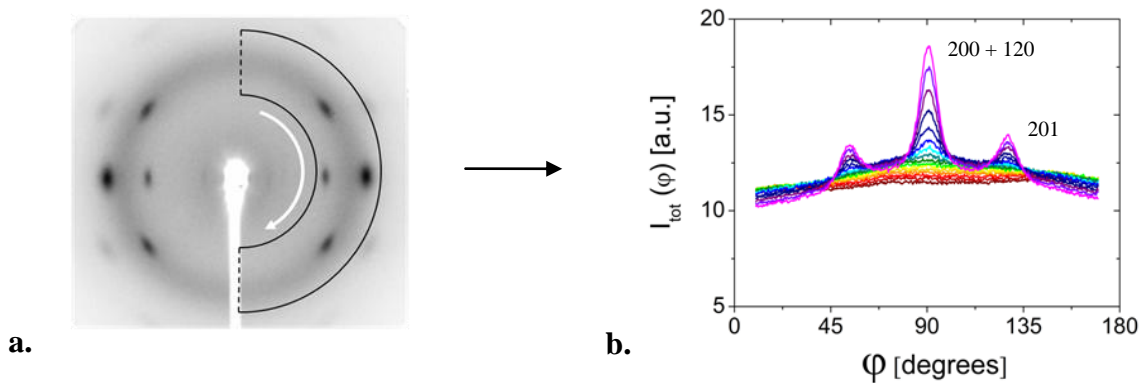


Figure 4. **a.** Diffraction patterns of ENR-DA ( $p = 50$ ) at extension ratio  $\lambda=6.5$ . The black lines delimit the analyzed area and the white arrow the azimuthal scan along  $\varphi$ .

**b.** Superposition of all the integrated scattering intensity profiles during traction experiment (the purple line corresponds to the presented pattern).

The obtained profiles, plotted in function of the azimuthal angle  $\varphi$  are shown in Figure 4b. The overall intensity ( $I_{tot}(\varphi)$ ) of these profiles can be divided into two contributions: an amorphous halo ( $I_{am}(\varphi)$ ) and three crystalline peaks ( $I_{cryst}(\varphi)$ ):

$$I_{tot}(\varphi) = I_{am}(\varphi) + I_{crys}(\varphi) \quad (7)$$

The amorphous anisotropic contribution was fitted with:  $I_{am}(\varphi) = A + B \sin^2 \varphi$  and the crystalline contribution with a set of Pearson VII functions.<sup>7</sup> Using the expression of  $I_{am}(\varphi)$  in equations (6) and (5), the orientation parameter may be calculated:

$$\langle P_2^{RX}(\cos \varphi) \rangle = \langle P_2^{RX} \rangle = -\frac{2B}{15A + 10B} \quad (8)$$

The air contribution to the scattered intensity was subtracted by measuring the direct beam and scattered intensity (respectively  $I_0$  and  $A_{air}$ ) in the absence of a sample. In the presence of a sample, the direct beam intensity  $I_t$  was then used to estimate the intensity due to air scattering  $A_{air}(I_t/I_0)$ . This contribution was subtracted to the amorphous contribution and a corrected A parameter was obtained:

$$A_{corr} = A - A_{air} \left( \frac{I_t}{I_0} \right) \quad (9)$$

Then, from Equation (8), we obtain:

$$\langle P_2^{RX} \rangle = -\frac{2B}{15A_{corr} + 10B} \quad (10)$$

The value of this coefficient will always be negative since the scattering intensity is higher in the perpendicular direction ( $\varphi = \pi/2$ ) for an orientation of the amorphous chains along the stretching direction ( $\varphi = 0$ ).

For each elongation ratio, the integrated intensity was fitted and  $A$  and  $B$  parameters were extracted. Then  $\langle P_2^{RX} \rangle$  was calculated and plotted *versus* the elongation ratio  $\lambda$ .

#### *Degree of crystallinity*

Assuming a cylindrical symmetry around the stretching direction, and that the main diffraction peaks are contained in the integrated  $2\theta$  domain (Figure 4a), the crystal ratio may be estimated with an azimuthal integration of the 2D pattern. This degree of crystallinity is defined as:

$$\chi_c = \frac{\int_0^\pi I_{crist}(\varphi) \cdot d\varphi}{\int_0^\pi I_{am}(\varphi) \cdot d\varphi + \int_0^\pi I_{crist}(\varphi) \cdot d\varphi} \quad (11)$$

This parameter is thus calculated for each elongation ratio using the fitted parameters  $A_{corr}$ ,  $B$  and the Pearson VII functions.

### Lattice parameters

The diffraction peaks observed for the crystallization of ENR were indexed in the orthorhombic system (Figure 3d), for which the  $a$ ,  $b$ ,  $c$  lattice parameters may be deduced from the inter-reticular distances  $d_{hkl}$  defined as:

$$d_{hkl} = \frac{1}{\sqrt{\frac{h^2}{a^2} + \frac{k^2}{b^2} + \frac{l^2}{c^2}}} \quad (12)$$

## 1.3. Results and discussion

### 1.3.1. Crosslinking and thermo-mechanical characterisation of ENR-DA networks

ENR25 was crosslinked by reaction with dodecanedioic acid (DA) according to a previously reported mechanism.<sup>16-18, 20</sup> Comparison was made between three different degrees of crosslinking ( $p = 25, 50$  and  $100$ ),  $p$  being the epoxy/DA molecule ratio as defined in the experimental section. For example,  $p = 25$  means one DA molecule for 25 epoxy functions in the material. The ratios  $p = 50$  and  $100$  should produce lower crosslink densities (two and four times lower, respectively).

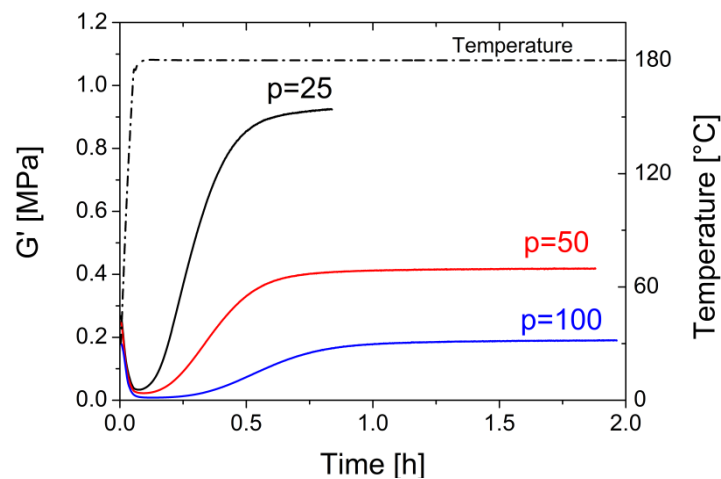


Figure 5. Kinetic study of the DA-curing of ENR25 with temperature in the rheometer (temperature is plotted as a dash-dot line to show the very fast initial ramp). Different  $p$  ratios are compared.

The evolution of the storage modulus  $G'$  followed by rheology is plotted against time in Figure 5. The crosslinking time for each material was chosen as the time needed to get to 90 % of the plateau value. The storage modulus  $G'$  is theoretically proportional to the number of crosslinks. The plateau modulus was plotted in Figure 6 against the theoretical percentage of linked monomers (number of acid functions compared to the total number of monomers, for example  $p = 25$  means 1 DA for 25 epoxy that is 1 DA for 100 monomers in ENR25 and thus corresponds to 2 % of linked monomers). For moderate DA amounts, the  $G'$  plateau is expected to vary linearly with the number of linked monomers.<sup>16</sup> The linearity observed in Figure 6 indicates that most of the diacid has reacted during the curing process.

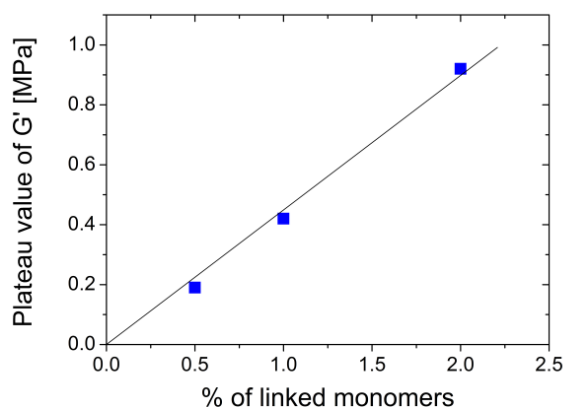


Figure 6. Variation of  $G'$  plateau value in function of the crosslink density.

The three crosslinked ENR25 networks were characterized by DMA (Figure 7). Above the glass transition temperature marked by a sharp decrease of  $E'$  (and a peak of  $E''$ ), each sample exhibits a rubbery plateau. The value of the plateau is in accordance with the crosslink densities: the higher the density the higher the plateau.

As a complementary experiment, DSC measurements were performed to differentiate the  $T_g$ s of the three networks. The obtained values were respectively  $-42.2$ ,  $-41.9$  and  $-41.6$  °C for samples  $p = 100$ , 50 and 25. This slight increase is due to the decrease in mobility of the polymer chains with increasing content of crosslinker.<sup>16</sup>

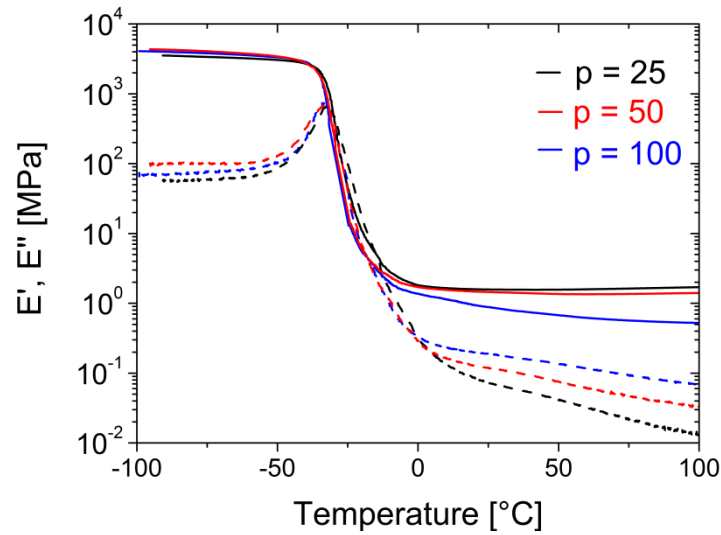


Figure 7. Dynamic mechanical analysis of the three ENR25 networks (line:  $E'$ ; dashed line:  $E''$ ).

Swelling tests were performed to quantify the crosslink density of the networks. Since the Flory-Huggins parameter for ENR is necessary to calculate the crosslink density from the Flory-Rehner equation but is not known, the inverse of the swelling ratio ( $1/Q$ ) was calculated. This does not give an absolute value but only an apparent crosslink density. This apparent value was plotted against the percentage of linked monomers in Figure 8. As expected, the crosslink density of the samples increases with increasing percentage of linked monomers (decreasing  $p$  ratios). The non-zero ordinate intercept at origin is related to truly trapped entanglements that still contribute even in the swollen state.<sup>9</sup>

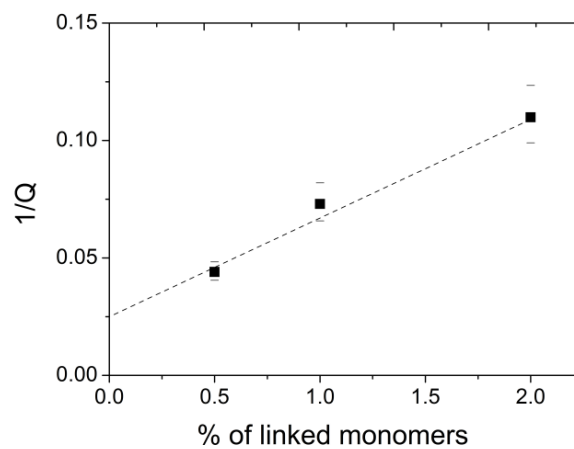


Figure 8. Apparent crosslink density deduced from swelling measurements.

1.3.2. Tensile tests and in situ X-ray experiments

- Rupture properties

The mechanical properties until break are plotted in Figure 9. The samples were pre-cycled to get rid of the Mullins effect. The Young's modulus, corresponding to the initial slope of the stress-strain curve, increases with increasing crosslink densities. The ultimate properties vary in opposite ways: the stress increases while the strain decreases with increasing crosslink densities. During tensile experiments, X-ray diffraction patterns (WAXS) were recorded. Some representative patterns are shown in Figure 9b for the sample  $p = 50$ . These patterns clearly indicate that ENR25 crystallizes upon elongation.

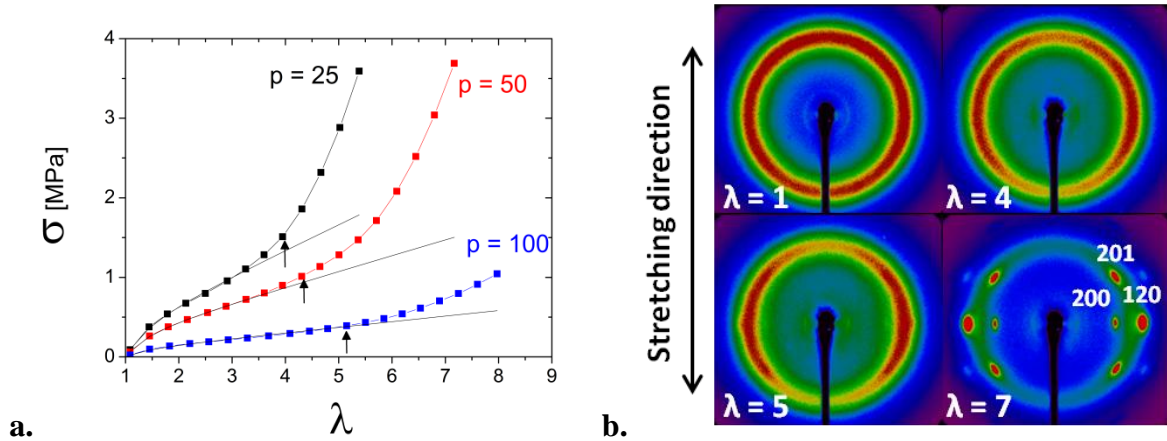


Figure 9. a. Mechanical properties until break; black arrows mark the crystallization onsets determined by X-ray scattering and black lines are Mooney-Rivlin fits from Equation (14).

b. X-ray diffraction patterns during stretching for sample  $p = 50$  (traction direction is vertical). Peaks at  $\lambda = 7$  have been indexed in the orthorhombic system. (No intensity normalization has been performed on the patterns).

The shape of the mechanical curve (Figure 9a) is the same for the three ENR-DA (as are the X-ray patterns). Two regimes can be differentiated in the curves and physically understood by the theory of rubber elasticity. The limit between the two regimes is marked by the up-turn of the stress that corresponds quite well to the onset of crystallization (marked with black arrows). At the beginning of the traction experiment ( $\lambda = 1$ ), the pattern is fully isotropic. Just before the crystallization onset the intensity is concentrated around the equator because of the alignment of the chains in the traction direction ( $\lambda = 4$ ). After the crystallization onset, characteristic crystalline peaks appear ( $\lambda = 5$ ) and intensify until break.

The classical theory of elasticity predicts that the engineering stress is proportional to  $(\lambda - 1/\lambda^2)$  as shown in Equation (13):<sup>13</sup>

$$\sigma = G \cdot \left( \lambda - \frac{1}{\lambda^2} \right) \quad (13)$$

where  $G$  is the shear modulus. However, even before the crystallization onset, the experimental results cannot be correctly fitted by this equation because of the slight turndown observed for small  $\lambda$  values. To account for this, we used the semi-empirical law proposed by Mooney and Rivlin (black lines in Figure 9 a):

$$\sigma = 2 \left( C_1 + \frac{C_2}{\lambda} \right) \cdot \left( \lambda - \frac{1}{\lambda^2} \right) \quad (14)$$

where  $C_1$  and  $C_2$  are the Mooney-Rivlin (MR) parameters. Above a certain elongation, the stress shows an upturn (attributed to SIC) and the MR equation is no longer in accordance with the data.

The first parameter  $C_1$  is directly related to the crosslink density  $\nu_{mecha}$  by Equation (15):

$$\nu_{mecha} = \frac{2C_1}{\rho RT} \quad (15)$$

where  $\rho$  is the density of the rubber (taken as 0.97 for ENR25),  $R$  the gas constant and  $T$  the temperature. The origin of the second parameter  $C_2$  is less straightforward.

The first part of the mechanical curve, corresponding to the orientation of the material and the alignment of the chains (increasing anisotropy, Figure 9b), was well fitted by the MR equation (Equation (14), Figure 9a). Values of the crosslink density calculated using Equation (15) as well as the fit parameters  $C_1$  and  $C_2$  were collected in Table 2.

Table 2. Parameters of Mooney-Rivlin fits and calculated crosslink density

	$2C_1$ [MPa]	$2C_2$ [MPa]	$C_2/C_1$	$\nu_{mecha} \cdot 10^4$ (mol.g <sup>-1</sup> )
$p = 25$	0.319	0.079	0.25	1.35
$p = 50$	0.198	0.095	0.48	0.85
$p = 100$	0.070	0.062	0.89	0.30

From Equation (14), it can be deduced that at small extensions ( $\lambda \approx 1 + \varepsilon$ , with  $\varepsilon \rightarrow 0$ ),  $\sigma \approx 6(C_1 + C_2)\varepsilon$ . The initial slope of the mechanical curve, also corresponding to the Young's modulus  $E$ , is thus  $E \approx 6(C_1 + C_2)$ . The Young's modulus was calculated to be

around 1.2 MPa for the more crosslinked network ( $p = 25$ ), in accordance with the modulus measured by DMA ( $E_{DMA} \approx 1.6$  MPa at room temperature, Figure 7) and already reported values for ENR25 crosslinked by a functional diacid.<sup>22</sup> The ratio  $C_2/C_1$  increases with decreasing crosslink densities (increasing  $p$  ratios), in accordance with previous observations,<sup>31</sup> and interpreted as the decreasing relative effect of entanglements with increasing number of crosslinks.

The crosslink density  $v_{mecha}$ , plotted against the percentage of linked monomers in Figure 10 is a linear law as expected. This experiment confirms that the crosslink density of the samples increases linearly with increasing percentage of linked monomers (decreasing  $p$  ratios). The calculation of the crosslink density from  $C_1$  does not take into account the entanglement contribution, so the ordinate intercept at origin is null.

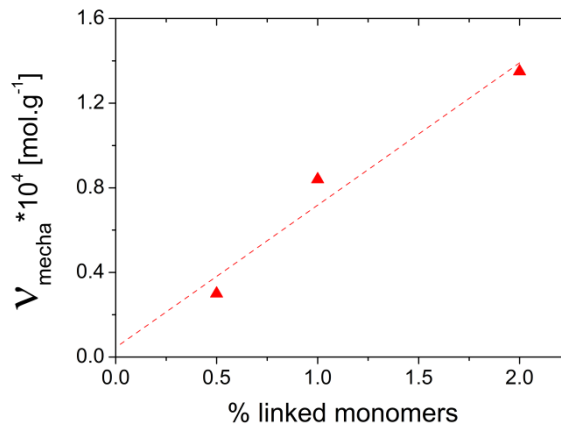


Figure 10. Crosslink density deduced from mechanical experiments, Equation (15) (the dashed line is a linear fit of the data).

In the first part of the mechanical curves (Figure 9a, before the up-turn), the chain segments gradually align towards the traction direction prior to crystallize. To quantify the orientation of this amorphous phase, we defined an orientation parameter  $\langle P_2 \rangle$ . As seen in Figure 9b, the chain alignment is visible in the X-ray diffraction patterns (concentration of the intensity in the equator region), and the diffracted amorphous intensity can be used to calculate the orientation parameter (see experimental section). In the classical theory of elasticity, this parameter is proportional to the crosslink density and to the elongation function ( $\lambda^2 - \lambda^{-1}$ ) as shown in Equation (16):

$$\langle P_2 \rangle = K\nu_X \left( \lambda^2 - \frac{1}{\lambda} \right) \quad (16)$$

where  $K$  is a factor related to the local structure of the amorphous phase.<sup>9</sup> This factor is unknown, but it is not dependent on strain or crosslink density, so comparisons are reliable. The variation of  $\langle P_2^{RX} \rangle$  as a function of  $(\lambda^2 - \lambda^{-1})$  is shown in Figure 11a. As in the case of tensile tests, the curves exhibit two distinct regimes. The separation between both regimes corresponds approximately to the crystallization onset. Below this onset,  $\langle P_2^{RX} \rangle$  follows the rubber elasticity theory (Equation (16)). The curves are linear until  $(\lambda^2 - \lambda^{-1})$  values around 15-25 that correspond quite well to the crystallization onsets. If plotted against the true stress (Figure 11b), the two regimes of  $\langle P_2^{RX} \rangle$  are still visible. Moreover it can be seen that all the curves collapse onto a single master curve below the SIC onset, in accordance with the prediction of the elasticity theory. Indeed, from Equations (13) and (16),  $\langle P_2^{RX} \rangle$  and the stress should both be proportional to the crosslink density ( $G \propto \nu$ ). Above the SIC onset, the curves deviate from linearity and reach a plateau due to the so-called strain-regulation effect.<sup>32</sup>

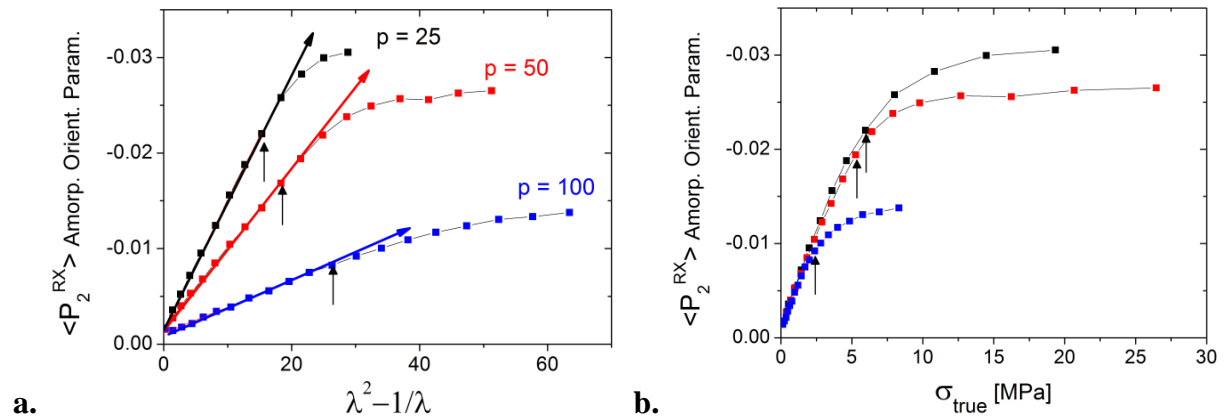


Figure 11. Evolution of the amorphous orientation parameter  $\langle P_2^{RX} \rangle$  obtained from X-ray scattering. Crystallization onsets are indicated by arrows.

The slope of  $\langle P_2^{RX} \rangle$  as a function of  $(\lambda^2 - \lambda^{-1})$  gives access to the crosslink density measured by X-ray scattering ( $\nu_X$ ). As discussed before, the measure of this crosslink density is not absolute since  $K$  is unknown. The crosslink density measured by mechanical experiments is plotted against  $K\nu_X$  in Figure 12. The very good linear behaviour of this plot confirms the agreement between all our experiments.

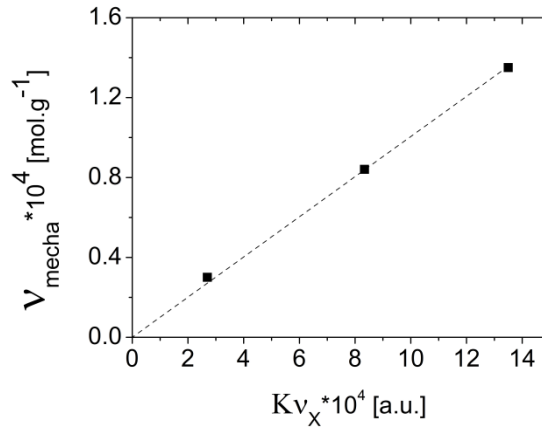


Figure 12. Crosslink density deduced from mechanical experiments in function of the  $\langle P_2^{RX} \rangle$  parameter's slope:  $Kv_X$ . The dashed line is a linear fit of the data (intercept was fixed at zero).

For larger elongation ratios (after the up-turn of the stress in Figure 9a), the MR equation no longer fits the data, and  $\langle P_2^{RX} \rangle$  reaches a plateau. This also corresponds to the appearance of sharp diffraction peaks in the X-ray patterns (Figure 9b), confirming the occurrence of SIC. The crystallization of the chains creates new physical crosslinks. The number of crosslinks being suddenly different and variable, the MR equation is no longer valid. Crystals form and support the additional elongation, resulting in a fast increase of the measured stress; the portion of amorphous phase left is no longer solicited (saturation of the  $\langle P_2^{RX} \rangle$  values). The crystallinity of the samples was measured as described in the experimental section and is plotted against the elongation ratio in Figure 13.

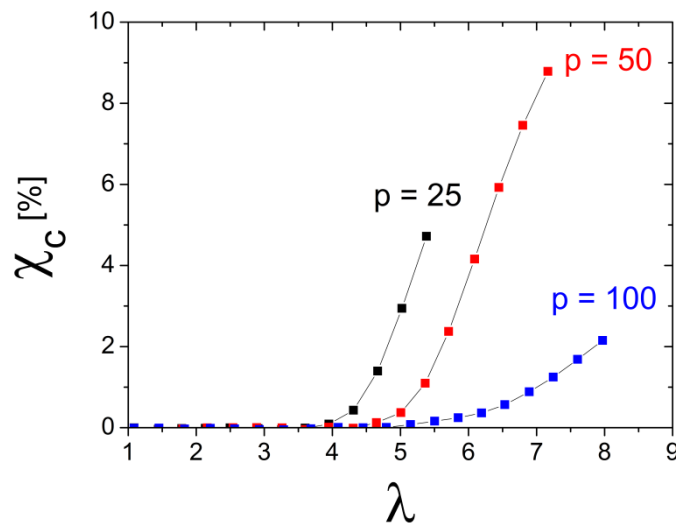


Figure 13. Evolution of the crystallinity of the three samples in function of the elongation ratio.

Degrees of crystallinity up to around 10 % were found in the samples. The onsets of crystallization vary with the crosslink density (Figure 13). For our three samples, the higher the crosslink density the lower the elongation at crystallization onset ( $\lambda_c$ ). Moreover, the rate of crystallization is lower for sample  $p = 100$  than for the two other samples.

The patterns showing the highest crystallinity were used to determine the lattice parameters in the orthorhombic system. Peaks are indexed in Figure 9b and the obtained parameters are gathered in Table 3.

Table 3. Lattice parameters

	a (nm)	b (nm)	c (nm)	Volume (nm <sup>3</sup> )	Degree of crystallinity <sup>a</sup> (%)
Literature (NR+sulphur) <sup>33</sup>	1.25	0.90	0.815	0.920	10-20
Literature (ENR25+sulphur) <sup>3</sup>	1.254	0.950	0.827	0.985	11 <sup>b</sup>
$p = 25$	1.25	0.95	0.82	0.973	5
$p = 50$	1.25	0.94	0.81	0.955	9
$p = 100$	1.24	0.94	0.82	0.956	2

Uncertainties were  $\pm 0.01$  nm for lattice parameters and  $\pm 0.03$  nm<sup>3</sup> for the volume

<sup>a</sup>Measured just before break

<sup>b</sup>Measured at 400 % strain

ENR is thus shown to be able to crystallize under strain when crosslinked differently than by classical sulphur vulcanization. Cyclic experiments enabled to further explore the crystallization behaviour of crosslinked ENR.

#### - Cyclic experiments

Mechanical properties and X-ray scattering patterns were recorded during cyclic experiments as explained in the experimental section. The maximal elongation was limited to values around 90-95 % of the rupture strain. In Figure 14, only the second mechanical cycle was plotted, to get rid of the Mullin's effect. After unloading, the shape of the sample is fully recovered and the unloading curve eventually superimposes with the loading confirming the good elasticity of the samples. For the less crosslinked sample ( $p = 100$ ), the shape recovery is slower because of a more visco-elastic behaviour. At the highest elongations, a hysteresis is observed. This hysteresis is more pronounced for the  $p = 50$  sample, because of its higher crystallinity (Figure 13).

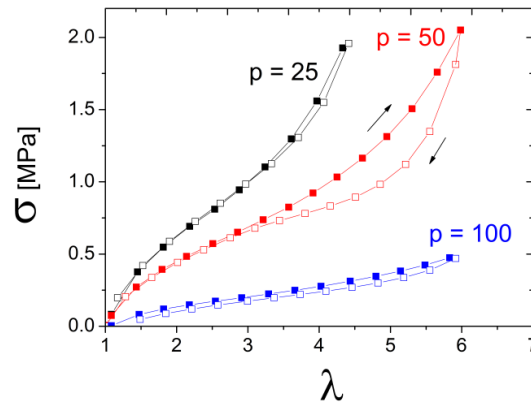


Figure 14. Cyclic mechanical properties (full symbols: loading, open symbols: unloading).

Representative WAXS patterns during a cycle are presented in Figure 15a to show the evolution during the traction experiment. Only  $p = 50$  is presented since this sample exhibits the higher crystallinity. Figure 15 clearly shows that crystals form upon stretching and then melt when the sample is allowed to go back to its original shape.

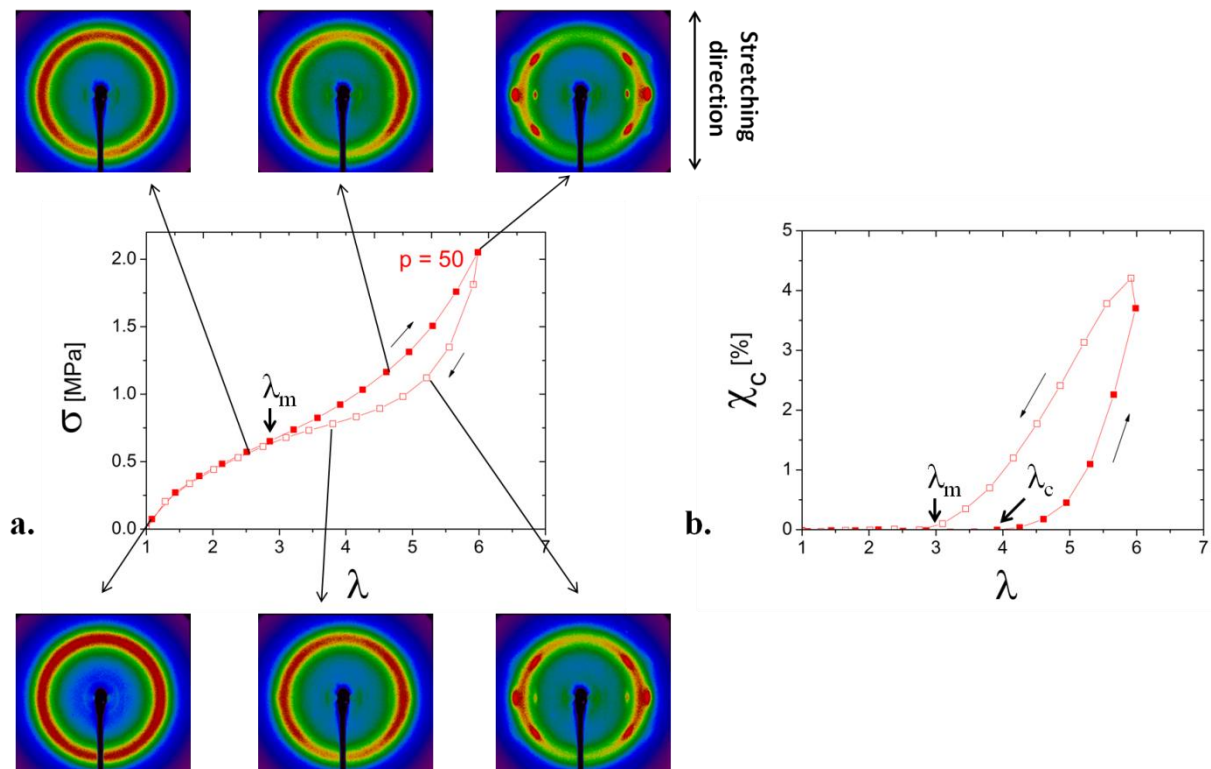


Figure 15. **a.** Diffraction pattern evolution during the cycle for the sample  $p = 50$ . **b.** Evolution of the degree of crystallinity (Full symbols: loading, open symbols: unloading).

The degree of crystallinity of the  $p = 50$  sample was extracted from the WAXS patterns and plotted against the elongation ratio  $\lambda$  in Figure 15b. The behaviour of the two other samples was qualitatively similar, although they were less crystalline. The degree of crystallinity starts increasing during stretching from a certain elongation ratio  $\lambda_c$  called the crystallization onset ( $\lambda_c = 4$  in Figure 15b). A hysteresis is observed, during unloading the crystallinity is higher than during loading for the same  $\lambda$ . The degree of crystallinity eventually goes back to zero for an elongation ratio  $\lambda_m$  (melting elongation) smaller than  $\lambda_c$  ( $\lambda_m = 3$  in Figure 15b).  $\lambda_m$  also corresponds to the point when the mechanical loading and unloading curves superimpose again (Figure 15a).

### 1.3.3. Comparison with literature

To our knowledge, only one article reported on X-ray diffraction of ENR networks.<sup>3</sup> In this work, ENR was vulcanized with sulphur and the X-ray diffraction was measured in static conditions by clamping the sample at 400% elongation. Here, ENR is crosslinked through an original method using diacids that react on the epoxy rings by esterification. Tensile tests, coupled with *in situ* dynamic X-ray experiments, show that the ENR-DA crosslinked rubbers crystallize upon stretching. The lattice parameters, calculated in the orthorhombic system, are very similar to the ones reported in the case of sulphur-crosslinked ENR25.<sup>3</sup> One therefore can conclude that the lattice parameters of ENR strain-induced crystals are independent of the crosslink density as well as of the curing method. ENR lattice parameters are slightly higher than the ones reported for NR, resulting in a larger cell volume. This confirms that the oxirane rings of ENR are integrated into the strain-induced crystals.<sup>3</sup>

Conversely, the SIC of NR was extensively studied in the literature. The X-ray diffraction patterns and amorphous orientation parameters obtained here for ENR are very similar to the ones reported for NR.<sup>7, 9, 32</sup> The strain-induced crystals reversibly form and melt at each traction cycle with maximum degrees of crystallization in the range of what can be found for NR (around 10 %).<sup>32</sup> The evolution of the rate of crystallization is in full agreement with the literature, this rate being markedly lower at low crosslink densities.<sup>34</sup> Besides, the crosslink density in sulphur-cured NR is commonly considered to have no effect on the crystallization onset  $\lambda_c$ .<sup>5, 34-36</sup> The results presented here highlight a decrease of  $\lambda_c$  with increasing crosslink densities in ENR. It is to notice that a similar dependence was observed in peroxide crosslinked samples,<sup>36</sup> this difference being tentatively attributed to a higher inhomogeneity of peroxide cross-linked samples.<sup>37</sup> In our case, the homogeneity of the network was not tested.

## 1.4. Conclusions

Strain-induced crystallization was observed by dynamic X-ray scattering measurements in ENR networks crosslinked by dodecanedioic diacid (DA). Different crosslink densities were studied by varying the amount of crosslinker. The samples were characterized by rheological, swelling, tensile and *in-situ* X-ray measurements, giving access to the crosslink densities, the orientation of the molten phase as well as the degree of crystallinity. The networks crystallize upon stretching at all the crosslink densities studied. Higher crosslink densities induce sooner crystallization. The SIC lattice parameters of ENR were found to be independent of the crosslink density or the crosslinking method. The unit cell volume is larger for our material than the reported values for NR, confirming that the oxirane rings are included into the lattice. The degree of crystallinity is significant (around 10 % at break), confirming that the diacid does not impede crystallization conversely to what was reported for other crosslinkers as lignin.<sup>25</sup>

Stress-strain curves exhibit two regimes, the first one being essentially linked with the orientation of the polymer chains between crosslinks. After a certain elongation  $\lambda_c$ , SIC of ENR is observed. Conversely to what was observed for NR,  $\lambda_c$  seems to depend on the density of crosslinks. When crystals appear, the molten phase no longer orientates as indicated by the plateau of the orientation parameter. The newly formed crystals support the additional strain and act as physical crosslinks, modifying the mechanical behaviour of the rubber. Upon unloading, the oriented amorphous phase relaxes first, and crystals melt more slowly. The samples eventually recover their shape and their isotropy.

This work proves that ENR crosslinked through an environmentally friendly process still presents SIC, making DA-crosslinked ENR an attractive fully bio-based rubber.

## 2. Crystallizable grafts and physical network

### 2.1. Introduction

To obtain a physical network, moieties capable of bonding through physical interactions must be introduced. For example supramolecular bonds<sup>38, 39</sup> or ionic interactions<sup>40</sup> could be used. Simple phase separation is also widely used as a possible path towards the obtaining of physical networks in thermoplastic elastomers.<sup>1</sup> Here, physical interactions were introduced in ENR using crystallizable grafts.

NR is usually grafted using the reactivity of the allylic carbon next to the double bond. For example, maleic anhydride can be grafted by means of radical reaction using benzoyl peroxide as a radical initiator.<sup>41</sup> No commercial product has yet been developed based on maleated NR, but this type of material was used for compatibilization effects.<sup>42, 43</sup> Graft copolymerization of a vinyl monomer onto NR can also be achieved through radical process. For example, styrene or methyl methacrylate can be polymerized from the NR chain.<sup>44</sup> NR grafted with styrene was shown to present thermoplastic elastomer properties when the grafting content was around 40 wt%.<sup>12</sup>

The epoxy functions of ENR can be used as functional sites for grafting, which represents an advantage over NR. The esterification reaction used for the crosslinking of ENR with carboxylic diacids (previous section and Chapter 2) can in principle permit to graft any molecule presenting a carboxylic acid function. Fatty acids are well adapted to such a grafting because the aliphatic chains are not reactive towards any function of ENR and side reactions will be unlikely. Behenic acid (BA) was selected here because its long 22-carbon chain is able to crystallize. If this property is retained after grafting, the crystals will play the role of crosslink points and the material will be a thermoplastic elastomer.

BA is among the most widely used surfactant for preparing Langmuir-Blodgett films. The crystalline structure of a BA monolayer has been well studied.<sup>45, 46</sup> It was previously established that the long-chain fatty acid molecules crystallize in polymorphic forms.<sup>47</sup>

Most of the experimental information about material characterization was already described in the previous section. Some complements, more specific to this section, can be found in Appendix B.

## 2.2. Characterization of the BA-grafting onto ENR

### 2.2.1. Grafting reaction

The proposed reaction between ENR and BA is the same than for the DA-crosslinking of ENR: an acid function reacts with an oxirane ring to create an ester (Figure 16). Again, DMI was added in stoichiometry to the acid functions to accelerate the esterification reaction. Unless otherwise specified, the BA content was fixed to one acid molecule for two epoxy functions. This high content of grafted molecules was necessary to render the crystallization observable.

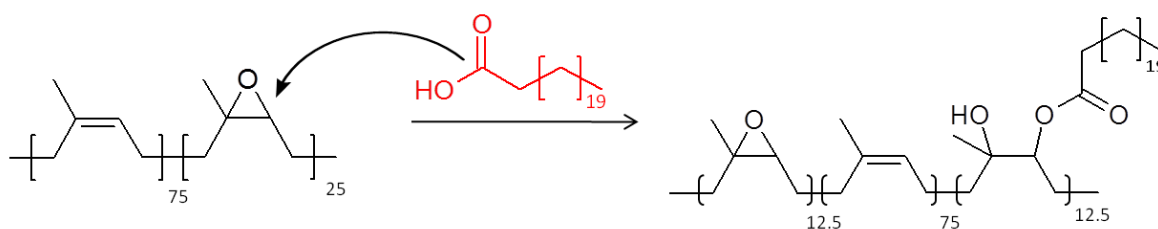


Figure 16. Scheme of the reaction of ENR25 with BA.

### 2.2.2. Thermo-physical characterization of the grafting

*Extrusion profiles.* BA was grafted onto ENR25 through reactive extrusion at 180 °C. During the extrusion process, the axial force exerted by the screws on the cavity of the extruder was followed. This force, which varies with the loading, the temperature and the polymer composition, is an indirect measure of the torque. An increase of this force is related to a viscosity increase of the extruded mass. For all of the extrusion experiments, this axial force was measured in function of the time. A typical curve obtained for the grafting of BA onto ENR25 chains is presented in Figure 17a. For a better understanding of the process and for comparison, the force corresponding to the extrusion of pure ENR25 in the same conditions is presented in Figure 17b.

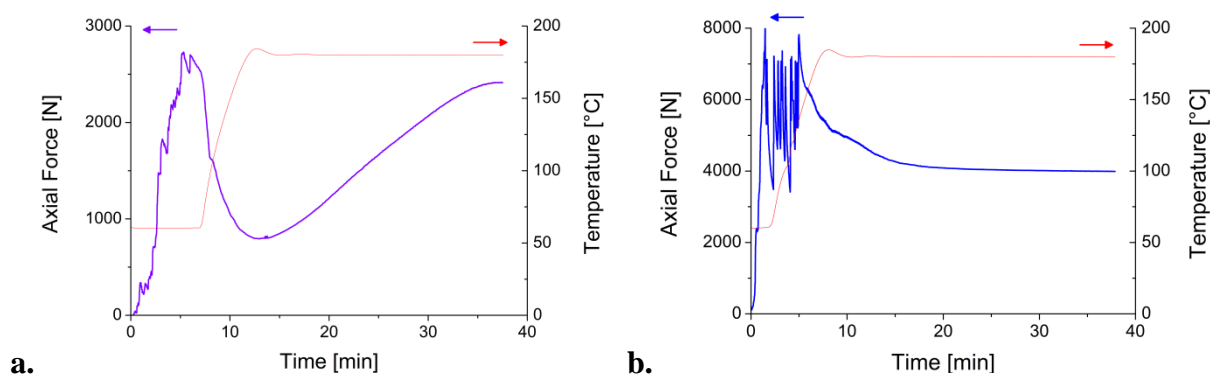


Figure 17. Extrusion profiles. **a.** Reactive extrusion of ENR25 with BA and DMI (one BA molecule for two epoxy functions.) **b.** Extrusion of pure ENR25.

On both curves, the first few minutes correspond to the introduction of the materials into the extruder. During this filling step, the force increases and oscillates due to the increasing amount of product inside the cavity. As soon as all the products were introduced, the extruder was closed and the temperature raised to 180 °C to start the grafting reaction. A nitrogen flux was used to prevent thermal oxidation. High temperature favouring molecular motion, the force decreases. In the case of neat ENR25, considering that no crosslinking side reaction can happen thanks to the nitrogen flux, the only possible reaction is the scission of the long chains into shorter segments because of the high applied shear. This scission results in a decrease of viscosity. As seen in Figure 17**b**, the force eventually reaches a plateau indicating that the scission process stays limited under the chosen conditions. In the case of the reactive extrusion (Figure 17**a**), the initial decrease is sharper, probably because of the plasticizing effect of BA that melts around 80 °C. Then, when the temperature is high enough, the axial force starts increasing again. This was interpreted as the consumption of the plasticizer by the grafting reaction. This reaction creates a branched polymer from a linear one and the change of morphology could also play a role in the increase of the torque. The extrusion was stopped after 25 minutes, when the force reached a plateau that indicates the end of the reaction.

*DSC measurements.* For this DSC study, the BA content was fixed at one BA molecule for four epoxy rings. As shown in Figure 18**a**, free BA crystals melt around 78 °C and form around 74 °C. When mixed with ENR25 and DMI, the DSC trace becomes more complicated, even before grafting (Figure 18**b**). The  $T_g$  of ENR25 is visible ( $\approx -45$  °C), and some melting and crystallization peaks appear between 17 and 90 °C. Those peaks were attributed to BA and DMI but also to the corresponding imidazolium salt. After the grafting of BA onto ENR

chains (Figure 18c), the  $T_g$  of ENR25 is still visible and almost unchanged, but there is only one other large peak left. The change in the DSC traces before and after reactive extrusion confirms the occurring of the grafting reaction. The peaks around 30 and 14 °C were attributed to the fusion and crystallization of the grafted acid, respectively. Melting of these grafted BA crystals occurs at much lower temperature than free BA molecules, probably because the chemical links hinder crystallization.

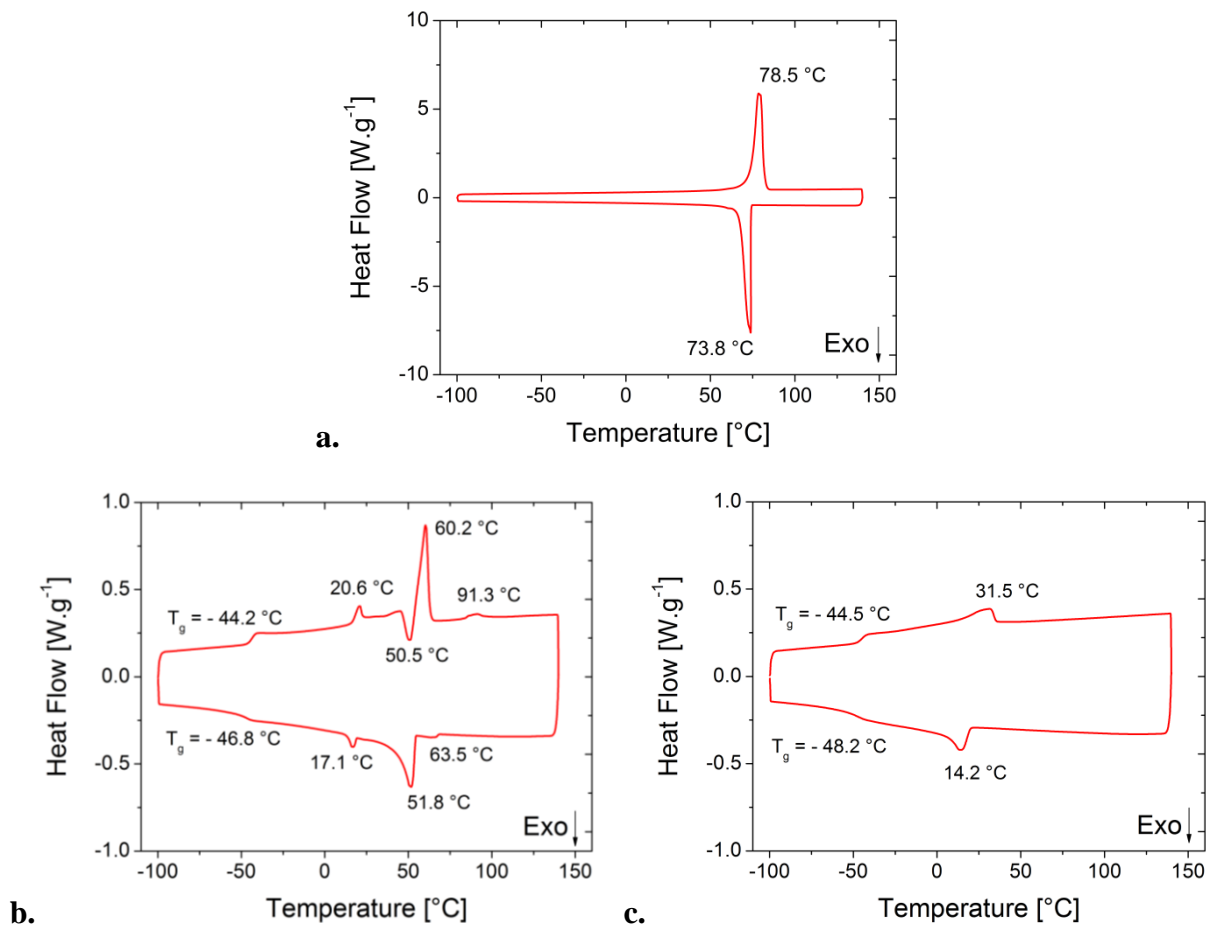


Figure 18. DSC traces of (a) pure BA, and mixes between ENR, BA and DMI before (b) and after (c) reactive extrusion. (BA/epoxy ratio: 1/4)

## 2.2.3. Spectroscopic characterization

*Infrared spectroscopy.* IR was used to confirm the occurrence of grafting through esterification. Indeed, hydroxyl, acid and ester functions have characteristic absorption bands that are well visible and easily identified in ENR spectrum. The FTIR spectra of the blend before and after grafting are superimposed in Figure 19a. One can notice the emerging of a broad band around  $3400\text{ cm}^{-1}$  after grafting. This band corresponds to the stretching vibration of O-H bonds, confirming the opening of the epoxy rings during the reaction. A zoom around  $1700\text{ cm}^{-1}$  (Figure 19b) shows that the peak of the carboxylic acid completely disappeared after extrusion, and that a new peak appeared, corresponding to the newly formed ester bond.

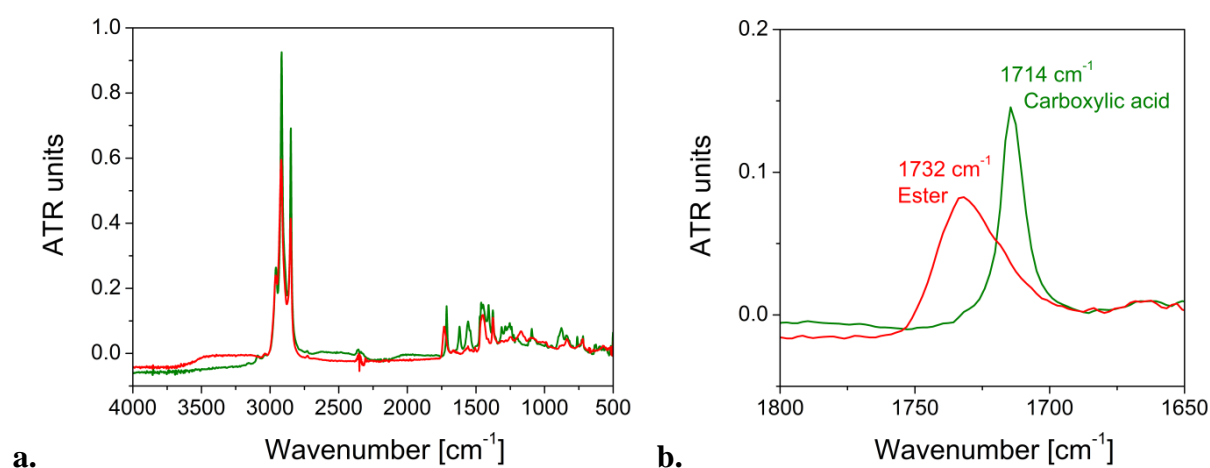


Figure 19. FTIR spectra of the blend (ENR25 + BA + DMI) before (green) and after (red) grafting: **a.** complete spectrum; **b.** zoom in the carbonyl group area.

*<sup>1</sup>H NMR experiments.* The NMR spectra of a blend containing ENR25, BA (one molecule for two epoxy functions) and DMI at different stages of grafting are shown in Figure 20. The signals of the protons on the epoxy rings (2.7 ppm) and the double bonds (5.13 ppm) as well as the appearance of new signals corresponding to the grafted products will be discussed. Like in Chapter 2, the integration of the olefinic protons was fixed to 1 in each case to facilitate comparison and an epoxidation ratio could be calculated (see Equation (1) in Chapter 2).

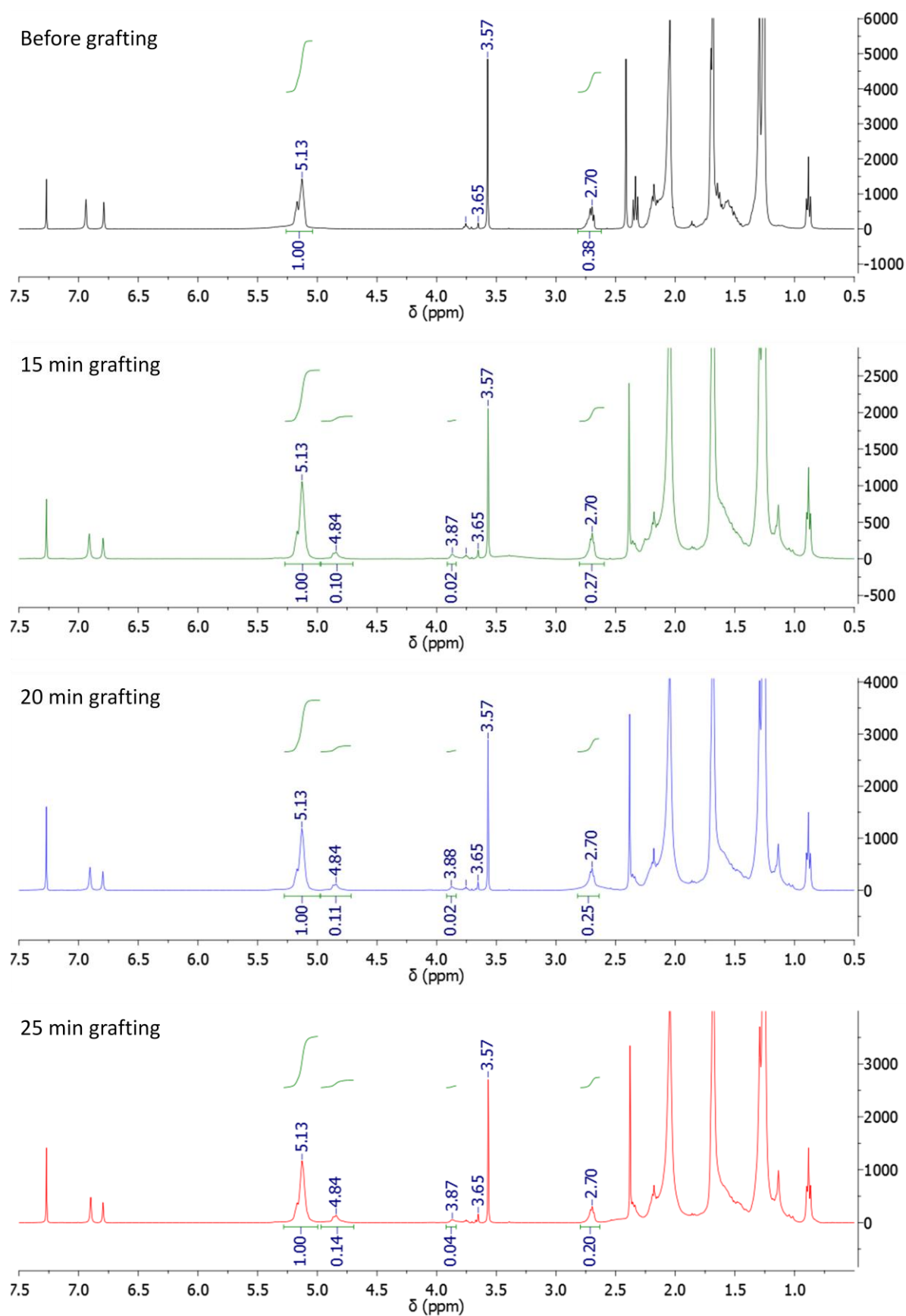


Figure 20.  $^1\text{H}$  NMR spectra in  $\text{CDCl}_3$  of the extrusion product after different grafting times at  $180^\circ\text{C}$  (BA/epoxy ratio:  $1/2$ ).

Before grafting, the epoxidation ratio was calculated to be around 28 % (as in Chapter 2). Then, with increasing grafting times, the integration of the epoxy protons decreases, indicating the reaction of oxirane rings. At the same time, two new peaks appear at 4.8 and 3.9 ppm that were attributed respectively to protons of carbon number 8 and 3 in Figure 21. Indeed, there are two possible addition products depending on the regioselectivity of the epoxy opening. The grafting of BA on the less crowded side of the epoxy seems favoured, in accordance with the NMR study conducted by Pire *et al.* on DA-crosslinking of ENR.<sup>18</sup> This side of the epoxy reacts preferentially when the mechanism is base-catalyzed as it is the case here. After 25 minutes of grafting at 180 °C, about half of the epoxy functions have been consumed. As BA was introduced in a ratio 1:2 to epoxy rings, this confirms that the reaction is over in about 25 minutes. To ensure complete grafting of BA onto ENR, the grafting time will be fixed to 30 minutes in the following.

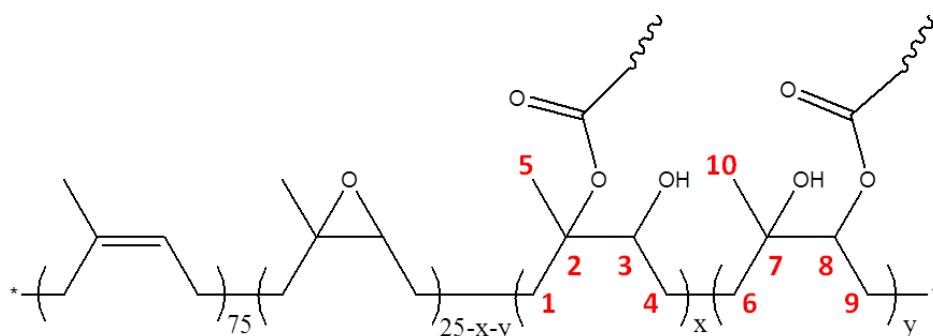


Figure 21. Possible locations of grafting and NMR peak attribution.

ENR is composed of very long molecules. This high molecular weight (around  $10^6 \text{ g}\cdot\text{mol}^{-1}$ ) renders chemical modification difficult because of solubility and viscosity problems as well as unfavourable neighbouring group effect that impedes the reactivity of the polymer.<sup>12</sup> The grafting method proposed here is an efficient and easy bulk process which allows quantitative modification of the backbone without the use of a solvent.

## 2.3. Properties of BA-grafted ENR25

### 2.3.1. Thermo-mechanical properties

*DSC experiments.* The DSC trace of the grafted ENR25 with the chosen BA content (one BA molecule for two epoxy functions) is shown in Figure 22a. The crucial point here is that BA is still able to crystallize even after chemical grafting onto ENR chains. Fusion of the grafted BA occurs around 39 °C and crystallization around 27 °C, just above room temperature. The properties of this crystallized ENR will be studied here, and comparison will be made with the chemical networks of section (1) (ENR-DA, that contained kaolin). For a better comparison, a comparable quantity of kaolin was added to the physical network.

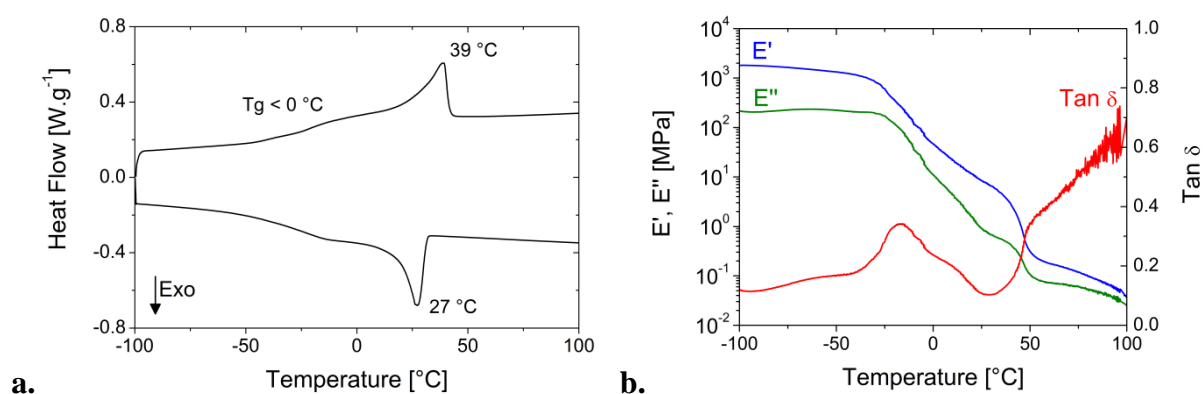


Figure 22. DSC trace (a) and dynamic mechanical analysis (b) of BA-grafted ENR25.

*Dynamic mechanical analysis.* A plot of the storage and loss moduli as well as  $Tan \delta$  in function of temperature is given in Figure 22b. The  $T_g$  of the material corresponds to the first decrease of  $E'$  (and to the peak of  $Tan \delta$ ). After grafting, the transition zone broadens a lot, but the  $T_g$  is still negative, confirming the rubbery character of the material at room temperature. The second sharp decrease of  $E'$  around 50 °C corresponds to the melting of grafted BA in accordance with the DSC measurements. Above this temperature, ENR chains are no longer linked to each other and can move freely, inducing flow. At room temperature, the grafted ENR can thus be seen as a physical network crosslinked by BA crystallites. The operating range of this TPE is in between the  $T_g$  ( $\approx -15$  °C) and the melting temperature of the BA crystals (around 40-50 °C). Within this range, the modulus is quite dependent on

temperature (Figure 22b). Two temperatures will be selected for mechanical testing and diffraction experiments: 20 °C, to account for the properties around room temperature, and 10 °C (below the melting endotherm, Figure 22a) to test a more crystalline material.

### 2.3.2. Morphology and structure of the physical network

*Microscopic observation.* The morphology of the physical network was investigated by transmission electron microscopy. The staining of the sample reveals white (unstained) rows that were interpreted as crystalline lamellae (Figure 23). Images of ultrathin cuts thus confirm the crystallizable nature of these materials already seen by DSC measurements. The lamellae seem to organize periodically and account for a high percentage of the material, in accordance with the formulation (BA represents 37 wt% of the total formulation, Table 6 in appendix B).

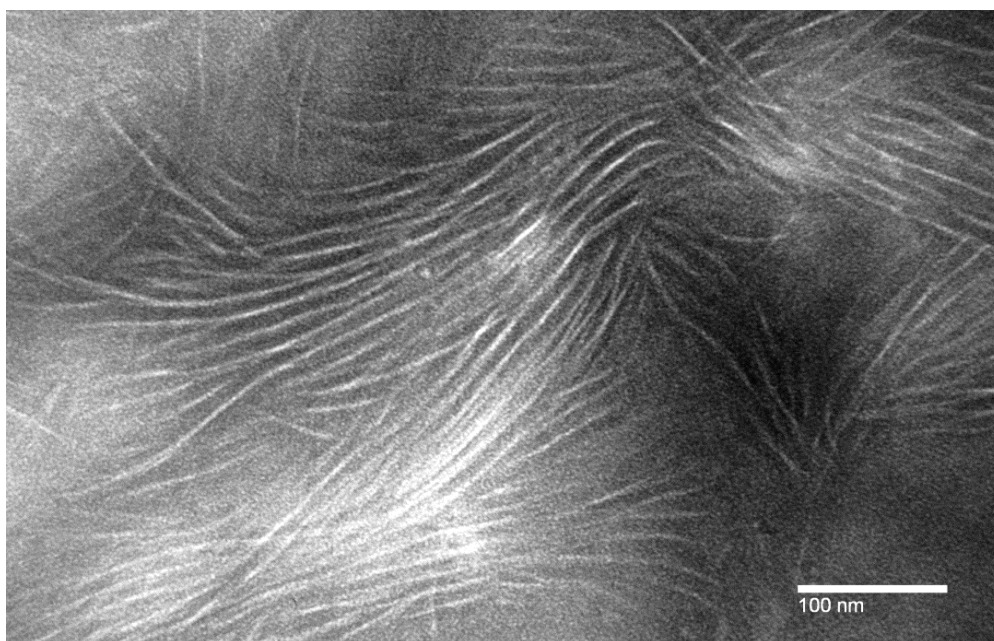


Figure 23. TEM image of the grafted ENR (physical network).  $\text{RuO}_4$  staining.

From this TEM image, the inter-lamellar distance was evaluated around 12 nm, a characteristic distance that should be visible in X-ray diffraction measurements. Small angle X-ray scattering measurements were thus performed at the LEM laboratory (Arkema Serquigny).

*Small angle X-ray scattering (SAXS).* The SAXS profiles are shown in Figure 24, in the  $q^2 I(q) = f(q)$  representation. The SAXS spectra of the physical network (containing kaolin, as it was studied in most of this work) presents a broad peak around  $0.075 \text{ \AA}^{-1}$  (corresponding to distances of about  $80 \text{ \AA}$ ), that was attributed to kaolin. Indeed, the chemical network described in the previous section (ENR-DA,  $p = 25$ ), that also contained kaolin, shows the same peak, whereas the peak is absent in the spectra of neat ENR25 and kaolin-free physical network. The SAXS profile of the kaolin-free physical network clearly presents a peak around  $0.04\text{-}0.05 \text{ \AA}^{-1}$ , corresponding to distances around  $140 \text{ \AA}$ . This peak is also visible, as a shoulder, on the spectrum of the physical network containing kaolin and absent in the other spectra. This distance corresponds quite well to the  $12 \text{ nm}$ -interlamellar distance measured from TEM images, confirming that this peak is due to BA lamellae.

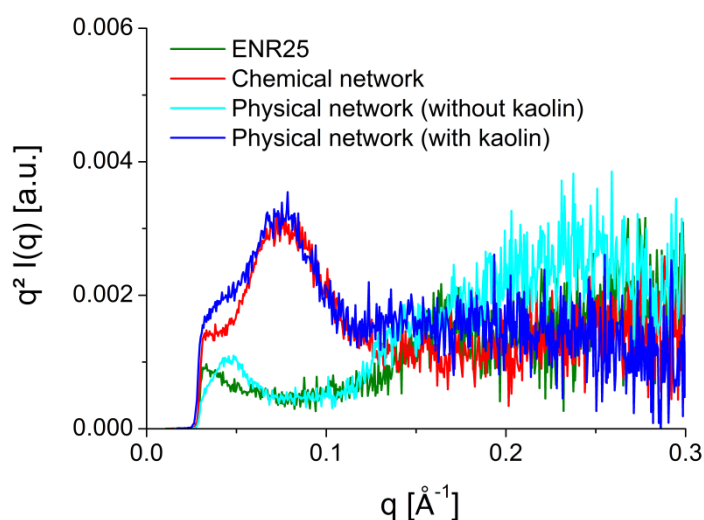


Figure 24. SAXS measurements of different samples of ENR25.

### 2.3.3. Mechanical properties and X-ray scattering

The mechanical properties of the grafted ENR, tested at  $20$  and  $10 \text{ }^\circ\text{C}$ , are shown in Figure 25. Two cycles were performed on the same sample which was finally stretched until break. The curves at both temperatures looked qualitatively similar. However, as expected from DMA measurements (Figure 22b), the moduli are quite different, more elevated at the lower temperature. This is due to the higher degree of crystallization of the grafts at  $10 \text{ }^\circ\text{C}$ . Either the number of crystals increased, leading to a greater modulus because crystals act as crosslinking points, or their size is bigger, which can potentially result in a higher reinforcing

effect. Both cases tend to increase the modulus, explaining the observed difference in the mechanical properties.

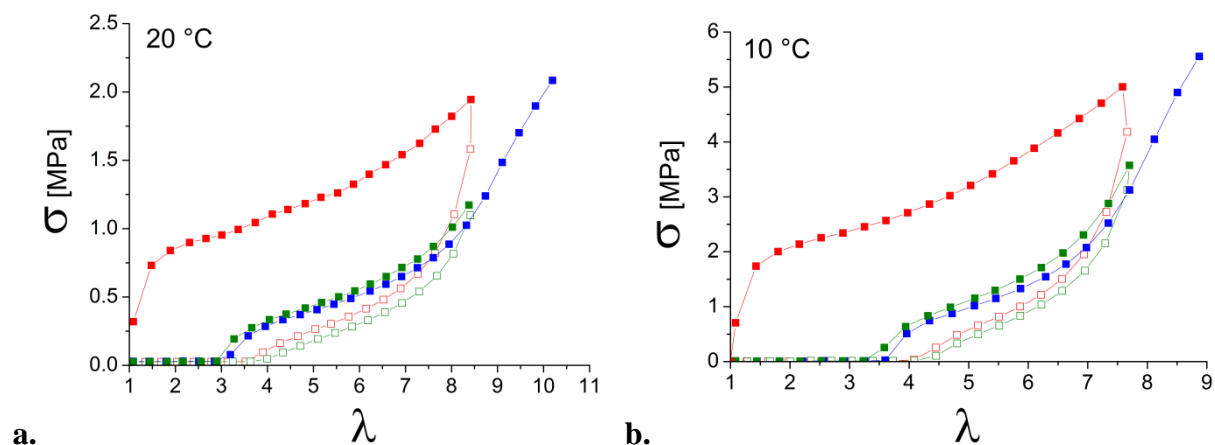


Figure 25. Mechanical properties of BA-grafted ENR25 at 20 °C (a) and 10 °C (b). (red) first cycle; (green) second cycle; (blue) final stretching until break. (full symbols: loading, open symbols: unloading)

The first cycle is tremendously different from the second and third ones. The corresponding Young's modulus, taken as the initial slope of the stress-strain plot, is very high (around 2.5 MPa at 20 °C and 5.5 MPa at 10 °C). For comparison, the chemical networks of section (1) (ENR-DA) showed Young's moduli around 1.5 MPa or less. Moreover, this first cycle does not present elasticity, an important residual strain of around 300 % is observed. The pristine material cannot be considered as an elastomer. Instead, it behaves in accordance with its semi-crystalline nature.

For the second cycle and last stretching, the behaviour is completely different. The corresponding curves were plotted after recalculation of the strain (Figure 26). The material presents a low hysteresis and a residual strain around 100 % after unloading. After five minutes rest, this residual strain has disappeared and the subsequent loading is almost identical to the previous one. After the pre-stretching step, the physically crosslinked ENR thus behaves as an elastomer.

The corresponding cycles for the chemical network (at different  $p$  ratios, see section (1.2)) were plotted for comparison. In Figure 26b, the cycle (corresponding to the second cycle in Figure 25b) of the physical network almost superimposed with the one of the chemical network with  $p = 25$ . At 20 °C (Figure 26a), the sample compares with the chemical

networks  $p = 50$  and  $100$  instead of  $25$ . This has to be linked with the lower crystallization at  $20\text{ °C}$  that most probably results in a lower physical crosslink density. At both temperatures, the physically crosslinked rubber presents elastomeric properties and even exhibits better ultimate properties than the corresponding chemical network.

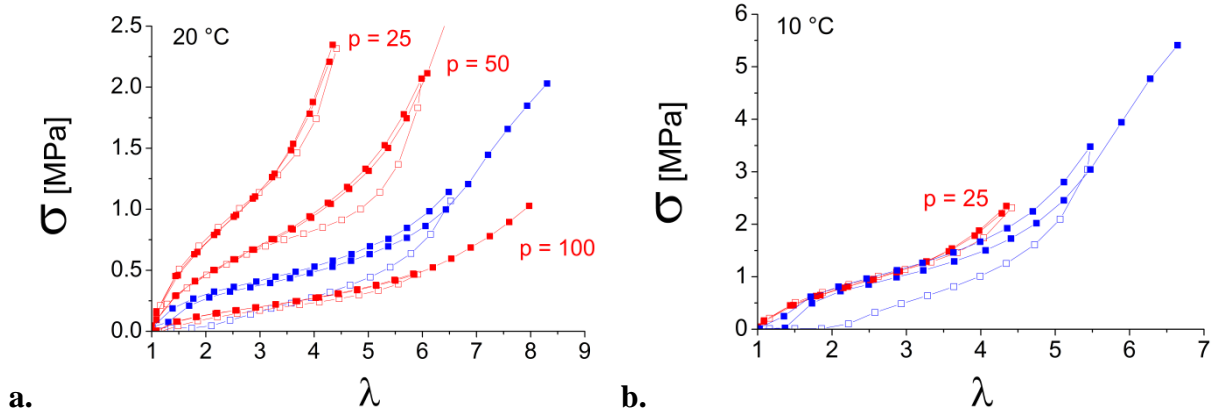


Figure 26. Mechanical properties of BA-grafted ENR25 after the first cycle (blue) and behaviour of ENR-DA (red) at different crosslink densities. (a)  $20\text{ °C}$ ; (b)  $10\text{ °C}$ .

The WAXS patterns were recorded during stretching and their evolution with strain during the first cycle is presented at both temperatures in Figure 27a and b. The scattering patterns and their evolution were much more complicated than what was observed in the previous section for the chemical ENR-DA networks due to additional diffraction by the grafted BA.

Before stretching, the patterns already show some crystallization (crystalline ratios calculated from the WAXS patterns at  $\lambda = 1$  are:  $9\%$  at  $20\text{ °C}$  and  $12\%$  at  $10\text{ °C}$ ). Indeed, contrarily to the chemical network patterns that only presented an amorphous halo (Figure 15a,  $\lambda = 1$ ), another ring is visible here, superimposed to the amorphous halo but at a higher Bragg angle (initial pattern in Figure 27a and b,  $\lambda = 1$ ). This Bragg angle corresponds to a distance around  $4.2\text{ \AA}$ , in accordance with the (110) inter-planar distance in polyethylene  $((\text{CH}_2)_x)$ .<sup>48</sup> Upon stretching, this outer ring rapidly orientates, showing an orientation of the BA crystals.

As described in the first section of this chapter, the X-ray patterns were analyzed by radial integration between two cycles in function of the azimuthal angle  $\varphi$ . For the chemical networks, this integration was limited to  $\varphi$  between  $-80$  and  $+80^\circ$ . However, the scattering

patterns of the physical network are more complicated, the integration was thus extended to  $\varphi$  in between  $-180$  and  $+180^\circ$ . The angular profiles obtained by radial integration are shown in Figure 27c and d. Each curve here corresponds to a point in the mechanical curve of Figure 27a and b.

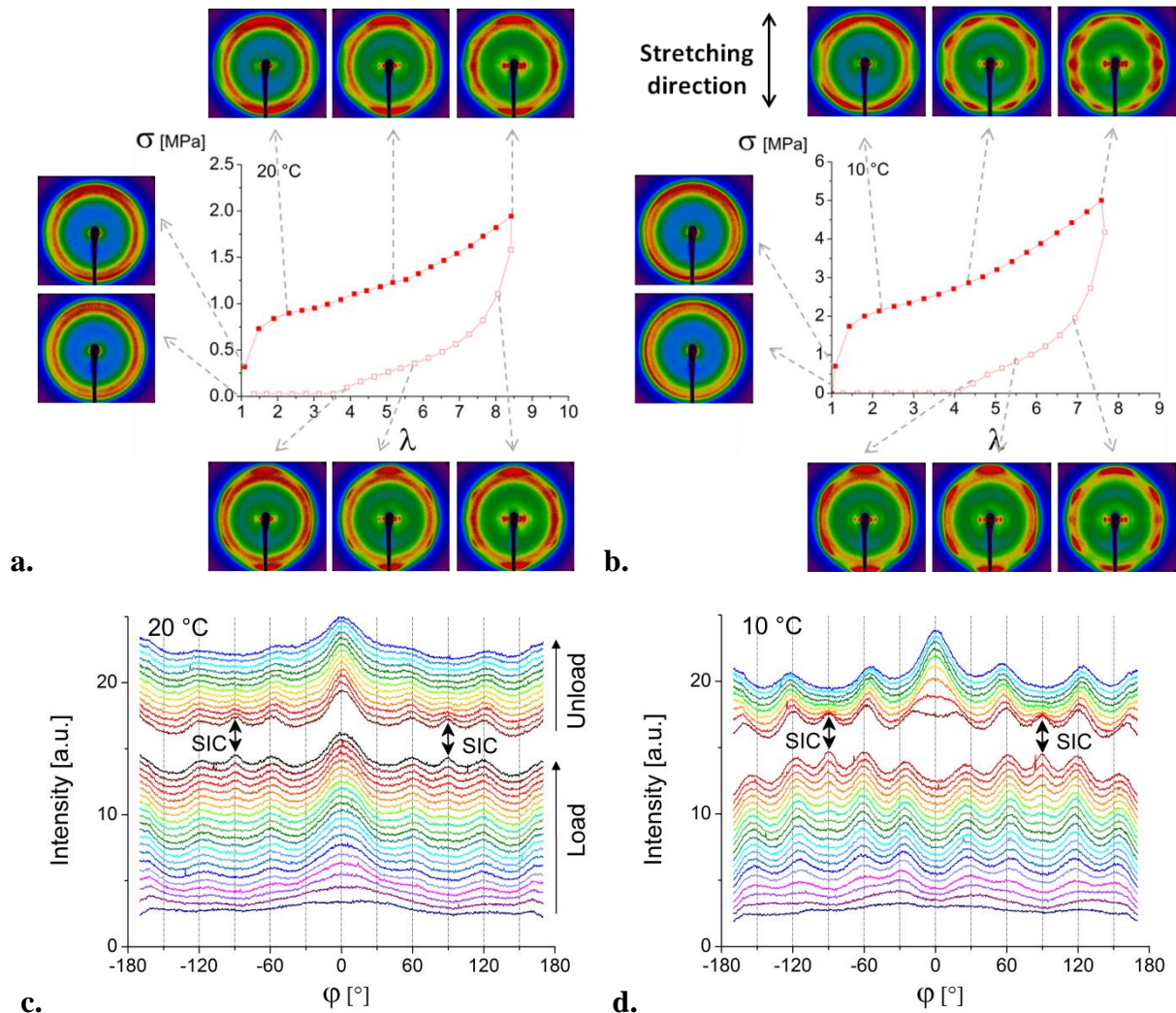


Figure 27. Diffraction patterns obtained during the first tensile cycle at  $20^\circ\text{C}$  (a) and  $10^\circ\text{C}$  (b), and radial integration profiles obtained at  $20^\circ\text{C}$  (c) and  $10^\circ\text{C}$  (d) during the first cycle.

The different curves correspond to different elongation ratios.

For small elongations ( $\lambda < 2$ ) a slight orientation is observed, to attain a minimum intensity along the equator ( $\varphi = \pm 90^\circ$ ), perpendicular to the stretching axis. For  $2 < \lambda < 6$ , at  $20^\circ\text{C}$ , the Bragg ring associated to BA crystals splits in several arcs, a main component

centered on the stretching direction ( $\varphi = 0^\circ$ ), corresponding to a large peak, and two other less intense and narrower peaks at  $\varphi = \pm 60^\circ$ . At 10 °C, the orientation is a little different. The main signal splits into two peaks centered around  $\varphi = \pm 25^\circ$ . For elongation ratios above  $\lambda \approx 6$ , the BA crystal orientation is unchanged and peaks from ENR's SIC superimpose. This SIC will be studied in more detail later.

Upon unloading, for experiments at 20 °C, strain-induced ENR crystals melt, but the orientation of BA crystals is preserved with only a partial relaxation, the isotropic outer ring does not reappear. At 10 °C, after the melting of strain induced crystals, the orientation of the BA crystals evolves differently. The main peaks evolve from  $\varphi = \pm 25^\circ$  to  $\varphi = 0^\circ$  while the others remain around  $\varphi = \pm 60^\circ$  (Figure 27d). This differences in behaviour are to be related to the different crystal ratios (quantity and size of the crystals are higher at 10 °C) resulting in different physical crosslink densities.

At both temperatures, the BA crystals remain oriented after unloading, whereas the strain-induced crystals disappear. This persistent orientation of BA crystals is responsible for the high residual elongation at the end of the first cycle (300 %).

The WAXS patterns obtained during the second cycle and last load are presented in Figure 28, along with the corresponding radial profiles. The evolution of these patterns and profiles permits to follow the orientation of BA crystals. The small arcs located at  $\varphi = \pm 60^\circ$  do not evolve during the second cycle. Contrarily, the large arc centered at  $\varphi = 0^\circ$  for the measurement at 20 °C tightens upon stretching and relaxes at unloading. At 10 °C, the intensity localized at  $\varphi = 0^\circ$  before stretching evolves continuously to split into two arcs at  $\varphi = \pm 25^\circ$  for  $\lambda = 8$  and relaxes progressively towards  $\varphi = 0^\circ$  upon unloading.

These cyclic tests indicate that the four small arcs at  $\varphi = \pm 60^\circ$  (white arrows in Figure 29) that appear at both temperatures during the first load show very little evolution during the following loadings and unloadings. These arcs are associated to wide crystalline domains (narrow peaks) that fracture and orientate during the first cycle, and do not play a role afterwards in the traction mechanism. Conversely, the orientation of the other crystalline domains (smaller, associated to wider peaks) evolves during stretching. These domains are associated with crystals that would form physical crosslinking points supporting the elongation during the subsequent cycles. At 10 °C, there are more physical crosslinks because of the higher crystallinity, and these crosslinks are tilted reversibly upon stretching, as shown in Figure 29.

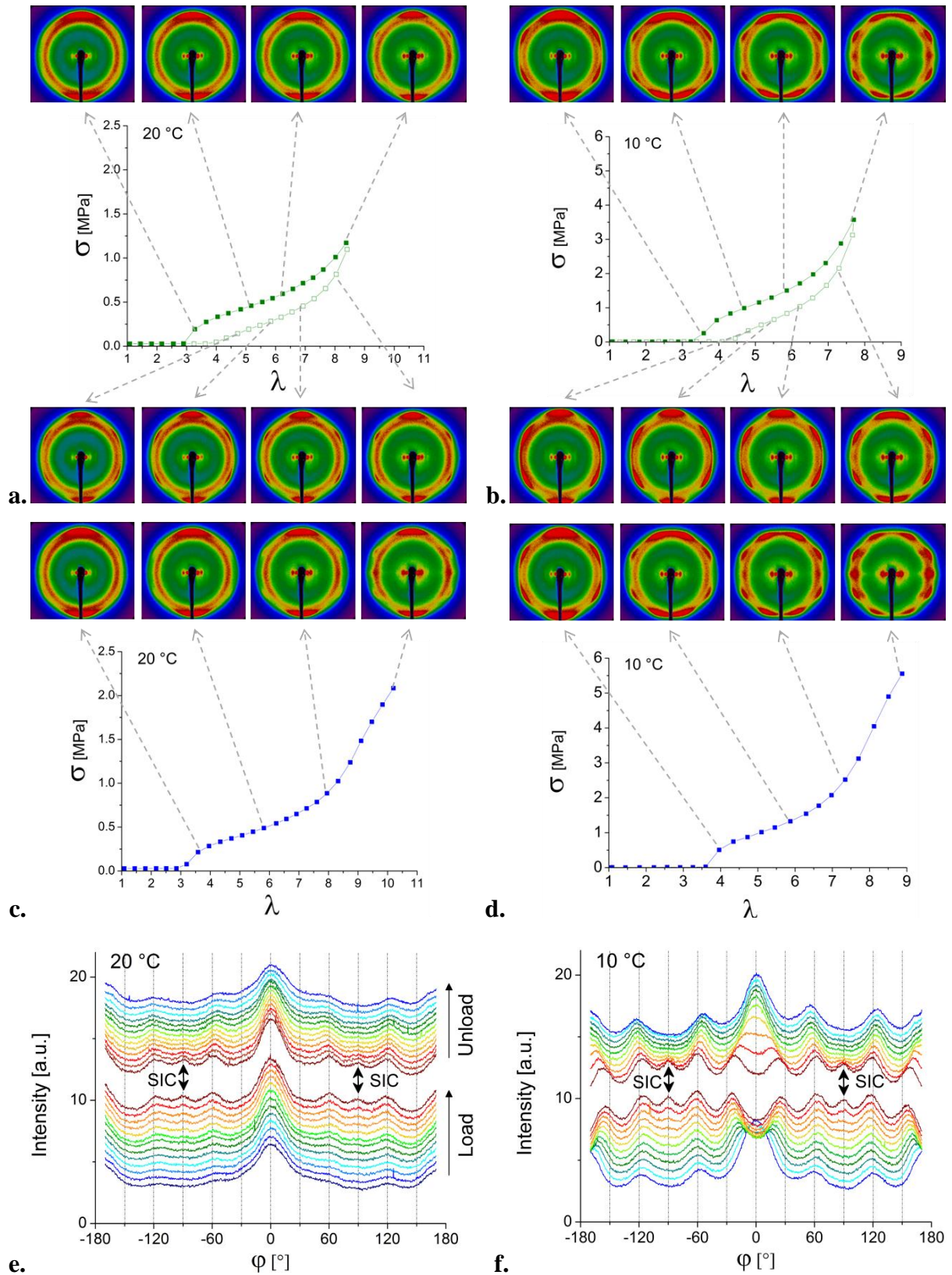


Figure 28. Diffraction patterns obtained during the second cycle and third load at 20 °C (a and c) and 10 °C (b and d). The radial integration profiles corresponding to the second cycle are plotted at 20 °C (e) and 10 °C (f).

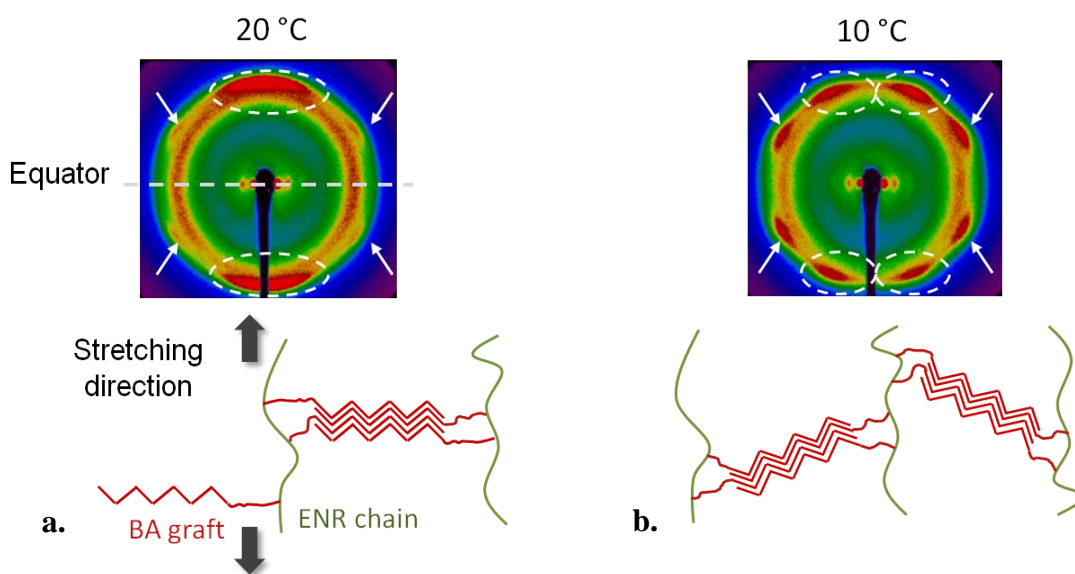


Figure 29. WAXS patterns and schematization of the BA crystal orientation during the first loading  $\lambda \approx 5$  at 20 °C (a) and at 10 °C (b).

On the diffraction patterns, the SIC of ENR is well visible for the experiments at 10 °C (peak located on the equator for high  $\lambda$ , Figure 28b and d) and a little weaker at 20 °C. It is also recognized in the radial integration profile by the appearance of an equatorial peak at  $\varphi = 90^\circ$  and the symmetric one at  $-90^\circ$  (black arrows in Figure 28e and f) corresponding to the added contributions of reflections (200) and (120) (Figure 9b, in section (1)). The attribution of this peak to SIC of ENR chains is also supported by the fact that it reversibly appears during loading and disappears at unloading.

By extracting linear intensity profiles ( $I(2\theta)$ ) at the equator ( $\varphi = 90^\circ$ ) and at  $\varphi = 53^\circ$  (angle at which the (201) reflection appears), the position of the peaks corresponding to strain-induced crystals could be identified. These peaks superimpose with the contributions of BA (at  $\varphi = 53^\circ$ ), complicating their precise determination. At 20 °C, even if SIC is clearly observed in Figure 28a, c or e, the characteristic diffraction peaks were too low to be determined. The corresponding lattice parameters were thus calculated only from measurement at 10 °C with the formulas given in experimental section (1.2) and are collected in Table 4.

Table 4. Lattice parameters (orthorhombic system)

		a (nm)	b (nm)	c (nm)	Volume (nm <sup>3</sup> )
ENR-DA ( $p = 25$ ) <sup>a</sup>	20 °C	1.25	0.95	0.82	0.973
BA-grafted ENR25	10 °C	1.22	0.93	0.84	0.95

<sup>a</sup> Results from the previous section

The calculated lattice parameters were close to what was found for ENR-DA in the previous section, confirming that the observed peaks are indeed due to SIC. The crystallizable grafts thus not only do not hamper the strain-induced crystallization, but help reinforcement of the mechanical properties of the material.

## 2.4. Summary and conclusions

ENR was efficiently grafted with BA by a reactive extrusion process without the need of organic solvents. The grafting reaction was fully characterized and resulted in a semi-crystalline material. The crystallites self-organize into lamellae that could be observed by electronic microscopy and SAXS measurements.

Mechanical experiments showed that after one pre-stretching cycle, the material behaves as an elastomer while being crosslinked only through BA crystals. During the pre-stretching step, the grafts orientate and remain in a position compatible with further stretching cycles, giving rise to a thermoplastic elastomer.

This thermoplastic elastomer also demonstrates a SIC behaviour, associated with the fact that it is based on a natural rubber derivative. This should confer to our strain-crystallizing TPE unique mechanical properties (resistance to tearing and to crack propagation for example) that should be investigated further.

### 3. Dual networks

Two different crosslinking methods, based on the opening of epoxy functions on ENR chains, were studied in this chapter, a chemical one (using carboxylic diacids), and a physical one (grafting of crystallizable monoacid chains). By combining chemical and physical bonds, the resulting materials can potentially benefit from the advantages of both types of networks. The chemical bonds provide heat and solvent resistance while the physical bonds can lead to higher ultimate mechanical properties. The preliminary results obtained on those dual networks are briefly presented here.

Two different ways were used to combine both types of crosslinks:

- *Simple dual networks* were synthesized by addition of DA and DMI (to get to  $p = 25$ ) to BA-grafted ENR (with the same BA content than in the previous section) and subsequent crosslinking in a hot-press. The result is a BA-grafted ENR crosslinked by DA.
- *Mixed dual networks* were made in two steps. Pure ENR25 was first mixed with DA and DMI without curing ( $p = 25$ ), this blend was then mixed with the grafted material (same BA content again), and eventually, the resulting binary ENR blend was cured by hot-pressing. The result is a mixture of immiscible ENR and BA-grafted ENR both potentially crosslinked by DA.

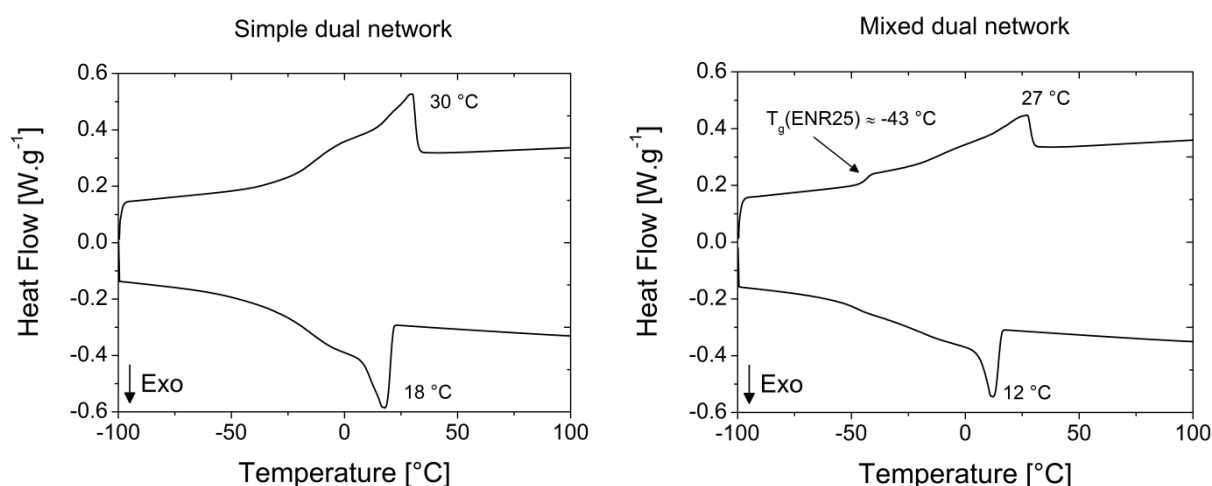


Figure 30. DSC traces of the dual networks

The networks were firstly characterized by DSC (Figure 30). The trace of the simple dual network resembles much the one of the physical network (Figure 22a). The

crystallization and melting of the grafts is well visible. Crystallization occurs at lower temperature than in the physical network, probably because the chemical bonds hinder the formation of the crystals. In the trace of the mixed dual network, the  $T_g$  of pure ENR25 is visible, additionally to a signal very similar to the one of the physical network. This is a sign of the non-miscibility of pure and grafted ENRs. Crystallization and melting of the grafts occurs at even lower temperature for mixed networks indicating that their crystallization is also hindered (resulting in smaller and fewer crystallites).

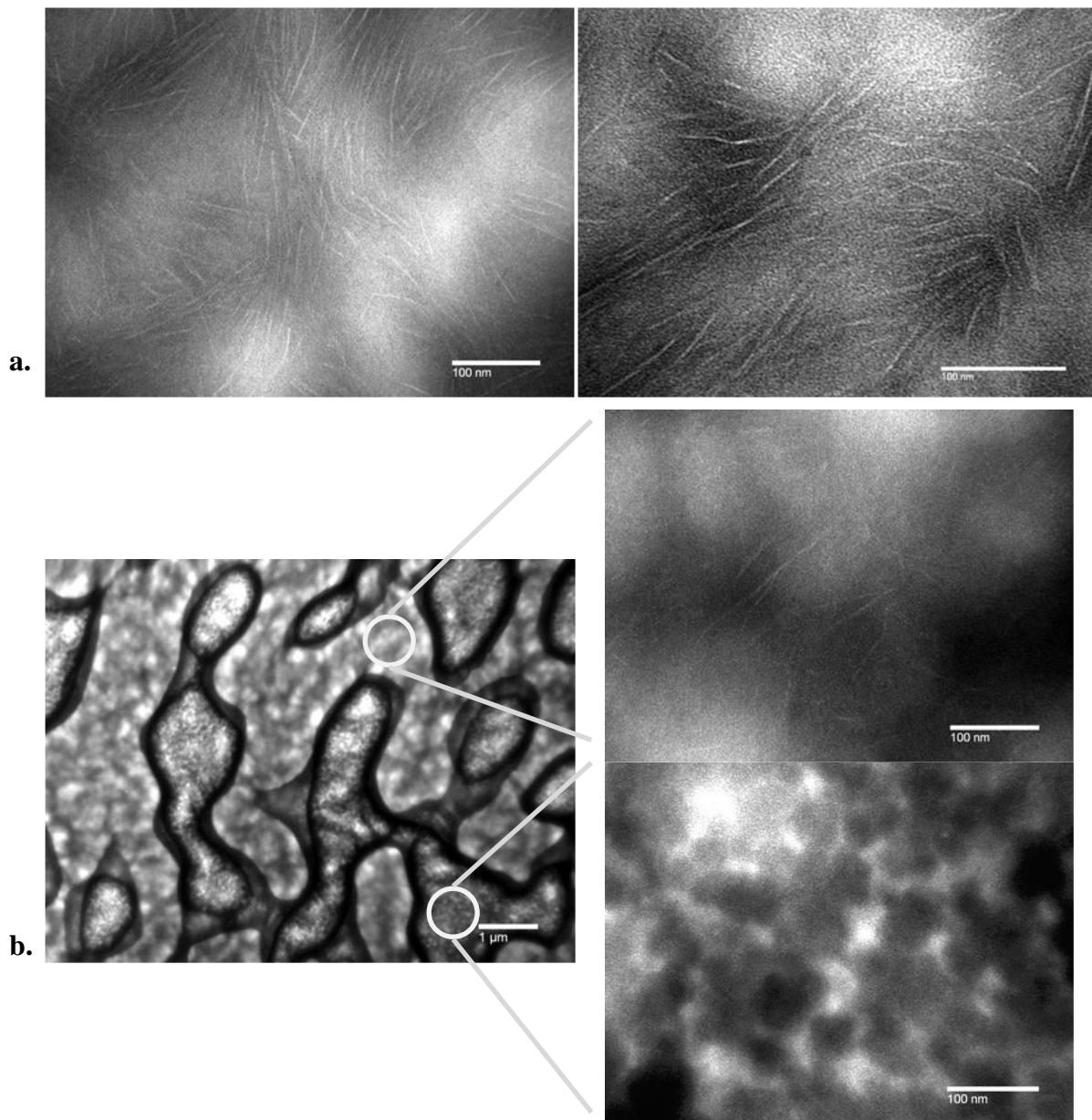


Figure 31. TEM images of dual networks. **a.** Simple dual network at two different scales. **b.** Mixed dual network with a zoom on each of the two phases. The scale bars represent 100 nm in each picture except the left bottom one for which it represents 1  $\mu\text{m}$ ).

The morphology of the materials was studied by transmission electronic microscopy (Figure 31). As expected from DSC, the simple dual network exhibits a similar morphology to the physical network (Figure 31a). The observed lamellae seem shorter and more widely-spaced than the ones observed for the physical network (Figure 23). This lower crystallinity is in accordance with the lower calculated area under the melting peak in DSC (around  $20 \text{ J.g}^{-1}$  for the physical network but only around  $15 \text{ J.g}^{-1}$  for the simple dual network) as well as with the lower crystallization and melting temperatures. The TEM images of the mixed dual network clearly show two phases, confirming the non-miscibility of ENR and BA-grafted ENR. Indeed by zooming on each phase, isolated crystallites are observable (top zoom image, mainly the BA-grafted ENR) or not (bottom zoom image, mainly the ENR phase).

DSC and TEM indicated that both dual networks contain crystallized grafts. The mechanical properties were studied at  $10 \text{ }^\circ\text{C}$ , temperature which promotes crystallization (Figure 32). For both dual networks, a hysteresis is observed during the first cycle. However the residual strain is much lower than in the case of the physical network thanks to the presence of the chemical bonds (around 100 % residual strain instead of 300 %, Figure 25).

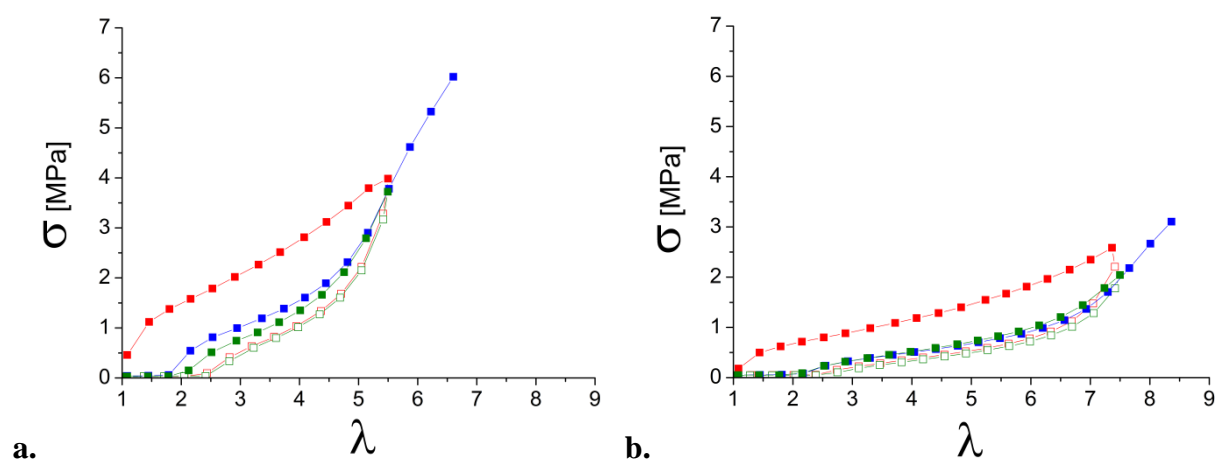


Figure 32. Mechanical properties at  $10 \text{ }^\circ\text{C}$  of the simple dual network (a), and mixed dual network (b). (red) first cycle; (green) second cycle; (blue) subsequent stretching until break. (full symbols: loading, open symbols: unloading)

The estimated chemical crosslink densities of the dual networks were compared to the three chemical networks by measuring the swelling ratio  $Q$  (see section (1)). The values of the apparent crosslink densities  $1/Q$  are given in Table 5.

Table 5. Apparent crosslink densities of chemical and dual ENR networks.

Type of network	$1/Q$
Chemical $p = 25$	0.10
Chemical $p = 50$	0.073
Chemical $p = 100$	0.044
Simple dual	0.071
Mixed dual	0.052

The chemical crosslink density of the simple dual network is comparable to the one of ENR-DA  $p = 50$ . As DA was introduced in order to get  $p = 25$ , we can conclude that the DA did not fully react, probably because of the high percentage of already grafted epoxy functions. For the mixed dual network, the chemical crosslink density is in between those of  $p = 50$  and  $p = 100$  ENR-DA samples.

The mechanical properties of the mixed dual network after one cycle (the strain has been recalculated as for the physical network) are compared in Figure 33 to those of the two less crosslinked chemical networks. The stress values are in between those of the two chemical networks as expected from swelling measurements. However, the stress and strain at break are higher. This heterogeneous type of dual crosslinking permitted to have a low residual strain in cyclic experiments and to improve the strain and stress at break while retaining the same stress values than with fully chemical crosslinking.

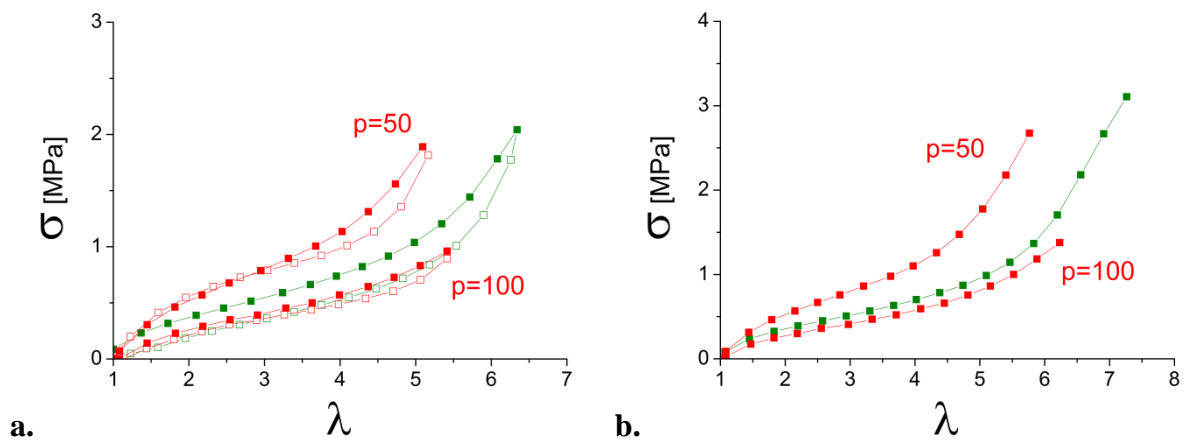


Figure 33. Comparison of chemical (red) and mixed dual (green) networks at 10 °C during the second mechanical cycle (a), and the last stretching until break (b).

For the simple dual network, comparison is made with the physical and chemical ( $p = 25$ ) networks (Figure 34). Very similar stress values are obtained, but the hysteresis is different. The residual strain of the simple dual network is in between the two other values. Its properties at break (Figure 34b) are higher than the ones of the chemical network, and comparable to those of the physical network. Even if the crosslink density of this dual network is lower (comparable to  $p = 50$ ), the curve almost superimposes to the one of the chemical network until rupture, showing the reinforcing effect of the grafts. Combining physical and chemical bonds permitted to reduce the hysteresis of the physical network while preserving its higher properties at break.

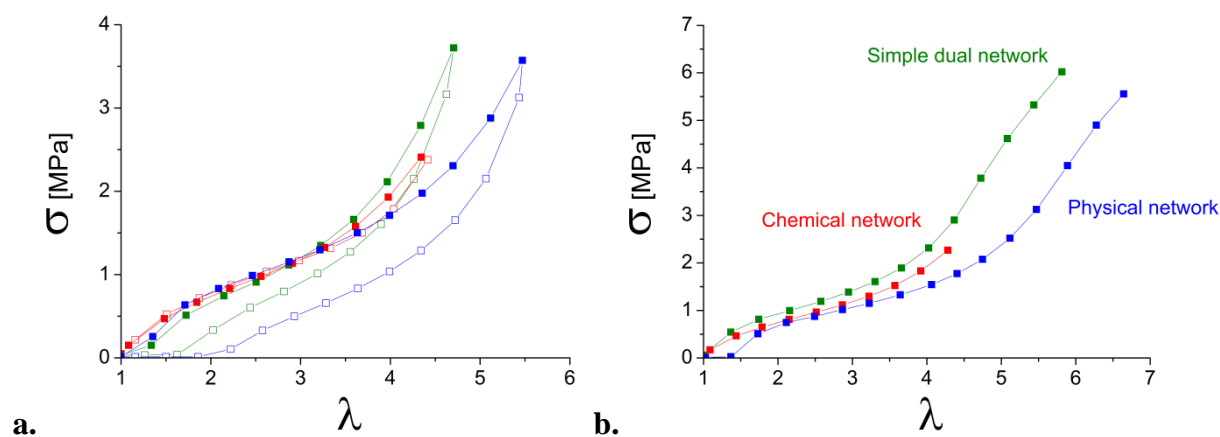


Figure 34. Comparison of three network types (chemical network is ENR-DA  $p = 25$ ) at 10 °C during the second mechanical cycle (a), and the last stretching until break (b).

## Appendix A: Presentation of the *in situ* tensile X-ray scattering set-up

The experimental set-up is composed of three main elements: the tensile machine, the X-ray source and the CCD camera for the detection of the diffracted intensity (Figure 35).

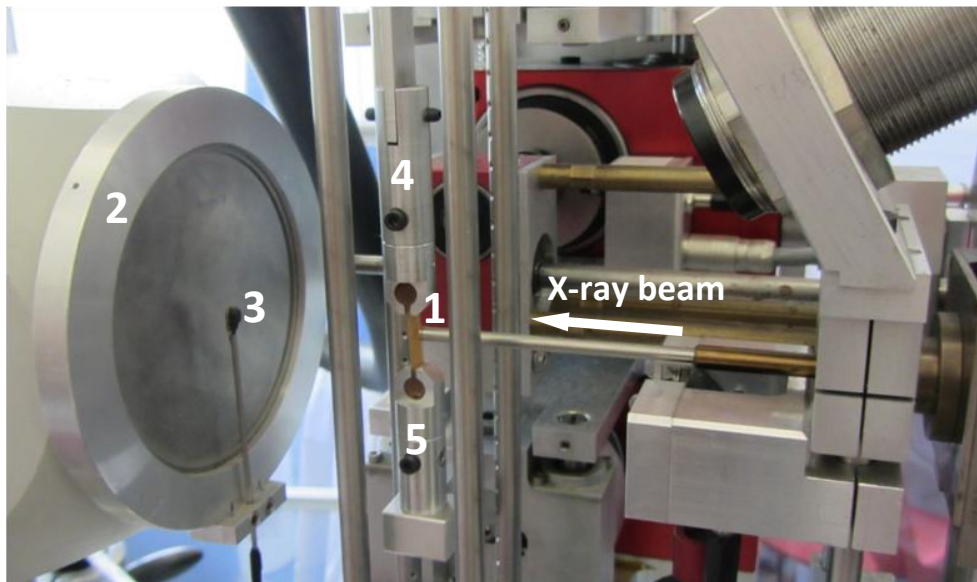


Figure 35. Experimental set up. 1: sample and collimator exit; 2: X-ray CCD camera; 3: beam stop; 4 and 5: moving clamps. (Traction direction is vertical)

The sample is located at the focalization point close to the collimator exit to ensure a maximum diffracted intensity. The extension of the sample is symmetric relative to the fixed point where the X-ray beam is focalized. The speed of the traction machine is controlled by a stepper motor that allows traction speeds between 1 and 800 mm.min<sup>-1</sup>. In this study, all the experiments were conducted at 25 mm.min<sup>-1</sup> (corresponding to a strain rate of 1.25 min<sup>-1</sup>). The exposure time of the CCD camera is 10 seconds and the data transfer takes about 6 seconds. We thus obtain one X-ray diffraction pattern every 16 seconds, ensuring an appropriate number of measurement points during tensile tests. The temperature is controlled through air flow and can be adapted between -10 and 110 °C. During the experiment, force, temperature, time, dimension of the sample, transmitted intensity and diffracted intensity are recorded at the same time.

## Appendix B: Experimental section (physical networks)

### 1. Materials

Behenic acid (BA,  $\geq 80\%$ ) was purchased from Fluka and used as received. The other materials (ENR25, DMI and kaolin) were already described in experimental section (1.2).

### 2. Blend preparation

#### *Masterbatch*

Mixtures of ENR, BA and DMI were made in a Haake Polydrive mixer equipped with cam rotors at 40 °C for about 20 minutes, following a protocol already described.<sup>16</sup> During mixing the temperature increased to about 60 °C. The amount of behenic acid was fixed to one molecule per two epoxy rings, that is to say, one per eight monomers for ENR25. DMI, liquid in the mixing conditions (mp  $\approx 38$  °C), was premixed with behenic acid to facilitate its incorporation in the rubber.

#### *Grafting process*

The grafting reaction was conducted by reactive extrusion under N<sub>2</sub> flow at a 60 rpm rate using a DSM micro-extruder with a capacity of 15 cm<sup>3</sup>. About 12 g of masterbatch were first added at 60 °C, and then the extruder was closed and the temperature raised to 180 °C for grafting. The high temperature was maintained during 30 minutes while mixing to ensure the complete grafting of BA onto ENR. Then, the mixture was cooled; kaolin was added at 60 °C and blended during 7 minutes. Kaolin was added only for comparison with chemical networks studied in section (1). The final composition of the grafted ENR is given in Table 6.

Table 6. Final composition of the grafted ENR.<sup>a</sup>

<b>Component</b>	<b>Physical network</b>
ENR25	100
BA	74
DMI	17
kaolin	10.1

<sup>a</sup> amounts in *phr* (part per hundred rubber)

### *Sample shaping*

Finally, the grafted rubber was shaped by compression moulding for 5 min at 80°C and 8 tons in a home-made mould to obtain the tensile samples described in Figure 2b in experimental section (1.2).

## 3. Characterization

Swelling experiments and tensile tests were conducted as already described in experimental section (1.2). The stretching apparatus is described in Appendix A.

### *Infra-red spectroscopy*

Vibrational (IR) spectra were recorded from the bulk using a Bruker TENSOR 37 spectrometer fitted with a Specac golden gate ATR heating cell.

### *Nuclear Magnetic Resonance spectroscopy (NMR):*

<sup>1</sup>H NMR spectra were recorded in CDCl<sub>3</sub> using a Bruker Avance 400 spectrometer (400 MHz).

### *Electronic microscopy*

Blend morphologies were observed using a CEM 902 Zeiss transmission electron microscope operated under a voltage acceleration of 80 kV. Thin sections (60-100 nm) were cut from the cured blends at -80 °C using an ultra-cryomicrotome (Leica Ultracut) with a diamond knife. Staining was achieved by exposing the thin sections to ruthenium tetroxide (RuO<sub>4</sub>) vapours during 2 minutes at room temperature.

### *Dynamic Mechanical Analysis*

Temperature evolution of storage and loss moduli was measured using a Q800 series TA Instruments Dynamical Mechanical Analyzer (DMA), in tension-film configuration. Samples cut in a cured rubber sheet (1.5 mm thickness) were submitted to a 3 °C.min<sup>-1</sup> temperature ramp from -100 °C to 200 °C (1 Hz, 0.1 % strain).

### *Differential Scanning Calorimetry*

DSC measurements were performed using a Q1000 series TA Instrument under nitrogen flow. Samples (≈ 10 mg) encapsulated in hermetic pans were first cooled down to -100 °C for 5 minutes to equilibrate the system, and then samples underwent a complete cycle up to 140 °C and a second heating from -100 °C to 180 °C, at a rate of 10 °C.min<sup>-1</sup>.

*SAXS measurements*

Small angle X-ray scattering experiments were performed at room temperature in transmission mode by using Cu K $\alpha$  radiation ( $\lambda_{Cu} = 0.1542 \text{ nm}$ ) from an X-ray generator (XRG3D Inel) operating at 40 kV and 25 mA. SAXS curves were acquired with a linear detector (LPS50 Inel). The sample-to-detector distance was 41 cm, so the  $q$  range covered was 0.03-0.32  $\text{\AA}^{-1}$ . Standard data corrections were applied; they have been normalized by the transmission, the thickness, the intensity of the incident beam, the acquisition duration, and finally corrected for background scattering. The scattering profiles were plotted as a function of the scattering vector  $q$  defined according to equation (17), where  $\theta$  is the scattering angle,  $d$  the Bragg distance, and  $\lambda$  the radiation wavelength.

$$q = \frac{4\pi \sin \theta}{\lambda_{Cu}} = \frac{2\pi}{d} \quad (17)$$

## References

1. J. G. Drobný, *Handbook of thermoplastic elastomers*, Elsevier, 2nd edn., 2014.
2. M. Morton, *Rubber technology*, Springer Science & Business Media, 2013.
3. C. Davies, S. Wolfe, I. Gelling and A. Thomas, *Polymer*, 1983, **24**, 107-113.
4. S. Trabelsi, P.-A. Albouy and J. Rault, *Macromolecules*, 2002, **35**, 10054-10061.
5. S. Trabelsi, P.-A. Albouy and J. Rault, *Macromolecules*, 2003, **36**, 7624-7639.
6. J. Rault, J. Marchal, P. Judeinstein and P. Albouy, *Macromolecules*, 2006, **39**, 8356-8368.
7. P.-A. Albouy, G. Guillier, D. Petermann, A. Vieyres, O. Sanseau and P. Sotta, *Polymer*, 2012, **53**, 3313-3324.
8. R. Pérez-Aparicio, A. Vieyres, P.-A. Albouy, O. Sanséau, L. Vanel, D. R. Long and P. Sotta, *Macromolecules*, 2013, **46**, 8964-8972.
9. A. Vieyres, R. Pérez-Aparicio, P.-A. Albouy, O. Sanseau, K. Saalwächter, D. R. Long and P. Sotta, *Macromolecules*, 2013, **46**, 889-899.
10. N. Murthy and H. Minor, *Polymer*, 1990, **31**, 996-1002.
11. U. Göschel, K. Deutscher and V. Abetz, *Polymer*, 1996, **37**, 1-6.
12. S. Kohjiya and Y. Ikeda, *Chemistry, manufacture and applications of natural rubber*, Elsevier, 2014.
13. L. R. G. Treloar, *The physics of rubber elasticity*, Oxford university press, 1975.
14. A. Gent, *Transactions of the Faraday Society*, 1954, **50**, 521-533.
15. B. Huneau, *Rubber Chemistry and Technology*, 2011, **84**, 425-452.
16. M. Pire, S. Norvez, I. Iliopoulos, B. Le Rossignol and L. Leibler, *Polymer*, 2010, **51**, 5903-5909.
17. M. Pire, S. Norvez, I. Iliopoulos, B. Le Rossignol and L. Leibler, *Polymer*, 2011, **52**, 5243-5249.
18. M. Pire, C. Lorthioir, E. K. Oikonomou, S. Norvez, I. Iliopoulos, B. Le Rossignol and L. Leibler, *Polymer Chemistry*, 2012, **3**, 946-953.
19. M. Pire, E. K. Oikonomou, L. Imbernon, C. Lorthioir, I. Iliopoulos and S. Norvez, *Macromolecular Symposia*, 2013, **331-332**, 89-96.
20. M. Pire, S. Norvez, I. Iliopoulos, B. Le Rossignol and L. Leibler, *Composite Interfaces*, 2014, **21**, 45-50.
21. L. Imbernon, M. Pire, E. K. Oikonomou and S. Norvez, *Macromolecular Chemistry and Physics*, 2013, **214**, 806-811.
22. L. Imbernon, E. Oikonomou, S. Norvez and L. Leibler, *Polymer Chemistry*, 2015, **6**, 4271-4278.
23. C. Ding and A. S. Matharu, *ACS Sustainable Chemistry & Engineering*, 2014, **2**, 2217-2236.
24. T. Lin, X. Zhang, Z. Tang and B. Guo, *Green Chemistry*, 2015, **17**, 3301-3305.
25. C. Jiang, H. He, X. Yao, P. Yu, L. Zhou and D. Jia, *Journal of applied polymer science*, 2014, **131**, 41166.
26. T. Lin and B. Guo, *Industrial & Engineering Chemistry Research*, 2013, **52**, 18123-18130.
27. L. Mascia, P. Russo, M. Lavorgna, L. Verdolotti, J. Clarke, A. Vignali and D. Acierno, *AIP Conference Proceedings*, 2014, **1599**, 26-29.
28. L. Mascia, J. Clarke, K. S. Ng, K. S. Chua and P. Russo, *Journal of applied polymer science*, 2015, **132**.
29. A. S. Hashim and S. Kohjiya, *Polymer Gels and Networks*, 1994, **2**, 219-227.
30. A. S. Hashim, S. Kohjiya and Y. Ikeda, *Polymer International*, 1995, **38**, 111-117.

31. J. Mark, *Rubber Chemistry and Technology*, 1975, **48**, 495-512.
32. P.-A. Albouy, A. Vieyres, R. Pérez-Aparicio, O. Sanséau and P. Sotta, *Polymer*, 2014, **55**, 4022-4031.
33. M. Tosaka, S. Murakami, S. Poompradub, S. Kohjiya, Y. Ikeda, S. Toki, I. Sics and B. S. Hsiao, *Macromolecules*, 2004, **37**, 3299-3309.
34. J.-M. Chenal, L. Chazeau, L. Guy, Y. Bomal and C. Gauthier, *Polymer*, 2007, **48**, 1042-1046.
35. M. Tosaka, S. Kohjiya, S. Murakami, S. Poompradub, Y. Ikeda, S. Toki, I. Sics and B. S. Hsiao, *Rubber Chemistry and Technology*, 2004, **77**, 711-723.
36. Y. Ikeda, Y. Yasuda, K. Hijikata, M. Tosaka and S. Kohjiya, *Macromolecules*, 2008, **41**, 5876-5884.
37. J. Valentin, P. Posadas, A. Fernandez-Torres, M. Malmierca, L. Gonzalez, W. Chasse and K. Saalwächter, *Macromolecules*, 2010, **43**, 4210-4222.
38. J.-M. Lehn, *Supramolecular chemistry*, Vch, Weinheim, 1995.
39. P. Cordier, F. Tournilhac, C. Soulié-Ziakovic and L. Leibler, *Nature*, 2008, **451**, 977-980.
40. M. R. Tant, K. A. Mauritz and G. L. Wilkes, *Ionomers: synthesis, structure, properties and applications*, Springer Science & Business Media, 1997.
41. R. Bacon and E. Farmer, *Rubber Chemistry and Technology*, 1939, **12**, 200-209.
42. C. Nakason, A. Kaesaman, Z. Samoh, S. Homsin and S. Kiatkamjornwong, *Polymer testing*, 2002, **21**, 449-455.
43. C. Nakason, S. Saiwaree, S. Tatun and A. Kaesaman, *Polymer testing*, 2006, **25**, 656-667.
44. W. Arayaprane, P. Prasassarakich and G. Rempel, *Journal of applied polymer science*, 2003, **89**, 63-74.
45. R. Kenn, C. Böhm, A. Bibo, I. Peterson, H. Möhwald, J. Als-Nielsen and K. Kjaer, *The Journal of Physical Chemistry*, 1991, **95**, 2092-2097.
46. Y. Ren, K. Iimura and T. Kato, *The Journal of Chemical Physics*, 2001, **114**, 6502-6504.
47. N. Garti and K. Sato, *Crystallization and polymorphism of fats and fatty acids*, M. Dekker, 1988.
48. C. W. Bunn, *Transactions of the Faraday Society*, 1939, **35**, 482-491.

## **Conclusion générale**

---



Les élastomères font partie des matériaux les plus importants à l'échelle industrielle pour leurs propriétés extraordinaires. Qui dit forte utilisation dit aussi grande quantité de déchets associés (matériaux en fin de vie et autres rebuts de production). Malheureusement, le recyclage des caoutchoucs est fortement compliqué par leur nature thermodurcissable, ce qui représente donc un réel problème écologique. Il est nécessaire de trouver des solutions alliant à la fois bonnes propriétés mécaniques, et impact environnemental réduit. La réduction de l'impact environnemental des caoutchoucs passe par l'allongement de leur cycle de vie, la capacité de remodelage des objets en fin de vie, ou même dans le cas idéal la récupération du polymère initial avant réticulation.

Au cours de ce travail, nous avons cherché de nouvelles méthodes de réticulation du caoutchouc naturel époxydé. Nous avons mis en place et étudié trois types de réticulation différents, tous basés sur des chimies non-permanentes (chimique ou physique, réversible ou échangeable).

Dans le **Chapitre 2**, l'ENR a été réticulé par des diacides carboxyliques capables d'ouvrir les fonctions époxy en formant des liaisons esters. En présence d'un catalyseur de transestérification, ces réseaux montrent des propriétés vitrimères limitées, probablement à cause du faible pourcentage de fonction hydroxyles libres pour la réaction d'échange. Cependant, ce matériau permet de mettre en évidence les avantages de la chimie vitrimère face à des réseaux permanents peu réticulés (avec l'exemple ici d'une réticulation au peroxyde). En effet, si ces réseaux non denses permettent d'obtenir des propriétés de relaxation de contrainte et d'adhésion, celles-ci sont limitées et non contrôlables. Le matériau présente donc de faibles propriétés mécaniques et flue irrémédiablement, même à basse température. Face à cela, notre élastomère dynamique, bien que possédant des propriétés vitrimères limitées, présente à la fois une bonne tenue mécanique et des propriétés de relaxation et d'adhésion. Ses avantages majeurs sont le contrôle du temps de relaxation par la quantité et la nature du catalyseur, ainsi que la déclenchabilité des propriétés dynamiques par le levier température. Ainsi, le matériau présente de bonnes propriétés mécaniques à la température d'usage, mais peut également être soudé ou réparé à plus haute température.

La chimie covalente dynamique du soufre a été mise à profit dans le **Chapitre 3**. Depuis longtemps utilisé pour la vulcanisation des caoutchoucs, le soufre élémentaire produit des ponts polysulfures entre les chaînes de polymère. Dans ce travail, des liaisons sulfures ont été introduites dans l'ENR de deux manières différentes. D'une part par réticulation classique au

soufre (production de liens polysulfures principalement), et d'autre part, par l'utilisation d'un diacide commercial, contenant une fonction disulfure au centre de la chaîne aliphatique. La vulcanisation au soufre produit des liens variables selon les quantités de réactifs utilisés (vulcanisation classique, efficace ou semi-efficace). Le système de vulcanisation choisi pour cette étude a permis de minimiser la présence de ponts mono-sulfures, maximiser celle des ponts polysulfures, et donc de se placer dans le meilleur des cas du point de vue des échanges de liaisons sulfures. Malgré l'occurrence de réactions parasites qui créent peu à peu des liaisons permanentes à haute température, des propriétés de relaxation de contrainte, d'adhésion et de recyclage ont été mises en évidence et sont comparables pour les deux types de matériaux étudiés. Cependant, la réticulation aux disulfures montre des propriétés légèrement meilleures en fluage et thermo-oxydation, et surtout, présente le grand avantage de ne pas nécessiter l'utilisation de produits toxiques tels que les activateurs et accélérateurs utilisés pour la vulcanisation.

Dans le **Chapitre 4**, sous prétexte de l'étude par rayons-X d'un réseau physique d'ENR, nous avons également eu l'occasion d'étudier les propriétés de cristallisation sous contrainte de l'ENR réticulé par les diacides (réseau chimique). La cristallisation sous contrainte de l'ENR n'est pas gênée par le diacide et ressemble beaucoup à celle de NR puisqu'une légère modification des paramètres de maille permet l'inclusion des cycles oxirane dans la structure des cristaux. L'étude démontre que ces paramètres sont indépendants de la méthode ou de la densité de réticulation. Le greffage de monoacides gras sur les chaînes d'ENR a été réalisé efficacement en l'absence de solvant par une méthode d'extrusion réactive. Le polymère greffé présente une structure semi-cristalline observable par microscopie électronique. Après un cycle préliminaire de traction, ce matériau présente des propriétés mécaniques comparables à celle d'un élastomère classique tout en n'étant réticulé que par les greffons cristallisés, d'où la dénomination d'élastomère thermoplastique. Du fait de la proximité des températures de fusion et de cristallisation des greffons avec la température ambiante, les propriétés mécaniques du matériau sont très dépendantes de la température. L'utilisation d'autres greffons, par exemple des chaînes cristallisables plus longues, pourrait permettre d'augmenter la température maximale d'utilisation de ce matériau et d'en stabiliser les propriétés. L'ENR greffé a démontré une capacité de cristallisation sous contrainte, ce qui d'une part montre l'efficacité de la réticulation physique, et d'autre part laisse envisager de bonnes propriétés de résistance au déchirement ou à la propagation de fissures. Ces propriétés n'ont pas été testées dans ce travail. Enfin, les deux méthodes de réticulation chimique et

physique vues dans ce chapitre ont été combinées pour créer des matériaux duals qui peuvent apporter de nouveaux compromis en termes de propriétés.

Nous avons donc mis en place et étudié trois nouveaux types de réticulation non-permanente de l'ENR qui tous trois produisent des caoutchoucs dont l'impact environnemental est moindre par rapport à un caoutchouc réticulé de manière permanente. L'intérêt d'utiliser l'ENR comme matériau de base est de bénéficier de sa nature biosourcée ainsi que de ses propriétés mécaniques excellentes héritées du caoutchouc naturel. Le **Chapitre 1** constitue le paysage de toutes les autres propositions existantes dans lequel s'inscrit cette thèse. De nombreuses avancées restent encore à faire dans ce vaste et dynamique domaine.

## **Réticulation non-permanente, chimique ou physique, du caoutchouc naturel époxydé. Propriétés dynamiques et recyclage.**

### Résumé :

Améliorer le recyclage des caoutchoucs est un enjeu majeur de la société actuelle. Ces matériaux sont classiquement réticulés de manière permanente par chimie covalente, ce qui empêche toute modification ultérieure de la structure du réseau. Au cours de cette thèse, nous avons cherché à concevoir le recyclage en amont, en utilisant des méthodes de réticulation non-permanentes. Le caoutchouc naturel époxydé (ENR), choisi comme élastomère de base de l'étude, est efficacement réticulé par l'action de diacides carboxyliques qui réagissent sur les fonctions oxiranes pour former des ponts esters. D'une part, l'ajout d'un catalyseur de transestérification au sein du matériau a permis d'envisager l'obtention de propriétés vitrimères. Les avantages de cette chimie covalente échangeable sont mis en évidence par comparaison avec les réseaux permanents faiblement réticulés qui montrent eux aussi des propriétés de relaxation et d'adhésion. D'autre part, l'utilisation d'un diacide comportant dans sa chaîne une fonction disulfure dynamique apporte un certain degré de recyclabilité, comparable à ce qui peut être obtenu par vulcanisation conventionnelle au soufre. La chimie décrite ici présente cependant l'avantage majeur de ne pas être toxique pour l'environnement, contrairement à la vulcanisation. Enfin, le greffage d'acides gras à chaîne cristallisable sur l'ENR conduit à l'obtention d'élastomères thermoplastiques. L'étude par diffraction des rayons-X sous traction cyclique montre que ces réseaux physiques cristallisent sous contrainte aussi bien que l'ENR réticulé chimiquement aux diacides.

Mots clés : [Caoutchouc naturel époxydé, Réticulation, Chimie dynamique, Recyclage, Vitrimères, Greffons cristallisables]

## **Chemical or physical non-permanent crosslinking of epoxidized natural rubber. Dynamic properties and recyclability.**

### Abstract:

Improving rubber recyclability is a major challenge of today's society. These materials are usually crosslinked through permanent covalent chemistry, which prevents any further modification of the network structure. The aim of this thesis was to design the recyclability up-stream by using non-permanent chemistry for rubber crosslinking. Epoxidized natural rubber (ENR), chosen as the base rubber, is efficiently crosslinked by reaction of dicarboxylic acids on oxirane rings to form ester bonds. On the one hand, the addition of a transesterification catalyst let foresee the obtaining of vitrimer properties. The advantages of this exchangeable chemistry are shown by comparison to lightly permanently crosslinked rubbers that also show stress relaxation and adhesion properties. On the other hand, using a functionalized diacid with a central disulphide function, a certain degree of reprocessability could be obtained, comparable to what was obtained by conventional sulphur vulcanization. A major advantage of the presented diacid chemistry over vulcanization is the non-toxicity towards the environment. Lastly, by grafting long crystallizable fatty acids onto ENR, we synthesized thermoplastic elastomers. Like diacid-crosslinked ENR (chemical network), these physical networks show strain-induced crystallization measured by X-ray diffraction during cyclic tensile tests.

Keywords: [Epoxidized natural rubber, Crosslinking, Dynamic chemistry, Recycling, Vitrimers, Crystallizable grafts]